INTERNATIONAL DOCTORAL
SCHOOL OF THE USC

Estefanía
Fernández Paz

PhD Thesis

New pulmonary delivery platform based on chitosan nanocapsules with potential application in gene therapy

Santiago de Compostela, 2022

Doctoral Programme in Drug Research and Development

DOCTORAL THESIS

NEW PULMONARY DELIVERY PLATFORM BASED ON CHITOSAN NANOCAPSULES WITH POTENTIAL APPLICATION IN GENE THERAPY

Estefanía Fernández Paz

INTERNATIONAL DOCTORAL SCHOOL

DOCTORAL PROGRAM IN DRUG RESEARCH AND DEVELOPMENT

SANTIAGO DE COMPOSTELA

2022

TESIS DOCTORAL

NUEVA PLATAFORMA DE ADMINISTRACIÓN PULMONAR BASADA EN NANOCÁPSULAS DE QUITOSANO CON POTENCIAL APLICACIÓN EN TERAPIA GÉNICA

Estefanía Fernández Paz

ESCUELA DE DOCTORADO INTERNACIONAL

PROGRAMA DE DOCTORADO EN INVESTIGACIÓN Y DESARROLLO DE MEDICAMENTOS

SANTIAGO DE COMPOSTELA

2022

PhD CANDIDATE STATEMENT

New pulmonary delivery platform based on chitosan nanocapsules with potential application in gene therapy

Miss Estefanía Fernández Paz

I submit my Doctoral thesis, following the procedure according to the Regulation, stating that:

1) This thesis gathers the results corresponding to my work.
2) When applicable, explicit mention is given to the collaborations the work may have had.
3) The present document is the final version submitted for its defense and coincides with the document sent in electronic format.
4) I confirm that this thesis does not incur in any plagiarism of any other authors or documents submitted by me for obtaining other degrees.

Narón, …… 2022

Fdo. Estefanía Fernández Paz

DECLARACIÓN DEL AUTOR DE LA TESIS

Nueva plataforma de administración pulmonar basada en nanocápsulas de quitosano con potencial aplicación en terapia génica

Dña. Estefanía Fernández Paz

Presento mi tesis, siguiendo el procedimiento adecuado al Reglamento, y declaro que:

1) La tesis abarca los resultados de la elaboración de mi trabajo.
2) En su caso, en la tesis se hace referencia a las colaboraciones que tuvo este trabajo.
3) La tesis es la versión definitiva presentada para su defensa y coincide con la versión enviada en formato electrónico.
4) Confirmo que la tesis no incurre en ningún tipo de plagio de otros autores ni de trabajos presentados por mí para la obtención de otros títulos.

Narón, …… 2022

Fdo. Estefanía Fernández Paz

AUTHORIZATION OF THE THESIS SUPERVISORS

New pulmonary delivery platform based on chitosan nanocapsules with potential application in gene therapy

Prof. María del Carmen Remuñán López

REPORT:

That the present thesis corresponds to the work carried out by Miss Estefanía Fernández Paz, under my supervision, and that I authorize its presentation considering that it gathers the necessary requirements of the USC Doctoral Studies Regulation, and that as supervisor of this thesis, it does not incur in the abstention causes established by the Law 40/2015.

According to the Regulation of Doctorate Studies, I also declare that the present doctoral thesis is suitable to be defended on the basis of the Monographic modality with reproduction of publications, in which the participation of the doctoral student was decisive for its elaboration and that the publications correspond to the research plan.

Santiago de Compostela, …… 2022

Fdo. María del Carmen Remuñán López

AUTORIZACIÓN DEL DIRECTOR / TUTOR DE LA TESIS

Nueva plataforma de administración pulmonar basada en nanocápsulas de quitosano con potencial aplicación en terapia génica

Dª. María del Carmen Remuñán López

INFORMA:

Que la presente tesis, se corresponde con el trabajo realizado por Dª. Estefanía Fernández Paz, bajo mi dirección, y autorizo su presentación, considerando que reúne los requisitos exigidos en el Reglamento de Estudios de Doctorado de la USC, y que como directora de ésta no incurre en las causas de abstención establecidas en la Ley 40/2015.

De acuerdo con lo indicado en el Reglamento de Estudios de Doctorado, declaro también que la presente tesis doctoral es idónea para ser defendida en base a la modalidad de Monográfica con reproducción de publicaciones, en los que la participación de la doctoranda fue decisiva para su elaboración y las publicaciones se ajustan al Plan de Investigación.

Santiago de Compostela, …… 2022

Fdo. María del Carmen Remuñán López

A mis padres y hermanos

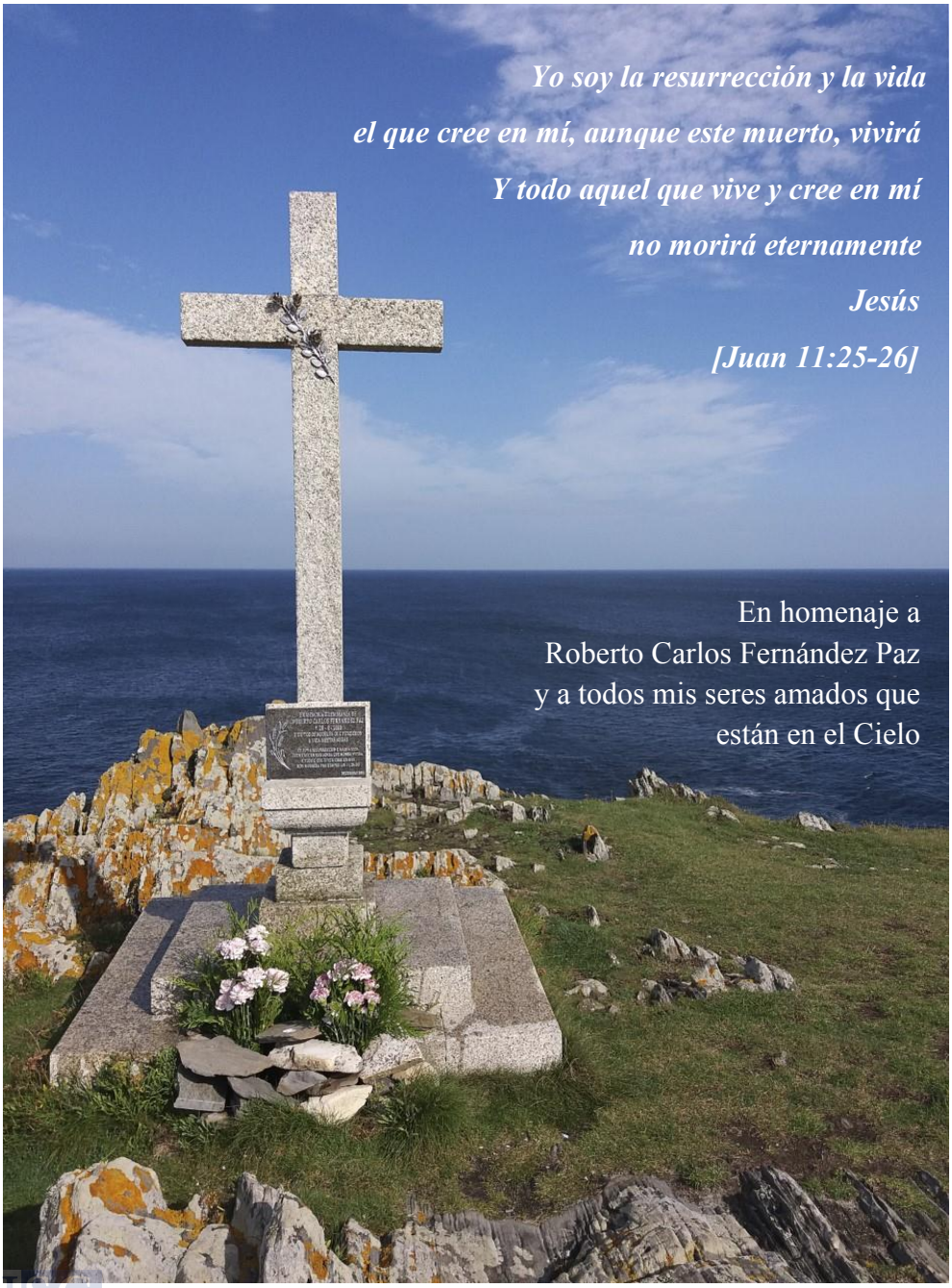

“No dejes de pensar en la vida como una aventura.
No tienes ninguna seguridad,
al menos que puedas vivir con valentía, emoción, imaginación;
al menos, que puedas elegir un desafío”

Eleanore Roosevelt

AGRADECIMIENTOS

Es para mí un honor escribir estas palabras… Y es que nadie sabe cuánto significa para mí la educación y la satisfacción que me produce ser Doctora. En realidad, llevo unos cuantos años imaginándome cómo sería el momento de escribir estos Agradecimientos… Y ahora siento que estoy viviendo uno de los momentos más especiales de mi vida. Gracias a Dios y a la vida, tengo mucho que agradecer porque tengo una vida muy rica en el amor de los que me rodean, en oportunidades y en aprendizajes.

Quisiera empezar dando el reconocimiento que se merece a mi Tutora y Directora de Tesis, Carmen Remuñán López (Carmucha). Es muy importante para mí que me permitiera cumplir el sueño de llegar a lo más alto académicamente junto con mi hermana Cris, porque los retos y los logros son más grandes y satisfactorios cuando los comparto con ella. Siempre estaré agradecida a Carmucha por toda la confianza que depositó en mí… y, sobre todo, por todas sus lecciones y enseñanzas. Más allá de todo lo que aprendí en investigación, que es mucho, para mí es más importante todo lo que aprendí como persona a lo largo de todos estos años junto a ella… Llegué a sobrepasar con creces mis límites y barreas, dándome cuenta de que puedo llegar mucho más lejos de lo que pensaba… Mis sueños y expectativas académicas más altas están cumplidas, gracias a sus oportunidades y ayuda. ¡Siempre te lo agradeceré!

A Noemí Csaba, de quien admiro muchísimo su enorme profesionalidad. No puedo estar más agradecida por todos y cada uno de sus consejos, la ayuda que me brindó, la confianza que depositó en mi hermana y en mí… y por dejarnos formar parte de su laboratorio durante meses.

A todos los profesores del Departamento de Farmacología, Farmacia y Tecnología Farmacéutica de la Universidad de Santiago de Compostela, recordando especialmente a los que ya partieron: Begoña Seijo Rey, Juan Torres Lavandeira y José Luis Gómez Amoza. Quisiera hacer mención especial a Begoña Seijo y a Dolores Torres, profesoras del Departamento de Tecnología Farmacéutica, por su calidad humana, por todas sus enseñanzas, apoyo, confianza, consejos y ayuda…

A todos los maestros de mi vida, que me han dado un pedacito de sus conocimientos y de su sabiduría personal. Aprecio toda la dedicación y el cariño con el que nos han tratado a mi hermana y a mí. Me gustaría hacer mención especial a Antonio Dopico y a Purita. A Antonio Dopico por la forma tan bella, didáctica y alegre de darnos clase a sus alumnos. ¡Gracias por tus visitas a casa!... ¡Por querernos tanto a mis hermanos y a mí!... ¡Y por ser un maestro y persona ejemplar!... A Purita, agradecerle lo buena y maravillosa maestra que ha sido siempre para nosotras… Por despertarnos la curiosidad desde pequeñitas y asombrarnos siempre con su conocimiento… ¡Gracias a ti, me nació la vocación por la enseñanza!... ¡Siempre os llevaré en el corazón!

A Rafael Romero… a quien admiro por su ingenio, simpatía, eficiencia, enorme profesionalidad y ayuda incondicional. Una persona por la que hablan sus actos y su nobleza… ¡Gracias por estar siempre ahí!

A los técnicos de la USC: Raquel, Mercedes, María José, Ramiro, Ezequiel, Javier, Montse, Ana, Luz, Gonzalo y Miguel Anxo por vuestra enorme ayuda, generosidad y profesionalidad; pero, también, por vuestra cercanía, amabilidad y hacerme sentir como en casa.

Al Decano Francisco Otero, a la anterior Decana Isabel Sández, a la Vicedecana Reyes Laguna, a la Vicedecana Paz García, a Teresa (Asuntos Económicos), a la técnica Chus, al técnico Julio y a la Secretaria del Departamento Sagrario, por vuestra ayuda. A los conserjes Joses, Vicky, María, Alfonso y Chelo, por ser tan buenas personas, grandes profesionales, voluntariosos y tan simpáticos. Especialmente, quisiera agradecerle a Chelo su hermosa amistad y todos los buenos momentos vividos juntas… que, a decir verdad, fueron todos… A las señoras encargadas de la limpieza, con enorme cariño a Socorro, Merche, Celsa y Sandra… por haberme hecho compañía en este largo camino, por habernos compartido las alegrías y las penas, por haber creado un ambiente tan familiar que siempre agradeceré.

Por supuesto, me encantaría recordar a los profesores Monteagudo, Arturo, Cristina, Matilde y a Creus, por esos encuentros en el café en donde nos reímos tanto y tan bien nos lo pasamos.

A Carlos Calderón, por haberme ayudado incondicionalmente… con profesionalidad, eficiencia y cariño… por ser tan honesto conmigo, estar siempre ahí y hacernos amigos.

A mi exjefe David por haberme dado la oportunidad de ganarme la vida honradamente en su oficina de farmacia, verano tras verano y durante años, gracias a lo cual pude costearme mis estudios de Máster y Doctorado. Le agradezco, también, por permitirme desarrollarme profesionalmente en este otro ámbito de la Farmacia y confiarme el trato a sus pacientes, que tantas alegrías me han dado. Con cariño, a todos mis compañeros de la Farmacia David López Fernández, por su ayuda, enseñanzas y momentos alegres. Por todo lo que aprendí con ellos… En especial, quisiera dar el reconocimiento y el valor que se merecen a Fran y a Merchy. Ambos me han enseñado lo que significa el absoluto amor y respeto por los pacientes, su total compromiso y profesionalidad con cada uno de ellos. Les agradezco por todo lo que me han enseñado y ayudado… Y la maravillosa experiencia de ser amigos y compartir cada segundo juntos.

A mis compañeros de laboratorio Inés, Jesús, Helena, Rita, Andrea, Diana, Jaccopo, Omar, Lorena, Patricia, Víctor, Sheila, Carla, Clara, Jose Luis, Santi, Alba, Virna y a las Rocíos… por ser tan buenas personas y por su compañerismo. Además, quisiera agradecer a Catherin, Catia, Celina y a Rebeca por el enorme apoyo y cariño que me han dado.

También, quisiera hacer una mención especial a todos y a cada uno de los compañeros a los que he enseñado y ayudado: Gabriel Armesto, Lucía Aragunde, Iago Vidal, Carlota Vila, Natalia Formigo, Silvia Vigo, Manuel Baladrón, Rubén Olmedo, H. Daniel Riascos, Altair V. Marcos, Laurin Schulze, Ana Villaverde y Ana Isabel García… Os agradezco a todos por la ilusión y el amor que pusisteis a vuestros trabajos… por vuestra compañía, respeto, alegría, las risas compartidas, por las batallas que superamos y por haberme hecho cumplir el sueño de ser maestra, la gran vocación de mi vida.

A mis amigos y también compañeros: Fernando David porque ser un hombre francamente especial, con gran valentía, honestidad, saber estar, sensibilidad y enorme corazón. A Lucía Feijoo, quien empezó siendo mi compañera y se ha convertido en mi amiga… Agradezco

toda su ayuda, pero también su nobleza y profesionalidad. A Eli, a Emi y a León, mi familia de Medellín, que tanto me han enseñado, me han querido y valorado…

A mi amigo Mou, por su amistad desde prácticamente niños, por abrir mi mente a nuevas formas de comprensión, por su cariño, apoyo y confianza absoluta en mí… ¡Gracias por el regalo de nuestra amistad, siempre duradera!

A mi amigos Carlos y Rosi… y a toda su familia, por el amor tan bonito e incondicional que nos dan a Cris y a mí, por abrirnos las puertas de su casa y de sus corazones… por ayudarnos, aconsejarnos y ser un gran apoyo para nosotras.

A todas mis "Guapísimas de Farmacia": María, Celsa, Lorena, Almudena, Noelia, Tatiana, Reyes, Eva María y Mariluz, por ser las mejores amigas y compis de carrera que podría tener… por quererme y apoyarme tanto. En especial, me gustaría agradecer a Eva por tanto cariño y por las charlas tan chulas que hemos tenido… Y a Mariluz, por ser tan bella y buena persona, por su amor y paciencia de hermana mayor, por el orgullo que nos tiene a Cris y a mí… y por el amor tan absoluto e incondicional que nos da… ¡Eres esa luz tan bonita en nuestras vidas!

A mi amiga Irene… La vida nos puso como amigas, pero podríamos haber sido perfectamente hermanas… De hecho, es mi hermana del alma… Le agradezco tanto por su cariño y amor, por estar siempre ahí, por compartir nuestras alegrías y penas, por su fidelidad y compromiso… por tu abrazo en los momentos tristes, pero también por todas las risas y helados… cabalgatas, procesiones, circo, ferias medievales y toda experiencia que vivimos y viviremos juntas… Eres mi trilliza… Y lo sabes…

A Sonia y a Manolo… Quisiera agradecerles por estos años tan felices en que fuimos familia… por todo el cariño que nos dieron a mi hermana y a mí, por abrirnos las puertas de su casa, por comprendernos, aconsejarnos y ayudarnos en todo cuanto estuvo en sus manos. ¡Gracias por haber formado parte de mi vida!

A mi primer amor, Óscar A. Ruso… por todo el amor que me dio y que me está dando desde el Cielo… por darme una experiencia única en la vida: descubrir el amor y lo que ello significa…

Agradeceré toda la vida por el tiempo que compartimos en que nos amamos y fuimos felices juntos… Agradezco por todo lo que aprendí en tu presencia y en tu ausencia… ¡Deseo que seas muy feliz!

A toda mi familia por creer en mi hermana y en mí… Por valorar nuestras capacidades desde pequeñas… por darnos su apoyo...

A mi familia espiritual… que siempre me cuidan y me dan su amor desde el cielo: a mi tía Rosa, por ser mi segunda mamá; a mi primo Fran, por su lucha y superación hasta el final; a mis abuelos paternos, Manolo y Magdalena, por su amor y generosidad inmensas; a mi abuelo Andrés, por su grandeza como abuelo, como hombre y como persona; y a mi hermano Roberto ("Killo"), al que llevo en mi alma y al que recuerdo cada día... de corazón gigante, valorado y admirado por todos… El mejor hermano mayor que pudiera tener… Agradezco todo su amor y cariño, sus enseñanzas, su energía y vitalidad, por enseñarme a ver y a amar la vida a través de sus ojos, siempre positivos. Agradezco a la vida porque fuimos, somos y seremos siempre tres hermanos… tres… ¡Te quiero muchísimo!

Quisiera darles las gracias a mis padres, Reme y Carlos, por su amor infinito y apoyo incondicional. Tanto Cris como yo, hemos tenido grandes aspiraciones en la vida y gracias a ellos hemos podido cumplir nuestros sueños... Se han sacrificado muchísimo para que tuviéramos todo lo que necesitáramos y mucho más… Y nos han enseñado grandes valores. A mi padre, agradecerle por su filosofía de vida de tratar bien a todo el mundo y a cada uno dedicarle el tiempo que se merece… de levantarse y seguir luchando cada vez que la vida nos tira al suelo… de sentir gratitud por todo lo bueno que nos pasa en la vida… ¡Gracias, papá!...por todos tus consejos, por tu franqueza, por hacerme reír, por cada beso y abrazo que me das… ¡Gracias por ser mi padre!... Y a mi madre… por ser el mejor ejemplo de súper mujer que conozco… Que nos ha enseñado a Cris y a mí a ser unas mujeres fuertes e independientes, íntegras y trabajadoras… Mamá… que nuestros triunfos siempre fueron los tuyos… y nuestra felicidad, la tuya… ¡Eres la mejor madre que tus hijos pudieran tener!… Ejemplo de cariño, bondad, generosidad, sacrificio, esfuerzo, amor y felicidad… ¡Gracias por ser nuestra mamá!

Quisiera darle las gracias a mi niña interior, y que aún vive dentro de mí, por despertarme la ilusión por cada cosa nueva en mi vida, por aprender y formarme… Por hacerme sentir desde pequeña la confianza en mí misma para conseguir todo lo que me hace feliz… Siento que, por fin, estoy cumpliendo la promesa que le hice, hace más de 20 años, a mi profesora Purita: "No sé lo que voy a hacer cuando sea mayor, pero lo que sí sé es que voy a llegar a lo más alto a lo que pueda llegar". Y es que siempre tuve esa fuerza interior para alcanzar mis metas y logros… esa pasión que me impulsa cada día a dar lo mejor de mí… esa inspiración que, sin duda, viene de mi niña interior.

Y, por supuesto, quisiera finalizar mis Agradecimientos dándole las gracias al amor de mi vida, a mi hermana Cris. Soy realmente afortunada y puedo decir que me tocó más que la Lotería antes de nacer. Muchas de las cosas que hago en la vida son mucho mejores porque las comparto con ella, desde el primer beso del día hasta ser Doctoras… y lo todo lo que está por venir, que es infinito… Me siento realmente agradecida y orgullosa de que sea mi hermana y "mi muy mejor amiga". Nuestro amor nos impulsa cada día a conseguir nuestros propósitos para lograr un futuro mejor para las dos. Y es que la vida es, sin duda, mucho más divertida y apasionante contigo.

También, me gustaría agradecerle a Dios y a la vida por permitirme ser tan dichosa, plena y afortunada.

Estefanía Fernández Paz
En Narón, 22 de Noviembre de 2021

TABLE OF CONTENTS

TABLE OF CONTENTS

LISTINGS

List of abbreviations (with Latin letters)

AAT	alpha-1 antitrypsin
AAV	adenoassociated virus
Abm	*Acinetobacter baumannii*
AI/s	active ingredient/s
ARDS	acute respiratory distress syndrome
ASGPR	asialoglycoprotein receptor
ASO/s	antisense oligonucleotide/s
ASTM	American Society for Testing and Materials
A549	line cell of adenocarcinoma human alveolar basal epithelial
Calu-3	human lung cancer cell line
CF	cystic fibrosis
CLSM	confocal laser scanning microscopy
CMC	Carboxymethylchitosan
CMCD	carboxymethyl-β-cyclodextrin
COPD	chronic obstructive pulmonary disease
CRISPR	clustered regularly interspaced palindromic repeats
CS	chitosan
Cu^6	coumarin 6
D_{aer}	aerodynamic diameter
DAPI	4′,6-diamino-2-phenylindole
DA	degree of acetylation
DD	degree of deacetylation
D_g	geometric diameter
D.L.	drug loading

DLS	dynamic light scattering
DMD	Duchenne muscular dystrophy
DMEM	Dulbecco´s Modified Eagle Medium
DMSO	dimethyl sulfoxide
DNA	deoxyribonucleic acid
DNMT1	DNA methyltransferase 1
ECMO	extracorporeal membrane oxygenation
E.E.	encapsulation efficiency
EGRF	epidermal growth factor receptor
EMA	European Medicines Agency
EPR	enhanced permeability and retention
FACS	fluorescence-activated cells sorting
FBS	fetal bovine serum
FDA	Food and Drug Administration
FITC	fluorescein isothyocianate
F.R.	flow rate
FSC	forward scattering
GVHD	graft-versus-host disease
HA	hyaluronic acid
HPLC	high performance liquid chromatography
HR	homologous recombination
INS	insulin
ISO	International Organization for Standardization
L	lipid
LB	Luria Bertani medium
LDA	laser doppler anemometry

Ma	D-mannitol
MIL	material of Institut Lavoisier
miRNA	microribonucleic acid
MOF/s	metal-organic framework/s
mRNA	messenger ribonucleic acid
MS	microsphere/s
MUC	mucin
Mw	molecular weight
N/P ratio	CS amino groups/Genetic material phosphate groups ratio
NC/s	nanocapsule/s
NCL	nanotechnology characterization laboratory
NHEJ	non-homologous end joining
NP/s	nanoparticle/s
NSCLC	non-small cells of lung cancer
PBS	phosphate buffered saline
pDNA	plasmid deoxyribonucleic acid
PdI	polydispersity index
PE	phosphatidylethanolamine
PEG	polyethylene glycol
PEI	polyethyleneimine
P.Y.	process yield
QD/s	quantum dot/s
rAAV	recombinant adenoassociated virus
RISC	RNA-induced silencing complex
RNA	ribonucleic acid

RNAi	interfering ribonucleic acid
SBRT	stereotactic body radiation therapy
SCLC	small cells of lung cancer
S.D.	standard deviation
SDS	sodium dodecyl sulphate
SEM	scanning electron microscope
siRNA	small interfering ribonucleic acid
SLN	solid lipid nanoparticles
SMA	spinal muscular atrophy
TALENs	translational activator-like effectors
TEM	transmission electron microscopy
$T_{Inlet/s}$	inlet temperature/s
TMC	N,N,N-Trimethylchitosan
TNF-alpha	alpha tumor necrosis factor
$T_{Outlet/s}$	outlet temperature/s
TPP	sodium tripolyphosphate
t.s.c.	total solids content
UV	ultraviolet
WHO	World Health Organization
X-Gal	5-bromo-4-chloro-3-indolylbeta-D-galactopyranoside
ZFNs	zinc finger nucleases

List of abbreviations (with Greek letters)

λ	dynamic shape factor
$\lambda_{Ex/Em}$	excitation and emission wavelength values
β-Gal	β-galactosidase
PLL	ε-poly-L-lysine

Micro- and nanoparticulated systems

CS NCs*	chitosan nanocapsules
HA/CS NCs*	hyaluronic acid /chitosan nanocapsules
pCMV-βGal-CS NCs	chitosan nanocapsules loaded with pCMV-βGal
pCMV-βGal-HA/CS NCs	hyaluronic acid /chitosan nanocapsules loaded with pCMV-βGal
Cu^6-CS NCs	chitosan nanocapsules labeled with coumarin 6
Cu^6-HA/CS NCs	hyaluronic acid /chitosan nanocapsules labeled with coumarin 6
Ma MS	mannitol microsphere/s
pCMV-βGal-Ma MS	mannitol microsphere/s loaded with pCMV-βGal
CS NCs-loaded Ma MS	mannitol microsphere/s loaded with chitosan nanocapsules
HA/CS NCs-loaded Ma MS	mannitol microsphere/s loaded with hyaluronic acid/chitosan nanocapsules
pCMV-βGal-CS NCs-loaded Ma MS	mannitol microsphere/s loaded with chitosan nanocapsules containing pCMV-βGal

pCMV-βGal-HA/CS NCs-loaded Ma MS	mannitol microsphere/s loaded with hyaluronic acid/chitosan nanocapsules containing pCMV-βGal
Cu^{6}-CS NCs-loaded Ma^{B} MS	Bodipy®-labeled mannitol microsphere/s loaded with chitosan nanocapsules labeled with coumarin 6

*In the Thesis book, sometimes to refer to both CS NCs and HA/CS NCs at the same time, it is used the expression "CS-based NCs".

Units

kDa	kilodalton
Nl/h	Newton liter per hour
rpm	revolutions per minute
tap/min	taps per minute
v/v	volume/volume
w/v	weight/volume
w/w	weight/weight

LIST OF FIGURES

LIST OF TABLES

ABSTRACT

ABSTRACT

Numerous lung diseases of genetic origin (such as some types of lung cancer) do not have a good prognosis due to their current established treatments. They might benefit from the application of gene therapy by the pulmonary route, since this allows a direct and more effective "in situ" treatment.

The main objective of this Doctoral Thesis is the design and development of a novel micro-nanoplatform based on chitosan (CS) nanocapsules (NCs) for pulmonary administration of genetic material.

CS-based NCs were prepared with/without hyaluronic acid (HA) using a solvent displacement procedure, and the model plasmid pCMV-βGal was associated. The stability of the NCs in the solution of the spray-drying excipient (mannitol, Ma) was tested. Afterwards, the NCs were microencapsulated using a simple spray-drying technique with good production yields. Once the dry powders were obtained, they were characterized, resulting in adequate morphological and aerodynamic properties for pulmonary administration. The release of NCs from Ma MS in MilliQ water and in simulated pulmonary medium (SPM) demonstrated that their sizes were maintained in the nanometric range. Biocompatibility studies, carried out using the A549 cell line (of human alveolar basal epithelial adenocarcinoma), demonstrated the low toxicity of CS NCs, HA/CS NCs and Ma. In addition, the adequate uptake of the systems in the cells was demonstrated by confocal laser scanning microscopy (CLSM), observing also an homogeneous cytoplasmic distribution. Subsequently, *in vivo* studies were carried out by administering the dry powders intratracheally to Wistar-Kyoto rats, simulating their physiological respiration. The pulmonary distribution of the microencapsulated NCs was determined using NCs that were labeled with Coumarin 6 (Cu^6) (green color), while the lungs were labeled with rhodamine (red color). The results confirmed the successful arrival of the micro-nanoplatform to the deep lung. Finally, a gene expression study was carried out, using the X-Gal reaction, in rat lungs extracted 3 days after the pulmonary administration of the formulations (CS NCs-loaded Ma MS, pCMV-βGal-CS NCs-loaded Ma MS, HA/CS NCs-loaded Ma MS, pCMV-βGal-HA/CS NCs-

loaded Ma MS and pCMV-βGal-Ma MS). The results confirmed that only the plasmid-loaded formulations produced blue deposits, confirming the integrity and functionality of the plasmid released in the lung cells. In addition, the formulations with NCs improved the dispersion of the plasmid in the tissue in a more homogeneously distributed way. The best results were obtained for the formulation of pCMV-βGal-HA/CS NCs-loaded Ma MS, thanks to the transfection promoting effect of the HA. The results of the histopathological examination of the lung sections showed absence of pulmonary embolism and inflammation, with presence of normal parenchyma and thin-walled alveoli, compared to the control group.

The results presented in this work confirm that the proposed micro-nanoplatform is of great interest for the treatment of lung diseases of genetic origin.

RESUMEN

Numerosas enfermedades pulmonares de origen genético (como algunos tipos de cáncer de pulmón) no tienen un buen pronóstico debido a los tratamientos establecidos actualmente. Podrían beneficiarse de la aplicación de terapia génica por vía pulmonar, ya que permite un tratamiento "in situ" directo y más eficaz.

El objetivo principal de esta Tesis Doctoral es el diseño y desarrollo de una nueva micro-nanoplataforma basada en nanocápsulas (NCs) de quitosano (CS) para la administración pulmonar de material genético.

Las NCs basadas en CS se prepararon con/sin ácido hialurónico (HA) usando un procedimiento de desplazamiento de solvente, y se asoció el plásmido modelo pCMV-βGal. Se probó la estabilidad de las NCs en la solución del excipiente de secado por aspersión (manitol, Ma). Posteriormente, las NCs se microencapsularon mediante una técnica simple de secado por aspersión con buenos rendimientos de producción. Una vez obtenidos los polvos secos, se procedió a su caracterización, resultando en propiedades morfológicas y aerodinámicas adecuadas para la administración pulmonar. La liberación de NCs desde las Ma MS en agua MilliQ y en medio pulmonar simulado (SPM) demostró que sus tamaños se mantuvieron en el rango nanométrico. Los estudios de biocompatibilidad, realizados con la línea celular A549 (de adenocarcinoma epitelial basal alveolar humano), demostraron la baja toxicidad de CS NCs, HA/CS NCs y Ma. Además, se demostró la adecuada captación de los sistemas en las células mediante microscopía de barrido láser confocal (CLSM), observándose también una distribución citoplasmática homogénea. Posteriormente, se realizaron estudios *in vivo* administrando los polvos secos por vía intratraqueal a ratas Wistar-Kyoto, simulando su respiración fisiológica. La distribución pulmonar de las NCs microencapsuladas se determinó utilizando NCs que se marcaron con Cumarina 6 (Cu^6) (color verde), mientras que los pulmones se marcaron con rodamina (color rojo). Los resultados confirmaron la exitosa llegada de la micro-nanoplataforma al pulmón profundo. Finalmente, se realizó un estudio de expresión génica, mediante la reacción X-Gal, en pulmones de rata extraídos 3 días

después de la administración pulmonar de las formulaciones (Ma MS cargadas con CS NCs, Ma MS cargadas con pCMV-βGal-CS NCs, Ma MS cargadas con HA/CS NCs, Ma MS cargadas con pCMV-βGal-HA/CS NCs y Ma MS cargadas con pCMV-βGal). Los resultados confirmaron que solo las formulaciones cargadas con plásmido produjeron depósitos azules, lo que confirma la integridad y funcionalidad del plásmido liberado en las células pulmonares. Además, las formulaciones con NCs mejoraron la dispersión del plásmido en el tejido de forma más homogéneamente distribuida. Los mejores resultados se obtuvieron para la formulación de Ma MS cargada con pCMV-βGal-HA/CS NCs, gracias al efecto promotor de la transfección del HA. Los resultados del examen histopatológico de las secciones de pulmón mostraron ausencia de embolismo e inflamación pulmonar, con presencia de parénquima normal y alvéolos de pared delgada, en comparación con el grupo control.

Los resultados presentados en este trabajo confirman que la micro-nanoplataforma propuesta es de gran interés para el tratamiento de enfermedades pulmonares de origen genético.

RESUMO

Moitas enfermidades pulmonares de orixe xenético (como algúns tipos de cancro de pulmón) non teñen un bo prognóstico debido aos tratamentos actualmente establecidos. Poderíanse beneficiar da aplicación da terapia xénica pola vía pulmonar, xa que permite un tratamento "in situ" directo e máis eficaz.

O obxectivo principal desta Tese Doutoral é o deseño e desenvolvemento dunha nova micro-nanoplataforma baseada en nanocápsulas (NCs) de quitosano (CS) para a administración pulmonar de material xenético.

Preparáronse NCs baseadas en CS con/sen ácido hialurónico (HA) mediante un procedemento de desprazamento do disolvente e asociouse o plásmido modelo pCMV-βGal. Probouse a estabilidade das NCs na solución de excipiente de secado por aspersión (manitol, Ma). As NCs foron posteriormente microencapsuladas mediante unha técnica sinxela de secado por aspersión con bos rendementos de produción. Unha vez obtidos os pos secos, caracterizáronse, dando como resultado propiedades morfolóxicas e aerodinámicas aptas para a administración pulmonar. A liberación de NCs dende Ma MS en auga MilliQ e medio pulmonar simulado (SPM) mostrou que os seus tamaños se mantiveron no rango nanométrico. Os estudos de biocompatibilidade, realizados coa liña celular A549 (adenocarcinoma epitelial basal alveolar humano), demostraron a baixa toxicidade das CS NCs, HA/CS NCs e Ma. Ademais, a adecuada captación dos sistemas nas células demostrouse mediante microscopía de barrido láser confocal (CLSM), observando tamén unha distribución citoplasmática homoxénea. Posteriormente, realizáronse estudos *in vivo* administrando os pos secos por vía intratraqueal a ratas Wistar-Kyoto, simulando a súa respiración fisiolóxica. A distribución pulmonar das NCs microencapsuladas determinouse usando NCs que foron etiquetadas con Cumarin 6 (Cu^6) (cor verde), mentres que os pulmóns foron etiquetados con rodamina (cor vermella). Os resultados confirmaron a entrega exitosa da micro-nanoplataforma ao pulmón profundo. Finalmente, realizouse un estudo da expresión xénica, mediante a reacción X-Gal, en pulmóns de rata extraídos 3 días despois da administración pulmonar das formulacións (Ma MS

cargado con CS NCs, Ma MS cargado con pCMV-βGal-CS NCs, Ma MS cargado con HA/CS NCs, Ma MS cargado con pCMV-βGal-HA/CS NCs e Ma MS cargado con pCMV-βGal). Os resultados confirmaron que só as formulacións cargadas con plásmido producían depósitos azuis, confirmando a integridade e a funcionalidade do plásmido liberado nas células pulmonares. Ademais, as formulacións con NCs melloraron a dispersión do plásmido no tecido dunha forma máis homoxénea e distribuída. Os mellores resultados obtivéronse para a formulación de Ma MS cargado con pCMV-βGal-HA/CS NCs, grazas ao efecto promotor da transfección do HA. Os resultados do exame histopatolóxico das seccións pulmonares mostraron a ausencia de embolia e inflamación pulmonar, con presenza de parénquima normal e alvéolos de parede delgada, en comparación co grupo control.

Os resultados presentados neste traballo confirman que a micro-nanoplataforma proposta é de gran interese para o tratamento de enfermidades pulmonares de orixe xenético.

RESUMO *IN EXTENSO*

1. Introdución

A terapia xénica é un conxunto de técnicas e métodos dirixidos ao tratamento de patoloxías, cuxa orixe é producida por un trastorno xenético. A terapia xénica ten un gran potencial para diversas indicacións clínicas para os cales non existen tratamentos estándar ben establecidos [1]. Para acadar o obxectivo, a administración de xenes pódese abordar mediante técnicas *ex vivo* e *en vivo* (Figura 1).

A terapia xénica *ex vivo* ocorre fóra do corpo. As células obtéñense dun paciente ou doador e cultívanse en laboratorio, onde se modifican co xene terapéutico e, posteriormente, as células modificadas son reintroducidas no paciente [1,2].

A terapia xénica *in vivo* ocorre dentro do corpo do paciente. Para iso, incorpórase directamente ao paciente [1].

Hoxe en día, as estratexias de terapia xénica empregadas limítanse ao seu uso en células somáticas. Na liña xerminal, a modificación do xenoma realizaríase nos gametos ou nas células preimplantacionais. Sen embargo, é un método tecnicamente moi complexo, é eticamente cuestionado e non hai evidencias reais de que as modificacións se herdan á seguinte xeración [2].

A terapia xénica pódese abordar mediante diferentes mecanismos (Figura 2): terapia de substitución xénica (mediante a substitución dun xene defectuoso por outro que funciona correctamente); adición de xenes; modificación da expresión do ARN mensaxeiro (ARNm) (xa sexa por silenciamento xenético (cun ARNi)) ou ben pola alteración do "splicing" do ARNm (empregando oligonucleótidos antisentido)); e edición xénica (facendo cambios específicos no xenoma da célula, usando nucleasas de deseño) [3-9].

As estratexias empregadas para introducir o material xenético dentro das células diana pódense dividir en métodos físicos e vectores.

Os métodos físicos son: transferencia hidrodinámica de material xenético, inxección, masaxe, ADN balístico (tamén chamado "bombardeo de ADN" ou "pistola xénica"), fotoporación, sonoporación, electroporación e magnetofección (Táboa 1) [10-12].

Os vectores pódense clasificar en vectores virais e non virais. Os primeiros son virus que usan o seu ciclo de replicación para introducir

material xenético dentro das células diana [2]. Hai vectores virais de ADN e vectores virais de ARN [1,13]. Os vectores non virais son nanoestruturas inferiores a 1 μm e de composición variable [14], que poden transportar tanto fármacos como outros AIs, material xenético como oligodesoxinucleótidos, moléculas de ARN (ARNm, ARNsi, ribocimas), macromoléculas de ADN (plásmido de ADN), etc. Poden transportar material xenético de forma segura (protexéndoo da degradación polas nucleasas extracelulares) e liberalo dentro das células do tecido diana [15]. Os vectores non virais pódense clasificar en: nanopartículas inorgánicas (NPs), nanosistemas baseados en péptidos, nanosistemas baseados en lípidos e nanosistemas baseados en polímeros. Estes últimos son a principal alternativa aos vectores virais [16]. Os polímeros que forman os vectores non virais poden ser: non biodegradables, sendo máis citotóxicos; e biodegradables, sendo máis empregados en terapia xénica [11]. Ademais, os nanosistemas baseados en polímeros poden aumentar a eficacia da endocitose, grazas á incorporación de ligandos de direccionamento, tales como a galactosa (Táboa 2) [11,14]. Os polímeros empregados pódense clasificar en polímeros sintéticos, polímeros bioreducibles e polímeros naturais, destacando este último.

Os vectores virais demostraron unha maior eficiencia de transfección con respecto aos vectores non virais, pero presentan serios problemas. Poden facer que os tratamentos sexan menos efectivos cando se repiten as doses, producir respostas inmunitarias e inflamatorias, e inducir toxicidade no paciente [2]. Existe risco de mutaxénese insercional, producindo a activación do oncoxene (fai malignas ás células) ou a inhibición da expresión do xene supresor [2]. Ademais, é importante ter en conta que hai virus (por exemplo, adenovirus) que non son capaces de integrar a nova información xénica dentro do material xenético celular e, polo tanto, non se pode herdar ás células fillas durante a división celular [2]. Todo isto levou nos últimos anos a realizar novas investigacións sobre vectores non virais como portadores de material xenético [10]. De feito, os vectores non virais teñen unha serie de vantaxes atractivas sobre os vectores virais, sendo a máis importante a súa bioseguridade [10]. Ademais, son quimicamente moi versátiles (especialmente os poliméricos) [15],

teñen gran capacidade de carga (incluso de material xenético de alto peso molecular), poden co-administrar o material xenético con outros fármacos (p. ex. anticanceríxenos) [11], teñen un menor custo de produción e son máis escalables [17]. Polo tanto, os vectores non virais xorden como unha opción importante para a terapia xénica.

Os polímeros naturais empregados para preparar vectores non virais son bioseguros, teñen alta solubilidade en auga e grandes propiedades de transfección. Ademais, os vectores non virais cargados positivamente únense facilmente ao ADN plasmídico (ADNp) (de carga negativa) mediante atraccións electrostáticas, e facilitan establecer contacto coa superficie celular e producir transfección [18]. Unha vez dentro, o material xenético é liberado, expresándose na célula diana con bos resultados *in vitro* e *in vivo* [18]. Ademais, son interesantes, tendo en conta que poden deseñarse para acadar unha terapia xénica dirixida a unha zona determinada [18].

Entre os polisacáridos, os máis investigados para a preparación de vectores non virais son o CS e o HA (Táboa 3), pero outros polisacáridos tamén deberían citarse brevemente: alxinato, glicosaminoglicanos (como o sulfato de condroitina e a heparina), dextrano, pululano e esquizofilano.

O CS non é tóxico, é biocompatible e biodegradable [19]. Obtense pola desacetilación parcial da quitina, que é un homopolímero natural formado por residuos de N-acetil-D-glucosamina unidos por enlaces β-1,4 (Figura 3) [20]. A quitina atópase nos exoesqueletos de crustáceos, moluscos e insectos, pero tamén na parede celular dos fungos miceliais. Recentemente, estudouse a produción de quitosano por métodos biotecnolóxicos [21]. É mucoadhesivo e, en consecuencia, mellora a absorción de moléculas hidrófilas a través dos epitelios (intestinal, nasal, etc.) e aumenta a concentración dos AIs no lugar de acción [22]. No organismo, o CS é hidrolizado por microorganismos intestinais, lipasas de diferentes fluídos (pancreático, gástrico, saliva, mucoso) e lisozimas séricas, degradándose a N-acetilglucosamina e eliminándose do organismo sen acumularse [23].

Unha utilidade importante dos nanoportadores baseados en CS é que poden acadar facilmente o seu lugar de acción, reducindo os

efectos secundarios [22]. Ademais, os nanosistemas baseados en CS conseguen un atraso na eliminación do sistema reticuloendotelial (RES), co que poden botar un tempo máis longo de circulación no torrente sanguíneo e permitir máis interaccións coas membranas celulares [22]. Ademais, unha vez que o vehículo de CS cargado co material xenético está dentro dun endosoma, prodúcese o chamado "efecto esponxa de protóns". Consiste en que os grupos amino do CS captan os protóns do espazo endosomal, de tal xeito que as bombas de protóns introducen máis protóns dentro do endosoma e, en consecuencia, ións cloruro e auga. Todo isto leva ao inchazón do endosoma provocando a súa ruptura e a liberación do material xenético ao citoplasma celular [24].

O primeiro estudo no que se utilizou o CS como vector de material xenético (ADNp) foi en 1995, e desde 2006 tamén se investigou para a administración de ARNsi para o silenciamento xenético [25]. O CS debe a súa capacidade de unir material xenético á protonación de grupos amina a pH ácido, o que lle confire carga positiva e, polo tanto, a posibilidade de establecer interaccións electrostáticas cos ácidos nucleicos cargados negativamente [25]. Por todo o anterior, o CS é un polisacárido importante para a preparación de vectores non virais de gran utilidade en terapia xénica.

O HA, tamén chamado hialuronato, é un polisacárido natural, do grupo dos glicosaminoglicanos, cuxa estrutura molecular está formada por unidades de N-acetil-D-glucosamina (enlaces β (1,3)) e Ácido D-glucurónico (unións β (1,4)) (Figura 5) [26]. Atópase naturalmente no cordón umbilical e no humor vítreo, pero principalmente na cartilaxe e no líquido sinovial [26]. Ten propiedades atractivas, como a alta biocompatibilidade, a baixa toxicidade e a biodegradabilidade [26].

O HA é moi interesante para cubrir nanotransportadores en terapia xénica, sendo moi salientable a súa combinación en NPs baseadas en CS, por exemplo, na terapia xénica ocular para a liberación de material xenético na córnea [27]. A vantaxe do HA é que, debido á súa carga aniónica, non establece unións electrostáticas co material xenético. Ten afinidade polo receptor CD44, que está presente en gran cantidade nas células tumorais. Polo tanto, o HA ten un gran potencial para a terapia do cancro [26].

Tendo en conta a situación pandémica actual, a importancia das enfermidades pulmonares é cada vez máis destacada. Polo tanto, é moi interesante mencionar a situación actual da terapia xénica pola vía pulmonar nos ensaios clínicos (Táboa 4). O panorama actual mostra que os estudos realizados centráronse principalmente no uso de vectores virais pero, tendo en conta que os vectores non virais son máis seguros que os vectores virais, existe un amplo campo aberto para a investigación de vectores non virais baseados en polisacáridos para terapia xénica por vía pulmonar.

Inicialmente, é importante coñecer que a árbore respiratoria é a responsable do intercambio de gases no organismo. Está constituído polo tracto superior (boca, cavidade nasal, farinxe e larinxe) e o tracto inferior (traquea, bronquios, bronquiolos, bronquiolos terminais e área alveolar). Esta última subdivídese funcionalmente en: zona de condución (traquea, bronquios, bronquiolos e bronquiolos terminais) e zona respiratoria (bronquiolos respiratorios, condutos alveolares e sacos alveolares) [28].

Cando se inhala unha formulación, as partículas depositanse nos pulmóns, dependendo do seu tamaño, por: impacto, sedimentación e difusión (Figura 6). Inicialmente, os inhalados entran de forma rápida e turbulenta no tracto respiratorio. As formulacións de máis de 10 μm sitúanse na área orofarínxea e aquelas de 5-10 μm, na tráquea e nos bronquios. Se os seus tamaños atópanse entre 3-5 μm, acadarán os bronquios e os bronquiolos. Se os seus tamaños están entre 1-3 μm, chegan aos alvéolos. Ademais, hai outras variables que tamén afectan á deposición de partículas no pulmón: a frecuencia respiratoria, o volume tidal, o diámetro das vías respiratorias, a cantidade de moco producido polo paciente e o oco das vías respiratorias.

A ruta pulmonar mostra as seguintes vantaxes: é unha vía non invasiva, presenta accesibilidade das vías aéreas (que permiten a administración directa á superficie pulmonar), mostra unha gran superficie (máis de 120 m^2), ten un epitelio alveolar extremadamente pequeno e unha gran vascularización (o que dá lugar a unha alta e rápida absorción), e permite unha diminución da dose e dos efectos secundarios (con respecto a outras rutas de administración, como a vía oral ou a vía parenteral) [29].

Non obstante, é importante ter en conta as principais desvantaxes da ruta pulmonar, que son os obstáculos que deben superar as partículas para chegar ao sitio pulmonar diana [30]. Son o estornudo, a tose, a estrutura da propia árbore respiratoria, o ascensor mucociliar (que é a combinación do líquido superficial (moco e fluído periciliar) xunto co movemento ciliar), os macrófagos, a actividade enzimática (é dicir, a lisozima), o surfactante e as barreiras celulares (Figura 7).

As enfermidades xénicas pulmonares poden alterar os mecanismos de defensa do tracto respiratorio, o que leva a unha maior propensión a outras enfermidades pulmonares como a COVID-19 [31]. As enfermidades tratables con terapia xénica son: infeccións (bacterianas, fúnxicas e virais, como o SARS-CoV-2), síndrome de distress respiratorio agudo (SDRA), asma, enfermidade pulmonar obstrutiva crónica (EPOC), fibrose quística (FC), deficiencia de alfa-1 antitripsina (AAT) e algúns tipos de cancro de pulmón. Hoxe en día, existen dúas vacinas baseadas na terapia xénica que están autorizadas pola Axencia Europea de Medicamentos para previr a COVID-19 [32]: Comirnaty (Pfizer-BioNTech) and Spikevax (Moderna).

As NCs teñen un enorme interese para terapia xénica, grazas á súa particular cuberta polimérica e ao seu núcleo líquido [33]. De feito, son moi útiles para a administración de moitos AIs, como metabolitos, hormonas, péptidos, proteínas, enzimas, fármacos e xenes con aplicacións terapéuticas [34]. Ademais, as NCs permiten a estabilización, aumentan a biodisponibilidade, realizan un tratamento dirixido e unha liberación sostida dos AIs.

Tendo en conta o enorme número de enfermidades pulmonares que poderían tratarse mediante inhalación, é esencial incluír as NCs baseadas en CS cargadas de material xenético nunha plataforma de características adecuadas para a súa chegada ao pulmón.

Para levar a cabo con éxito unha terapia xénica pulmonar, é moi importante superar os obstáculos mencionados anteriormente desta vía, pero tamén hai que ter en conta outros factores como a estabilidade, o tamaño de partícula e a inercia. Os nanosistemas administrados en suspensión mostran unha menor estabilidade que se se administrasen en forma de pos secos [35]. Polo tanto, é necesaria a administración de NCs en forma de pos secos con características

adecuadas para a súa chegada á rexión desexada do tracto respiratorio [30]. Ademais, as NCs teñen baixa inercia que, combinada co seu pequeno tamaño, teñen malas características para chegar por si soas ao pulmón profundo [35]. Tendo en conta que o noso grupo de investigación desenvolveu unha plataforma eficiente para a administración de nanosistemas en forma de pos secos para a vía pulmonar, consistente na microencapsulación de nanosistemas en microesferas de manitol (Ma MS) [35-38], resulta interesante unha micro-nanoplataforma baseada en NCs microencapsuladas en Ma MS. O Ma é un azucre non redutor biocompatible para os pulmóns que foi amplamente empregado para usos farmacéuticos [39]. É termoprotector, aumenta a fluidez, a dispersabilidade e a estabilidade das formulacións obtidas en po, ten efecto mucolítico e deixa pasar ás nanoestructuras facilmente a través do moco do tracto respiratorio [40].

En consecuencia, e en base ao anterior, destaca o interese da microencapsulación de NCs baseadas en CS para a administración pulmonar.

2. Obxectivos

O obxectivo principal desta Tese foi desenvolver unha micro-nanoplataforma baseada en NCs a base de CS (CS NCs e HA/CS NCs) microencapsuladas en Ma MS en forma de po seco para a administración pulmonar de material xenético, con potencial aplicación no tratamento de diferentes enfermidades pulmonares mediante terapia xénica.

Este obxectivo principal estaba composto polos seguintes obxectivos específicos:

Obxectivo I. Preparación de NCs baseadas en CS capaces de portar unha alta carga de plásmido modelo (pCMV-βGal)

Obxectivo II. Microencapsulación de NCs a base de CS cargadas con pCMV-βGal en Ma MS con características adecuadas para a inhalación

Obxectivo III. Liberación de NCs baseadas en CS dende as Ma MS en medios acuosos

Obxectivo IV. Avaliación *in vitro* da viabilidade e da captación celular na liña celular A549

Obxectivo V. Avaliación *in vivo* da distribución pulmonar e da expresión xénica empregando ratas Wistar-Kyoto

3. Materiais e Métodos

3.1.Preparación e caracterización de NCs baseadas en CS

Inicialmente, preparouse o plásmido modelo pCMV-βGal, empregando células competentes de Escherichia coli DH5α. Comprobouse o plásmido mediante un xel de agarosa ao 1% (Electrophoresis PowerPac 300, Bio Rad, Hercules, EE.UU.). A concentración do plásmido cuantificouse cun espectrofotómetro Nanodrop 1000 (ThermoFisher Scientific, Franklin, EE.UU.) e as mostras de plásmido conxeláronse a -20 °C ata que se realicen estudos posteriores.

A preparación de NCs baseadas en CS (con/sen plásmido modelo, Táboa 5) realizouse mediante un procedemento de desprazamento do solvente previamente desenvolvido polo noso grupo en "dous pasos" [41], que neste traballo foi modificado e simplificado para realizarse "nun paso". Os materiais empregados foron Protasan® UP CL 113 (quitosano ultrapuro, sal clorhidrato, CS), Epikuron® 145V (lecitina de soia), Miglyol® 812N (un aceite neutro composto polos ácidos cáprico e caprílico, ácidos graxos de cadea media), ácido hialurónico (HA) e plásmido pCMV-βGal.

Unha vez preparadas as NCs, determinouse o seu rendemento de produción (mediante gravimetría) (Fórmula 2), caracterizouse a súa morfoloxía mediante microscopía electrónica de transmisión (TEM) (Jem-2010 Electron Microscope, Oberkochen, Alemaña), e os seus tamaños e potenciais ζ se mediron mediante Dynamic Light Scattering (DLS) e Laser Doppler Anemometry (LDA) usando un Zetasizer® Nano-ZS (Malvern Instruments, Malvern, Worcestershire, Reino Unido).

A asociación de plásmido ás NCs baseadas en CS determinouse cualitativamente mediante electroforese en xel de agarosa (1% de agarosa); mentres que a eficiencia de asociación determinouse cuantitativamente (E.E. e D.L., Fórmulas 3 e 4) medindo a diferenza entre a cantidade total de plásmido engadido ás NCs e a cantidade de plásmido libre, empregando un Fluorímetro Qubit® 3.0 (Invitrogen Life Technologies, España).

Ademais, realizouse unha análise de estabilidade térmica das NCs mediante rampas de quentamento-arrefriamento (de 25 ºC a 90 ºC e viceversa), empregando un Zetasizer® Nano-ZS (Malvern Instruments, Malvern, Reino Unido).

3.2. Preparación e caracterización das formulacións en forma de pos secos

Antes da microencapsulación de NCs en Ma MS, analizouse a súa estabilidade fisicoquímica en solución de Ma. Para iso, analizáronse as características fisicoquímicas das NCs (tamaño e potencial ζ) a diferentes tempos (0, 0.5, 1, 2 e 4 h), polos métodos anteriormente descritos.

Para microencapsular correctamente as NCs, necesitouse axustar algúns parámetros do proceso de atomización: contido en sólidos totais (t.s.c) (*p/p*, %), caudal de aire (Nl/h), relación NCs:Ma, temperatura de entrada ($T_{Entrada}$) (°C), Aspirador (%) e taxa de fluxo (FR) (mL/min). Posteriormente, utilizáronse as condicións óptimas de atomización para microencapsular todas as NCs.

Para preparar os pos secos, o proceso de microencapsulación realizouse mediante un atomizador (Büchi® Mini Spray Dryer B-290, Flawil, Suíza), empregando as condicións: velocidade de alimentación de 5 ml/min, Aspirador ao 100%, diámetro de boquilla de 0.7 mm, limpiador de boquilla fixouse a 5, a temperatura de entrada ($T_{Entrada}$) mantívose a 105 ± 2 °C e a taxa de fluxo de aire, a 600 Nl/h.

Entón, os pos secos caracterizáronse en termos de rendemento do proceso de atomización (por gravimetría, %, Fórmula 6), morfoloxía e tamaño (mediante Microscopía Electrónica de Varrido (SEM, FESEM Ultra-Plus, Zeiss, Alemaña) e propiedades aerodinámicas (diámetro xeométrico (μm), densidade aparente (g/cm^3), densidade real (g/cm^3) e diámetro aerodinámico teórico (μm)) [42] (Fórmula 1).

A distribución das NCs nas Ma MS comprobouse mediante Microscopía Raman Confocal WITec (modelo Alpha 300R) e Microscopía Láser Confocal de Varrido (CLSM, microscopio Leica TCS-SP5X-AOBS).

Para a liberación de NCs dende os pos secos, os pos incubáronse en medios acuosos: auga MilliQ ou medio pulmonar simulado (0.1% Curosurf® en PBS 10 mM (*v/v*, pH = 7.4)). A diferentes tempos (0, 0.5, 1, 2 e 4 h), as NCs liberadas analizáronse para determinar o seu tamaño e o seu potencial ζ usando un Zetasizer, como se describiu anteriormente.

3.3. Estudos *in vitro* na liña celular A549

Previamente aos estudos celulares *in vitro*, comprobouse a estabilidade das NCs en medio de crecemento celular. Especificamente, verificouse a estabilidade das NCs en auga MilliQ (control), no Medio Dulbecco's Modified Eagle (DMEM) sen suplementación e en DMEM suplementado con L-Glutamina e Soro Fetal Bovino (FBS). En diferentes momentos (0, 2 e 4 h), caracterizáronse as NCs en termos de tamaño de partícula e desviación estándar.

Os estudos *in vitro* realizáronse na liña celular A549. Probouse a viabilidade celular (Luna II, e ás 24 e 48 h despois da incubación cos sistemas, Fórmula 7), a captación intracelular (por CLSM, Leica TCS SP5 X, Alemaña) e a cuantificación de células A549 que conteñen NCs (mediante citometría, técnica Fluorescence-Activated Cells Sorting, FACS).

3.4. Estudos *in vivo*

Realizáronse estudos *in vivo* con ratas femias Wistar-Kyoto. Examinouse a distribución pulmonar das NCs microencapsuladas (por CLSM, Leica TCS-SP5X-AOBS), pero tamén estudouse a expresión xénica *in vivo* (mediante a reacción de X-Gal) [43]. Neste estudo, as mostras observáronse mediante microscopía óptica de campo claro (Leica Microsystems Heidelberg GmbH, Alemaña).

4. Resultados e discusión

4.1. Caracterización de NCs baseadas en CS

As características fisicoquímicas das NCs baseadas en CS son amosadas na Táboa 6. As CS NCs presentan un tamaño de partícula duns 160 nm e un potencial ζ positivo, de aproximadamente +56 mV. A asociación electrostática de HA (cargada negativamente) na súa superficie provocou unha lixeira redución de tamaño ata 154 nm e unha diminución do potencial ζ a +35 mV, quedando positiva. Estes resultados son consistentes con aqueles de NPs a base de CS e TPP aos que lles engadiu HA [44]. CS Cando se engadiu pCMV-βGal ás CS NCs, o tamaño e o potencial ζ eran de 165 nm e +54 mV; mentres que, para as NCs que conteñen HA, foron de 162 nm e +29 mV. Esta lixeira diminución do potencial ζ tamén se observou para as NPs de CS/TPP con cantidades crecentes de ADNp [45]. Para as NCs marcadas con Cu^6 pre-dializadas, tanto o tamaño como o potencial ζ mantivéronse practicamente constantes con respecto ás NCs sen marcar. O proceso de diálise non afectou ao tamaño das NCs marcadas con Cu^6, pero produciu unha redución dos seus potenciais ζ de case 18 mV e 11 mV para as Cu^6-CS NCs e Cu^6-HA/CS NCs, respectivamente, en comparación coas súas formas pre-dializadas.

Os rendementos de produción (Táboa 6) foron ao redor do 83% e do 79% para as CS NCs e as pCMV-βGal-CS NCs, respectivamente; e ao redor do 67% e do 65% para as HA/CS NCs e as pCMV-βGal-HA/CS NCs, correspondentemente. As formulacións preparadas con HA tiveron menores rendementos de producción, feito que concorda cos resultados obtidos paras as NPs de CS/HA/TPP [44].

As imaxes TEM mostraron NCs que, en todos os casos, presentaban unha morfoloxía esférica coa presenza dunha estrutura núcleo-cuberta (Figura 9).

A asociación de pCMV-βGal determinada cualitativamente mediante electroforese (Figura 10) mostrou unha unión do plásmido de ata o 40%, revelando unha forte asociación plásmido-NCs. A caracterización posterior da asociación do plásmido ás NCs cuantificada por fluorimetría, revelou que a eficiencia de

encapsulación (E.E.) e a carga de fármaco (D.L.) das NCs eran altas e similares para ambas NCs (Táboa 7), sendo do 91% e do 36% para as pCMV-βGal-CS NCs; e do 89% e do 36% para as pCMV-βGal-HA/CS NCs, sendo resultados consistentes coas das NPs de CS/TPP [45].

O efecto da temperatura sobre as características fisicoquímicas das NCs (tamaño e PdI, Figura 11) mostrou en ambos os casos unha diminución do tamaño de 48 nm e 16 nm para as CS NCs e HA/CS NCs, correspondentemente, na rampa de quentamento ata 90 ºC. Ademais, revélase unha desestabilización da estrutura das NCs despois de 80.5 ºC, mostrada por un PdI superior a 0.7. No caso das HA/CS NCs, estas desestabilizáronse a partir dunha temperatura superior a 72 ºC, revelada por un PdI de 1. Cando a temperatura volveu a 25 ºC, o tamaño das CS NCs diminuíu, quedando 17 nm por debaixo do tamaño orixinal, mentres que o tamaño das HA/CS NCs aumentou ata permanecer uns 7 nm por riba do seu tamaño orixinal. Noutras palabras, durante a rampa de arrefriamento gradual, as NCs volveron aproximadamente aos seus tamaños orixinais, suceso tamén observado para as NPs lipídicas sólidas (SLNs) [46].

4.2. Caracterización das formulacións en forma de pos secos

O estudo da estabilidade das NCs na solución do excipiente de atomización (Figura 12) mostrou un aumento de tamaño en ambas NCs, que se mantivo practicamente constante a medida en que avanzaba o tempo de incubación, manténdose en ambos casos por riba dos seus valores orixinais durante todo o proceso de incubación. Por outra banda, os potenciais ζ de ambos tipos de NCs foron algo máis baixos que os das súas correspondentes formas frescas en todo o proceso. Estes resultados producíronse probablemente por certas interaccións das NCs co Ma [37]. Os resultados confirmaron a idoneidade das NCs para estudos posteriores.

Para a correcta microencapsulación das NCs, foi fundamental axustar as variables do seu proceso de atomización (Táboa 8). Os valores optimizados son: t.s.c. = 11 %, taxa de fluxo de aire = 600 Nl/h, NCs:Ma = 1:15, $T_{Entrada}$ = 105 ºC, Aspirador = 100%, taxa de

fluxo = 5 mL/min. Tendo en conta a natureza lipídica das NCs, foi necesario axustar a $T_{Entrada}$ a un valor baixo, temperatura que concorda coa empregada para a atomización das SLNs [38]. Como era de esperar, as $T_{Saída}$ foron baixas (entre 55 e 60 °C, Táboa 9), adecuadas para a microencapsulación das NCs. Ademais, os rendementos obtidos (Táboa 9) oscilaron entre o 64% e o 71%, aproximadamente, sendo similares aos obtidos para a microencapsulación de NPs baseadas en CS e TPP [35,40,44,47].

As microfotografías SEM mostraron que as Ma MS eran esféricas, de tamaño algo heteroxéneo, con límites ben definidos. Cando as CS NCs ou as HA/CS NCs foron incluídas nas Ma MS, as micro-nanoestructuras resultantes eran esféricas, con límites ben definidos e estaban comparativamente menos agregadas e de menor tamaño que as anteriores. A inclusión de plásmido nas MS non afectou as súas características en todos os casos (Figura 18). Ademais, todos os tipos de MS eran xeralmente sólidas, excepto as mais grandes (Figura 19), o que concorda coas Ma MS cargadas de CS NPs máis grandes [36].

Os resultados dos estudos das propiedades aerodinámicas (Táboa 10) confirmaron que as micro-nanoplataformas deseñadas e preparadas neste traballo son teoricamente adecuadas para a súa administración ao pulmón profundo (bronquiolos e alvéolos) [48].

Tanto o estudo de RAMAN como o de confocal concluíron que as CS NCs foron microencapsuladas con éxito nas Ma MS, estando as NCs amplamente distribuídas ata chegar ao borde da MS (Figuras 20 e 21, e Figura 23).

A capacidade das MS para liberar facilmente *in vitro* ás NCs en auga MilliQ e en medio pulmonar simulado, foi confirmada pola rápida disolución do excipiente Ma. As NCs liberadas (Figura 24) eran morfoloxicamente similares ás NCs recén preparadas (Figure 9), o que demostra que o proceso de atomización non afectou á estrutura das NCs, como se esperaba [49]. Os tamaños das CS NCs e das HA/CS NCs liberadas desde as Ma MS en auga MilliQ e en medio pulmonar simulado mostraron un aumento de tamaño con respecto ás NCs frescas, probablemente debido á presenza de Ma remanente das MS. Cando se liberaron as CS NCs e as HA/CS NCs en auga MilliQ,

os potenciais ζ non variaron, pero no medio pulmonar simulado as NCs adquiriron potenciais ζ negativos, probablemente debido á presenza de moléculas negativas do medio unidas por atraccións electrostáticas á superficie positiva das NCs (Figura 25). A liberación das NCs tamén foi confirmado polo número de contas (Táboa 11). Tendo en conta a alta solubilidade do Ma nos medios acuosos investigados e os resultados obtidos neste estudo, espérase que os pos secos administrados *in vivo* liberen as NCs no fluído pulmonar.

4.3. Estudos *in vitro* na liña celular A549

Antes dos estudos celulares *in vitro*, determinouse a estabilidade de CS NCs e HA/CS NCs en auga MilliQ, en DMEM suplementado e en DMEM sen suplementación a diferentes tempos (0, 2 e 4 h) (Figura 26). Ambos tipos de NCs mantivéronse practicamente constantes na auga MilliQ co tempo, como era de esperar. Sen embargo, observouse un aumento de tamaño co tempo cando as NCs baseadas en CS se incubaron en DMEM suplementado, acadando os 500 nm para as CS NCs ás 4 h, e sendo practicamente constante por debaixo dos 250 nm para as HA/CS NCs. Cando as NCs se incubaron en DMEM sen suplementación, os tamaños tamén aumentaron co tempo, acadando máis de 500 nm as CS NCs, e sobre os 400 nm as HA/CS NCs ás 4 h. A maior estabilidade das HA/CS NCs pódese explicar pola presenza de HA na súa estrutura, parecendo ser máis estables cas CS NCs en ambos medios celulares. Non obstante, ambas formulacións estiveron no rango nanométrico e foron adecuadas para o propósito dos estudos celulares *in vitro*.

O ensaio de viabilidade celular preliminar de Luna II (Figura 27) revelou que o control positivo presentou un máximo de viabilidade lixeiramente superior ao 95%, mentres que o control negativo mostrou un 0% de viabilidade, como se esperaba. Cando as células se incubaron con CS NCs e HA/CS NCs, presentaron unha viabilidade ao redor do 95% en ambos casos. Á vista dos resultados positivos deste ensaio preliminar, a continuación realizouse outro estudo de viabilidade para avaliar especificamente a actividade metabólica das células.

A viabilidade celular das células A549 estudadas empregando CellTiter-Blue® (AlamarBlue®) (Figura 28) mostrou que, as células tratadas con NCs baseadas en CS e o excipiente Ma tanto ás 24 como ás 48 h, presentaron altas viabilidades (superiores ao 90%) [50]. En resumo, o ensaio de viabilidade indicou que as NCs baseadas en CS e o excipiente Ma non foron tóxicas para a liña celular A549. Polo tanto, espérase que estes micro-nanosistemas sexan axeitados para a administración pulmonar.

O estudo de captación intracelular (Figuras 29 e 30) verificou a internalización dos nanosistemas dentro das células, en comparación coas células control. Ademais, as células mantiveron a súa integridade, así como unha sinal de fluorescencia máis intensa procedente das Cu^6-HA/CS NCs que a das Cu^6-CS NCs. Isto probablemente débese ao efecto promotor da penetración do HA [50].

Para cuantificar as células A549 que internalizaron CS NCs e HA/CS NCs, así coma a porcentaxe de viabilidade das células, empregouse a técnica FACS mediante a análise dun mínimo de 10000 eventos por mostra (Táboa 12). Os histogramas das células control consideráronse o sinal basal para corrixir o sinal obtido das células tratadas con Cu^6-NCs. O histograma das células control confirmou unha viabilidade positiva do 100%, como se esperaba. Cando as células se trataron con Cu^6-CS NCs e Cu^6-HA/CS NCs, os seus respectivos histogramas (previamente corrixidos por "compensación da cor") mostraron que as células foron negativas para a Aqua, indicando tamén unha alta viabilidade (99.83% e 99.93% de media para Cu^6-CS NCs e Cu^6-HA/CS NCs, respectivamente) (Figura 31).

Para determinar a porcentaxe de células internalizadas, comparouse o histograma das células control cos obtidos polas células tratadas con Cu^6-CS NCs e Cu^6-HA/CS NCs (Figura 32). Como se esperaba, as células control foron negativas para o sinal de Cu^6. Cando as células se trataron con Cu^6-CS NCs e Cu^6-HA/CS NCs, foron positivas para o sinal da Cumarina, mostrando que os nanosistemas foron internalizados no 100% das células. Os resultados deste estudo foron congruentes cos obtidos mediante CLSM porque pódese verificar a internalización celular dos nanosistemas, pero tamén cuantificar o % de células A549 internalizadas coas NCs. Pódese

concluír que tanto o estudo de confocal como o de citometría de fluxo mostraron unha internalización eficiente das NCs baseadas en CS na liña celular A549, revelando tamén que a internalización dos nanosistemas non afectou á viabilidade celular. Polo tanto, as NCs baseadas en CS microencapsuladas parecen ser seguras e axeitadas para a súa administración pola vía pulmonar.

4.4. Estudos *in vivo*

Os estudos *in vivo* comprendían a distribución pulmonar das NCs microencapsuladas e o estudo da expresión xénica. A distribución pulmonar *in vivo* das NCs microencapsuladas investigouse utilizando NCs marcadas con Cu^6 e a técnica CLSM. As imaxes de seccións pulmonares obtidas tras a administración das formulacións micro-nanoestructuradas marcadas con Cu^6 a ratas (Figura 33) mostraron que, á 1h despois da administración das formulacións, as micro-nanoestructuras foron detectadas no epitelio pulmonar, sendo algunhas delas capturadas por macrófagos, fenómeno tamén observado para as Ma MS cargadas con NPs de CS/TPP-insulina [35]. Os resultados confirmaron que a nova plataforma micro-nanoestructurada ten un gran potencial para a administración pulmonar de nanoestructuras, máis concretamente de NCs, conducindo á súa liberación no pulmón profundo. O seguinte estudo tivo como obxectivo demostrar a capacidade dos pos secos micro-nanoestructurados cargados de plásmido para producir transfección pulmonar despois da súa administración *in vivo*.

Para o estudo da expresión xénica *in vivo* utilizouse o plásmido pCMV-βGal (ou xene LacZ), que codifica o enzima β-Gal. O substrato usado para probar a funcionalidade do β-Gal é o 5-Bromo-4-cloro-3-indolil-beta-D-galactopiranósido (X-Gal). Cando os tecidos pulmonares de ratas tratadas con formulacións cargadas de plásmido foron incubados nunha solución de X-Gal, o β-Gal presente nos tecidos transforma as moléculas de X-Gal en precipitados azuis. É importante sinalar que os tecidos dos mamíferos tamén posúen enzimas endóxenos coa mesma actividade β-galactosidasa. Polo tanto, foi crucial inhibir a actividade β-galactosidasa endóxena para evitar

falsos positivos. Para iso, os tecidos foron previamente procesados correctamente, mediante a incubación en solucións de pH ao redor de 7.4 [43,51], mantendo ao mesmo tempo a actividade β-galactosidasa esóxena a nivel óptimo. A inhibición puido manterse ata as 2 h, unha vez iniciada a reacción con X-Gal. Polo tanto, os tecidos pulmonares incubáronse durante exactamente 2 h na solución de X-Gal. Ademais, foi mellor procesar o pulmón en seccións que en bloque porque permite unha inhibición máis eficaz da actividade β-galactosidasa endóxena, así como unha mellor detección da actividade β-galactosidasa exóxena [43]. Polo tanto, despois da administración pulmonar a ratas de Ma MS cargadas con pCMV-βGal-CS NCs e Ma MS cargadas con pCMV-βGal-HA/CS NCs, así como os seus controis (Ma MS cargadas con CS NCs, Ma MS cargadas con HA/CS NCs e Ma MS cargadas con pCMV-βGal), a expresión de β-Gal estudouse en seccións dos pulmóns extraídos tres días despois da administración dos pos [45]. As seccións de pulmón de rata (Figura 34) que non foron tratadas con pos non mostraron depósitos azuis, o que indica que a actividade β-galactosidasa endóxena foi inhibida correctamente para evitar falsos positivos. Tampouco apareceron depósitos azuis cando as ratas foron administradas cos pos control sen plásmido: Ma MS cargadas con CS NCs e Ma MS cargadas con HA/CS NCs. Pola contra, os depósitos azuis apareceron de forma clara e reproducible nos pulmóns de ratas tratadas coas formulacións cargadas de plásmido (Ma MS cargadas de pCMV-βGal-CS NCs, Ma MS cargadas de pCMV-βGal-HA/CS NCs e Ma MS cargadas de pCMV-βGal), indicando unha expresión xénica eficiente *in vivo*. Ademais, observáronse importantes diferenzas entre os patróns de transfección das formulacións cargadas de plásmido, dependendo de se o material xenético estaba asociado ou non ás NCs e se as NCs contiñan ou non HA. De feito, nos pulmóns das ratas tratadas con pos secos de Ma MS contendo plásmido espido (Ma MS cargadas de pCMV-βGal), os depósitos azuis formaron agregados. Isto podería explicarse porque as MS en contacto co fluído pulmonar liberaba o plásmido moi rapidamente no epitelio pulmonar. En cambio, cando pCMV-βGal se incorporou previamente ás CS NCs e ás HA/CS NCs (Ma MS cargadas con pCMV-βGal-CS NCs, Ma MS cargadas con pCMV-

βGal-HA/CS NCs), os depósitos azuis resultantes estiveron máis espallados por todo o epitelio pulmonar. Ademais, e como era de esperar [52], a adición de HA á cuberta das NCs mellorou as súas propiedades de transfección. Para as Ma MS cargadas con pCMV-βGal-HA/CS NCs había depósitos azuis estendidos máis aló do borde dos alvéolos pulmonares e a transfección produciuse de forma homoxénea nunha área máis ampla.

A principal novidade deste traballo é que ideamos a microencapsulación das NCs baseadas en CS cargadas de material xenético en Ma MS para facilitar a súa administración pulmonar en forma de pos secos, o que leva a resultados reveladores. Ademais, é moi importante destacar que os sistemas presentados neste traballo non son tóxicos para a liña celular A549, e os resultados do exame histopatolóxico das seccións pulmonares foron notables, tendo en conta que os pulmóns foron extirpados 3 días despois da administración das formulacións de po seco, tempo suficiente para avaliar a posible toxicidade dos micro-nanosistemas. En concreto, houbo ausencia tanto de embolia como de inflamación pulmonar, así como a presenza de parénquima normal, con alvéolos de parede delgada, sendo comparables aos observados en cortes de tecido pulmonar non tratados con formulacións, o que confirma a non toxicidade e, polo tanto, a seguridade das formulacións para a administración pulmonar. Ademais, unha vantaxe interesante das NCs baseadas en CS é que poden usarse para unha terapia xénica combinada, cargando o material xenético na cuberta e unha molécula lipófila adxuvante, no núcleo. Esta molécula pode mellorar a transfección, como a capsaicina [53]. A versatilidade do transporte simultáneo de HA e diferentes moléculas activas nunha mesma estrutura sinxela permite levar a cabo un efecto de transfección sinérxico, sendo de enorme valor para un tratamento máis eficaz das enfermidades pulmonares xenéticas.

5. Conclusións

Conclusións específicas:

A partir dos resultados deste traballo de Tese Doutoral extraíronse as seguintes conclusións:

1. Preparáronse NCs baseadas en CS, que conteñen ou non HA, capaces de portar unha alta carga do plásmido modelo pCMV-βGal, sendo a eficiencia de asociación de arredor do 90%.

2. As NCs baseadas en CS cargadas con pCMV-βGal foron microencapsuladas en Ma MS mediante unha técnica de secado por pulverización, dando como resultado altos rendementos do proceso (> 60%) e microesferas con características morfolóxicas e aerodinámicas adecuadas para a súa administración pulmonar.

3. As NCs baseadas en CS liberadas dende Ma MS en medios acuosos mantiveron o seu tamaño no rango nanométrico, sendo apenas afectadas polo proceso de secado por pulverización. En consecuencia, espérase que despois da administración *in vivo*, as nanoestruturas recuperadas conserven as súas características orixinais no fluído pulmonar.

4. As NCs baseadas en CS e o excipiente Ma son biocompatibles coas células A549, o que leva a viabilidades superiores ao 90%. Ademais, a captación celular foi producida polo 100% das células.

5. A administración *in vivo* dos micro-nanosistemas desenvolvidos confirmou a chegada das NCs microencapsuladas ao pulmón profundo. Ademais, a reacción de X-Gal revelou altos niveis de transfección. Os mellores resultados foron obtidos polas Ma MS cargadas con pCMV-βGal-HA/CS NCs, producindo depósitos azuis estendidos de forma homoxénea máis aló do bordo dos alvéolos pulmonares. As imaxes de microscopía óptica de campo claro confirmaron visiblemente a ausencia de toxicidade e, polo tanto, a

seguridade das formulacións en po seco para a administración pulmonar.

Conclusión xeral:

Neste traballo deseñamos e desenvolvemos unha micro-nanoplataforma baseada en CS NCs e HA/CS NCs microencapsuladas en Ma MS en forma de po seco para a administración "in situ" eficiente e segura de material xenético no pulmón. Esta plataforma pode atopar unha aplicación en terapia xénica para o tratamento de enfermidades pulmonares xenéticas, abrindo unha fiestra de esperanza para o tratamento daquelas que actualmente non están ben resoltas.

6. Perspectivas Futuras

As NCs baseadas en CS microencapsuladas mostraron un enorme potencial para a súa aplicación na terapia xénica pola vía pulmonar. Por iso, esperta o interese de futuros estudos que complementen e reforcen a utilidade desta micro-nanoplataforma. Os posibles estudos nos que contemplamos afondar con esta liña de investigación son os seguintes:

1. Avaliar a estabilidade das formulacións en po seco (NCs microencapsuladas) no tempo, tendo en conta o efecto de determinados factores como a temperatura e a humidade.

2. Mellorar a caracterización das propiedades aerodinámicas dos pos secos seleccionados respecto do seu diámetro aerodinámico e distribución *in vitro*, utilizando un Andersen Cascade Impactor.

3. Investigar a asociación na cuberta das HA/CS NCs dun material xenético terapéutico para unha enfermidade pulmonar xenética específica, xunto cunha molécula adxuvante lipófila no seu núcleo oleoso, como a capsaicina (proposta como molécula adxuvante para favorecer a transfección celular). Ademais, estamos a pensar no tratamento das infeccións producidas por *A. baumannii* e *M. tuberculosis*, con material xenético específico e antibiótico na súa cuberta e núcleo, respectivamente. Outra idea é investigar a micro-nanoplataforma para a entrega pulmonar de vacinas xenéticas, como no caso, por exemplo, da COVID-19.

4. Probar a viabilidade *in vitro*, a transfección e a capacidade para modificar a expresión xénica en células alteradas, utilizando as formulacións en po seco que conteñan os principios activos propostos no punto 3.

5. Avaliar a eficacia terapéutica *in vivo* nun modelo animal axeitado (por exemplo, rato) cun defecto xenético que revele unha enfermidade

pulmonar, ao que se lle puidese administrar a formulación en po seco que conteña as moléculas activas propostas no punto 3.

6. Afondar nos perfís de seguridade da micro-nanoplataforma proposta.

7. Referencias

[1] R. Tang, Z. Xu, Gene therapy: a double-edged sword with great powers, Mol. Cell. Biochem. 474 (2020) 73–81. doi:10.1007/s11010-020-03834-3.

[2] M. Jafarlou, B. Baradaran, T.A. Saedi, V. Jafarlou, D. Shanehbandi, M. Maralani, F. Othman, An overview of the history, applications, advantages, disadvantages and prospects of gene therapy, J. Biol. Regul. Homeost. Agents. 30 (2016) 315–321.

[3] D. Wang, G. Gao, State of the art human gene therapy: part II. Gene therapy strategies and clinical applications, Discov. Med. 18 (2014) 151–161.

[4] K.A. Hoadley, C. Yau, T. Hinoue, D.M. Wolf, A.J. Lazar, E. Drill, R. Shen, A.M. Taylor, A.D. Cherniack, V. Thorsson, R. Akbani, R. Bowlby, C.K. Wong, M. Wiznerowicz, F. Sanchez-Vega, A.G. Robertson, B.G. Schneider, M.S. Lawrence, H. Noushmehr, T.M. Malta, J.M. Stuart, C.C. Benz, P.W. Laird, Cell of origin patterns dominate the molecular classification of 10,000 tumors from 33 types of cancer, Cell. 173 (2018) 291–304. doi:10.1016/j.cell.2018.03.022.

[5] E.P. Szymanski, J.M. Leung, C.J. Fowler, C. Haney, A.P. Hsu, F. Chen, P. Duggal, A.J. Oler, R. McCormack, E. Podack, R.A. Drummond, M.S. Lionakis, S.K. Browne, D.R. Prevots, M. Knowles, G. Cutting, X. Liu, S.E. Devine, C.M. Fraser, H. Tettelin, K.N. Olivier, S.M. Holland, Pulmonary nontuberculous mycobacterial infection- a multisystem, multigenic disease, Am. J. Respir. Crit. Care Med. 192 (2015) 618–628. doi:10.1164/rccm.201502-0387OC.

[6] R. Thwaite, G. Pagès, M. Chillón, A. Bosch, AAVrh.10 immunogenicity in mice and humans. Relevance of antibody cross-reactivity in human gene therapy, Gene Ther. 22 (2015) 196–201. doi:10.1038/gt.2014.103.

[7] Y. Deng, C.C. Wang, K.W. Choy, Q. Du, J. Chen, Q. Wang, L. Li, T.K.H. Chung, T. Tang, Therapeutic potentials of gene silencing by RNA interference: Principles, challenges, and new strategies, Gene. 538 (2014) 217–227. doi:10.1016/j.gene.2013.12.019.

[8] G. Cuccato, A. Polynikis, V. Siciliano, M. Graziano, M. di Bernardo, D. di Bernardo, Modeling RNA interference in mammalian cells, BMC Syst. Biol. 5 (2011) 19. doi:10.1186/1752-0509-5-19.

[9] H. Borna, S. Imani, M. Iman, S. Azimzadeh Jamalkandi, Therapeutic face of RNAi: In vivo challenges, Expert Opin. Biol. Ther. 15 (2015) 269–285. doi:10.1517/14712598.2015.983070.

[10] M. Ramamoorth, A. Narvekar, Non viral vectors in gene therapy - an overview, J. Clin. Diagn. Res. 9 (2015) 1–6. doi:10.7860/jcdr/2015/10443.5394.

[11] M. Alsaggar, D. Liu, Physical methods for gene transfer, Adv. Genet. 89 (2015) 1–24. doi:10.1016/bs.adgen.2014.10.001.

[12] J. Pahle, W. Walther, Vectors and strategies for nonviral cancer gene therapy, Expert Opin. Biol. Ther. 16 (2016) 443–461. doi:10.1517/14712598.2016.1134480.

[13] S.M. Alnasser, Review on mechanistic strategy of gene therapy in the treatment of disease, Gene. 769 (2020) 1–30. doi:10.1016/j.gene.2020.145246.

[14] C.L. Hardee, L.M. Arévalo-Soliz, B.D. Hornstein, L. Zechiedrich, Advances in non-viral DNA vectors for gene therapy, Genes. 8 (2017) 65. doi:10.3390/genes8020065.

[15] C.-K. Chen, P.-K. Huang, W.-C. Law, C.-H. Chu, N.-T. Chen, L.-W. Lo, Biodegradable polymers for gene-delivery applications, Int. J. Nanomed. 15 (2020) 2131–2150. doi:10.2147/IJN.S222419.

[16] T.V. Mashel, Y.V. Tarakanchikova, A.R. Muslimov, M.V. Zyuzin, A.S. Timin, K.V. Lepik, B. Fehse, Overcoming the delivery problem for therapeutic genome editing: Current status and perspective of non-viral methods, Biomater. 258 (2020) 120282. doi:10.1016/j.biomaterials.2020.120282.

[17] D. Wang, G. Gao, State of the art human gene therapy: Part I. Gene delivery technologies, Discov. Med. 18 (2014) 67–77.

[18] W. Khan, H. Hosseinkhani, D. Ickowicz, P.-D. Hong, D.-S. Yu, A.J. Domb, Polysaccharide gene transfection agents, Acta Biomater. 8 (2012) 4224–4232. doi:10.1016/j.actbio.2012.09.022.

[19] J. Zhao, J. Li, Z. Jiang, R. Tong, X. Duan, L. Bai, J. Shi, Chitosan, N,N,N-trimethyl chitosan (TMC) and 2-hydroxypropyltrimethyl ammonium chloride chitosan (HTCC): The potential immune adjuvants and nano carriers, Int. J. Biol. Macromol. 154 (2020) 339–348. doi:10.1016/j.ijbiomac.2020.03.065.

[20] A. Bernkop-Schnurch, S. Dunnhaupt, Chitosan-based drug delivery systems, Eur. J. Pharm. Biopharm. 81 (2012) 463–469. doi:10.1016/j.ejpb.2012.04.007.

[21] A.S. Erenler, Capsular polysaccharide biosynthesis from recombinant E. coli and chondroitin sülfate production, Cell. Mol. Biol. 65 (2019) 17–21. doi:10.14715/cmb/2019.65.6.4.

[22] W. Yu, T. Hu, Conjugation with an inulin-chitosan adjuvant markedly improves the immunogenicity of Mycobacterium tuberculosis CFP10-TB10.4 fusion protein, Mol. Pharm. 13 (2016) 3626–3635. doi:10.1021/acs.molpharmaceut.6b00138.

[23] R.C. Cheung, T.B. Ng, J.H. Wong, W.Y. Chan, Chitosan: An update on potential biomedical and pharmaceutical applications, Mar. Drugs. 13 (2015) 5156–5186. doi:10.3390/md13085156.

[24] D. Chuan, T. Jin, R. Fan, L. Zhou, G. Guo, Chitosan for gene delivery: Methods for improvement and applications, Adv. Coll. Interface Sci. 268 (2019) 25–38. doi:10.1016/j.cis.2019.03.007.

[25] B. Santos-Carballal, E. Fernández Fernández, F.M. Goycoolea, Chitosan in non-viral gene delivery: Role of structure, characterization methods, and insights in cancer and rare diseases therapies, Polym. 10 (2018) 444. doi:10.3390/polym10040444.

[26] M.S. Huh, E.J. Lee, H. Koo, J.Y. Yhee, K.S. Oh, S. Son, S. Lee, S.H. Kim, I.C. Kwon, K. Kim, Polysaccharide-based nanoparticles for gene delivery, Top. Curr. Chem. 375 (2017) 31–50. doi:10.1007/s41061-017-0114-y.

[27] S.J. Hong, M.H. Ahn, J. Sangshetti, P.H. Choung, R.B. Arote, Sugar-based gene delivery systems: Current knowledge and new perspectives, Carbohydr. Polym. 181 (2018) 1180–1193. doi:10.1016/j.carbpol.2017.11.105.

[28] S.M. More, S.S. Kale, A review on pulmonary drug delivery system, World J. Pharm. Pharm. Sci. 10 (2021) 625–641. doi:10.17605/OSF.IO/29J6A.

[29] A. Grenha, D. Carrión-Recio, D. Teijeiro-Osorio, B. Seijo, C. Remuñán-López, Nano-and microparticulate carriers for pulmonary drug delivery. In Handbook of Particulate Drug Delivery; Kumar, M.N.V., Ed.; Ranch, Stevenson; American Scientific Publishers: Valencia, CA, USA, 2008; Volume 2, pp. 165–192.

[30] S.P. Newman, Drug delivery to the lungs: Challenges and opportunities. Ther. Deliv. 8 (2017) 647–661. doi:10.4155/tde-2017-0037.

[31] Adivitiya, M.S. Kaushik, S. Chakraborty, S. Veleri, S. Kateriya, Mucociliary respiratory epithelium integrity in molecular defense and

susceptibility to pulmonary viral infections, Biol. 10 (2021) 95. doi:10.3390/biology10020095.

[32] European Medicines Agency: Science Medicines Health. COVID-19 vaccines: Authorised for use in the European Union. https://www.ema.europa.eu/en/human-regulatory/overview/public-health-threats/coronavirus-disease-covid-19/treatments-vaccines/covid-19-vaccines. (Accessed 1 September 2021).

[33] S. Deng, M.R. Gigliobianco, R. Censi, P. Di Martino, Polymeric nanocapsules as nanotechnological alternative for drug delivery system: Current status, challenges and opportunities, Nanomater. 10 (2020) 847. doi:10.3390/nano10050847.

[34] A.M. Ledo, M.S. Sasso, V. Bronte, I. Marigo, B.J. Boyd, M. Garcia-Fuentes, M.J. Alonso, Co-delivery of RNAi and chemokine by polyarginine nanocapsules enables the modulation of myeloid-derived suppressor cells, J. Control. Release. 295 (2019) 60–73. doi:10.1016/j.jconrel.2018.12.041.

[35] S. Al-Qadi, A. Grenha, D. Carrión-Recio, B. Seijo, C. Remuñán-López, Microencapsulated chitosan nanoparticles for pulmonary protein delivery: In vivo evaluation of insulin-loaded formulations, J. Control. Rel. 157 (2012) 383–390. doi:10.1016/j.jconrel.2011.08.008.

[36] A. Grenha, B. Seijo, C. Remuñán-López, Microencapsulated chitosan nanoparticles for lung protein delivery, Eur. J. Pharm. Sci. 25 (2005) 427–437. doi:10.1016/j.ejps.2005.04.009.

[37] C. Fernández-Paz, S. Rojas, P. Salcedo-Abraira, T. Simón-Yarza, C. Remuñán-López, P. Horcajada, Metal-organic frame-work microsphere formulation for pulmonary administration, ACS Appl. Mater. Interfaces. 12 (2020) 25676–25682. doi:10.1021/acsami.0c07356.

[38] D.P. Gaspar, M.M. Gaspar, C.V. Eleutério, A. Grenha, M. Blanco, L.M.D. Gonçalves, P. Taboada, A.J. Almeida, C. Remuñán-López, Microencapsulated solid lipid nanoparticles as a hybrid platform for pulmonary antibiotic delivery, Mol. Pharm. 14 (2017) 2977–2990. doi:10.1021/acs.molpharmaceut.7b00169.

[39] H.L. Ohrem, E. Schornick, A. Kalivoda, R. Ognibene, Why is mannitol becoming more and more popular as a pharmaceutical excipient in solid dosage forms? Pharm. Dev. Technol. 19 (2014) 257–262. doi:10.3109/10837450.2013.775154.

[40] S. Al-Qadi, P. Taboada, C. Remuñán-López, Micro/nanostructured inhalable formulation based on polysaccharides: Effect of a thermoprotectant on powder properties and protein integrity, Int. J. Pharm. 551 (2018) 23–33. doi:10.1016/j.ijpharm.2018.08.049.

[41] P. Calvo, C. Remuñán-López, J.L. Vila-Jato, M.J. Alonso, Development of positively charged colloidal drug carriers: Chitosan-coated polyester nanocapsules and submicron-emulsions, Colloid Polym. Sci. 275 (1997) 46–53. doi:10.1007/s003960050050.

[42] A.D. Alves, J.S. Cavaco, F. Guerreiro, J.P. Lourenço, A.M.R. da Costa, A. Grenha, Inhalable antitubercular therapy mediated by locust bean gum microparticles, Mol. 21 (2016) 702. doi:10.3390/molecules21060702.

[43] P. Bell, M. Limberis, G. Gao, D. Wu, M.S. Bove, J.C. Sanmiguel, J.M. Wilson, An optimized protocol for detection of E. Coli β-Galactosidase in lung tissue following gene transfer, Histochem. Cell Biol. 124 (2005) 77–85. doi:10.1007/s00418-005-0793-2.

[44] S. Al-Qadi, A. Grenha, C. Remuñán-López, Microspheres loaded with polysaccharide nanoparticles for pulmonary delivery: Preparation, structure and surface analysis, Carbohydr. Polym. 86 (2011) 25–34. doi:10.1016/j.carbpol.2011.03.022.

[45] N. Csaba, M. Köping-Höggård, M.J. Alonso, Ionically crosslinked chitosan/tripolyphosphate nanoparticles for oligonucleotide and plasmid DNA delivery, Int. J. Pharm. 382 (2009) 205–214. doi:10.1016/j.ijpharm.2009.07.028.

[46] D.P. Gaspar, V. Faria, L.M.D. Gonçalves, P. Taboada, C. Remuñán-López, A.J. Almeida, Rifabutin-loaded solid lipid nanoparticles for inhaled antitubercular therapy: Physicochemical and in vitro studies, Int. J. Pharm. 497 (2016) 199–209. doi:10.1016/j.ijpharm.2015.11.050.

[47] S. Al-Qadi, C. Remuñán-López, A micro-and nano-structured drug carrier based on biocompatible, hybrid polymeric nanoparticles for potential application in dry powder inhalation therapy, Polymer. 55 (2014) 4012–4021. doi:10.1016/j.polymer.2014.06.046.

[48] M. Paranjpe, C.C. Müller-Goymann, Nanoparticle-mediated pulmonary drug delivery: A review. Int. J. Mol. Sci. 15 (2014) 5852–5873. doi:10.3390/ijms15045852.

[49] J. Broadhead, S.K. Edmond-Rouan, C.T. Rhodes, The spray drying of pharmaceuticals, Drug Dev. Ind. Pharm. 18 (1992) 1169–1206. doi:10.3109/03639049209046327.

[50] A. Grenha, C.I. Grainger, L.A. Dailey, B. Seijo, G.P. Martin, C. Remuñán-López, B. Forbes, Chitosan nanoparticles are compatible with respiratory epithelial cells in vitro, Eur. J. Pharm. Sci. 31 (2007) 73–84. doi:10.1016/j.ejps.2007.02.008.

[51] D.J. Weiss, D. Liggitt, J.G. Clark, Histochemical discrimination of endogenous mammalian β-Galactosidase activity from that resulting from Lac-Z gene expression, Histochem. J. 31 (1999) 231–236. doi:10.1023/a:1003642025421.

[52] S. Al-Qadi, M. Alatorre-Meda, E.M. Zaghloul, P. Taboada, C. Remunán-López, Chitosan– hyaluronic acid nanoparticles for gene silencing: The role of hyaluronic acid on the nanoparticles' formation and activity, Colloids Surf. B: Biointerfaces. 103 (2013) 615–623. doi:10.1016/j.colsurfb.2012.11.009.

[53] A.K. Kolonko, J. Efing, Y. González-Espinosa, N. Bangel-Ruland, W. van Driessche, F.M. Goycoolea, W.-M. Weber, Capsaicin-loaded chitosan nanocapsules for wtCFTR-mRNA delivery to a cystic fibrosis cell line, Biomed. 8 (2020) 364. doi:10.3390/biomedicines8090364.

1. INTRODUCTION

1.1. Concept of gene therapy

Gene therapy is a set of techniques and methods aimed at the treatment of pathologies, whose origin is produced by a genetic disorder. Initially, it arose to treat hereditary monogenetic disorders and its advance extended in the area of cancer, as well as in other diseases like infections (e.g. Cytomegalovirus retinitis). Nowadays, gene therapy has great potential for several clinical indications for which there are no well-established standard treatments [1].

More specifically, gene therapy consists in the administration of genetic material (DNA or RNA) into cells to restore or change their functionality in order to prevent or treat certain diseases [1], whether the pathologies are hereditary or not [1,2]. It is important to know that gene is the functional unit of heredity, being the nucleic acids that encode the information for the synthesis of proteins, necessary for the life. To achieve the objective, the gene delivery can be approached by *ex vivo* and *in vivo* techniques (Figure 1).

The *ex vivo* gene therapy occurs outside the body. For that, cells are collected from a patient or donor and cultured in laboratory, where they are modified with the therapeutic gene and later the modified cells are reintroduced into the patient [1,3]. This method is poorly immunogenic, it does not produce graft-versus-host disease (GVHD) [1]; therefore, it is not necessary a histocompatible donor [1]. This type of therapy was studied in the treatment of severe combined immunodeficiencies associated to adenosine deaminase, in recessive dystrophic epidermolysis bullosa, peripheral artery disease, between others [1,4,5].

The *in vivo* gene therapy occurs within the patient's body. For that, a transgene is incorporated directly into the patient, with the advantage of avoiding all the problems related to the practical process of the *ex vivo* gene therapy: cell collection, culture, genetic modification and reintroduction [1]. This method is of interest for the familial deficiency of lipoprotein lipase, in ovarian cancer related to DNA methyltransferase 1 (DNMT1) gene (gDNMT1) and in reepithelialization, among other diseases [1,6,7].

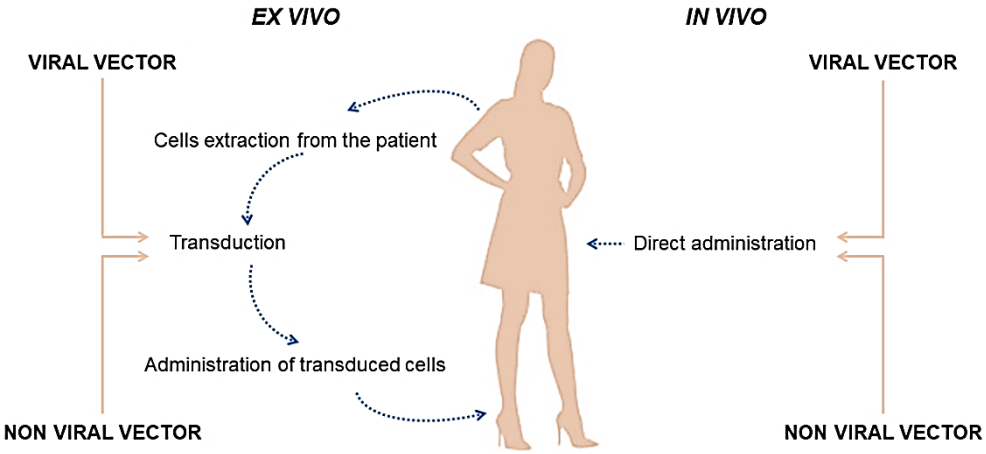

Figure 1. Scheme of the administration of genetic material *in vivo* and *ex vivo*. (Copyright free image)

Nowadays, the gene therapy strategies used are limited to their use in somatic cells, although promising studies are currently being developed with great expectations using the germinal line [1]. In this case, the genome modification would be carried out in the gametes or in preimplantation cells. So, theoretically, the genetic information would be transmitted hereditarily; but is a method technically very complex (which requires *in vitro* fertilization, as well as preimplantation genetic tests (PGT) [3]) and nowadays it is ethically questioned. However, there is no real evidences that the modifications are inherited to the next generation and, therefore, would not be maintained in the long term [3].

1.2. Mechanisms of gene therapy

In gene therapy, it is essential to know the mechanism by which the disease occurs and to evaluate the genetic defect to treat the disease [8]. Based on that, the gene therapy can be approached using different strategies (Figure 2), depending on the disorder to be repaired [2,9]:

1.2.1. Gene replacement therapy

It is based on the replacement or substitution of a defective gene for another that works correctly and, hence, it is useful for the treatment of monogenetic diseases, like certain respiratory diseases (cystic fibrosis (CF), alpha-1 antitrypsin (AAT) deficiency) [9], blood disorders (Hemophilia B), leukodystrophies, etc. [9].

1.2.2. Addition of genes

This method is interesting for more complex diseases resulting from the combination of multiple genes and environmental factors. It comprises diverse groups of diseases such as some types of cancer, heart failure, infections, etc. [9-12]. Multigenic and infectious diseases cause high mortality, so it is essential the development of cutting-edge therapies of this type [9].

1.2.3. Modification of the expression of messenger RNA (mRNA)

Taking into account that mRNA is a key element in the expression of a gene, different strategies have been proposed to affect these molecules, being classified in two groups:

1.2.3.1. Gene silencing by interfering RNA (RNAi)

This method is very useful when the overexpression of a gene occurs, producing physiological problems. Thus, the expression of certain genes can be silenced by adding an RNAi. This is a small double-stranded RNA (siRNA) that is added to the RNA-induced silencing complex (RISC), whereby the chains are separated and are directed to the complementary sequence of the target mRNA, blocking its transcription or degrading the chain of mRNA, managing to suppress the expression of the gene [13-15]. This prevents the synthesis of toxic proteins, such as superoxide dismutase I (in amyotrophic lateral sclerosis) or hungtingtin (for Huntington's disease) [16,17].

1.2.3.2. Alteration of mRNA splicing by antisense oligonucleotides

The RNA splicing phenomenon is a mechanism by which the pre-mRNA (an initial mRNA) loses the introns to constitute the mature RNA, which has only exons. This process occurs in the cytoplasm, thanks to a complex called spliceosome [18]. Thanks to antisense oligonucleotides (ASOs), the splicing phenomenon can be interfered by two mechanisms: either the introns are not properly eliminated or that the exons are modified, altering the protein resulting from the transcription process [9]. This technique is very interesting in diseases whose genes are very large and cannot be replaced, as in the case of spinal muscular atrophy (SMA) [19] or Duchenne muscular dystrophy (DMD) [9,20].

1.2.4. Genetic editing

It consists of making specific changes in the genome of the cell, using design nucleases that are specific of the target sequence [9]. To make the genetic edition, zinc finger nucleases (ZFNs) [21], translational activator-like effectors (TALENs) [22,23], or grouped and spaced palindromic short repeats (CRISPR/Cas9) [22,23] can be used. In this way, the double strand of DNA is broken and the necessary changes are made for the reparation, either by homologous recombination (HR) or by non-homologous end joining (NHEJ) [9].

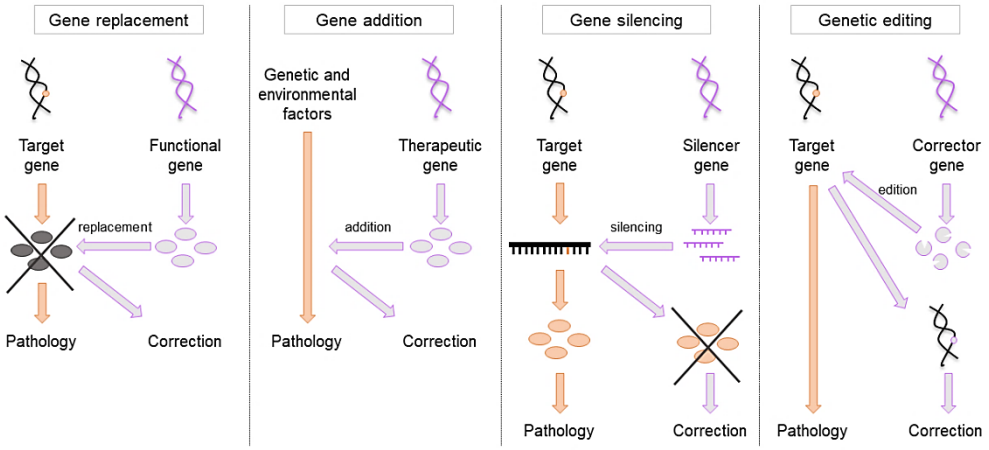

Figure 2. Scheme of gene therapy mechanisms. (New creation figure)

1.3. Procedures of genes administration into target cells

The strategies employed to introduce the genetic material into the target cells can be mostly divided in two main groups: physical methods and vectors.

1.3.1. Physical methods

They are based in the use of external forces to overcome the cell membrane and carry out the transfer of the genetic material [8,24,25]. A few examples of physical techniques applied to gene therapy are:

1.3.1.1. Hydrodynamic transfer of genetic material

This method consists in the intravenous application of a large quantity of DNA suspension, in such a way that it crosses the vascular endothelium, diffusing to the tissues [26,27].

1.3.1.2. Injection

It is a simple technique in which an injection is used to put the genetic material in free form in the tissues to be treated, with a few side effects [28]. A limitation is that the naked genes are exposed to degradation by nucleases.

1.3.1.3. Massage

It is applied a mechanical massage in the area to be treated, which temporarily modify the cellular membranes, in such a way that the DNA can access to their interior. Actually, the efficacy of this method has not been firmly demonstrated [8].

1.3.1.4. Ballistic DNA, also called "DNA bombardment" or "gene gun"

It is based on the use of heavy metal particles (tungsten, silver or gold) covered with DNA in precise doses. The use of electric shocks or helium under pressure give speed to the particles to cross the cell membrane [8,29]. It was used for the first time in plants [8].

1.3.1.5. Photoporation

Genetic material is introduced into cells thanks to transient pores of the target cells produced by a laser light beam. Its results are doubtful [8].

1.3.1.6. Sonoporation

Cell permeability is increased by applying ultrasound waves to DNA mixed with a contrast reagent (e.g. Optison® and Levovist®), producing cavitation. It is an effective and minimally invasive technique, highly dependent of the frequency, intensity and duration of the used ultrasound waves [24]. It is more useful in *in vivo* tests than in *in vitro* tests [24].

1.3.1.7. Electroporation

It consists on the application of electric pulses that generate pores in the cell membranes and, consequently, increase the cellular permeability. In this sense, the genetic material is normally introduced by electrophoresis through the pores [26]. It is commonly used in *in vitro* and *in vivo* assays with muscle and skin cells, employing needle-type or plate-type electrodes [24]. This physical method is the one that produces the highest transfection efficiency [30].

1.3.1.8. Magnetofection

It is based on magnetic particles that are coated with DNA in precise doses and are incorporated in a cell culture with electromagnets underneath. By magnetic attraction, it is possible to increase the sedimentation and, therefore, the cellular transfer of genetic material in any body tissue [8,31]. In addition, it can be used *in vitro* for the most complicated cases of cell transfection.

The following table (Table 1) summarizes the physical methods that can be used in gene therapy, emphasizing the mechanisms, the tissues in which they are applicable, their advantages and disadvantages:

Table 1. Summary of physical methods used in gene therapy.

Method	Mechanism	Tissue	Advantages	Disadvantages	References
Hydrodynamic transfer of genetic material	Increased permeability in the cell membrane	Hepatic	Transfection of high quantities of DNA	Tissue injury	[26,27]
Injection	Endocytosis	Tumoral, muscular, hepatic, cardiac, cutaneous	Safety, facility	Low efficiency	[28]
Massage	Difussion	Hepatic	Transient membrane permeability, cellular recovery	Efficacy not firmly demonstrated	[8]
Ballistic DNA	High pressure of a stream of helium	Tumoral (in ovary)	Low toxicity	Poor cellular penetration	[29]

Table 1 (continuation). Summary of physical methods used in gene therapy.

Method	Mechanism	Tissue	Advantages	Disadvantages	References
Photoporation	Appearance of pores in cell membrane	Tumoral, hepatic,	Non-invasiveness	Doubtful results	[8]
Sonoporation	Increased permeability in the cell membrane	Corneal, cerebral, peritoneal, cardiac, renal, muscular	Safety	Low efficiency	[24]
Electroporation	Increased permeability in the cell membrane	Skeletal, dermal	Good transfection efficiency and also with large genetic material	Need of surgery, electrode accessibility, tissue injury	[24,26,30]
Magnetofection	Pinocytosis and endocytosis	Tissues not treated by other methods	Low toxicity, targeting, non-invasiveness	Transitory transfection	[8,31]

1.3.2. Vectors

To achieve a successful therapy, the genetic material must be transported to the target cell and be efficiently released, either within its cytoplasm (RNA) or inside the nucleus (DNA) [8]. In order to achieve this goal, in the recent years, different types of vectors were designed [32], having all them in common that can carry genetic material (DNA or RNA) specifically to the target cells and protect it from degradation, thanks to their physicochemical characteristics, such as: positive charge, high hydrophilicity and elevated molecular weight [3]. Once the vector reaches the target cell, it delivers the genetic material, allowing it to correct the genetic defect with maximum efficiency and minimal adverse effects for the patient [8,33,34]. The vectors are divided in two big groups: viral and non-viral vectors. The most appropriate vector will be chosen according to different factors, such as type of target cell; size, molecular weight and quantity of genetic material; duration of the expression, biocompatibility, safety, etc. [8].

1.3.2.1. Viral vectors

They are modified viruses that use their replication cycle to introduce genetic material into the target cells [3]. It is important to identify in the virus the genome sequences that cause the immune response in the patient to eliminate them and, therefore, reduce the production of the antigens responsible for the aforementioned immune responses [2]. Viral vectors are subdivided into two groups:

a) DNA viral vectors. Transfect DNA, which is incorporated into the genetic material of the target cell. They are normally used for *in vivo* gene therapy [1], being some examples: herpes simplex virus, adenoviruses, adeno-associated viruses and poxviruses [35].

b) RNA viral vectors. From single-stranded RNA, a double-stranded DNA is synthesized by the reverse transcription process and the DNA is introduced into the target cell DNA. They are often used

in transplanted cells in *ex vivo* gene therapy [1,35]. Common examples are γ-retrovirus (simple retrovirus) and lentivirus (complex retrovirus) [1].

Currently, two viral-based vaccines are been used to immunize the population against the SARS-CoV-2:

b.1) Vaxzevria (AstraZeneca). This British vaccine has its origin in a collaboration between the University of Oxford and the company Astra Zeneca. It is the third approved for its use in Europe. Its composition uses an attenuated virus (adenovirus) that produces an immune response against SARS-CoV-2. It is stored between 2 and 8 ºC, which allows easier production and logistics than mRNA-based vaccines. It is used in 2 doses separated between 10 and 12 weeks (preferably 12 weeks) [36].

b.2) Vaccine Janssen. This vaccine is developed by the American company Johnson & Johnson, being the fourth approved in Europe for it use. It is also based on an adenovirus that produces an immune response against SARS-CoV-2, making its production and logistics easier than mRNA-based vaccines. It can be stored between 2 and 8 ºC for weeks and up to 2 h at room temperature. Janssen required 1 dose, but a second dose of another vaccine was necessary (Comirnaty and Spikevax) [37].

1.3.2.2. Non-viral vectors

They are nanostructures smaller than 1 μm and variable composition [32], which can transport both drugs and other AIs, genetic material like oligodeoxynucleotides, RNA molecules (mRNA, siRNA, ribozymes), DNA macromolecules (DNA plasmid), etc. [8]. They can transport genetic material in a safe way (protecting it from degradation by extracellular nucleases) and release it into the cells of the target tissue [33]. Among the non-viral vectors, the following can be highlighted:

a) Inorganic nanoparticles (NPs). They can be: soluble carbon molecules (fullerenes), carbon nanotubes (cylindrical fullerenes) [38,39], colloidal quantum dots (QDs) (nanocrystalline semiconductors) [40,41], calcium phosphate [42], silica NPs [8] and gold NPs [8,43]. The last let a controlled release of the genetic material thanks to a photothermic effect [8].

b) Peptides-based nanosystems. Their peptides-based composition allows them to transport and release DNA in the nucleus, thanks to their ability to interact with specific receptors and easily cross endosomal membranes [8]. In fact, the cationic peptides are used to functionalize other nanosystems, providing them a nuclear localization signal that improves their efficiency of transport to the cellular nuclei [8].

c) Lipids-based nanosystems. They are proposed mainly to avoid the AIs degradation in endosomes or lysosomes. They consist in different types of lipid-based nanosystems. Initially, the DNA was included in liposomes, forming lipoplexes or cationic lipids [8,24], in which the hydrophilic positive head of these structures are those that formed electrostatic interactions with the negatively charged phosphate groups of the genetic material. There are also lipid nanoemulsions, which are dispersions of oil in water with surfactant; and solid lipid NPs (SLNs), which are NPs with solid lipid core matrix stabilized with surfactant, being the latter the most used for the transport and transfer of siRNA [8].

d) Polymers-based nanosystems. They are organic vehicles that have cationic groups or that can be decorated with positively charged groups (such as quaternary ammonium groups) to electrostatically bond the genetic material (negatively charged), initially forming nanometric structures called polyplexes [8,32]. They are very significant for the transfection of the CRISPR/Cas9 plasmid, as the main alternative to viral vectors [44].

The polymers that make up the non-viral vectors are classified in two groups based on their biodegradability: non-biodegradable and biodegradable polymers. Non-biodegradable polymers have high molecular weight, but also amide and vinyl bonds that are not degradable and, therefore, make it difficult the elimination from the body [33]. For that, they are more cytotoxic. However, biodegradable polymers are the most used in gene therapy [24] because they degrade in low molecular weight components, which facilitates their expulsion and guarantee the safety [33].

Furthermore, the polymers-based nanosystems can increase the efficiency of endocytosis, thanks to the incorporation of targeting ligands that attach membrane receptors of target cells [24,32]. They achieve a sustained concentration of genetic material, preventing its deterioration [32]. As an example, we can mention galactose, a ligand that binds the asialoglycoprotein receptor (ASGPR), increasing the uptake in liver cells [24]. Another important ligand is polyethylene glycol, which allows to the vector to escape from the phagocytosis and act in the target site, improving the therapeutic efficacy [24,44]. This ligand also lets the accumulation of the therapeutic gene in inflamed areas or in tumors, increasing the therapeutic benefits [24]. This is called "enhanced permeability and retention (EPR) effect" [24].

The polymers that make up this type of vectors are very varied, and can be classified into three large groups, depending on their nature:

d.1) Synthetic polymers. Polymers as polyurethanes, amphiphilic polyesters and polycarbonates, of interest for their biocompatibility properties. Polyurethanes have biodegradability, flexibility and elasticity characteristics. Amphiphilic polyesters are also biodegradable, highlighting the poly (4-hydroxy-L-proline) ester for its biodegradability under physiological conditions, as well as for its good binding to DNA. Polycarbonates have low toxicity and good mechanical properties. There is a variety of cationic polycarbonate prepared by organocatalytic ring-opening polymerization of cyclic carbonates, with low cytotoxicity and high transfection capacity [33].

d.2) Bioreducible polymers. They are created to solve the problems caused by the high molecular weight polymers that do not degrade well. For this, degradable bonds are introduced, which are not broken in the outer cell space (oxidative environment), but that degrade in the cytoplasm (reducing environment). Disulfide bonds are an example of this type of bonds, and poly (amidoethylamine) is a type of bioreducible polymer [33].

d.3) Natural polymers. They are composed of glucose units that are joined by glycosidic bonds. Among the natural polymers, CS stands out (due to its positive charge), as well as HA (which is useful as targeting ligand to certain cells [33], such as lung cancer cells [45]) due to its transfection capacity.

1.3.2.3. Advantages of the non-viral vectors

Viral vectors have demonstrated higher transfection efficiency with respect to the non-viral vectors, but present serious problems. They can make treatments less effective when the doses are repeated, since they produce immune and inflammatory responses, and induce toxicity in the patient [3]. Besides, there is risk of insertional mutagenesis, producing the activation of the oncogene (makes cells malignant) or the inhibition of the expression of the suppression gene [3]. In addition, it is important to note that there are viruses (e.g. adenovirus) that are not capable of integrating the new genetic information into the cellular genetic material and, therefore, it cannot be inherited to daughter cells during the cell division [3]. More seriously, there was a very relevant death produced by gene therapy carried out with a viral vector. This was the case of Jesse Gelsinger (18 years old), while participating in a clinical trial in the Institute for Human Gene Therapy of the University of Pennsylvania, directed by James Wilson. Death occurred due to an immunological reaction produced by an adeno-associated virus used as vector for the genetic treatment of the ornithine transcarbamylase deficiency suffered by the patient [46]. All this has led in the recent years to a further investigations of non-viral vectors as carriers of genetic material [8]. In fact, the non-viral vectors have a number of attractive advantages

over the viral vectors, being the most important their biosafety [8]. In addition, they are chemically very versatile (tunable structure, especially polymeric ones) [33], have high loading capacity (even of genetic material of high molecular weight), can co-administer the genetic material with other drugs (e.g. anticancers) [24], have a lower production cost and are more scalable [47]. Therefore, non-viral vectors emerge as an important option for gene therapy.

1.4. Non-viral vectors based on polysaccharides

Thanks to the advantages of the non-viral vectors mentioned above, the researchers have put their efforts into the development of non-viral vectors. Among them, nanostructures of polysaccharides are especially interesting due to their enormous demonstrated utility in the transport and release of AIs [48]. In addition, the prepared with natural polymers are very biosecure, have high solubility in water and great transfection properties, being cheaper than viral vectors. Some of them also present antitumor activity and are immunostimulants [49]. In addition, non-viral vectors positively charged bind easily plasmid DNA (pDNA) (of negative charge) by electrostatic attractions, maintaining a positive charge on their surface. This facilitates to stablish contact with the cell surface and to produce transfection [50]. Once inside, the genetic material is released, expressing itself in the target cell with good results *in vitro* and *in vivo* [50]. These vectors are also very interesting since they can act at the post-transcriptional level carrying siRNA, by which it is achieved the gene silencing. They are very interesting, for example, in the treatment of cancers [50], especially considering that these vectors can be designed to achieve a gene therapy directed to a particular area [50].

Among the polysaccharides, the most investigated for the preparation of non-viral vectors are CS and HA, but other polysaccharides should also be mentioned briefly, such as: alginate, glycosaminoglycans (chondroitin sulfate and heparin), dextran, pullulan and schizophyllan.

1.4.1. Chitosan

CS is obtained from chitin, a natural homopolymer that is made of N-acetyl-D-glucosamine residues linked by β-1,4 bonds (Figure 3). Chitin is found in the exoskeletons of crustaceans, mollusks and insects, but also in the cell wall of mycelial fungi [51], with varied molecular weights (< 100 KDa to > 300 KDa) [52]. By partial deacetylation of chitin, CS is obtained that is a polysaccharide made up of N-acetyl-D-glucosamine and β-D-glucosamine units linked by β-1,4 bonds [51, 53-55].

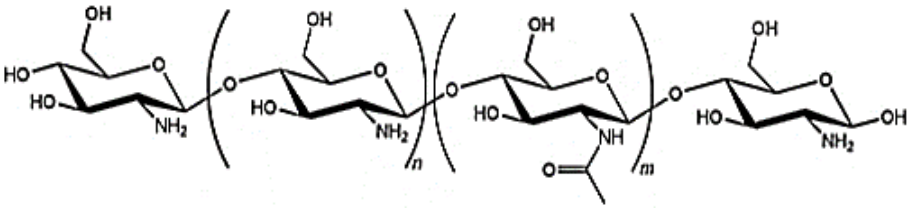

Figure 3. Basic structure of the CS polysaccharide. (Figure adapted from the work of Rodrigues et al. [56], J. Funct. Biomater. 3 (2012) 615–641. Open access article distributed under the Creative Commons Attribution License)

CS is non-toxic, biocompatible and biodegradable [54]. It has the ability to modify the inflammatory response and it is useful for tissue healing after wounds formation, thanks to the increase of the activity of neutrophils, macrophages and fibroblasts [57]. Besides, it is even capable of increasing the tissue repair through the use of CS-based nanocarriers loaded with growth factors (FGF, EGF), achieving more focused and prolonged effects [58]. CS has antiviral, antimicrobial, antitumor and hemostatic properties; and it is an adjuvant of the immune system [54,59]. In addition, CS can act as antioxidant and chelating agent (of magnesium, copper and iron) [57,60]. It is mucoadhesive, increases the concentration of the AIs at the site of action and enhances the absorption of hydrophilic molecules through epithelia (intestinal, nasal, etc.) [59]. Finally, the CS in the body is hydrolyzed by microorganisms of the intestine and lysozymes, being degraded to N-acetylglucosamine [52,58]. In this way, CS is

eliminated from the human body without accumulating, even if it is administered over a long period of time [54,59].

An important utility of CS-based nanocarriers is that can easily achieve their site of action, reducing side effects [59]. As example, the effect of estradiol used for Alzheimer's disease can be transported in CS NPs by the nasal route. It was shown that the residence time of estradiol in the area was increased, which facilitated its capture by olfactory neuronal cells and reach the brain, increasing its amount in the central nervous system [59]. In addition, CS-based nanosystems conjugated with other molecules (like PEG) achieve a delay in the clearance of the reticuloendothelial system (RES), with which they can spend a longer time of circulation in the bloodstream, allow more interactions with and cross the cell membranes, as well as traverse the intercellular spaces [59]. Moreover, it is important to note that, once the CS vehicle loaded with genetic material is into an endosome, the called "proton sponge effect" occurs. This consists in that the amino groups of the CS capture the protons of the endosomal space, in such a way that the proton pumps introduce more protons into the endosome and, consequently, chloride ions and water. All this leads to the swelling of the endosome causing its rupture and the release of the genetic material to the cellular cytoplasm [61].

The first study in that CS was used as vector of genetic material was in 1995 to carry pDNA; while, since 2006, it has been also employed to deliver siRNA intended to gene silencing [62]. CS owes its ability of bind genetic material to the protonation of amine groups at acidic pH, which gives it positive charge and, therefore, the possibility of establishing electrostatic interactions with the negatively charged nucleic acids [62]. For all the aforementioned, CS is an interesting polysaccharide for the preparation of non-viral vectors of great utility in gene therapy.

1.4.1.1. CS physicochemical properties

To achieve a successful gene transfection, it is important to put attention to some CS physicochemical properties:

a) Degree of deacetylation (DD). It determines the amount of primary amines that has the CS. It can also be expressed inversely, as degree of acetylation (DA). DD influences the CS solubility, the nucleic acid binding sites, the cell uptake capacity and, therefore, its transfection capacity. The higher is the DD, the more positively charged has the CS and the stronger are the electrostatic bonds with the genetic material. In addition, the nanosystems prepared with the CS of higher DD will have more capacity to be released from lysosomes or endosomes, improving the transfection [62,63]. The optimal degree of deacetylation to compact pDNA should be higher than 65% and to compact siRNA, above 80% [64].

b) Molecular weight. It is determined by the extension of the CS chain and influences, in turn, the size of the NPs. For example, the CS of 20 kDa corresponds to NPs of 200 nm, while CS of 80 kDa, to NPs of 300 nm [65]. However, the size can also vary depending on the transported genetic material. In addition, it is important to highlight that the molecular weight of CS determines the stability of the loaded genetic material. In this sense, usually it is more protected from degradation with CS of higher molecular weight; but, on the contrary, it is more difficult to release the DNA/RNA by the strong electrostatic binding [64]. For this reason, is so essential to choose very well a CS of suitable molecular weight to prepare the nanocarriers [64,65].

1.4.1.2. Preparation techniques of CS-based nanocarriers for gene delivery.

The techniques most used for the preparation of nanocarriers (Figure 4) are listed below:

a) Complexation of polyelectrolytes. Polyplexes, also called polyelectrolytes complexes, are formed upon mixing solutions of CS with solutions of genetic material in appropriated concentrations as consequence of electrostatic interactions between the polysaccharide and the genetic material [64,66]. It is very important the CS amino groups/Genetic material phosphate groups ratio (N/P ratio) because determines the proportion between the amount of CS and of genetic material that conforms the polyplexe. If the ratio is less than 1, it means that the proportion of nucleic acid is greater than of CS, producing a large and unstable polyplexe of poor complexation level. When the ratio is greater than 1 means that there is more proportion of CS, resulting in a stable polyplexe. If this ratio is very large, an enormous stability would be produced, which would hinder the transfer of genetic material to the cell and, therefore, the transfection. Therefore, within stable limits, the positive polyplexe interacts adequately with the cell surface, promoting the uptake, favoring the "proton sponge effect" and releasing the genetic material.

b) Ionic gelation. It is a process to prepare nanosystems by the electrostatic union of a potitively charged polymer (like CS) and a negatively charged crosslinking agent (such as tripolyphosphate, TPP). This carrier can release genetic material in the cell for a longer time. Furthermore, in these systems the co-loading of molecules that favor the cellular internalization and the tracing of the released DNA/RNA can be carried out [64,67].

c) Adsorption. It consists in the electrostatic binding of genetic material (negatively charged) to the surface of previously formed CS-based nanocarriers (positively charged) [62].

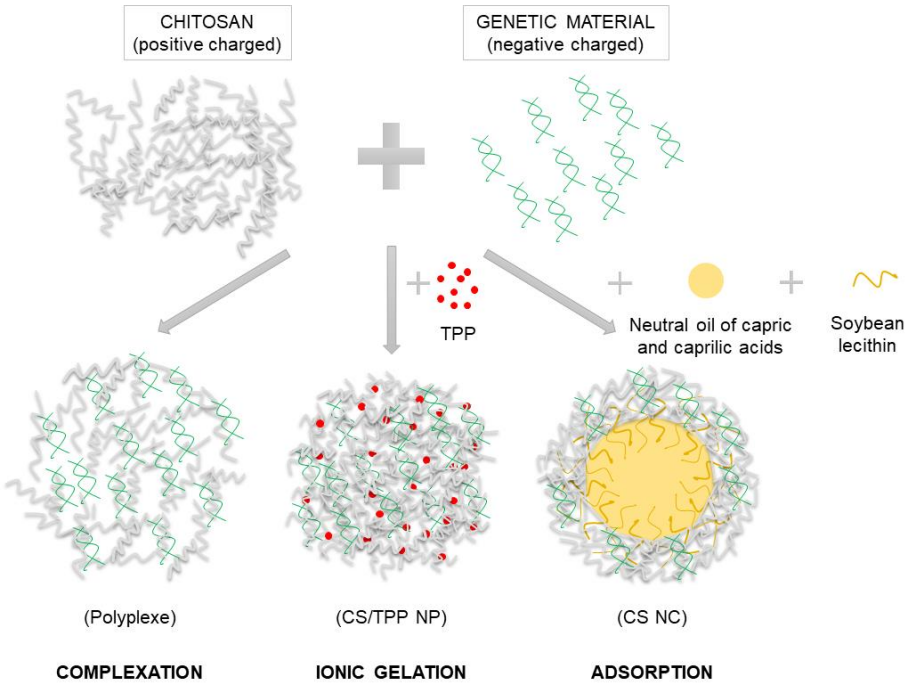

Figure 4. Scheme of preparation techniques of CS-based nanosystems. (New creation figure)

1.4.1.3. Interest of CS derivatives

Although CS has valuable characteristics for its use in non-viral vectors, certain modifications of the hydroxyl and amino groups produce CS derivatives with improved properties to prepare this type of nanocarriers [54,61]. Among the characteristics that can be improved are: the CS solubility, the tracking of the CS-based nanosystems, the specificity of action, the CS-based nanosystems absorption, and the transfection capacity [55].

1.4.1.4. Modulation of CS solubility

CS is soluble at a pH below 6.5, while its solubility is compromised at a basic or neutral pH (like physiological pH) [61]. The solubility of the CS can be increased using several methods:

a) CS chain breaking, by enzymatic or acidic hydrolysis, or even by redox reactions. Thereby, CS of lower molecular weight is produced with a higher amount of amino groups, which allows a better interaction with the water, improving the solubility [61].

b) CS chain modification, with certain molecular structures that make it solubilize at an alkaline pH [61]. Three examples of derivatives can be highlighted:

b.1) PEGylated CS. The addition of polyethylene glycol (PEG) to CS promotes its solubility at different pHs. PEGylated CS-based nanosystems have a higher half-life in blood and internalize worse in cells. Therefore, they accumulate worse in tumor cells and certain amount of therapeutic genetic material is lost. This situation can be resolved by incorporating a targeting ligand in the nanostructure, like folic acid [61].

b.2) Carboxymethylchitosan (CMC). It is an amphoteric derivative. For one side, the added carboxyl groups (pKa of 4.5) deprotonate at physiological pH, giving negative charge to the molecule and allowing it to be soluble. On the other hand, amino groups protonate in an acidic environment, like in tumor areas, producing positive charge to the molecule. For this reason, this derivative is of special interest for the preparation of pH-dependent non-viral vectors [61].

b.3) N,N,N-Trimethylchitosan (TMC). TMC is a derivative that is more soluble with a 40% of quaternization. This derivative can be further modified to increase the transfection capacity, as in the case of trimethylchitosan-cysteine modified with mannose for the

administration of siRNA, of alpha tumor necrosis factor (TNF-alpha) that showed higher silencing with respect to other vehicles, such as Lipofectamine 2000 [61].

1.4.1.5. Tracking capacity of CS-based nanosystems

The ability of track CS-based non-viral vectors and checking their interaction with tissues or target sites can be verified, thanks to the addition of organic colorants to the CS structure. As example, fluorescein isothyocianate (FITC) can be covalently bound to amines groups of the CS. This colorant does not affect the cellular uptake capacity of the obtained nanosystems, but it allows their monitorization using techniques, such as flow cytometry [59].

1.4.1.6. Improvement of the specificity of action of CS-based nanosystems

The incorporation of ligands to target CS-based nanosystems improves the recognition by cells, increasing the endocytosis [61]. Some examples of ligands are as follows:

a) Folic acid. It is very interesting to achieve the uptake by tumor cells, such as lung cancer cells because overexpress alpha folate receptors. It can be used for the treatment of various lung cancers, such as bronchioalveolar carcinoma, adenocarcinoma and large cells carcinoma [45].

b) Transferrin. It is a glycoprotein that controls the process of cell growth, as well as the uptake of iron. Pulmonary adenocarcinoma cells, as well as squamous carcinoma cells overexpress transferrin recognition receptors. Therefore, this ligand is useful to target the CS nanosystem to these cells [45].

c) Anti-EGFR Antibodies. EGRF is the epidermal growth factor receptor and participates in the cell proliferation, being overexpressed in malignant neoplastic cells. In addition, a higher proportion of the

receptor is associated with greater resistance to chemotherapy, producing more mortality in the patients. Hence, the incorporation of anti-EGFR antibodies in CS-based nanosystems promote uptake in these cells, showing great promise for the treatment of cancer, like in lung cancer [45].

d) Galactose. It has been shown that Galactose increases the CS-based nanosystems specificity of low molecular weight to the liver cells in both *in vitro* and *in vivo* studies, using as model liver parenchymal cells [59,68].

The following table (Table 2) summarizes examples of ligands used in CS-based vehicles, emphasizing their resulting complexes, the employed genetic material and their results.

Table 2. Examples of ligands used in CS-based vehicles.

Ligand	Resulting complex	Genetic material	Results	Reference
Folic Acid	Complexes of CS/PEI modified with folate	ARNhc AKt1	Good *in vitro* gene silencing in A549 cells. Good *in vivo* suppression of tumorigenesis in mice.	[68]
Transferrin	CS NPs complexed with transferrin	Model gene	Better *in vitro* transfection efficiency for the CS NPs with transferrin in HEK293 and HeLa cells compared to the systems without transferrin.	[68]
Anti-EGFR	CS NPs linked with anti-EGFR	siRNA Mad 2 co-administered with cisplatin	Low toxicity in normal tissues and good tumor suppression in cisplatin-resistant pulmonary tumors.	[45]
Galactose	CS/galactosylated complexes	Model gene	Good transfection in HepG2 cells, but not in HeLa cells.	[68]

1.4.2. Hyaluronic acid

HA, also called hyaluronate, is a natural polysaccharide, from the group of the glycosaminoglycans [48], whose molecular structure is made up of units of N-acetyl-D-glucosamine (β (1,3) bonds) and D-glucuronic acid (β (1,4) junctions) (Figure 5) [48,69]. It is found naturally in the umbilical cord and in the vitreous humor, but mainly in cartilage and in the synovial fluid [48,69].

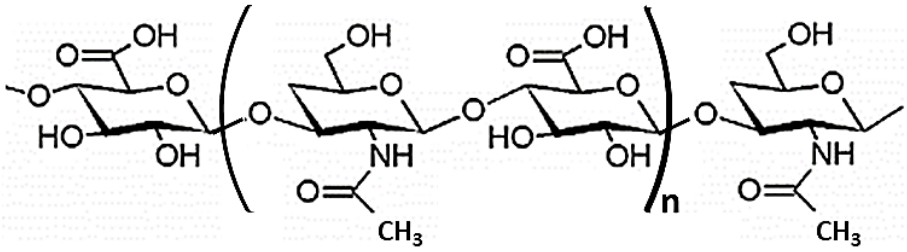

Figure 5. Basic structure of the HA polysaccharide. (Figure adapted from the work of Huang et al. [70], Drug Deliv. 25 (2018), 766–772. Open access article distributed under the terms of the Creative Commons CC BY License)

HA has attractive properties, such as high biocompatibility, low toxicity and biodegradability, which has been useful for different applications [48]. More popularly, it is known for its cosmetic use as a wrinkle corrector [69], but it is also important in the manufacture of medical materials, such as implants that are in contact with blood due to its antiplatelet activity [69] or in the preparation of sponges and dressings, useful in osteoarthritis by improving joint lubrication [48,69] and in ocular surgery [48]. In fact, sponges prepared with CS, HA and nanosilver have been shown to have good antimicrobial activity and decrease the chances of infection, creating an optimal moist environment for healing [69]. HA has been used in the pharmaceutical industry as vehicle for the administration of imaging agents and drugs, thanks to its good biological properties [71]. Specifically, the nanosystem consisting in cholanic acid and HA has proven to be useful in the image-mediated administration of anticancer drugs [71].

HA is very interesting in the coating of nanocarriers in gene therapy [49], being very noteworthy its combination in CS-based NPs, for example, in ocular gene therapy for the release the genetic material in the cornea [49]. HA has anionic charge and does not establish electrostatic bonds with the genetic material. Therefore, the genetic material is able to stablish electrostatic bindings with cationic polymers [71]. In addition, HA has affinity for the CD44 receptor, which is present in high quantity in tumoral cells. Therefore, HA has a great potential for targeting to tumoral cells [48].

1.4.2.1. HA physicochemical properties

HA can be found in a number of molecular weights (from 20 kDa to 4000 kDa), is highly hydrophilic and negatively charged at physiological pH (pKa: 3-4) [71]. It produces very viscous and elastic solutions [71]. All these properties are important for its use in the preparation of surgical devices [69]. Its structure can be modified to achieve medical and therapeutic benefits [71]; and is degradated by the hyaluronidase enzyme [69].

1.4.2.2. Interest of HA derivatives

It is interesting to obtain derivatives of low molecular weight, by the use of ozone in the original polysaccharide. These derivatives have a molecular weight between 45.2 - 145 kDa, with good antioxidant activity and are useful for wounds healing [69]. Furthermore, HA can be incorporated in nanosystems to transport genetic material with a improve of the transfection capacity.

1.4.2.3. Affinity of HA for the CD44 receptor

As HA has high affinity for the CD44 cell receptor, it is used as targeting ligand towards tumor cells [72-74]. Thus, cytotoxicity problems related to the administration of chemotherapy drugs by systemic route are avoided, such as cardiotoxicity, damage to the immune system and bone marrow, hair loss, etc. [72]. For other hand,

CD44 receptor is a set of transmembrane glycoproteins that present different isoforms [73]. Structurally, it has three domains, the intracellular domain and the transmembrane domain, being common to all variants. Only the extracellular domain or ectodomain is different from one isoform to another [73]. Under healthy conditions, the normal isoform (CD44s) is expressed; while under pathological conditions, variant isoforms (CD44v) are overexpressed in tumor cells [73]. Thanks to the affinity of HA for the CD44 receptor, as well as its utility in nanotechnology, specific and efficient non-viral vectors have been designed employing HA aimed to bind CD44 receptors of tumoral cells [74]. Two strategies were used:

a) Modification of nanosystems with HA, of great value to target nanocarriers to cancer cells. This is the example of doxorubicin-loaded liposomes linked to HA-derived phosphotidylethanolamine (HA-PE), which were efficiently taken up by murine melanoma cells B16F10 [74].

b) Self-assembled HA NPs. They can be prepared in two ways, either by hydrophobic interactions of HA hydrophobic areas in aqueous medium, or by the electrostatic conjugation due to its structural groups. The resulting nanocarriers (positively charged) electrostatically binds genetic material (negatively charged). It can be mentioned for example NPs prepared with polyethyleneimine (PEI), polyethylene glycol (PEG) and HA (HA-PEI/PEG). This type of nanocarrier transported SSB/PLK1 siRNA and was tested in A549 cells (of lung adenocarcinoma), resulting in good gene silencing due to its high cellular transfection [74].

The following table (Table 3) summarizes examples of CS and/or HA-based nanosystems, emphasizing the employed genetic material and their results:

Table 3. Examples of CS and/or HA-based nanosystems employed in gene therapy.

Nanosystem	Genetic material	Results	Reference
CS/TPP NPs	pCMV-Gal plasmid	High levels of expression in HEK293 cells and *in* vivo in mice.	[75]
Pegylated diethylaminoethyl-CS NPs	siRNA-SSB	NPs fulfill the existing ISO (International Organization for Standardization), ASTM (American Society for Testing and Materials) and NCL (Nanotechnology Characterization Laboratory) guidelines' threshold criteria. Low toxicity in murine Raw 264.7 macrophages, human MG-63 cells and human peripheral blood mononuclear cells (PBMC). Blood biocompatibility. High *in vitro* transfection efficiency.	[76]
CS-based polyelectrolyte NPs	Human SET1 antisense (hSET1, 17mer DNA-base oligonucleotide)	No toxicity in the MCF7 cell line. High transfection (>90%) in tumor cells. Low accumulation in heart, liver and lungs.	[77]

Table 3 (continuation 1). Examples of CS and/or HA-based nanosystems employed in gene therapy.

Nanosystem	Genetic material	Results	Reference
CS polyplexes substituted by the trisaccharide GlcNAc-GlcNAc-2,5 anhydroMan (A-A-M)	Fluorescein isothiocyanate (FITC)-labeled pDNA	Higher plasmid delivery efficiency than linear CS polyplexes in HEK293 cells. Ten times more transfection efficiency than PEIs in human bronchial epithelial cells. Good levels of gene expression *in vivo*.	[49]
Lipid coated CS-DNA NPs	pCMV-GFP plasmid	They show higher transfection *in vitro* than PEI in HEK 293 cell line.	[78]
Self-assembled NPs of poly(ethylene glycol) and HA	pGL3	Negligible cytotoxicity in HeLa and A549 lung cells. High gene expression in HeLa and A549 cell lines.	[79]

Table 3 (continuation 2). Examples of CS and/or HA-based nanosystems employed in gene therapy.

Nanosystem	Genetic material	Results	Reference
SLNs of protamine and HA	pCMS-EGFP plasmid	Transfection versatility in cells with different division rates: ARPE-19 and HEK-293. Transfection increased, by almost seven times, in ARPE-19 cells compared to the same systems without HA.	[80]
Polyplexes DNA/PEI coated of reduced HA	DNA	Low cytotoxicity and high attraction for carcinoma HA receptors, with high transfection efficiency.	[69]
Graft copolymer of pDMAEMA and HA modified with 2-(2-pyridyldithio) ethylamine hydrochloride	siRNA	Greater stability thanks to HA, which protects circulating siRNA. Affinity towards CD44 receptors in cancer tissue and good gene release, resulting in good gene silencing.	[71]

Table 3 (continuation 3). Examples of CS and/or HA-based nanosystems employed in gene therapy.

Nanosystem	Genetic material	Results	Reference
Layer-by-layer assembled AuNCs/PEI/miRNA/HA nanocomplexes	miRNA	Efficient miRNA delivery to liver tumor cells. Good antitumor effect combined with photothermal therapy in liver carcinoma.	[81]
Oleoyl-carboxymethyl-chitosan NPs (OCMCS) modified with HA	Aeromonas hydrophila aerolysin gene	Great DNA permeability and transfection in Caco-2 cells.	[49]

Table 3 (continuation 4). Examples of CS and/or HA-based nanosystems employed in gene therapy.

Nanosystem	Genetic material	Results	Reference
CS/HA/TPP NPs	siRNA	Increased interaction with the CD44 receptor thanks to the HA and great plasmid release (by weakening of the CS-siRNA binding). High gene silencing in A549-Luc cells.	[82]
	pEGFP plasmid	High transfection efficiency in human conjunctival and corneal cells.	[83]
	MiR-34a gene silencer of the anticancer resistance gene (Bcl-2) and DOX	High transfection efficiency in MDA-MB-231 cells and good *in vivo* antineoplastic effect in SCC7 tumor bearing mice.	[71]
PEGylated CS/HA/TPP NPs	siRNA	Stable intravenously. Successful silencing in B16F10 cells.	[71]

Table 3 (continuation 5). Examples of CS and/or HA-based nanosystems employed in gene therapy.

Nanosystem	Genetic material	Results	Reference
Hyaluronate-N,N,N-trimethyl CS NPs	IL-6- and STAT3-specific small interfering RNAs (siRNAs)	Low toxicity. High transfection efficiency in 4T1 (breast cancer), CT26 (colorectal), and B16-F10 (melanoma) cell lines. Controlled release of siRNA. High silencing of IL-6 and STAT3, blocking of the cell proliferation and of the angiogenesis in the tested cell lines.	[84]

1.4.3. Alginate

Alginate or alginic acid is a natural polysaccharide, hydrophilic, of low toxicity, with mucoadhesive and chelating properties, which allows the expulsion of harmful heavy metals [48-50]. Its structure is a linear chain made up of D-mannuronic acid monosaccharides linked to α-L-glucuronic acid residues, through β-1,4 bonds [49]. It is attractive as adjuvant of antibiotic drugs in CF against Pseudomonas aeruginosa [49,50]. Furthermore, as it is pH dependent, it is interesting for the oral administration of drugs [48]. For this reason, it has been used for the design of prolonged-release pharmaceutical forms of, for example, vascular endothelial growth factor (VEGF) [48]. Additionally, alginate NPs were studied for gene therapy, showing a transfection efficiency of 60% for those loaded with pDNA [48].

1.4.4. Glycosaminoglycans

The most important are the chondroitin sulfate and heparin [50].

1.4.4.1. Chondroitin sulfate

Chondroitin sulfate or sulfate of chondroitin is a natural polysaccharide present in mammalian tissues like skin, cartilage and blood vessels. [85]. It is biocompatible and biodegradable, has very low toxicity, is anti-inflammatory, anticoagulant and antithrombotic [85]. Structurally, it is made up of N-acetyl-glucosamine units (β-1,3 bonds) and D-glucuronic acid units (β-1,4 bonds) sulphated in different position [85]. This polysaccharide it is subclassified in four groups: A (chondroitin-4-sulfate), C (chondroitin-6-sulfate), D (chondroitin-2,6-sulfate) and E (chondroitin-4,6-sulfate). Chondroitin sulfate is a very useful biomaterial for the preparation and, specifically, for the modification of non-viral vectors. In fact, the addition of this polysaccharide to cationic polyplexes increases their specificity, decreasing the interactions with serum compounds that cause immunogenic problems, although these are always lower than in the case of viral vectors. Therefore, it improves the safety, at the same

time that gives rise to a better transfection of the nanosystems [85]. This adjuvant effect is higher in the case of tumor cells because chondroitin sulfate has affinity for CD44 receptors, overexpressed in these cells [50,85]. Indeed, nanosystems composed of PEI and a variety of chondroitin sulfate have been formulated for gene therapy in tumors [85, 86].

1.4.4.2. Heparin

It is a polysaccharide of high negative charge with important antiangiogenic, anti-inflammatory and anticoagulant properties. Its structure is made up of alternate units of glucosamine and glucuronic acid or iduronic acid (α-1,4 glycosidic bonds). Heparin is interesting to treat different diseases, but in gene therapy it must be chemically modified to avoid bleeding derived from the prolonged use over time [49]. This is the case of heparin-modified PEI and pDNA complexes (Hep/PEI/DNA complexes) that exhibited high transgene expression levels and low cytotoxicity in HeLa and 293T cells [49].

1.4.5. Dextran

It is a natural polysaccharide, soluble in water, chemically versatile composed of repetitive α-1,6 glycosidic bonds with branched chains of α-1,3 bonds [48,49]. In the pharmaceutical industry it has been used in the preparation of prodrugs (such as paclitaxel-carboxymethyl dextran, improving the treatment of colorectal carcinoma) [48]. In addition, it has been used as cholesterol reducer and as plasma expander [49,50]. In gene therapy, cationic dextran is important for the construction of non-viral vectors because they have low toxicity and can efficiently carry nucleic acids [49,50]. As example, cationized dextran/NK4 plasmid DNA complexes modified with PEG was used to transfect mouse Lewis lung carcinoma cells [87].

1.4.6. Pullulan

It is a polysaccharide with low toxicity, good adhesiveness and linear structure, composed of maltrose units linked by two glucosidic type bonds: α-1,4 and α-1,6 [49]. It is useful in the administration of drugs because it is capable of forming colloidal NPs [49,50], being also considered for the preparation of non-viral vectors for the transport and delivery of pDNA in *in vitro* and *in vivo* studies [48,50]. Taking into account that pullulan has high affinity by asialoglycoprotein receptors in the liver, the PEI-pullulan/siRNA complexes showed an excellent targeting to the liver with great results of transfection [48].

1.4.7. Schizophyllan

It is a hydrophilic polysaccharide, with 1,3-β-glucan structure and branches in β-1,6 of D-glucopyranosyl [50,88] that, in aqueous medium, adopts a triple helix conformation and can be modified to a single chain conformation if the pH is changed to basic or if the temperature is raised [88]. In turn, it can return to its original shape and load drugs into its interior cavity, generating circular, collapsed balloon or hairpin structures, among others. Although it is used in the cosmetic field, it stands out for its anticancer and immunomodulatory characteristics [88], being used in gene therapy for the transfection of antisense oligonucleotides in melanoma and leukemia [50]. Its internal cavity is flexible and adaptable, so it can accommodate the genetic material [88], being a good candidate to prepare non-viral vector.

Therefore, non-viral vectors based on polysaccharides are promising for treating numerous diseases using gene therapy. Specifically, there are serious lung diseases of genetic origin (such as some types of lung cancer) that are not well resolved therapeutically. For that, it is very interesting the use of new, more direct and effective trategies to resolve them. In that sense, gene therapy administered by the pulmonary route is very promising, taking into account that can be achieved better results, while reducing the side effects associated to the conventional oral/parenteral treatments.

1.5. Lung gene therapy

Initially, it is important to know the structure of the respiratory tract and its functionality in order to later understand how AIs reach the lung desired area. In addition, it is necessary to know the advantages, but also the disadvantages of the pulmonary route, as well as the defense mechanisms of the lung to determine the possibilities of a pulmonary gene therapy. Finally, lung diseases candidates to be treated by gene therapy will be analyzed.

1.5.1. Anatomical features and functionality of the respiratory tree

The respiratory tree is responsible of the gases exchange that, together with the cardiovascular system, is capable of transporting oxygen from the outside to all the organism cells, as well as of the expulsion of carbon dioxide [89,90]. Specifically, the lungs have very special anatomical-physiological characteristics to perform the gases exchange. Firstly, it is essential to know that the lungs are connected to the outside by canals that are dichotomously divided into narrower conduits, as they deepen into this organ. That lets to the lung gain in gas exchange surface and, as we will see later, in absorption surface [91].

Regarding the anatomy, the respiratory system is made up of upper tract (mouth, nasal cavity, pharynx and larynx) and lower tract (trachea, bronchi, primary bronchioles, terminal bronchioles and alveolar area) [92]. This latter is functionally subdivided in conduction zone (trachea, bronchi, primary bronchioles) and respiratory zone (terminal bronchioles, alveolar ducts and alveolar sacs (about 120 m^2)). The conduction zone filters, heats and humidifies the air that enters the lungs, while the respiratory zone deals with the gas exchange [93].

The airways are lined with epithelial tissue, which varies depending on the area. Specifically, as it approaches the alveolar area, the epithelial tissue becomes less thick and more permeable [94]. At the cellular level, in the upper respiratory tract, there are basal, ciliated and goblet cells (responsible for the secretion of mucus), forming a cylindrical pseudostratified epithelium; while in the bronchioles there

are mainly ciliated cells and Clara´s cells forming a simple cylindrical epithelium. By the contrary, goblet cells are already unusual [94]. At the level of the respiratory bronchioles (the most distant part of the bronchioles), non-ciliated cells abound, such as Clara's cells, and cells that are more typical of the alveolar area appear leading to gases exchange [94]. The alveolar zone is composed of epithelial cells of the type I (pneumocytes I) and epithelial cells of the type II (pneumocytes II), constituting a simple epithelium. Pneumocytes I are the majority cells of the alveolar epithelium. They are flat and through them the gas exchange is established. On the other hand, pneumocytes II are a minority and their shape varies between spherical and cubic. They are precursors of the pneumocytes I and are dedicated to secreting pulmonary surfactant, very important in the coating of pneumocytes for the reduction of the alveolar surface tension [95].

1.5.2. Deposit of inhaled particles in the respiratory tract

By the use of an inhalation device, aerosolized AIs can be introduced into the respiratory tract. An aerosol is a biphasic system of solid or liquid particles dispersed in a gaseous phase that must be stable [93].

To achieve therapeutic success, it is necessary to take into account that both the specific area of action, as well as the dose of AI that can reach that area [96]. Furthermore, it is very important to take into consideration that, depending on the pulmonary zone where the particle are deposited, one effect or another is achieved. Namely, to achieve a systemic effect, the AIs must reach the alveoli where they are absorbed, reaching the circulatory system; while if a local effect is required, it is recommended a deposit in the target area (bronchi and bronchioles) [96]. As example, it can be mentioned salbutamol, which acts on the epithelium between the primary bronchi and terminal bronchioles, activating the β2 adrenergic receptors [97]. In addition, it must be taking into account the physical and aerodynamic characteristics of the inhaled particles because significantly influence the lung deposit region. These properties are the size, density, hygroscopicity and electric charge of the particles. Specifically, the most influential factor is the aerodynamic diameter (D_{aer}) that is

defined as the diameter of a sphere of unit density with the same terminal settlement velocity as the particle under consideration [98]. It is calculated as follows:

$$D_{aer} = D_g \sqrt{\frac{\rho_{real}}{\rho_0 \lambda}} \quad (1)$$

where: Dg: geometric diameter (μm), ρ_{real}: real density of MS (g/cm^3), ρ_0 = 1 g/cm^3 and λ: MS dynamic shape factor (spherical MS: λ = 1; irregular MS: λ = 2) [99].

There are three types of mechanisms by which inhaled particles are deposited in the lungs, depending on their size. These mechanisms are impact, sedimentation, and diffusion (Figure 6).

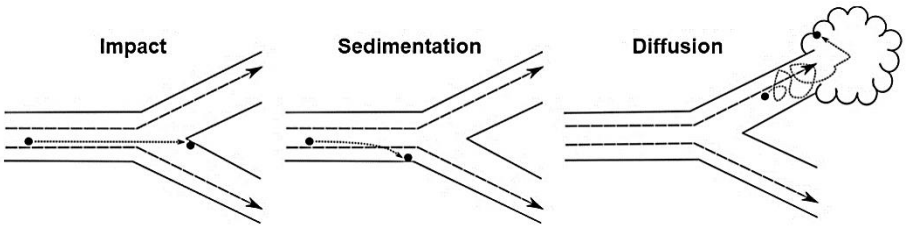

Figure 6. Deposition mechanisms of inhaled particles in the respiratory tract. (Figure adapted from the work of Sou et al. [100], J. Pharm. Sci. (Philadelphia, PA, United States) 110 (2021) 66–86. Open Access)

When the particles are inhaled, they enter quickly and turbulently in the respiratory tract. The larger ones impact and are retained in the upper section, basically because it is difficult for them to follow the curvilinear trajectories of the respiratory passages. In fact, those of size higher than 10 μm are located in the oropharyngeal area, and those of 5-10 μm, in the trachea and bronchi. Particles with a size between 1-5 μm are deposited in deeper airways (of smaller diameter) and in alveoli. In these regions, the particles move through a slow and laminar flow, remaining long enough time in the respiratory tract to be affected by gravity and, then, they sediment [101]. In effect, it has

been found that 80% of the particles with a size smaller than 3 μm have deposited in the alveoli. The smallest (< 1μm) present erratic movements (Brownian movements) that make difficult their deposit and they are usually eliminated in suspension from the body by exhalation [101]. In summary, the particles must have an aerodynamic size of less than 5 μm to ensure that they reach the lower respiratory tract. If their sizes are between 3-5 μm, they will achieve a local effect at the level of the bronchi and bronchioles. If their sizes are between 1-3 μm, a systemic effect will be achieved following their arrival at the alveoli.

In any case, the particles size may be increased and the density decreased by the effect of the environmental humidity of the respiratory tract, slightly varying the initial deposit pattern. This occurs because there are a relative humidity of the respiratory tract of 99.5%, a temperature of 37 ºC and a possible hygroscopic nature of the particles [102]. Furthermore, the size growth depends on its intrinsic properties, its initial size and the environmental characteristics of the respiratory tree [101].

The surface charge is the last of the factors that determines the deposit of the inhaled particles. Indeed, positively charged particles are able to bind better to the respiratory tract than the less charged particles. This is due to the electrostatic interactions that are established between the negative charges of the mucosa mucins with the positive charges of the surface of the systems [101].

There are other physiological and pathological factors (different from one person to another) that also affect the deposit of particles in the lung. These are the respiratory rate, the tidal volume, the diameter of the respiratory airways, the amount of mucus produced by the patient and the diseases that diminish the diameter of the respiratory conducts.

The tidal volume is the inspired/expired air volume during a normal respiration. The respiratory rate is the number of times that it breathed during 1 minute [103]. The higher is the tidal volume, the better is the therapeutic effectiveness of the inhaled aerosol because it reaches deeper and distal areas. The inspiratory flow is the volume of air that is inspired per minute (L/min) and is conditioned by the two

parameters mentioned above. If it is high, it is produced a greater retention of particles in the upper respiratory tract by impact; while if it is low, the particles can sediment in deeper areas. In fact, the most suitable inspiratory flow values are between 30-60 L/min. With a deep and homogeneous inspiration, followed by apnea (approx. 10 s), it is promoted the particles sedimentation in the lower tract of the respiratory tree [104]. Besides, it must be taken into account that, when the diameters of the respiratory ducts are decreased (such as in the natural physiological case of pediatric patients or in the case of obstructive pathologies), the impact of particles is greater, increasing their deposit [105].

1.5.3. Advantages and disadvantages of the pulmonary route

Pulmonary route has the following advantages: non-invasive route, accessibility of the airways (which allows the direct administration to the pulmonary surface), large surface (over 120 m^2), extremely thin alveolar epithelium, great vascularization (which led to high and fast absorption), and allows treatments with diminished doses and side effects (with respect to other routes, such as the oral or parenteral) [106-109]. Taking into account that there are several pulmonary diseases that can be efficiently treated by gene therapy, the inhalation route is appropriate because avoids certain problems associated to the parenteral via, such as the presence of a high concentration of enzymes, the interaction with serum proteins or the necessity of cross endothelial barriers [106]. For all the aforementioned advantages, the pulmonary route stands out for the treatment of genetic lung diseases.

However, it is important to consider the main disadvantages of the pulmonary route, which are the obstacles that the particles must overcome to reach the target lung site [110]. The respiratory tree has its own defense mechanisms that help it to eliminate microorganisms and undesirable particles to the outside. These mechanisms are beneficial to maintain the proper pulmonary function, but are also obstacles to take into account for that the therapeutic particles reach the mentioned lung desired area.

1.5.4. Defense mechanisms of the lung

There are different defense mechanisms that difficult the arrival of therapeutics genes to the lung cells (Figure 7):

1.5.4.1. Sneeze

Sneeze is one of the first defense mechanisms of the respiratory tract. When an irritant agent is inspired, it stimulates the sensory nerve endings of the trigeminal nerve (in the nose or oropharyngeal), generating a stimulus that is directed to the center of the sneeze (in the medulla of the brainstem). Then, several neurons are activated, such as the parasympathetic neuron, which innervate the tear glands and the motor neurons that supply the respiratory and facial muscles. With this mechanism, the respiratory system defends itself from harmful and irritating particles, but also from the formation of bacterial biofilms [111].

1.5.4.2. Cough

Cough is a reflex action that normally serves to unblock the airways. The process begins with the stimulation of certain receptors that are in areas such as the buccal cords, larynx, tracheal mucosa, bronchial mucosa and in the pleura. A signal is sent to the cough center (in the medulla oblongata) through certain nerves such as the trigeminal, vagus, glossopharyngeal or superior laryngeal. In the cough center, a response signal is elaborated and transferred by the efferent nerves, resulting in an inspiration, closure of the glottis with increased pulmonary pressure and subsequent abrupt opening of the glottis with a strong exhalation [111].

1.5.4.3. Structure of the respiratory tree

The particle that has avoided the sneeze and cough will be influenced by the next “defense mechanism”, the structure of the respiratory tree itself. In fact, it is physiologically designed to trap and

expel the foreign particles to the outside, achieving this purpose by the tortuous and increasingly narrow subdivided ducts. Afterwards, the particles can be eliminated by mechanisms that will be explained below, from top to bottom of the respiratory tree.

1.5.4.4. Mucociliary elevator

In the respiratory tract, from the top to the terminal bronchioles, there is a fluid at superficial level that is divided into two phases: the mucus (which is the closest layer to the lumen) and the periciliary fluid (which is below, in contact with the cells of the respiratory epithelium).

The mucus is a water-based fluid with viscoelastic properties, due to its high content of mucins, which serves as humectant and lubricant. Its secretion is produced mainly by goblet cells [112]. Mucus is where particles are deposited and retained after inhalation.

The periciliary fluid is a film of low-viscosity that is located above the respiratory epithelium. The goblet cells produce the secretions of this fluid, while the ciliated cells move the superficial fluid outwards [112,113]. Periciliary fluid film contains electrolytes (such as bicarbonate, chlorine and sodium) [114,115] that make difficult the pass of particles [17].

The mucociliary elevator is the combination of the superficial fluid (mucus and periciliary fluid) together with the ciliary movement, constituting one of the most relevant lung protection mechanisms [112]. When particles have been inhaled and deposited in the bronchi and bronchioles, they are retained by the mucus layer. Subsequently, and thanks to the movement of the cilia in the periciliary fluid, the superficial fluid containing particles is moved towards the pharynx. Then, it can be expectorated outwards or it can be swallowed. Once in the gastrointestinal tract, many particles are eliminated by lysozymes, peroxidases and other enzymes, while the rest of particles are minimally absorbed and hardly exert a systemic therapeutic effect [112].

It is very important to take into account that the daily mucus clearance is of 1L under normal physiological conditions, but it can be

increased in certain diseases such as asthma or chronic obstructive pulmonary disease (COPD), even producing obstructions.

1.5.4.5. Macrophages

Macrophages are phagocytic cells (derived from monocytes) that play an important role in the homeostasis and conservation of the lung. They are dedicated to tissue remodeling and the defense of the organism from foreign particles through their phagocytosis [116-118]. Macrophages are the most important defense mechanism of the alveolar surface because there are no cilia that help to the expulsion of inhaled foreign particles.

Phagocytosis process increases when the particles have any of these characteristics [118,119]:

a) Size: 100-200 nm or 1-6 μm
b) Shape: spherical
c) Surface charge: high positive or negative charge
d) Composition: phosphatidylserine, phosphatidylglycerol, hyaluronic acid, etc.
e) Ligands: mannose, surfactant protein A and D, O-steroyl amylopectin, maleylated bovine serum albumin, tuftsin, etc.

Phagocytosed particles are eliminated through the lymphatic system or by taking them to the mucociliary elevator, thanks to which from the pharynx they will subsequently be swallowed or expectorated [118].

1.5.4.6. Enzymatic activity

The inhaled particles can suffer degradation by the enzymes present in the respiratory tree (lysozyme, protease inhibitors, isozymes of the cytochrome P-450 family…) [120]. Therefore, from a therapeutic point of view, the enzymes can reduce the pharmacological activity, decreasing the therapeutic effect. In any case, the pulmonary route is still very attractive because its enzymatic activity is lower compared to other routes, such as the oral [120].

1.5.4.7. Surfactant

Lung surfactant is located on the alveolar surface, preventing its collapse during respiration [121]. It is abundant in one phospholipid (dipalmitoylphosphatidylcholine) and four proteins (SP-A, SP-B, SP-C, and SP-D) [122]. Surfactant can affect the vectors used to transport AIs, so it must be taken into account when preparing pulmonary delivery systems [123-125].

1.5.4.8. Cell barriers

To achieve therapeutic success in gene therapy, the nanosystems must access inside cells. If the payload is RNA, it is enough its arrival to cytoplasmic level; while if it is DNA, it must access to the cell nucleus. Therefore, the nanosystems must be able to pass through the membranes. It is important to take into account that the airway tissue has tight junctions, as well as low endocytic activity, which oppose the passage of nanosystems into cells [126-128]. These obstacles are modified in certain pathologies. For example, the permeability is reduced in CF [129]; while it is increased in the case of asthma or chronic obstructive pulmonary disease (COPD) [130,131]. Fortunately, non-viral vectors are a good option to carry genetic material in the lung tissue because they can cross the tight junctions and achieve the target cells.

The pulmonary administration of free genetic material in suspension form leads to transfection problems [106]. As previously mentioned, in order to deliver genetic material, it is necessary the use of vectors to efficiently protect and transfect it in the respiratory cells. Therefore, the vectors must be carefully prepared to optimize the arrival of this genetic material to the desired area of the respiratory tract, taking into account the lung defense mechanisms and the pathophysiological conditions of the disease.

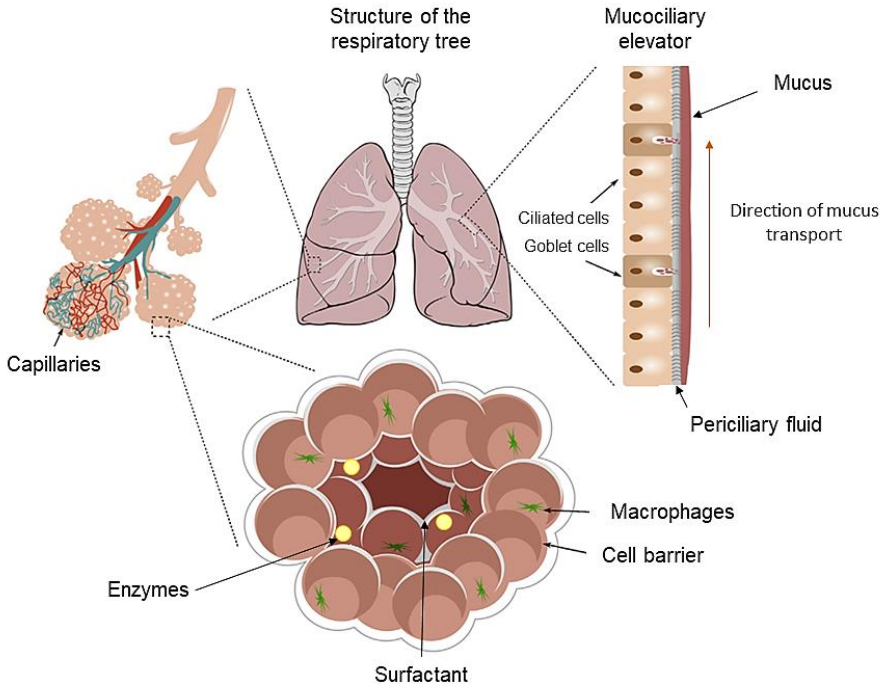

Figure 7. Illustration of different physiological barriers and defense mechanisms in the respiratory tract. (Figure adapted from the work of Sou et al. [100], J. Pharm. Sci. (Philadelphia, PA, United States) 110 (2021) 66–86. Open Access)

1.5.5. Lung diseases candidates for gene therapy

Some monogenic diseases (such as CF or AAT deficiency), or more complex diseases of polygenic origin (such as asthma, COPD or cancer, which require more sophisticated treatments), can be treated by gene therapy. It is very important to have in mind that these genetic diseases can alter the defense mechanisms of the respiratory tract, leading to a higher propensity to other lung diseases such as COVID-19 [132,133]. Next, three large groups of diseases treatable by gene therapy will be highlighted:

1.5.5.1. Infections

There is a global concern about the spread of lung infections. These can be subdivided into three groups:

a) Bacterial infections. Pulmonary pathogens are captured by alveolar macrophages. However, due to their biocidal mechanisms, they can proliferate uncontrollably causing serious respiratory problems [134]. One example is pneumonia, caused by fungi, viruses and, mainly, bacteria. In fact, bacterial pneumonia is the most common and one of the most infective, producing many resistances and making difficult its cure [135]. Among the pathogenic bacteria, it must be highlighted *Mycobacterium tuberculosis* (Mtb), which produces the tuberculosis disease, widely spread throughout the planet, generating a serious global public health problem and millions of deaths annually (around 1.5 million deaths/year) [136]. TB principally affects the respiratory tract, being the bacillus mainly located within the macrophages and is generally disseminated through sputum expelled in the environment [136]. There are also other very dangerous resistant bacteria, such as *Acinetobacter baumannii* (Abm). This bacterium poses a high risk to human health because it is associated with many diseases such as wound infections, pneumonia, sepsis and meningitis [137]. It is an opportunistic pathogen with great survival success due to its intrinsic genetic composition, as well as its rapid evolution by induced mutagenesis and horizontal gene transfer [138]. Abm is very persistent in hospital environments and easily causes outbreaks [137]. Taking into account the multi-resistance of Mtb and Abm, the development of new therapeutic strategies is crucial. The treatment of bacterial infections using gene silencing therapy is a less studied field compared to other diseases, such as cancer [134]. For example, the administration of siRNA has been studied using dimethylaminoethyl methacrylate NPs. These were able to enter into macrophages and demonstrated to be five times more effective against the pathogen gene, compared to the naked siRNA. In the case of Abm, the *in vitro* inhibition of aac(6')-Ib mRNA was studied. The expression of this mRNA produces the bacterial

resistance to antibiotics, like amikacin and other aminoglycosides. The administration of an antisense oligodeoxynucleotide (ODN4) specific for aac(6 ')-Ib mRNA inhibited its *in vitro* translation [139]. Polymeric NCs, such as CS-based NCs, arouse interest because they allow a combined administration of genetic material in their polymeric coat, and a lipophilic molecule in their core, either an antibiotic agent (rifabutin) or a cellular absorption promoter adjuvant (capsaicin) [140]. The use of cationic polymeric nanosystems has a growing interest in the treatment of infections, not only due to their biocompatibility and their better stabilization of the genetic material, but also because they allow to achieve a better cellular internalization, being very interesting in the case of infected macrophages. In addition, as CS acts like mediator of the immune response and presents antimicrobic effect, the use of CS-based nanosysems leads to an enhanced antimicrobial and anti-inflammatory therapy in the lungs [134].

b) Fungal infections. Infections caused by fungi are especially dangerous in the case of immunocompromised patients (as those with hematological neoplasms) [141] or when is associated to another diseases (like CF) [142]. Fungal pulmonary infections are very common and can be diagnosed by cytology [143]. An accurate diagnosis can be made, thanks to the specific characteristics of each type of fungus. There are certain pathogenic diseases that can compromise the lungs such as candidiasis, aspergillosis, coccidioidomycosis, histoplasmosis or cryptococcosis. The treatment possibilities are limited, being reduced to drugs (polyenes, triazoles, echinocandins and flucytosine); but the fungi reach resistance to antifungal agents over time [144]. In addition, the use of fungicides in the agricultural field (similar to those for human use) contributes to the appearance of resistances [144]. In addition, intrinsic resistances can happen, as in the case of *Candida krusei* [144]. Fungi resistances can occur intrinsically or be acquired [144-148], which represents a real threat to human health. Therefore, antifungal strategies should be expanded, being critical the prevention of future resistances [144]. Therapeutics treatment studies are focusing on the signals transduction

pathways in metabolic routes, cell membranes and walls, as well as in the expression of their genes [144]. For that reason, the detection of genes or mutations responsible of the fungi resistance is very important. The development of the fungal genomic allows the discovery of new targets for the treatment of fungi resistance [149], being also of interest the use of gene therapy to silence the genes responsible of their pathogenicity.

c) Viral infections. There are viral infections that cause great damage to the lungs, for example to the ciliated respiratory epithelium, whose integrity is altered. This leads to important problems because the mucociliary clearance is compromised, allowing the entrance of foreign particles and microbial infections at the lung level that can be very harmful [132]. These viral infections require of different vaccines for their prevention because stimulate the patients´ immune responses. In this sense, it is interesting the use of non-viral vectors.

Among the different pulmonary viruses, we can highlight three groups:

c.1) Influenza virus. Different strategies have been developed to deal the flu caused by the influenza virus. From a point of view of gene therapy, liposome-based vaccines (which imitate lung surfactant) carrying cyclic guanosine monophosphate-adenosine monophosphate 2'-3'-cGAMP (mimicking the initial stages of infection), lead to an improvement of the immune response [136]. In addition, it can be improved the immunity at the lung level by adding of Ag NPs to the inactivated influenza vaccine [150]. This approach using non-viral vectors encourages to future improvements regarding the treatment of the disease caused by this virus [136].

c.2) MERS-CoV. The coronavirus MERS-CoV produces the Middle east respiratory syndrome, highly infective, which requires a rapid and accurate diagnosis. Vaccines have been developed based on non-viral vectors, such as inorganic hollow/porous NPs loaded with

viral antigens, but also with subunits of stimulator of interferon (IFN) gene agonists, which improve the immune response.

c.3) SARS-CoV-2. The new type of coronavirus called SARS-CoV-2, which recently devastated the world producing a new disease called Covid-19, causes a severe acute respiratory tract syndrome. This virus was initially detected in December 2019 in Wuhan (China), and Covid-19 was declared as pandemic by the WHO in March 2020. Among the most common symptoms are dry cough, fatigue and acute respiratory distress syndrome (ARDS), but also other consequences beyond of the respiratory tract, such as fever and headaches, pains of joints and of muscles and diarrhea. The patients can also lose the smell, the taste and the hair. Sars-CoV-2 produces effects never seen before in the immune system, producing an increase of pro-inflammatory cytokines. This reaction can lead to pulmonary fibrosis and other pathological conditions [151], being probably that, like other viral infections, can generate carcinogenesis in different organs [151]. Furthermore, the elderly and patients with other concomitant pathologies (such as diabetes, cardiovascular problems, chronic respiratory disorders or even cancer) are more likely to suffer more severely this infection, reaching certain conditions such as pneumonia, neurological disorders and multi-organ failure [151]. In the most severe and dangerous cases, respiratory problems are so serious that the patients have to be hospitalized for respiratory resuscitation (by invasive mechanical ventilation) to save them of the death, but many patients end up losing their lives [151].

As the virus mutates, often virulent strains emerge; so the design of new vaccines and drugs is more and more important. The efforts have been focused both on the development of therapies that shorten the hospitalization period and increase the survival of affected patients, as well as developing prophylactic vaccines with the mission of increasing immunity against SARS-CoV-2 in the population [152]. For that reason, pharmaceutical industries and research institutions rush to prepare vaccines against this virus, ranging from traditional protein-based vaccines to more novel gene therapy-based vaccines.

The administration of DNA and mRNA is interesting for the encoding of certain protein-type SARS-CoV-2 antigens, but they have the problem of their molecular instability and low cellular internalization if they are administered in a naked way. For that reason, it is necessary to use a non-viral vector that promotes their uptake [152]. In fact, non-viral vectors are being employed to formulate some vaccines, such as Comirnaty and Spikevax (based on PEG-lipid NPs [153,154]), for the treatment of COVID-19 [136].

Currently, there are four vaccines authorized by the European Medicines Agency to prevent COVID-19 [155], two of them based in gene therapy:

c.3.1) Comirnaty (Pfizer-BioNTech). This vaccine is developed by the pharmaceutical company Pfizer (USA) and the biotechnology company BioNTech (German), being the first authorized in Europe against the COVID-19. It is based on the use of viral mRNA to provoke an immune response in the patient. It must be stored between -70 and -80 ºC, which implies complicated logistics. It was first administered in 2 doses, with a separation of, at least, 21 days between them. Thereafter, a third dose was approved. In addition, in Israel a fourth dose is being administered.

c.3.2) Spikevax (Moderna). This vaccine is produced in Switzerland and is the second that was approved in Europe. It is also based on mRNA, but can be stored at -20 ° C, with less complicated logistics. It was firstly applied in 2 doses, but with a separation of 28 days. Thereafter, a third dose was approved.

Specifically, both vaccines have mRNA that produces the spike protein, which is a protein found in the coat of SARS-CoV-2 and used by the virus to enter in the cells of the body. When a person receives any of these vaccine, temporarily produces the spike protein and his/her immune system will recognize it as foreign, producing antibodies and activated T cells to defend the organism. When the vaccinated people comes into contact with the SARS-CoV-2 virus, their immune system will recognize it and will be ready to defend

itself. The mRNA of these vaccines are destroyed shortly after vaccination [156,157].

1.5.5.2. Acute respiratory distress syndrome (ARDS)

It can be very dangerous for patients and can lead to death in the most serious cases. Around 3 million people per year are affected by this disease [158], leaving serious sequelae in 70% of survivors, such as damage in the lung, muscle and cognitive functions [159]. In the lung is an acute and diffuse lesion of alveolar cells that causes respiratory failure, being caused by inflammation (of infectious origin or not) by extra- or intra-pulmonary agents [160]. To treat it, certain strategies have been used without great results [158], such as placing the patient in the prone position [161], extracorporeal membrane oxygenation (ECMO) [162], nitric oxide inhalation [159], incorporation of exogenous surfactant [163,164] or the controlled administration of intravenous fluids [165]. Therefore, more specific and efficient treatments for ARDS are demanded [166]. Although the etiology of ARDS is not fully understood, in recent years gene therapy is pointed as a promising method for its therapy. It is tried to regulate the response genes of ARDS, maintaining normality in the endothelial cells and the epithelial cells of the alveoli, and preventing the fibrosis as well as the appearance of the disease.

For that, non-viral vectors are also becoming the best option to deliver genetic material for the therapy of ARDS. In fact, in the specific case of biodegradable polymeric systems, the release of genetic material into target cells could be controlled in long term, prolonging the gene expression. Furthermore, if targeting molecules are incorporated in the non-viral vectors, the specificity for the target cells increases. All these highlight great expectations in clinical studies [166].

1.5.5.3. Asthma

This disease difficults the breathing due to bronchial hyperresponsiveness, as well as chronic inflammation and reversible obstruction of the airway [167]. Its origin is usually produced by an allergenic agent that causes inflammation, constriction, cough and respiratory difficulty. The problem of this pathology is that is chronic and the inflammations produced over time damage the respiratory epithelium. Normally, asthma is treated with bronchodilators together with corticosteroids, relaxing the bronchial tissue as well as reducing inflammation [168]. These treatments have limitations, especially the inhaled corticosteroids, because they can produce many unwanted effects, even increasing the mortality [136]. Gene therapy has been proposed for the treatment of asthma [169] by reducing the inflammatory response [170,171].

1.5.5.4. Chronic obstructive pulmonary disease (COPD)

It is a lung disease with a high mortality rate [136]. It is based on the recurrent inflammation of the lungs, join to a reduction of the pulmonary ventilation. The most common symptoms are sputum, chronic cough and asthma. It is strongly predisposed by genetic factors [172], affecting the synthesis of collagenases, gelatinases, elastases, proteases and antiproteases; but also, can be caused by the inhalation of harmful particles [173,174]. As example, the tobacco smoke causes damage of the DNA, producing the disease [175]. In addition, there are irregularities in the mucosa due to phagocytic lung cells that produce reactive oxygen species, such as H_2O_2 [176-178]. Its current treatment is focused on bronchodilators, corticosteroids and antibiotics [136] but, given the risks that the disease still carries, it is more relevant a treatment directed to the focus, being the gene therapy a novel and promising strategy. In this sense, gene therapy is oriented to the epigenetic editing, specifically by gene silencing with miRNA and siRNA [179-182].

1.5.5.5. Cystic fibrosis (CF)

It is a recessive autosomal pathology caused by mutation in the CFTR gene, which was discovered in 1987 [183]. This gene encodes the transmembrane conductance protein, which forms a channel responsible of the transport of ions (such as bicarbonate and chloride [183]) in different tissues, mainly in the pulmonary epithelium [62]. The incorrect functionality of this channel produces decompensation of the ionic flow, which causes a change in the composition of the surface liquid of the respiratory tract, making it more acidic [184]. This hinders the mucociliary clearance and also produces a hyperplasia of the mucous glands, generating an abundant accumulation of thick and dense mucus, which promotes infections (mainly with *Pseudomonas aeruginosa* [136]), inflammation and tissue damage, as well as shortness of breath and pulmonary insufficiency [62].

The treatments proposed for CF have low efficacy [185]. For that reason, gene therapy stands out as a treatment of great potential and interest. It requires an efficient non-viral vector capable of delivering genetic material in ciliated epithelial cells and in submucosal glands [62,186].

With this purpose, the use of CS is remarkable [62]. NCs were prepared with a CS shell loaded with the wtCFTR-mRNA gene, and with a hydrophobic core of lecithin, where capsaicin was encapsulated. This nanocarrier efficiently delivered the gene because the capsaicin made a synergistic effect with the CS, returning the correct functionality of the CFTR gene [140]. The nanosystem adheres to the mucus due to the mucoadhesive effect of the CS, remaining for a longer time and holding the release of the gene [187].

It is important to note that lung fibroblasts from people with CF have many CD44 receptors. For that, the incorporation of HA in non-viral vectors (such as liposomes) is interesting to treat more efficiently this disease [188]. It was demonstrated that HA helps to the penetration of nanosystems into the cells. Concretely, as higher was the HA molecular weight, better was the cellular uptake of the nanosystems [188].

1.5.5.6. Alpha-1 antitrypsin (AAT) deficiency

AAT is a globulin protein present in serum and its deficiency produces one of the most common lethal hereditary diseases in caucasian patients of european origin [189]. This pathology was discovered by Laurell and Eriksson in 1963, and is produced by a error in a gene called SERPINA1 [190]. AAT is synthesized mostly in hepatocytes, but at the pulmonary level is also produced by epithelial cells and alveolar macrophages. The functions of the AAT globulin include protection from protein damage produced by neutrophil elastases in the lower pulmonary tract [189] and anti-inflammatory effect by inhibiting inflammation mediators [191]. Therefore, AAT deficiency leaves to the lungs to be vulnerable to uncontrolled proteolytic activity [189], as well as to other lung diseases such as bronchiectasis, emphysema or asthma. Normally, AAT deficiency is treated with the purified globulin, obtained from the plasma of healthy people, administered intravenously [192]; but it has several disadvantages such as risk of allergic reactions, need of multiple administrations and high cost of the treatment [193]. Therefore, the use of non-viral vectors based on polymers is very interesting and promising for this disease.

1.5.5.7. Lung cancer

This disease has one of the highest morbidity and mortality rates in the world, posing a serious danger to health [136,194]. It is produced in the epithelium of the bronchial and alveolar mucosa [136] by mutations in the genetic information that result in an uncontrolled growth of the lung mass. Gene therapy emerges as a promising alternative to treat several types of lung cancer [45]. There are different types of lung cancer [45]:

a) Small cell (SCLC). It is the least common, accounting for 15% of lung cancer cases.

b) Non-small cell (NSCLC). It is the most common, affecting 85% of lung cancer cases. In turn, it is classified as:

b.1) Large cell carcinoma. It occurs in lung epithelial cells, accounting for 15% of NSCLC cases.

b.2) Squamous cell carcinoma. It affects the tissue of the proximal lung pathways, occupying a 25% of NSCLC cases.

b.3) Adenocarcinoma. It is located in the surrounding tissue of the lung, with 40% of the cases of NSCLC.

There are several gene therapy strategies that are used in the treatment of lung cancer. Among them, it can be highlighted the use of siRNA. This molecule, once inside the neoplastic cells, silences the expression of the defective genes responsible of the tumor evolution. In addition, it can be used antisense oligonucleotides. To achieve the objective, the development of an efficient carrier is very important, for which the use of CS and HA in the preparation of this non-viral vector is very interesting [45]. CS facilitates the binding of genetic material and promotes the cell transfection [45]. On the other hand, HA directs the nanosystem towards cancer cells, thanks to its affinity for the CD44 receptor. This type of receptor is less common in SCLC cells than in NSCLC cells [45]. In fact, CS-based NPs prepared with HA have inhibited in a 60% the tumor (NSCLC) development, increasing the efficiency and duration of the transfection [195].

Taking into account the aforementioned, it seems reasonable to consider the inhalational gene therapy as a possible alternative for the treatment of certain lung diseases, with a more hopeful expectation.

1.6. Current situation of gene therapy by pulmonary route in clinical trials

After exploring the lung gene therapy, it is important to know what is its current situation in clinical trials. The current panorama of clinical trials performed for lung diseases treatable by gene therapy are showed below (Table 4) [196]:

Table 4. Complete clinical trials of pulmonary gene therapy compiled by the U.S. National Library of Medicine (01/09/21).

Study title	Conditions	Interventions
Trial of radiation and gene therapy before Nivolumab for metastatic non-small cell lung carcinoma and uveal melanoma	Lung squamous cell carcinoma stage IV Non-squamous non-small cell neoplasm of lung Metastatic uveal melanoma	ADV/HSV-tk (adenovirus-mediating expression of herpes simplex virus thymidine kinase) Valacyclovir SBRT: stereotactic body radiation therapy Nivolumab
Intrapleural AdV-tk therapy in patients with malignant pleural effusion	Lung cancer Malignant pleural effusion Mesothelioma Breast cancer Ovarian cancer	AdV-tk (adenovirus-mediated mediating expression of herpes thymidine kinase gene) Valacyclovir

Table 4 (continuation 1). Complete clinical trials of pulmonary gene therapy compiled by the U.S. National Library of Medicine (01/09/21).

Study title	Conditions	Interventions
Gene therapy plus radiation therapy in treating patients with non-small cell lung cancer	Lung cancer	Ad5CMV-p53 gene (adenovirus p53) Radiation therapy
Gene therapy to treat patients with non-small cell lung cancer that cannot be surgically removed	Lung cancer	Ad5CMV-p53 gene (adenovirus p53)
Phase I study of IV DOTAP: cholesterol-fus1 in non-small-cell lung cancer	Lung cancer	DOTAP:Chol-fus1 (DOTAP:cholesterol-fus1 liposome complex)
Phase II study of Lucanix™ in patients with stages II-IV non-small cell lung cancer	Lung neoplasm Carcinoma bronchogenic	Lucanix™

Table 4 (continuation 2). Complete clinical trials of pulmonary gene therapy compiled by the U.S. National Library of Medicine (01/09/21).

Study title	Conditions	Interventions
Vaccine therapy in treating patients with stage IIIB, stage IV, or recurrent non-small cell lung cancer	Lung cancer	Autologous dendritic cell-adenovirus CCL21 vaccine
Chemotherapy followed by vaccine therapy in treating patients with extensive-stage small cell lung cancer	Lung cancer	Autologous dendritic cell-adenovirus p53 vaccine Carboplatin Etoposide

Table 4 (continuation 3). Complete clinical trials of pulmonary gene therapy compiled by the U.S. National Library of Medicine (01/09/21).

Study title	Conditions	Interventions
Safety dose finding study of ADVM-043 gene therapy to treat Alpha-1 antitrypsin deficiency	Alpha 1-antitrypsin deficiency	ADVM-043 (investigational gene therapy product (serotype AAVrh.10 vector) expressing human A1AT)
Experimental gene transfer procedure to treat Alpha-1 antitrypsin deficiency	Alpha 1-antitrypsin deficiency	rAAV1-CB-hAAT gene vector (adeno-associated virus (AAV) genetically engineered to contain a normal copy of the AAT gene)
Experimental gene transfer procedure to treat Alpha-1 antitrypsin deficiency	Alpha 1-antitrypsin deficiency	rAAV2-CB-hAAT gene vector (adeno-associated virus (AAV) genetically engineered to contain a normal copy of the AAT gene)
Safety and efficacy study of rAAV1-CB-hAAT for Alpha-1 antitrypsin deficiency	Alpha-1 antitrypsin deficiency	rAAV2-CB-hAAT (recombinant adenoassociated virus (rAAV) alpha-1 antitrypsin (AAT) vector (rAAV1-CB-hAAT))
Safety and efficacy study of rAAV1-CB-hAAT for Alpha-1 antitrypsin deficiency	Alpha-1 antitrypsin deficiency	rAAV1-CB-hAAT (recombinant adenoassociated virus (rAAV) alpha-1 antitrypsin (AAT) vector (rAAV1-CB-hAAT))

Table 4 (continuation 4). Complete clinical trials of pulmonary gene therapy compiled by the U.S. National Library of Medicine (01/09/21).

Study title	Conditions	Interventions
Safety and efficacy of recombinant adeno-associated virus containing the CFTR gene in the treatment of cystic fibrosis	Cystic fibrosis	tgAAVCF (genetic design that contains the CFTR gene)
Repeated application of gene therapy in CF patients	Cystic fibrosis	pGM169/GL67A (product that encodes CFTR)
Phase I pilot study of gene therapy for cystic fibrosis using cationic liposome mediated gene transfer	Cystic fibrosis	pGT-1 gene lipid complex (lipid/DNA formulation (pGT-1 lipid complex))
Phase I study of liposome-mediated gene transfer in patients with cystic fibrosis	Cystic fibrosis	Cystic fibrosis transmembrane conductance regulator

As can be seen in Table 4, clinical studies performed on pulmonary gene therapy have focused mainly in the use of viral vectors; but, as mentioned above, non-viral vectors are safer showing a wide field of research.

1.7. Interest of nanocapsules for gene therapy

Polymeric NCs have received increasing interest in the recent years due to their versatility as nanocarrier related to their structure that consist of a polymeric shell and an oily liquid core [197]. NCs can encapsulate, protect and load metabolites, hormones, peptides, proteins, enzymes, drugs and genes [198-200]. For that reason, their research for biomedical applications increased in the last two decades [197]. In addition, there are certain properties that make NCs very useful as nanocarriers, such as stabilization, ability to increase the bioavailability, targeted treatment and sustained release of the AIs.

1.7.1. Stabilization

NCs are very interesting for the stabilization of different types of AIs, protecting them from hostile environments, such as determined temperatures, pHs, other substances or light, during the manufacture or the delivery of the AIs [201].

1.7.2. Ability to increase the bioavailability

It is important in the case of AIs slightly soluble in water, which are loaded in the NCs oily core and protected by the coat from the environmental conditions [202,203]. This is the case of imiquimod-loaded NCs (improving cytotoxicity in cervical cancer cell line) or PLGA-based NCs loaded with clarithromycin for nebulization (enhancing the treatment against *Mycobacterium abscessus* and *Staphylococcus aureus*) [202,203].

1.7.3. Targeted treatment

NCs can be decorated with bioactive smart molecules in order to direct them at specific tissues. Both NCs polymers and ligands have thiol, hydroxyl, carbonyl and amino groups that allow the conjugation [197,204]. Targeting is a very valuable option in diseases such as cancer because it increases the concentration and the effect in the tumor area, while decrease the adverse effects in healthy tissues [205,206]. In fact, there are micro/nanocapsules formulated with ε-poly-L-lysine (PLL) and oily core for the delivery of lipophilic molecules. This structures use folic acid as targeting ligand for achieve tumors [207]. It is because folic acid has a high affinity for folate receptors, recognized as remarkable tumor markers, and which are overexpressed in many tumor-type cells, such as in pulmonary tumors [207].

1.7.4. Sustained release

This property is very useful in pathologies whose treatments must be prolonged in time. Thereby, NCs allow high loads of AIs, reducing the administered doses and the adverse effects derived from the repeated doses [208-211]. Between other, it was investigated the use of brinzolamide-loaded CS-based NCs for the treatment of glaucoma and NCs loaded with damnacanthal or simvastatin for the treatment of breast cancer.

All the aforementioned properties make that polymeric NCs have an increase interest for gene therapy because they are natural and biocompatible non-viral vectors that efficiently deliver genetic material [212]. They are versatile in the variety of materials with which they can be prepared (highlighting of CS and HA for their shell and with an oily core). In addition, they can carry a diversity of AIs, even at the same time, hydrophilic molecules in the shell (such as genetic material) and lipophilic molecules in the core (like transfection adjuvant molecules, like capsaicin [213-215], improving the efficacy of the therapy. In fact, NCs can transport genetic material even of higher molecular weight and in higher payloads compared to

viral vectors [140]. For other hand, and taking into account the poor stability of naked genetic material by the nucleases *in vivo* [216], the use of NCs is a good option because, as it was previously mentioned, they can adequately protect it [51,140,212]. Furthermore, these polymeric shells also offer the advantage of being functionalized with targeting molecules that interact with specific structures [217-219], being very interesting in gene therapy to target the genes to the cells that cause the diseases. It can be highlighted that the gene therapy using genetic material-loaded CS-based NCs in the tumor area is also favored due to the "tumor-homing effect" [220]. As example of successful gene therapy mediated by CS-based NCs, it can be mentioned a recent work of Kolonko et al. [140] for treatment of CF. In this study, NCs were loaded with wtCFTR-mRNA (on the NCs surface), as well as capsaicin (on the NCs core), being tested *in vitro* in CF cell lines (16HBE14o- and CFBE41o- cells). The results showed the recovery of the function of the cystic fibrosis transmembrane conductance regulator (CFTR) gene [140]. CS-based NCs open a huge field for gene therapy, yet to be explored in depth, being not only successful in the CF [140], but also for the therapeutic delivery of genes in others diseases of genetic origin.

It is important to stand out that NCs have relevant interest for gene therapy beyond pulmonary diseases [221,222], such as brain tumors [223]. In this case, surgical operations are used as treatment and, sometimes, the tumor area cannot be accessed or, even, malignant cells may reappear in the area where the tumor was removed or in surrounding areas, causing worse prognoses [223]. In addition, taking into account that is a very invasive treatment, it is often used more standard treatments such as chemotherapy and radiotherapy, which are very limited. There is little pharmacological arrival to the affected area due to the blood-brain barrier [224,225]. For this reason, the nanocarrier approach, specifically CS-based NCs, are very interesting because they exhibit very high specificity and internalization in the affected area, reducing the systemic toxicity [53,226]. Specifically, the targeted silencing by CS-based NCs carrying EGFR and galectin-1 siRNA via nose-to-brain has been investigated, demonstrating a decrease of the gene expression in the tumor area and a notable

increase of the survival in mice with brain tumors [227,228]. In fact, it was observed a great potential for the administration of genetic material *in vitro* and *in vivo* [229,230].

The above information leads us to confirm the importance of NCs for gene therapy, taking into account the enormous number of lung diseases that could be treated by their inhalation. For that reason, it is vital to include the genetic material-loaded CS-based NCs in a platform of suitable characteristics for their deliver to the lung.

1.8. Interest of microencapsulation of CS-based NCs for pulmonary administration

In order to carry out a successful pulmonary gene therapy, it is very important to overcome the previously mentioned obstacles of this route to deliver the payload in the desired region of the lung. In this sense, formulations factors must also be taken into account, such as the stability, and the particle size and inertia.

1.8.1. Stability

Nanosystems administered in suspension show lower stability than when they are administered in dry powders [231]; therefore, nanocarriers suspensions are not recommendable. Furthermore, if the nanosystems are directly lyophilized, it would not be possible to ensure the particle homogeneity, or a suitable size for their correct inhaled administration, being seriously affected their reconstitution in the lung environment. Taking all this into account, it is necessary to allow the pulmonary administration of NCs in dry powders form to achieve their arrival to the desired region of the respiratory tract [110].

1.8.2. Particle size and inertia

The geometric and aerodynamic sizes of the inhaled particles have a crucial influence on their pulmonary deposit. Traditionally, it was considered that particles with a size between 1-5 μm were deposited in the deep lung area, while the larger ones were retained in

the upper respiratory tract, and those with a size lower than 1μm were expelled with the expired air [232]. Furthermore, nanostructures have low inertia that, combined to their small size, have poor characteristics to reach the deep lung by themselves [231,232].

In that sense, our research group developed an efficient platform for the administration of nanocrriers in dry powders form for the pulmonary route, consisting of Ma MS that encapsulate the nanosystems [212].

Ma is a non-reducing sugar biocompatible for the lungs that has been widely employed for pharmaceutical uses [233,234]. It has adequate properties as spray-drying excipient, such as its thermoprotective effect on the microencapsulated AIs [231,235], which is very interesting to ensure the genetic material integrity. Furthermore, it is capable to modulate the morphology and the size of the MS [236], and to increase the fluidity, dispersibility and stability of the obtained powder formulations [235]. Thanks to the Ma mucolytic effect, the nanostructures easily cross the mucus of the respiratory tract [237].

Our research group has efficiently microencapsulated CS-based NPs (CS NPs), SLNs and MOF MIL-100(Fe) NPs in Ma MS with suitable properties that allowed to the nanosystems to achieve the deep lung, where the drug could be efficiently released [120,231,232,238].

Consequently, and based on the aforementioned, highlights the interest of the microencapsulation of CS-based NCs for pulmonary administration.

2. BACKGROUND, HYPOTHESES AND OBJECTIVES

2.1. Background

Nanotechnology highlights within Pharmaceutical Technology because it deals with the research and development of vehicles of nanometric size, whose function is delivery one or more active ingredients (AIs) to treat diseases [239].

1. Currently, there is a number of poorly resolved lung diseases that are potential candidates to be treated by gene therapy. This is the case of bacterial, fungal and viral infections, acute respiratory distress syndrome (ARDS), asthma, chronic obstructive pulmonary disease (COPD), cystic fibrosis (CF) and several types of lung cancer. Therefore, gene therapy offers encouraging prospects for improving the current therapeutic scenario of these diseases.
2. CS NCs are receiving enormous interest in drug delivery due to their versatility related to their core-shell structure, which is also tunable [240-242]. Their oily core allows loading lipophilic molecules, while their positive polymeric shell allows the association of hydrophilic molecules of either low or high molecular weight such as genetic material [243]. More specifically, their application in gene therapy as non-viral vectors is receiving great attention. Indeed, they may for example load genetic material on their surface, as well as a lipophilic adjuvant molecule inside [140]. NCs have been administered by different routes like the ocular, nasal and oral, but never by the pulmonary route [140] with gene therapy purposes.
3. The pulmonary administration of nanosystems requires of their incorporation in a vehicle of micrometric size dry powder that provides them of the appropriate morphological and aerodynamic characteristics for their correct inhalation and arrival at the desired target site of the lung.
4. The great potential offered by the spray-drying technique for the microencapsulation of nanosystems has been demonstrated [187,231,238]. It is suitable for the microencapsulation of

nanostructures containing thermolabile molecules because it respects their integrity [235] and allows modulating the characteristics of the obtained powder [244].

5. The pulmonary administration of dry powders produced by the microencapsulation of nanosystems can allow a localized and specific treatment at the target site of the lung, reducing both administered dose and side effects. These micro-nanoplatforms are promising candidates to solve the current therapeutic needs of lung diseases.

2.2. Hypothesis

We hypothesize that it is possible to develop a dry powder formulation based on microencapsulated CS-based NCs with suitable characteristics for its administration by the pulmonary route and that efficiently release the associated genetic material at the target site of the lung for the treatment of genetic lung diseases. This main hypothesis can be divided into three partial hypotheses:

Hypothesis I: Considering that there are lung diseases of genetic origin that are currently not well treated, it is reasonable to consider that the administration of genetic material directly in the lung site where it is desired to exert its effect could improve the prognosis of these diseases.

Hypothesis II: As CS-based NCs are positively charged on their surface, it is expected that they could load high amounts of genetic material (negatively charged) on their shell, opening the possibility in the future of jointly load adjuvant lipophilic molecules in the core.

Hypothesis III: Taking into account the good results obtained in previous studies of microencapsulation of nanosystems of different nature in mannitol microspheres (Ma MS), it could be expected that the microencapsulation of CS-based NCs using also Ma as spray-drying excipient, would give rise to dry powders of suitable characteristics for pulmonary administration.

2.3. Objectives

The main objective of this Thesis was to develop a micro-nanoplatform based on CS-based NCs (CS NCs and HA/CS NCs) microencapsulated in Ma MS in dry powder form for the pulmonary administration of genetic material, with potential application in the treatment by gene therapy of different lung diseases.

This main objective was composed of the following specific objectives:

Objective I. Preparation of CS-based NCs capable of carrying a high load of model plasmid (pCMV-βGal)

Objective II. Microencapsulation of the pCMV-βGal-loaded CS-based NCs in Ma MS with suitable characteristics for inhalation

Objective III. Release of CS-based NCs from Ma MS in aqueous media

Objective IV. *In vitro* evaluation of viability and cellular uptake in the A549 cell line

Objective V. *In vivo* evaluation of lung distribution and gene expression using Wistar-Kyoto rats

In order to achieve these objectives, the following work stages were established:

Objective I. Preparation of CS-based NCs capable of carrying a high load of model plasmid (pCMV-βGal):

- Preparation of CS NCs using a solvent displacement procedure in one step, and association of HA and/or plasmid on their surface to obtain HA/CS NCs and pCMV-βGal-loaded CS-based NCs; and physicochemical characterization of the NCs.

- Determination of the maximum percentage of model plasmid that can be loaded by the NCs and of the plasmid association.

Objective II. Microencapsulation of the pCMV-βGal-loaded CS-based NCs in Ma MS with suitable characteristics for inhalation:

- Determination of the NCs stability in the solution of the spray-dry excipient (Ma).
- Adjustment of the NCs microencapsulation process by modifying one by one the spray-drying process parameters.
- Spray-drying of CS-based NCs with/without pCMV-βGal in Ma MS, using the optimal conditions.
- Characterization of the obtained dry powders in terms of process yield, morphological properties (SEM), theoretical aerodynamic diameter, geometric diameter, real and apparent densities, and distribution of the NCs in the Ma MS using CLSM and RAMAN techniques.

Objective III. Release of CS-based NCs from Ma MS in aqueous media:

- Release studies of NCs from Ma MS in MilliQ water and in simulated pulmonary medium, and physicochemical characterization of the released NCs at different times to assess if their characteristics are maintained following their microencapsulation.

Objective IV. *In vitro* evaluation of viability and cellular uptake in the A549 cell line:

- Study of cell viability using the Luna II device and the Flow Cytometry method.
- Uptake and intracellular distribution of the nanosystems using CLSM.
- Quantification of A549 cells internalized with NCs by Flow Cytometry.

Objective V. *In vivo* evaluation of lung distribution and gene expression using Wistar-Kyoto rats:

- Study of the pulmonary distribution of microencapsulated NCs, using CLSM.
- Determination of *in vivo* gene expression by X-Gal reaction.

3. MATERIALS AND METHODS

3.1. Materials

Protasan® UP CL 113 (ultrapure chitosan, hydrochloride salt, CS, deacetylation degree: 75-90%, molecular weight (Mw) < 150 KDa) was acquired from Pronova Biopolymer, A.S. (Drammen, Norway); hyaluronic acid (HA, Mw~ 166 kDa) was donated from Bioiberica (Barcelona, Spain); Epikuron® 145V (soybean lecithin) was provided by Cargill (Madrid, Spain); Miglyol® 812N (a neutral oil composed of capric and caprylic acids, medium-chain fatty acids) was a gift from Cremer Oleo Division (Hamburg, Germany); Curosurf® (pulmonary surfactant: 80 mg/mL of pig lung phospholipids) was gently provided by Professor Almeida (University of Lisbon, Portugal), who acquired it to Angelini Pharmacêutica, Lda. (Lisbon, Portugal); A549 cell line was obtained from ATCC (Manassas, USA); PureLink™ HiPure Expi Plasmid DNA Gigaprep Kit, Dulbecco´s Modified Eagle Medium (DMEM), Fetal Bovine Serum (FBS), Trypsin-EDTA (0.05%) and Fluoromount® were purchased to Gibco™ (ThermoFisher Scientific, Madrid, Spain); Bodipy® 630/650-X was got from Molecular Probes (Eugene, USA); β-Galactosidase Reporter Gene Staining kit, Nuclear Fast Red solution, Coumarin 6 (Cu^6, > 99%), D-mannitol (Ma, ≥ 98%, Mw: 182.17 g/mol), phosphate buffered saline tablets (PBS, pH = 7.4), L-Glutamine and sodium dodecyl sulfate (SDS) were purchased to Sigma Aldrich (Madrid, Spain); AlamarBlue® (CellTiter-Blue) was obtained from Promega (Fitchburg, USA); Triton® X-100 (molecular biology grade) was purchased to Scharlab S.L. Laboratories (Barcelona, Spain); 4´,6-diamino-2-phenylindole (DAPI) was acquired from Emp-Biotech (Berlin, Germany); LIVE/DEAD™ Fixable Aqua Dead Cell Stain Kit was acquired to Invitrogen™ (Waltham, USA); Trypan Blue was obtained of Logos Biosystems (Sainghin-en-Mélantois, France); Neutral Buffered Formalin (10% *v/v*) was bought to Bio-Optica (Milan, Italy); acetone and ethanol were grade HPLC; MilliQ water (ultrapure filtered water, using filters of 0.2 µm, Millex®-GN, Millipore Iberica, Madrid, Spain). The other chemical products were reagent grade.

3.2. Production of pCMV-βGal

Competent Escherichia coli DH5α cells were thawed on ice and 0.11 µg of pCMV-βGal were mixed gently with E. coli, remaining 30 min on ice. Then, it was incubated for 45 s in a bath at 42 °C and another 5 min on the ice. After the thermal shock, the bacteria were placed in a volume of 1 mL of Luria Bertani medium (LB) for 1 h, at 37 °C under stirring (260 rpm) and then 100 µL were grown on LB ampicillin-agar plates (100 µg/mL) and incubated during 14 h at 37 °C. One colony was incubated in 5 mL of LB medium supplemented with ampicillin for 20 h at 37 °C. After that time, the 5 mL of bacteria were transferred to a volume of 400 mL of LB (containing 400 µL of antibiotic) and allowed to incubate for 24 h at 37 °C under agitation (320 rpm). After that time, the 400 mL of bacteria were taken to a volume of 3200 mL and incubated for 24 h at 37 °C. The bacteria were then collected by centrifugation and frozen until use. The purification of pCMV-βGal was performed according to the protocol specified in PureLinkTM HiPure Expi Plasmid DNA Gigaprep Kit (ThermoFisher Scientific, Madrid, Spain). The plasmid was checked by a 1% agarose gel containing 12 µL of SYBR Safe DNA gel stain at 70 mV and 90 min (Electrophoresis PowerPac 300, Bio Rad, Hercules, USA). The concentration of the extracted plasmid was quantified by a Nanodrop 1000 Spectrophotometer (ThermoFisher Scientific, Franklin, USA) and the plasmid samples were frozen at −20 °C until further studies.

3.3. Preparation of CS-based NCs

The CS NCs were prepared using a solvent displacement procedure previously developed by our group in “two steps” [243], which in this work was modified and simplified to be carried out in “one step”. Briefly, an organic phase composed of 10 mg of lecithin (dissolved in 250 µL of ethanol at 37 °C), 31.2 µL of Miglyol® 812N and 4.75 mL of acetone was added quickly over an aqueous phase consisting in 10 mL of a CS solution (0.25 mg/mL) under constant magnetic stirring (2000 rpm) for 10 min. Immediately, the mixture

turned milky. Next, the solvents were eliminated under vacuum (Rotavapor Büchi R-210®, Flawil, Switzerland) to a final volume of 5 mL. In some cases, the CS NCs were further modified by incorporating HA to their surface. This was done by addition of HA (625 µg/mL) to the CS NCs suspension, producing HA/CS NCs. The association of the pCMV-βGal to the CS NCs (pCMV-βGal-CS NCs) was performed by its drop-by-drop addition on the previously prepared NCs suspension and incubation with gentle magnetic stirring at room temperature for 1 h. To prepare plasmid-loaded HA/CS NCs (pCMV-βGal-HA/CS NCs), the plasmid was firstly added to the CS NCs suspension and next, the HA. Specifically, the volumes and concentrations of the components employed to obtain the pCMV-βGal-loaded NCs are shown in Table 5.

Table 5. Theoretical concentrations and volumes of the components employed to prepare pCMV-βGal-loaded CS-based NCs.

Formulation	MilliQ Water (µL)	pCMV-βGal (628 µg/mL) (µL)	CS NCs suspension (34.3 mg/mL) (µL)	Hyaluronic acid (HA) solution (625 µg/mL) (µL)
pCMV-βGal-CS NCs	125	125	250	-
pCMV-βGal-HA/CS NCs	125	93.80	250	31.20

3.4. Determination of NCs production yield

The NCs production yield was determined by gravimetry. For that, fixed volumes of NCs suspensions were centrifuged (60000 rpm, 1 h, 15 °C) in an Ultracentrifuge Beckman Coulter (OptimaTM TLX Ultracentrifuge. Rotor: TLA_100.3, Minnesota, USA). The NCs creams were freeze-dried (over 24 h at −80 °C and gradual ascent until 20 °C), using a Tel-star Freeze Dryer (Telstar LyoQuest −85, Barcelona, Spain) (n = 3).

The production yield (P.Y.) was calculated using the following formula:

$$\text{P.Y. (\%)} = \frac{\text{NCs weight}}{\text{Total solids weight}} \times 100 \quad (2)$$

Where total solids = CS + (HA) + Lecithin + Miglyol®

3.5. Morphological and physicochemical characterization of NCs

The NCs morphology was characterized by transmission electron microscopy (TEM) (Jem-2010 Electron Microscope, Oberkochen, Germany) at 120 KV. For TEM observation, 10 μL of sample were placed on copper grids with carbon films and were stained for 2 min with 2% (w/v) phosphotungstic acid. Their size and ζ-potential were determined by Dynamic Light Scattering (DLS) and Laser Doppler Anemometry (LDA) using a Zetasizer® Nano-ZS (Malvern Instruments, Malvern, Worcestershire, United Kingdom). The analysis was performed at 25 °C. Size and ζ-potential of each sample was measured in triplicate (n = 3).

3.6. Preliminary study of the pCMV-βGal association to the NCs

The association of plasmid to the CS-based NCs was determined qualitatively by agarose gel electrophoresis (1% agarose, SYBR Safe DNA gel stain, 70 mV, 90 min). The samples were prepared in 96-well plates. Free plasmid (pCMV-βGal, 5% with respect to the amount of CS used to prepare the NCs) and control CS-based NCs (without plasmid) were introduced in the first and second wells of the gel, respectively. NCs with increasing amounts of plasmid, from 10% (*w/w*) to 100% (*w/w*) with respect to the total amount of CS used to prepare the NCs, were included in the next wells. The images of the gels were obtained with a Gel Doc™ XR 302 nm ultraviolet light system (Bio-Rad, Hercules, USA).

3.7. Determination of the pCMV-βGal association to the NCs

The plasmid association efficiency was quantitatively determined by measuring the difference between the added total plasmid amount and the free plasmid amount. For that, pCMV-βGal-CS-based NCs were centrifuged in an ultracentrifuge at 60000 rpm, during 1 h at 15 °C (Ultracentrifuge Beckman Coulter: Optima™ TLX Ultracentrifuge. Rotor: TLA_100.3, Minnesota, USA). The NCs creams were discarded and the liquids containing free plasmid were quantified by fluorimetry using a Qubit® 3.0 Fluorometer (Invitrogen Life Technologies, Madrid, España). The experiment was done in triplicate (n = 3). The encapsulation efficiency (E.E.) and drug loading (D.L.) of plasmid were calculated using the following formulas:

$$\text{E.E.}(\%) = \frac{\text{Total plasmid amount - Free plasmid amount}}{\text{Total plasmid amount}} \times 100 \qquad (3)$$

$$\text{D.L.}(\%) = \frac{\text{Total plasmid amount - Free plasmid amount}}{\text{CS-based NCs amount}} \times 100 \qquad (4)$$

3.8. NCs thermal stability analysis: Heating-cooling ramps

It is very important to bear in mind that the structural stability of the NCs is conditioned by the temperature. Taking into account that the NCs will be microencapsulated in Ma MS by a spray-dry process, these nanostructures will be exposed for a certain time to a temperature (T_{Outlet}), which depends on the prefixed temperature (T_{Inlet}), among other factors. Therefore, the stability of the NCs could be compromised by the T_{Outlet}. For that, it is crucial to perform a thermal stability analysis to determine the critical temperature at which each nanosystem (CS NCs and HA/CS NCs) could destabilize. It must be ensured that during the spray-drying process, the T_{Outlet} remains below the destabilization temperature to ensure structural integrity and, hence, the quality of the microencapsulated NCs. The

structural destabilization is detected by a strong increase of NCs PdI (> 0.7), which will produce large standard deviations.

To investigate the structural stability of the NCs at different temperatures, suspensions of CS NCs and HA/CS NCs were exposed to heating-cooling ramps from 25 to 90 ºC (large range of possible $T_{Outlets}$) and vice versa (with a rate of 0.5 ºC/min), into quartz cuvette covered to prevent evaporation. The NCs sizes and PdI were measured each 0.5 °C by Dynamic Light Scattering (DLS) using the Zetasizer® Nano-ZS (Malvern Instruments, Malvern, UK) with an Attenuator fixed at 7. The study was done in triplicate (n = 3).

3.9. Stability of NCs in the spray-drying excipient solution

Before the NCs microencapsulation in Ma MS (the selected spray-drying excipient), their physicochemical stability in Ma solution was checked. For that purpose, 5 mL of NCs suspension was mixed with 5 mL of a concentrated solution of Ma (16%, *w/v*). The mixture was incubated at room temperature under magnetic stirring (300 rpm) (CIMAREC i Multipoint, Fisher Scientific, Spain). The NCs physicochemical characteristics (size and ζ-potential) were analyzed in triplicate (n = 3) at different times (0, 0.5, 1, 2 and 4 h), by the methods previously described.

3.10. Preparation of dry powders

NCs microencapsulation was carried out using a co-current Büchi spray-dryer (Büchi® Mini Spray Dryer B-290, Flawil, Switzerland) with two fluids 0.7 mm nozzle. Volume of drying chamber was 9.3 L, with a residence time of the particles of 55.8 s. This was calculated as follows [245]:

$$t_r = \frac{V_c}{\text{Air flow rate}} \quad (5)$$

Where: t_r: residence time of the particles; V_c: volume of drying chamber: 9.3 L; air flow rate: 600 Nl/h.

To microencapsulate NCs correctly, firstly it was necessary to adjust some parameters of the spray-dry process: total solids content (t.s.c.) (*w/w,* %), air flow rate (Nl/h), NCs:Ma ratio, Outlet temperature (T_{Outlet}, mainly determined by the Inlet temperature (T_{Inlet})) (ºC), aspirator (%), and flow rate (F.R.) (mL/min). For this study, the CS NCs formulation was used and each variable of the process was modified step by step, while the other variables were kept constant. In the step 1, t.s.c. was tested, being the investigated values of 2.5, 5, 10, 11, and 12%, fixing the parameters air flow rate = 400, NCs:Ma = 1:10, T_{Inlet} = 170 °C, Aspirator = 75% and Flow Rate = 2 mL/min. In the step 2, the Air flow rate was checked, for which two high values were chosen for the greatest dispersion of the suspension droplets: 400 and 600 Nl/h. In the step 3, the NCs:Ma ratio was verified by testing two ratios in which there was a high proportion of Ma. This is because in previous studies (data not shown) it was observed that a more similar ratio between the NCs and the excipient, does not lead to the preparation of MS, but rather agglomerates with a "flake" shape. Therefore, the 1:10 and 1:15 ratios were tested. In step 4, the effect of the T_{Outlet} was studied, considering two opposing values: 105 and 170 ºC, associated with $T_{Outlets}$ around 58 and 90 ºC, respectively. In this way, we want to check whether a low temperature (slightly more humid powder, but ensuring the stability of the NCs) or a high temperature (drier powder, but with risk of stability of the NCs) is better. In any case, the Aspirator was directly set at 100% in this step to decrease the T_{Outlet} and minimize the risk of instability of the NCs spray-dried at 170 ºC. In addition, a F.R. of 8.8 mL/min was punctually used with the intention that the temperature had less influence on the samples, especially considering the one that was spray-dried at 170 ºC. In the step 5, it was determined which F.R. was

the most appropriated, keeping the Aspirator at 100% to lower the T_{Outlet}. The compared values were: 5, 7, 8.8 and 10 mL, being higher than 2 mL/min in all cases because it was observed that low F.R. values lead to too small MS. We observed the powders in terms of morphology, sphericity and aggregation of the MS. The optimum spray-dry conditions were subsequently used to prepare all formultions: Ma MS, CS NCs-loaded Ma MS, HA/CS NCs-loaded Ma MS, pCMV-βGal-Ma MS, pCMV-βGal-CS NCs-loaded Ma MS and pCMV-βGal-HA/CS NCs-loaded Ma MS.

Before the spray-drying process, 13.12% (*w/v*) Ma solution was prepared; NCs suspensions (CS NCs and HA/CS NCs) (volume: 4.373 mL, concentration: 34.3 mg of NCs/mL) were mixed with an appropriate volume of Ma solution (15.627 mL at 13.12%, *w/v*) to reach a NCs:Ma ratio of 1:15 (*w/w*) and a total solids content (t.s.c.) of 11% (*w/v*). For the microencapsulation of pCMV-βGal-CS-based NCs in Ma MS (pCMV-βGal-CS-based NCs-loaded Ma MS), the t.s.c. was adjusted to 5.5% (*w/v*); while for the microencapsulation of pCMV-βGal (without NCs) (pCMV-βGal-Ma MS), the t.s.c. was fixed to 5.1% (*w/v*).

After the spray-drying process, the powders were collected and stored at room temperature in a desiccator until use.

3.11. Characterization of the dry powders

3.11.1. Spray-drying process yield

Process yield (P.Y.) was calculated by gravimetry by comparing the final amount of dry powder obtained by spray-drying (MS weight) with the theoretical (t.s.c. (NCs + Ma) weight), using the following formula (n = 3):

$$\text{P.Y. (\%)} = \frac{\text{MS weight}}{\text{t.s.c. (NCs + Ma) weight}} \times 100 \qquad (6)$$

3.11.2. Morphology and size

The MS morphology and size were characterized by Scanning Electron Microscopy (SEM) (FESEM Ultra-Plus, Zeiss, Germany). For that purpose, thin films of powders were fixed in double-sided adhesive graphite discs on stubs. The samples were metalized with a film of iridium (10 nm) by an Emitechk 550 Sputter Coater (London, England). The MS size was determined by measuring the space between two tangents of opposed margins (Feret´s diameter) by the z-SmartTiff program (Zeiss, Germany). The geometric diameter (D_g) was calculated as the mean of the Feret´s diameters, being employed in this study 50 MS measures for each powder (n = 50).

3.11.3. Aerodynamic properties of the dry powders

The tap density or apparent density of a powder (g/cm^3), which is the mass that occupies in 1 cm^3, was obtained using a tap density tester (Tecnociencia, A Coruña, Spain). For that, a volume of powder of weight comprised between 1.0–1.6 g was measured into a 10 mL test-tube before the mechanical tapping. The test-tube was tapped to a speed of 30 tap/min until the sample reached a constant volume [246] (n = 3).

The real density of the dry powder samples (g/cm^3) was determined by a helium pycnometer (Quantachrome MPY-2, New York, USA) (n = 3).

The aerodynamic diameter (D_{aer}), which is the diameter of a sphere of unit density with the same terminal settlement velocity as the particle under consideration, was theoretically calculated using the equation [98]:

$$D_{aer} = D_g \sqrt{\frac{\rho_{real}}{\rho_0 \lambda}} \quad (1)$$

Where: D_g: geometric diameter (μm), ρ_{real}: real density of MS (g/cm^3), ρ_0 = 1 g/cm^3 and λ: MS dynamic shape factor (spherical MS: λ = 1; irregular MS: λ = 2) [99].

3.12. Distribution of NCs in Ma MS

3.12.1. RAMAN images and spectra

RAMAN studies were carried out to demonstrate the presence and location of NCs in Ma MS. Ma MS containing CS NCs, the controls Ma MS and lyophilized CS NCs were characterized on their surface by Confocal Raman Microscopy WITec (model Alpha 300R) equipped with a DPSS laser (λ = 532 nm) and a piezo-electric table. A 532 nm laser with a power of 6.8 mW and integration time of 0.1s was used. The objective was Zeiss EC Epiplan-Neofluar 100x / 0.9 NA. A continuous scan range was employed reaching 20 μm in Z direction (accuracy position of < 0.2 nm) and 100 μm in the X and Y directions (accuracy position of < 1 nm). In addition, a Ultra-High-Throughput-Spectrometer UHTS300 for VIS employing 2 gratings (600 and 1800 lines/mm) and a detector CCD camera back-illuminated (with 1024x127 pixel format), VIS improved QE > 90%, Peltier cooling (to approx. -60 °C) were used. The registration time was approximately of 1h 15min. Results were processed with the software WITec Project Five 5.1. One CS NCs-loaded Ma MS (2.71 μm size) was analyzed in planes of different depth (Z cuts) to test the NCs presence in the structure. MS was cut in 30 planes (10x10 μm) (a plane every 90.5 nm depth), using a resolution of 30 lines and 30 points/line. The spectra of the CS NCs-loaded Ma MS surface, as well as of the planes 21, 22, 23, 24 and 25 (located at 1.90, 1.99, 2.08, 2.17, 2.26 μm of depth, respectively) were analyzed. Initially, the infiltrated cosmic rays (CRR) and the sub-background of every spectrum were corrected in

that order. After that, the corrected spectrum of the CS NCs-loaded Ma MS surface, as well as the spectra of the components of each plane were compared with the spectra of the controls Ma MS and lyophilized CS NCs to verify the presence of Ma and NCs in the different planes and in the surface of the CS NCs-loaded Ma MS.

RAMAN images were obtained by mathematical/computerized treatment of the spectra using the Project FIVE 5.0 (WITec focus innovations). A color was assigned to each component, being observed the Ma in blue color and the CS NCs in red color in the image of every tested plane of the CS NCs-loaded Ma MS.

3.12.2. Confocal Laser Scanning Microscopy (CLSM)

For this study, Coumarin 6 (Cu^6) was used to label the NCs, obtaining Cu^6-CS NCs and Cu^6-HA/CS NCs. Specifically, 4.5 µL of Cu^6 (10 mg Cu^6/mL of dichloromethane) was mixed homogeneously in the oil phase during the NCs preparation. Cu^6-labelled NCs were characterized for size, PdI and ζ-potential, as described above (Section 3.5.). To remove possible non-encapsulated Cu^6 residues, the labelled NCs were dialyzed (Spectra/Por® 3 MWCO Dialysis Membrane Standard RC Tube: 3.5 kD) overnight, before their microencapsulation. After dialysis, the Cu^6-labeled NCs were characterized newly. Then, both pre-dialyzed and dialyzed labelled NCs were compared by Confocal Laser Scanning Microscopy (CLSM) to confirm that the Cu^6 was perfectly encapsulated and not released. The CLSM microphotographs were taken using a Leica TCS-SP5X-AOBS microscope with a white laser (470-670 nm) and a UV laser (Leica), using LAS AF software (Leica Application Suite Advanced Fluorescence) and a 63X objective (PL oil APO63x /NA1.4-0.6 CS). The data were obtained using a green channel ($\lambda(Cu^6)$ = 455/461 nm ($\lambda_{Exc/Em}$)). Furthermore, Ma excipient was labelled with Bodipy® (λ(Bodipy®) = 558/568-651 nm, ($\lambda_{Exc/Em}$)) (Ma^B) (1 mg/mL of Bodipy® in DMSO) by addition of the fluorophore to the Ma solution (0.32 µg Bodipy®/1 mg Ma) under mild magnetic stirring for 2 h at room temperature. Then, the Cu^6-NCs were added to the Ma^B solution and were mixed for 1 h, before their spray-drying.

The powders samples were visualized by CLSM (Leica TCS-SP5X-AOBS microscope with LAS AF Leica Application Suite Advanced Fluorescence software, using an objective HCX PL APO CS 63.0x1.30 GLYC 21°C UV). Images were captured using separate channels. The grayscale images were colored with green for Cu^6 and red for Bodipy® and were overlapped to get a multicolor image.

3.13. Release of NCs from dry powders

Amounts of 100 mg of powders were incubated in 3 mL of MilliQ water or simulated pulmonary medium (0.1% Curosurf® in 10 mM PBS (*v/v*, pH = 7.4)) under magnetic stirring (300 rpm, CIMAREC i Multipoint, ThermoFisher Scientific, Madrid, Spain) at room temperature and 37 °C, respectively. At different times (0, 0.5, 1, 2 and 4 h), the released NCs were analyzed to determine their size and ζ-potential using a Zetasizer, as previously described (n = 3). The NCs morphology was observed in samples obtained at 1 h post-release in MilliQ water by TEM, as indicated above.

3.14. Stability of NCs in cell growth medium

The stability of CS NCs and HA/CS NCs was checked in MilliQ water (control), in Dulbecco's Modified Eagle Medium (DMEM) without supplementation and in DMEM supplemented with 200 mM L-Glutamine and 10% (*v/v*) Fetal Bovine Serum (FBS). For that purpose, suspensions of CS NCs and HA/CS NCs (2.74 mg/mL) were diluted in the different media (1:10 (*v/v*)) and mixed under gentle magnetic stirring (300 rpm) (CIMAREC i Multipoint, Fisher Scientific, Spain) at 37 ºC. At different times (0, 2 and 4 h), an aliquot of each sample was characterized in terms of particle size and standard deviation, fixing the temperature at 37 °C and the attenuator at 7. The NCs are considered stable if their sizes remain in the nanometric range. The study was carried out in triplicate (n = 3).

3.15. *In vitro* studies in the A549 cell line

A549 cell line was used in the cell passes from 12 to 32. Cells were grown in 10 mL plates (with TC treated surface), in a humidified incubator (inCu saFe Cooper Alloy Stainless) with 5% CO_2/95% atmospheric air at 37 °C, using DMEM supplemented with 200 mM L-Glutamine and 10% (*v/v*) FBS. *In vitro* cell studies were carried out using CS-based NCs and Ma separately and not in form of micro-nanostructured platform. This is because *in vivo* the Ma dissolves very rapidly, releasing the NCs that are the ones that, together with the dissolved Ma, really interact with the pulmonary cells.

3.15.1. Viability studies

CS NCs and HA/CS NCs were dialyzed overnight (Spectra/Por® 3 Dialysis Membrane Standard RC Tubing MWCO: 3.5 kD) to remove possible residues. Then, NCs were characterized to confirm the preservation of their physicochemical characteristics (n = 3).

To evaluate the initial viability of the A549 cells after incubation with the nanosystems, a preliminary study with Luna II (Luna II™ Automated Cell Counter, Logos Biosystems, USA) was carried out. For that purpose, 400 µL of cells in supplemented DMEM were seeded in 24-well plates (Falcon®, USA) at a density of 60000 A549 cells/well and incubated in the humidified incubator with 5% CO_2 and 95% atmospheric air at 37 °C until confluence (48 h). Then, the culture medium was removed and cells were treated as follows: (i) 40 µL of sterile filtered MilliQ water with 360 µL of supplemented DMEM (1:10) (positive control), (ii) 55.2 µg/well of CS NCs or HA/CS NCs until a final volume of 400 µL of supplemented DMEM and (iii) a mixture of 40 µL of 1% (*v/v*) Triton with 360 µL of supplemented DMEM (1:10) (negative control). After 4 h of incubation, cells were washed three times with 350 µL of 1X PBS (pH: 7.4) and subsequently detached by incubation with 120 µL of Trypsin for 5 min. Then, 280 µL of supplemented DMEM was added to each well in order to deactivate the Trypsin and the cells were

collected and centrifuged for 5 min at 1477 rpm (Eppendorf 5415R Refrigerated Centrifuge, Germany). The pellets were resuspended in 500 µL of 1X PBS (pH: 7.4) (supplemented with 10% (*v/v*) FBS). 10 µL of each sample were mixed homogeneously with 10 µL of (0.4%, *w/v*) Trypan Blue Stain. Finally, 10 µL of each mixture were loaded in a counting chamber to obtain images of the living and dead cells. The viability percentages of the cells incubated with the systems were obtained by automated counting in each image, taking into account the images of the positive and negative controls (n = 3).

Subsequently, another cell viability study was performed to check the cells recovery at 24 and 48 h after 4 hours of incubation with CS NCs, HA/CS NCs and Ma excipient. This study was carried out by seeding 9000 A549 cells/well in 96-well plates (Corning Incorporated costar®, USA) in a final volume of 100 µL of supplemented cell culture medium. After 48 h of incubation in a humidified incubator with 5% CO_2/95% atmospheric air at 37 °C, the cells were confluent. Then, the medium of each well was replaced with 90 µL of fresh supplemented cell culture medium and 10 µL of: (i) sterile filtered MilliQ water (positive control), (ii) 1% (*v/v*) Triton (negative control), and (iii) suspensions of NCs (CS or HA/CS) to obtain the following concentrations: 2.74, 0.69, 0.18, 0.05, 0.02, 0.005, 0.001 mg/mL (n = 4). In the case of the excipient, a 15% (*w/v*) Ma solution was directly prepared in supplemented DMEM, being the analyzed final concentrations of: 15, 3.75, 0.94, 0.23, 0.059, 0.015, 0.0037 mg/mL. The cells were incubated during 4 h at the same conditions with the controls and the systems. Then, the media were removed and the cells were washed three times with 1X PBS (pH: 7.4). Once the PBS was eliminated, 100 µL of fresh supplemented DMEM was added. The A549 cells were incubated for 24 and 48 h in the humidified incubator. Later, 20 µL of CellTiter-Blue® was added to each well in dark conditions. The cells were incubated in the same conditions during 3 h. This product was added to quantify the metabolic capacity of live A549 cells by reducing of the resazurin reagent of the CellTiter-Blue® (dark blue color) to resorufin (pink color). Finally, 50 µL of 3% (*w/v*) sodium dodecyl sulfate (SDS) was added to each well (30 min) to stop the reaction and to lysate the cells. Lysed samples

were transferred to a dark-bottom 96-well plate to measure the fluorescence emitted by resorufin. The fluorescence signal was measured at $\lambda_{Ex/Em}$: 539/620 nm by microplate reader (SYNERGY H1M BioTek®) with the Gen5 (Image Software BioTek®) program. The percentage of cell viability (%) was calculated as follows:

$$\text{Cell viability (\%)} = \frac{\text{Sample fluorescence}}{\text{Positive control fluorescence}} \times 100 \qquad (7)$$

3.15.2. Study of intracellular uptake

For the cell internalization study, 400 µL of cells in supplemented DMEM were seeded in 24-well plates (Falcon®, USA), corresponding to 60000 A549 cells/well, on polylysine-treated coverslips (Poly-L-Lysine Cellware 12 mm round Coverslips, Corning® BioCoat™). Cells were incubated in a humidified incubator for 48 h. Once the cells were confluent, the culture medium was substituted by: (i) 400 µL of supplemented DMEM (control) and (ii) 55.2 µg/well of Cu^6-CS NCs or Cu^6-HA/CS NCs until a final volume of 400 µL of supplemented DMEM. Cells were incubated for 4 h as described above. Afterwards, cells were washed three times with 350 µL of 1X PBS (pH: 7.4). Cells were fixed by adding 350 µL of 10% (*v/v*) neutral buffered formalin for 15 min. Then, the washing process was repeated three times with 350 µL of 1X PBS (pH: 7.4). Cell nuclei were labelled by adding 200 µL of a dilution 1:1000 (*v/v*) of DAPI (1 mg/mL in 1X PBS) for 30 min. The cells were washed three times again with 350 µL of 1X PBS (pH: 7.4) to eliminate the excess of DAPI. The covers were placed on slides, using Fluoromount® (Thermo Fisher Scientific, Spain). Samples were observed by confocal laser scanning microscopy (CLSM) (Leica TCS SP5 X, Germany) using an objective HCX PL APO CS 63.0 x 1.30 GLYC 21°C UV and a white light laser. The fluorescent emissions from Cu^6 ($\lambda_{Ex/Em}$ = 455/461 nm) and DAPI ($\lambda_{Ex/Em}$ = 405/414-440 nm) were captured and the images were colored with green for Cu^6 and blue for DAPI, and overlapped to get a multicolor image, using the LAS X Life Science Software.

3.15.3. Quantification of A549 cells containing NCs

To quantify the A549 cells that have internalized CS NCs and HA/CS NCs, the Fluorescence-Activated Cells Sorting technique (FACS) was employed using dialyzed Cu^6-CS-based NCs.

A number of 60000 A549 cells/well were seeded in 24-well plates (Falcon®, USA), and incubated in a humidified incubator with 5% CO_2/95% atmospheric air at 37 °C for 48 h. When the cells were confluent, the culture medium was replaced by: (i) 400 µL of supplemented DMEM (control) and (ii) 55.2 µg/well of CS NCs or HA/CS NCs until a final volume of 400 µL of supplemented DMEM (n = 3). Cells were incubated for 4 h at the same conditions. Afterwards, cells were washed three times with 350 µL of 1X PBS (pH: 7.4). When the PBS was removed, 200 µL of LIVE/DEAD™ fixable Aqua (dead cell stain reagent diluted in 1X PBS (1 µL of Aqua in 2 mL of the PBS, *v/v*)) were added for 15 min. Then, the cells were again washed three times with 1X PBS. They were detached by incubation with 120 µL of Trypsin for 5 min. Next, 280 µL of supplemented DMEM was added to deactivate the Trypsin and the cells were isolated by centrifugation for 5 min at 1477 rpm (Eppendorf 5415R Refrigerated Centrifuge, Germany). The supernatant was removed and the pellet was resuspended in 500 µL of 1X PBS (pH: 7.4) (supplemented with 10% (*v/v*) FBS). A minimum of 10000 events were excited at 488 nm using filters BP 525/50 for Cu^6 and BP 515/20 for Aqua viability reagent. It was employed the detector forward scatter (FSC-A) by Accuri Becton Dickinson cytometer (BD Accuri™), using a BD sample software (BD Biosciences, CA). To avoid false positives due to Cu^6 signal overlapping with the Aqua signal, "color compensation" was applied (data not shown), being the corrections of: 17.62%, 18.25% and 18.05% for the first, second, and third replicates, respectively, of the cells treated with Cu^6-labelled NCs.

3.16. *In vivo* studies

In vivo studies were made in accordance with the Principles of Laboratory Animal Care of the University of Santiago de Compostela and Faculty of Pharmacy of the University of Lisbon, and approved by the competent national authority, Direção Geral de Alimentação e Veterinária (DGAV) of Portugal in accordance with the EU Directive (2010/63/UE) for use and care of animals in research. Rats (female Wistar-Kyoto, 7 months old, 200-250 g) were provided by Charles River (Barcelona, Spain). This animal model was chosen for the *in vivo* studies due to the good results previously obtained [231] and, unlike other species such as Sprague, Wistar Kyoto rats have a clear lung tissue that lets the detection of possible results. To carry out the *in vivo* studies, the fewest number of rats was employed. They were aleatory separated in boxes of two animals per cage and stayed with air-conditioned at 20-24 °C with a 12 h light/dark cycle and had free access to water and food before and after the powder administration. Rats were anesthetized with a saline solution of ketamine and xylazine by inguinal injection (right groin). Anesthetized rats were positioned with the ventral side upwards, and the trachea was exposed by means of a longitudinal incision in the neck to administer the powder formulations. Samples of 20 mg of each dry powder were administered through a tracheal cannula (adaptor in Y, opening of 1.3 mm) connected to a Harvard® ventilator (Inspira ASV 55-7058, 80 breaths/min, tidal volume = 1.53 cm^3, Harvard Apparatus, Holliston, USA), simulating the physiological breathing mode of rats.

3.16.1. Lung distribution of microencapsulated NCs

For this study, the CS-based NCs were labelled with Coumarin 6 (Cu^6) (Cu^6-CS NCs and Cu^6-HA/CS NCs). For that, 4.5 µL of Cu^6 (10 mg Cu^6/mL dichloromethane) was added and homogenized in the oil phase during the NCs preparation. Cu^6-NCs were characterized in terms of size and ζ-potential, as described above. Prior to their microencapsulation in Ma MS, the labelled NCs were dialyzed overnight using a dialysis membrane (Spectra/Por® 3 Dialysis

Membrane Standard RC Tubing MWCO: 3.5 kD) to remove possible non-encapsulated Cu^6 residues and their physicochemical properties were characterized again. To verify that there was no release of Cu^6 from the nanosystems, the pre-dialyzed labelled NCs (with presence of non-encapsulated Cu^6 residues) and the dialyzed labelled NCs were compared by confocal laser scanning microscopy (CLSM). The photographs were taken using a microscope Leica TCS-SP5X-AOBS with a white laser (470–670 nm) and a UV laser (Leica) with LAS AF (Leica Application Suite Advanced Fluorescence) software, using a 63X objective (oil PL APO63x/N.A.1.4-0.6 CS). Data were collected using a green channel (Cu^6 emission, λ_{Em} = 455–461 nm).

Amounts of 20 mg of dry powders (including 1.4 mg of NCs) were administered in all the cases. At 1 h post-administration, the thoracic cavities of the rats were exposed and a microinfusor was deeply inserted into the left ventricle. The right atrium was cut to allow the movement of the administered fluids. Firstly, 100 mL of a solution of 0.1% rhodamine in PBS (pH = 7.4) was introduced through a peristaltic pump (Spetec GmbH, Perimax 12, Erding, Germany) at a flow rate of 20 mL/min. Then, the lungs were fixed employing 50 mL of fixing solution (50 mL of PBS containing 0.1% rhodamine, 0.6% formaldehyde and 0.9% glutaraldehyde, pH = 7.4) at a flow rate of 15 mL/min. Thereafter, the lungs were removed and fixed externally for 48 h in 100 mL of 10% buffered neutral formalin. Next, the upper right lobe was sectioned in cuts (50 and 60 μm thick) because it was expected to have the highest amount of formulation [231]. The cuts were placed over a holder and covered with a glass coverslip with an aqueous mounting medium (Fluoromount®) to be observed by CLSM. The photographs were taken using a microscope Leica TCS-SP5X-AOBS with a white laser (470-670 nm) and a UV laser (Leica) with LAS AF (Leica Application Suite Advanced Fluorescence) software, using a 63X objective (oil PL APO63x/N.A.1.4-0.6 CS). Data were collected employing sequential mode using green channel (Cu^6 emission, λ_{Em} = 455-461 nm) and red channel (rhodamine emission, λ_{Em} = 553-627 nm), and were superimposed to get a multi-colored image.

3.16.2. *In vivo* gene expression study

pCMV-βGal-CS NCs-loaded Ma MS and pCMV-βGal-HA/CS NCs-loaded Ma MS, as well as the controls (CS NCs-loaded Ma MS, HA/CS NCs-loaded Ma MS and pCMV-βGal-Ma MS) were intratracheally administered to anesthetized rats following the method described above. After administration, the cannula was removed from the trachea and the rats' necks were surgically sutured employing a surgical suture. At 1 or 2 h post-administration, the rats were allowed to recover from anesthesia. During the next three days, the rats had free access to food and water. Then, the rats were sacrificed and their lungs were removed to study the β-galactosidase expression in lung sections using a method previously described [247] that was adjusted in this study. Briefly, the endogenous β-galactosidase activity was inhibited by incubation of the lung tissues in solutions of pH around 7.4. For that, lung slices were incubated in a solution of 1X PBS for approximately 1 h at room temperature. Next, they were fixed in a 1X solution of 2% formaldehyde and 0.2% glutaraldehyde for 30 min at 4 °C and after, they were incubated again in a 1X PBS solution for 1 h at room temperature. The expression of the encoded β-Gal was studied by the 5-Bromo-4-chloro-3-indolylbeta-D-galactopyranoside (X-Gal) reaction. For that, lung slices were incubated in the X-Gal solution as specified by the β-galactosidase reporter gene staining kit. The cuts of lung tissue were removed from the X-Gal solution at 2 h and were washed in MilliQ water during 10 min at room temperature. Then, the lung sections were stained with Fast Red for 5 min and washed in MilliQ water during 1 min at room temperature. Once the lung samples were dried at room temperature, they were observed by light field optical microscopy in a Leica DMRE7 optical microscope (Leica Microsystems Heidelberg GmbH, Germany), using the HC PL APO CS 20x/0.7 lens.

4. RESULTS AND DISCUSSION

4.1. Preparation of CS-based NCs: Production yield and characterization

Various CS-based NCs formulations (CS NCs, HA/CS NCs, pCMV-βGal-CS NCs and pCMV-βGal-HA/CS NCs) were prepared using the procedure described in the section 3.3. Their theoretical structures are shown in Figure 8.

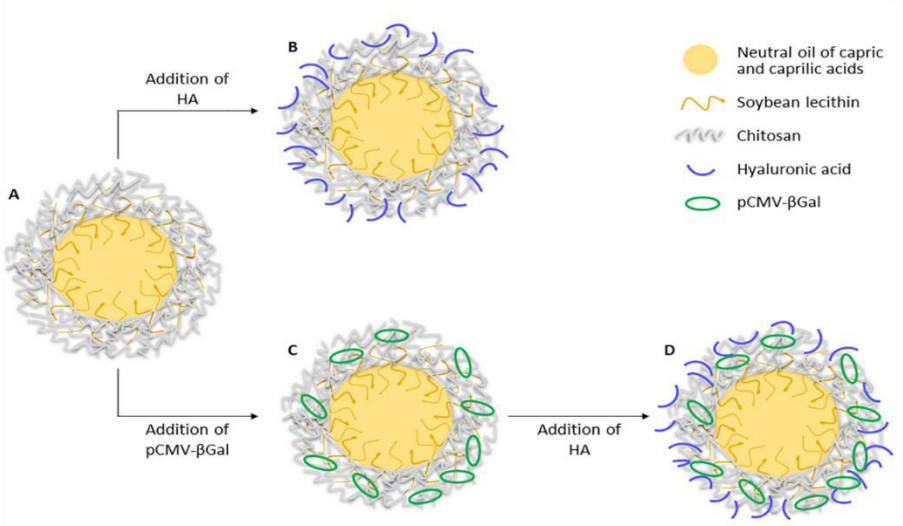

Figure 8. Theoretical structures of: (A) CS NC, (B) HA/CS NC, (C) pCMV-βGal-CS NC and (D) pCMV-βGal-HA/CS NC. (Figure from the work of Fernández-Paz et al. [212], Pharm. 13 (2021) 1377. Open access article distributed under the Creative Commons Attribution License)

As can be seen in Figure 8, CS NCs present the simplest core-shell structure (Figure 8A). They contain an oily core composed of a mixture of neutral oils of capric and caprilic acids, a soybean lecithin interface and a chitosan coating. The lipophilic core is useful for the encapsulation of hydrophobic molecules. The surfactant lecithin plays an important role in the composition of NCs thanks to its amphiphilic nature. It is located on the contact surface of the two apolar-polar phases (core-shell, respectively), providing binding and stability to the NC structure. The CS coating is hydrophilic and gives positive charge to the surface of the NCs. It allows to load negative molecules, such as

HA (Figure 8B), plasmid (Figure 8C) or both (Figure 8D). HA was incorporated on the NCs surface in order to improve the transfection properties. Therefore, CS-based NCs constitute versatile nanosystems for the simultaneous transport of molecules of different nature, thanks to their structure and composition. In fact, we have prepared NCs that simultaneously incorporate plasmid and the antibiotic rifabutin, on the surface and into the core of the NCs, respectively (data not shown).

As shown in Table 6, CS NCs present a particle size of about 160 nm and a positive ζ-potential of approximately +56 mV. The electrostatic association of HA (negatively charged) on their surface caused a slight reduction in size up to 154 nm and a decrease in the ζ-potential to +35 mV, remaining positive. These results could be explained by the electrostatic interaction between the amino groups of CS (positively charged) and the carbonyl groups of the HA (negatively charged), and are consistent with those of NPs prepared with CS, HA and TPP [248,249], in which keeping constant the TPP content, the size and ζ-potential of the NPs decreased as the amounts of HA increased with respect to CS.

When pCMV-βGal was added to the CS NCs, the size of the nanostructures was barely modified (from 160 nm to 165 nm for CS NCs and pCMV-βGal-CS NCs, respectively); while for the HA-containing NCs, slightly increased (from 154 nm to 162 nm for HA/CS NCs and pCMV-βGal-HA/CS NCs, correspondingly) (see Table 6). The ζ-potentials slightly decreased when the plasmid was associated to the NCs, being of approx. +56 mV to +54 mV for unloaded and plasmid-loaded CS NCs, respectively; and of +35 mV to +29 mV for unloaded and plasmid-loaded HA/CS NCs, correspondingly. The decrease of ζ-potential is explained by the electrostatic interaction between the plasmid (negatively charged) and the CS (positively charged). Slight decreases in ζ-potentials were also observed for CS/TPP NPs with increasing amounts of pDNA [75].

In order to determine the *in vivo* lung distribution of the powders, the CS NCs and HA/CS NCs were labelled with Cu^{6} and were dialyzed previously to their microencapsulation in Ma MS, as indicated in the Methodology section. The labelling of NCs with Cu^{6} hardly affected to their physicochemical properties. Both size and ζ-

potential of pre-dialyzed Cu^6-labelled NCs kept practically the same as those of the unlabeled NCs (see Table 6). The dialysis process did not affect to the size of Cu^6-labelled NCs but produced a reduction of their ζ-potentials of almost 18 mV and 11 mV for the Cu^6-CS NCs and Cu^6-HA/CS NCs, respectively, compared with their pre-dialyzed forms. This could be explained by the elimination of NCs remnants components, probably CS polymeric filaments (positively charged), which were in excess after the NCs formation.

Furthermore, it is very important to notice that all the formulations that contains HA present a decrease of size and of ζ-potential with respect to their counterpart without HA (Table 6). It is due to the electrostatic interactions of the HA to the NCs surface. This binding is more significantly corroborated in the case of the dialyzed NCs. When NCs are dialyzed, the possible debris, impurities and unbound CS and HA are eliminated. Anyway, the dialyzed Cu^6-HA/CS NCs presented a smallest size and a decrease in ζ-potential with respect to the dialyzed Cu^6-CS NCs (Table 6), which indicates that HA remained attached to the NCs.

The production yields were around 83% and 79% for the CS NCs and pCMV-βGal-CS NCs, respectively. However, they were lower, but still acceptable, around 67% and 65% for the HA/CS NCs and pCMV-βGal-HA/CS NCs, correspondingly (Table 6). It is striking that the formulations prepared with HA had lower yields with respect to their counterparts without HA, but the same was observed for the CS/HA/TPP NPs [248]: as the proportion of HA increased, the yield of the NPs decreased. This can be explained because it has been experimentally found that it is more difficult to isolate the NCs cream when the formulation contains HA, which results in a lower yield.

Table 6. Physicochemical properties and production yields of CS-based NCs (mean ± S.D.; $n = 3$).

Formulation	Size Range (nm)	PdI	ζ-Potential Range (mV)	Production Yield (%)
CS NCs	160 ± 3	0.19	+56.5 ± 1.4	83 ± 4
HA/CS NCs	154 ± 2	0.15	+34.7 ± 0.8	67 ± 7
pCMV-ßGal-CS NCs	165 ± 4	0.25	+54.0 ± 1.6	79 ± 6
pCMV-ßGal-HA/CS NCs	162 ± 3	0.21	+29.2 ± 1.2	65 ± 8
Pre-dialyzed Cu^6-CS NCs	161 ± 2	0.21	+57.4 ± 0.6	-
Pre-dialyzed Cu^6-HA/CS NCs	155 ± 1	0.16	+37.5 ± 0.4	-
Dialyzed Cu^6-CS NCs	162 ± 1	0.20	+39.6 ± 0.1	-
Dialyzed Cu^6-HA/CS NCs	156 ± 2	0.15	+26.2 ± 0.1	-

NCs exhibited a spherical morphology with the presence of a core-shell structure as revealed by TEM for the representative formulations (Figure 9). The incorporation of HA produced a change in the appearance of the NCs surface, where HA chains can be appreciated on their surface, generating an external layer (comparison of Figure 9B and Figure 9A). These NCs are similar to other CS-based NCs previously prepared [250-252]. For other hand, the incorporation of pCMV-βGal in the CS NCs modified the appearance of their structure, being the shell more fluted and producing invaginations towards the interior of the core. The presence of lecithin (amphiphilic) allowed the flexibility and deformation of the core-shell interface, maintaining the binding and the stability of the NC structure (Figure 9C). On the other hand, the pCMV-βGal-HA/CS NCs (Figure 9D) adopted a more compact conformation with respect to the HA/CS NCs (Figure 9B). The structures of the representative systems (Figure 9) are consistent with those described in the theoretical scheme (Figure 8), except for the pCMV-βGal-HA/CS NCs, being more compact (Figure 9D).

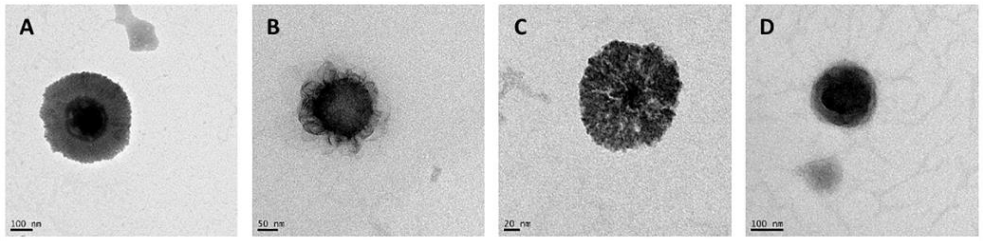

Figure 9. Transmission electron microscopy (TEM) microphotographs of freshly prepared: (A) CS NC, (B) HA/CS NC, (C) pCMV-βGal-CS NC and (D) pCMV-βGal-HA/CS NC. (Figure from the work of Fernández-Paz et al. [212], Pharm. 13 (2021) 1377. Open access article distributed under the Creative Commons Attribution License)

4.2. Determination of the pCMV-βGal association to the NCs

The ability of the NCs to associate pCMV-βGal was demonstrated by the agarose gel electrophoresis method (Section 3.6.), using increasing amounts of plasmid up to 100% (*w/w*) with respect to the total amount of CS used in the preparation of the NCs. As can be seen in the gels shown in Figure 10, corresponding to CS NCs (Figure 10A) and HA/CS NCs (Figure 10B), the free plasmid (in the first well) ran freely, while the control NCs (without plasmid) remained immovable in the second well. However, in presence of both CS NCs and HA/CS NCs, the plasmid stayed bound to the NCs without running from the well (as can be seen in the third and following wells) up to 40% (*w/w*) of plasmid (pointed by arrows in both images of Figure 10A,B). These results reveal a strong plasmid-to-NCs association. With amounts of plasmid higher than 40%, the excess of plasmid ran freely from the wells. Therefore, the decision was made to incorporate pCMV-βGal in the NCs with a theoretical percentage of 40% (*w/w*).

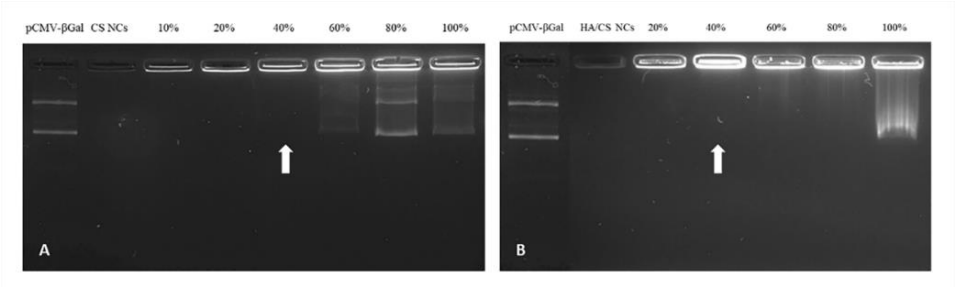

Figure 10. Association of pCMV-βGal to: (A) CS NCs and (B) HA/CS NCs by agarose gel electrophoresis (1% agarose), at different percentages (up to 100%) with respect to the total amount of CS employed to prepare a batch of NCs. (Figure from the work of Fernández-Paz et al. [212], Pharm. 13 (2021) 1377. Open access article distributed under the Creative Commons Attribution License)

To further characterize the association of the plasmid to the NCs, it was quantified by fluorimetry (using a Qubit®, Section 3.7.) the concentration of free plasmid of the supernatant liquid of the centrifuged plasmid-loaded NCs suspension. The E.E. and D.L. of the NCs (see Table 7) were high and similar for both pCMV-βGal-CS NCs and pCMV-βGal-HA/CS NCs (pCMV-βGal-CS NCs: 91% and 36%, respectively; pCMV-βGal-HA/CS NCs: 89% and 36%, correspondingly). These results are consistent with those of CS/TPP NPs loaded with pDNAs (pEGFP-C1 and pCMVβ-Gal) (70%–100%) [75], HA/CS NPs loaded with pDNA (pEGFP-C1) (87%–99%) [249] and HA/CS NPs loaded with siRNA (Luciferase-specific duplex siRNA) (> 95%) [82]. In the last case, although both types of nanostructures (CS-based NCs and CS-based NPs) presented the same CS and HA, the molecular structure of the genetic material was different, being much larger in the case of the plasmid (7164 bp) with respect to siRNA (21 bp), which could influence in the slightly lower E.E. of the CS-based NCs compared to the CS-based NPs.

Table 7. Encapsulation efficiency (E.E.) and drug loading (D.L.) of pCMV-βGal to the CS-based NCs (mean ± S.D.; $n = 3$).

Formulation	E.E. (%)	D.L. (%)
pCMV-βGal-CS NCs	90.6 ± 0.9	36.2 ± 0.4
pCMV-βGal-HA/CS NCs	89.0 ± 4.8	35.6 ± 1.9

4.3. NCs thermal stability analysis: Heating-cooling ramps

The effect of the temperature on the NCs physicochemical characteristics (size and PdI) was analyzed by DLS (Figure 11), using a heating ramp (from 25 ºC to 90 ºC), followed by a cooling ramp (from 90 ºC to 25 ºC) as was explained in the section 3.8. This study was carried out because the NCs will be subsequently subjected to elevated temperature during the spray-drying process and it is crucial to know their destabilization temperatures.

The initial mean sizes of the CS NCs and HA/CS NCs were of 165 ± 4 nm and 147 ± 10 nm, respectively. In both cases, the heating ramp at 90 ºC induced a decrease in size of 48 nm and 16 nm for CS NCs and HA/CS NCs, correspondingly. In addition, the heating ramp of CS NCs showed a destabilization of the NCs structure after 80.5 ºC, shown by a PdI greater than 0.7. In the case of HA/CS NCs, they were destabilized from a temperature above of 72 ºC, revealed by a PdI of 1. When the temperature returned to 25 ºC, the size of CS NCs decreased, staying 17 nm below the original size, while the size of HA/CS NCs increased to remain about 7 nm above their original size. In other words, during the gradual cooling ramp, the NCs returned approximately to their original sizes. This phenomenon was already reported for SLNs [253,254] in which, after the heating-cooling process, the SLNs could withstand the harsh conditions of temperature change. Surely, in the cooling process, the NCs constituent materials were relocated in function of their charges in the aqueous medium, in such a way that the Miglyol "took refuge" within the CS structure

thanks to the Lecithin interface, adopting the more stable structuring again.

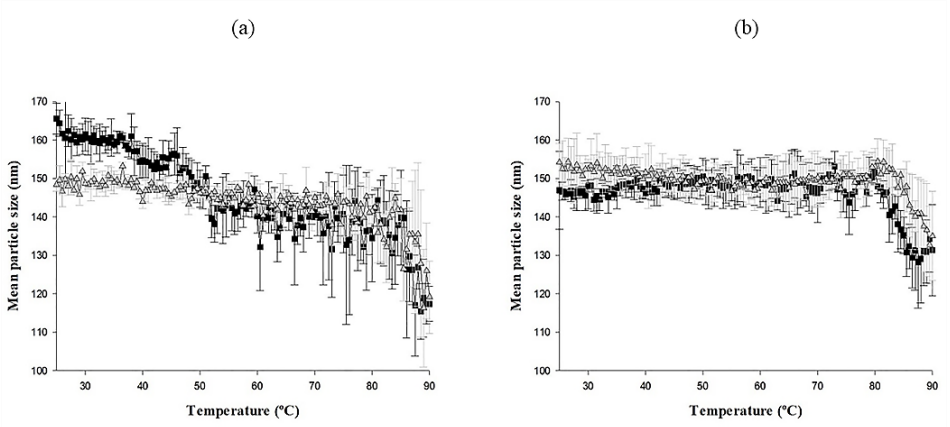

Figure 11. DLS thermograms of: (a) CS NCs and (b) HA/CS NCs, (■) from 25 °C to 90 ºC and (▲) from 90 °C to 25 °C (mean ± S.D., n = 3). (Figure from the work of Fernández-Paz et al. [255], article accepted for publication in Powder Technology)

4.4. Stability of NCs in the spray-drying excipient solution

Ma was selected as spray-drying excipient in previous microencapsulation studies of different NPs, such as: i) CS NPs, ii) SLN, and iii) mesoporous iron (III) trimesate (MIL-100(Fe) MOF), intended for pulmonary administration [120,231,232,238]. Encouraged by the good results, Ma has also been used in this work to microencapsulate NCs by spray-drying (Section 3.9.).

Initially, the size of the CS-based NCs increased about 60 nm and 30 nm for CS NCs and HA/CS NCs, respectively, when they were incubated in the Ma solution (see Figure 12). Later, the CS NCs sizes remained practically constant as the incubation time progressed, while the HA/CS NCs sizes decreased slightly, remaining in both cases above their original values (Table 6) during all the incubation process. In addition, the standard deviations of the CS-based NCs sizes were larger from the beginning until approximately 2 h, being less at 4 h. This suggests that the NCs sizes slightly stabilized over time. On the

other hand, ζ-potentials of both types of NCs were somewhat lower than those of their corresponding fresh forms (not incubated in excipient solution), being a decrease of around 10 mV and 4 mV for the CS NCs and HA/CS NCs, respectively. CS-based NCs kept their ζ-potentials practically constant at time 0 h and at 4 h, being more variable in the case of the CS NCs than HA/CS NCs. However, their standard deviations were very low (almost negligible in Figure 12). The increase in size, as well as the decrease in the ζ-potential, were probably produced by a certain interaction of the Ma excipient (of slight negative charge) with the CS polymeric shells (of positive charge) of the two NCs formulations [232].

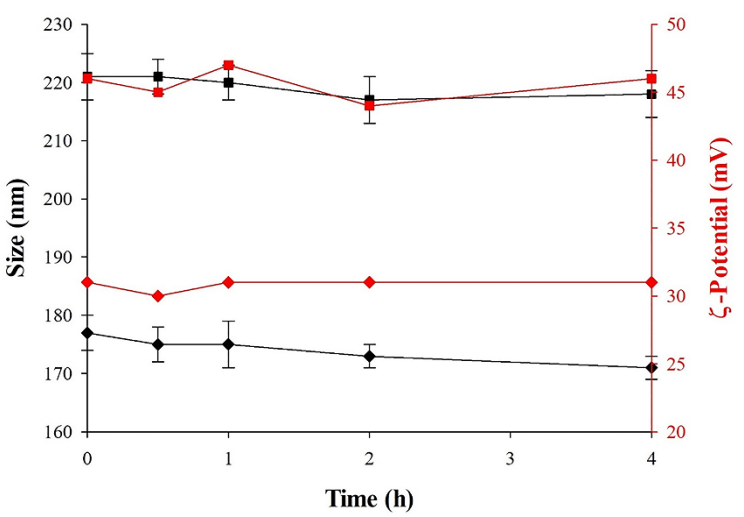

Figure 12. Evolution of sizes (nm) (black) and ζ-potentials (mV) (red) of: CS NCs (square) and HA/CS NCs (diamond) incubated in Ma solution (16%, *w/v*) over time (h) (mean ± S.D., n = 3). (Figure from the work of Fernández-Paz et al. [255], article accepted for publication in Powder Technology)

4.5. Preparation of dry powders

Spray-drying is a simple and rapid microencapsulation procedure that offers numerous advantages in the development of aerosolizable drug delivery systems. For example, it allows the use of different biomaterials to obtain versatile MS with different structures and surface characteristics, which permit controlling the release of drugs, as well as improve the aerosolization and the *in vivo* efficacy [256]. In addition, it has been reported that the spray-drying temperature do not compromises the stability of the encapsulated thermolabile molecules because, in the solvent evaporation process, the evaporated solvent absorbs a great amount of the heat applied to the system [257].

It shoud be taking into account that it is the first time that NCs are spray-dried to obtain dry powders for inhalation. Therefore, and as it was previously mentioned, for the suitable NCs microencapsulation to obtain quality powders, it is crucial to adjust the variables of their spray-dry process (Section 3.10.).

4.5.1. Adjustment of the NCs microencapsulation process

Table 8 shows the variable investigated (second column) at each stage (from 1 to 5, first column) of the NCs microencapsulation adjust process. In each step, the values of the studied variable appear on italic, being the selected value in bold. The other parameters remained unchanged.

Table 8. Investigated variables to adjust the NCs spray-drying process (Nozzle diameter: 0.7 mm, Nozzle cleaner: 5).

Step	Tested variable	Total solids content (*w/w*, %)	Air flow rate (Nl/h)	NCs:Ma ratio (*w/w*, %)	T_{Inlet} (°C)	Aspirator (%)	Flow rate (mL/min)
1	t.s.c.	*2.5*, *5*, *10*, ***11***, *12*	400	1:10	170	75	2
2	Air flow rate	11	*400*, ***600***	1:10	170	75	2
3	NCs:Ma ratio	11	600	*1:10*, ***1:15***	170	75	2
4	T_{Inlet} (T_{Outlet})	11	600	1:15	***105 (~58 °C)*** *170 (~90 °C)*	100[a]	8.8[b]
5	F.R.	11	600	1:15	105	100	***5***, *7*, *8.8*, *10*[c]
Optimal variables		**11**	**600**	**1:15**	**105**	**100**	**5**

T_{Inlet}: Inlet temperature (°C).
[a] Aspirator was increased to 100% to decrease the T_{Outlet}.
[b] F.R. was set at 8.8 mL/min for that the temperature did not affect the samples as much as possible.
[c] F.R. equal or higher than 5 mL/min were tested because lower F.R. lead to too small MS.

In the step 1, the optimal t.s.c. (%) was determined. For that, mixtures of CS NCs suspensions in Ma solutions were prepared with t.s.c. of 2.5%, 5%, 10%, 11% and 12% (*w/w*), and were spray-dried fixing the rest of parameters as described in the step 1 of the Table 8, being selected a t.s.c. of 11%. Next, the optimal air flow rate was identified by comparison between 400 and 600 Nl/h, maintaining the rest of the parameters stablished as showed in step 2 of the Table 8, obtaining the best results at an air flow rate of 600 Nl/h. The CS NCs:Ma ratio was studied by fixing of the other parameters as showed in the step 3 of the Table 8, being compared the ratios of 1:10 (*w/w,* %) and 1:15 (*w/w,* %), getting better MS with a ratio of 1:15. To

maintain a better stability of the NCs (whose core is liquid) it was important to increase the aspirator to 100% to produce a low T_{Outlet} and the F.R. was punctually selected at 8.8 mL/min so that the temperature had less influence on the samples, especially with that spray-dried at 170 °C. The selected T_{Inlets} were 105 ºC (low) and 170 °C (high), keeping the other parameters as indicated in the step 4 of the Table 8, achieving MS of best quality with a T_{Inlet} of 105 °C. The optimal F.R. was determined testing equal or higher values than 5 mL/min (5, 7, 8.8 and 10 mL/min) due to that MS of too small sizes were observed at lower F.R., and the other parameters were maintained as specified in step 5 of the Table 8. Finally, the best F.R. was of 5 mL/min. The complete optimal spray-drying conditions are shown in the bottom row of the Table 8.

In this study, it was observed that the sizes of the MS were not importantly affected by the changes of the investigated variables, being all the sizes comprised between 2.0 – 3.7 µm. For this reason, as mentioned above, only the characteristics of morphology, sphericity and aggregation of the MS were observed in order to select the most appropriate parameters values.

4.5.1.1. Determination of the optimal total solids content (t.s.c.) (%)

Suspensions of CS NCs in Ma solutions were spray-dried with different theoretical total solids content (t.s.c.) in order to identify the most appropriate one from a morphological and size point of view. As can be seen in the Figure 13, as the t.s.c. increased, the MS adopted a more spherical and defined morphology, with less aggregation, reaching the best characteristics when the t.s.c. was of 11% (*w/w*). Above this value, MS were less spherical, more aggregated and heterogeneous. This is the reason why t.s.c. of 11% (*w/w*) was selected as the optimum one for the CS NCs microencapsulation process. This t.s.c. is high compared to those required in other studies intended to the microencapsulation of CS NPs, in which the c.s.t. was of 2.1% - 3% [231,258], surely due to the high influence of the lipidic nature of the nanosystems.

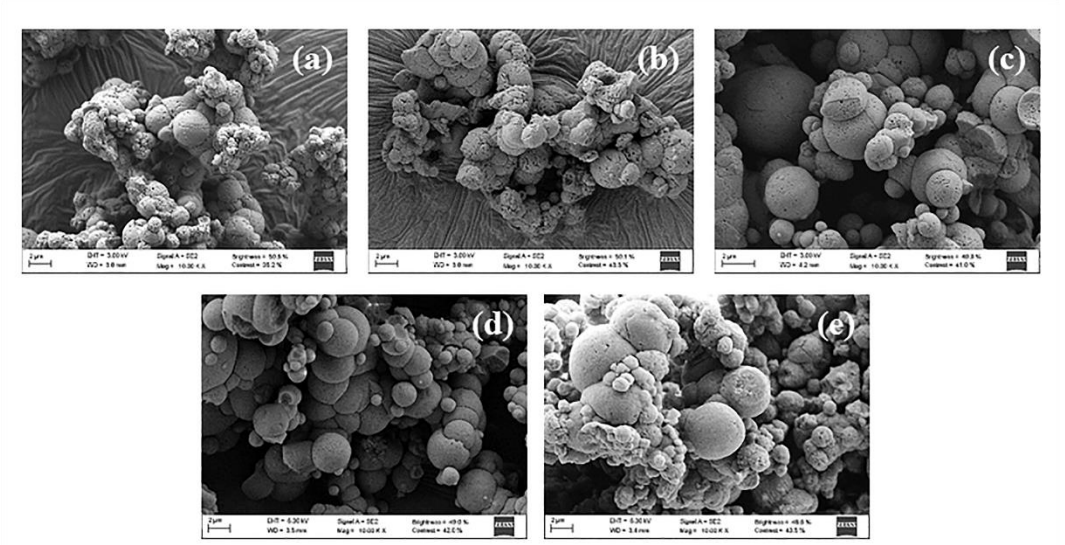

Figure 13. SEM microphotographs of CS NCs-loaded Ma MS with a total solid content of: (a) 2.5% (*w/w*), (b) 5% (*w/w*), (c) 10% (*w/w*), (d) 11% (*w/w*), and (e) 12% (*w/w*), respectively. (Figure from the work of Fernández-Paz et al. [255], article accepted for publication in Powder Technology)

4.5.1.2. Selection of the air flow rate (Nl/h)

The spray-drying was carried out at different pressures (400 Nl/h and 600 Nl/h) in order to find the most suitable one. According to the microphotographs depicted in Figure 14, the highest pressure produced MS more spherical and isolated. This could be explained by the better dispersion of the droplets during the spray-drying. Therefore, the pressure of 600 Nl/h was selected for further studies, being higher than the used for CS-based NPs (400 Nl/h) [231,258]. Perhaps, it is due to the lipidic nature of the NCs, which produces certain differences with respect to polymeric NPs (without oily core).

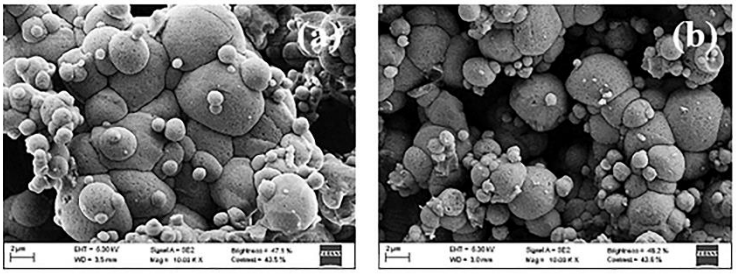

Figure 14. SEM microphotographs of CS NCs-loaded Ma MS spray-dried with a pressure of: (a) 400 Nl/h and (b) 600 Nl/h. (Figure from the work of Fernández-Paz et al. [255], article accepted for publication in Powder Technology)

4.5.1.3. Election of the NCs:Ma ratio (w/w)

Previous studies of NPs microencapsulation [231,258] employed a NPs:Ma ratio of 1:4 (*w/w*). However, when this ratio was used in preliminary studies of this work (data not shown), the MS were not formed. In fact, it is was an insufficient amount of Ma to constitute the MS, so only formed aggregates in form of "scales". Therefore, two ratios with higher proportion of Ma (1:10 and 1:15, (*w/w*)) were selected to improve homogeneity and spherical shape of MS. According to SEM images in the Figure 15, the MS with the 1:15 (*w/w*) ratio had a better and homogeneous appearance than those prepared with the 1:10 (*w/w*) ratio. As conclusion, the 1:15 (*w/w*) ratio was selected as the most suitable for the microencapsulation of CS NCs.

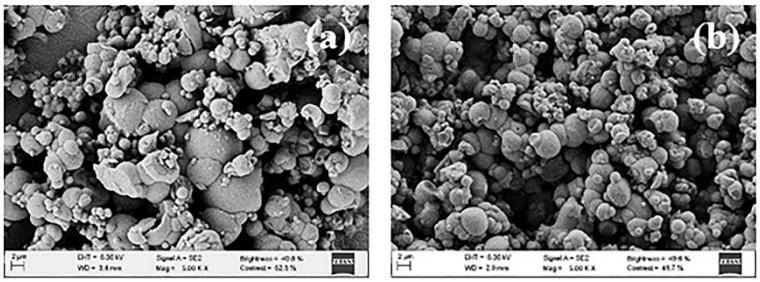

Figure 15. SEM microphotographs of CS NCs-loaded Ma MS with a NCs:Ma ratio of: (a) 1:10 (*w/w*) and (b) 1:15 (*w/w*). (Figure from the work of Fernández-Paz et al. [255], article accepted for publication in Powder Technology)

4.5.1.4. Determination of the suitable T_{Inlet} (°C) and Aspirator (%)

In this study, CS NCs were spray-dried at two different temperatures: 105 ºC and 170 ºC and the Aspirator was directly adjusted to 100% in both cases to favor the decrease of the T_{Outlet}. The Figure 16a shows that the MS prepared at the lowest temperature had more spherical morphology and were less aggregated compared with the MS obtained at the highest temperature (Figure 16b). It could be due to the heat treatment that NCs received during the spray-drying process. When the T_{Inlet} was of 170 °C, the T_{Outlet} was high (> 70 ºC) and, as demonstrated by the thermal stability analysis (Figure 11), the NCs stability could be compromised, at least in part, contributing to the worst appearance of the MS (Figure 16b). On the contrary, when the NCs were spray-dried at 105 ºC, a low T_{Outlet} was ensured (< 70 ºC) and the NCs remained stable, allowing an adequate microencapsulation. The T_{Inlet} selected in the present work (105 °C) was in agreement with the low T_{Inlet} employed for the microencapsulation of SLN (103 °C) and lipid – polymer hybrid NPs (LPNs) (100 °C) already reported [238,259], being these temperatures high enough to evaporate the water from the atomization suspension, generating a T_{Outlet} low enough (< 70 ºC) to avoid the systems destabilization.

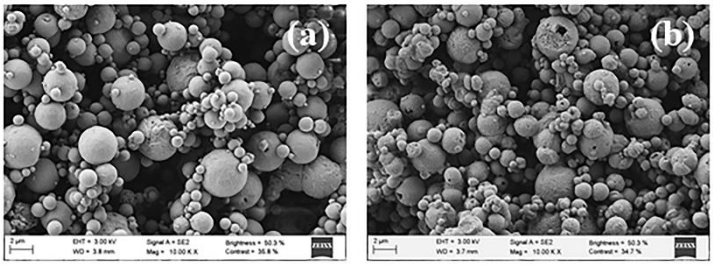

Figure 16. SEM microphotographs of CS NCs-loaded Ma MS spray-dried with a T_{Inlet} of: (a) 105 °C (T_{Outlet} ~58 °C) and (b) 170 °C (T_{Outlet} ~90 °C). (Figure from the work of Fernández-Paz et al. [255], article accepted for publication in Powder Technology)

4.5.1.5. Selection of the optimal flow rate (F.R.) (mL/min)

Different F.R. were tested: 5, 7, 8.8 and 10 mL/min. The MS obtained at low F.R. (2 mL/min) were small (Figures 13 to 15), as it was expected according to the results of previous studies. Figure 17a shows that the MS prepared at F.R. of 5 mL/min are spherical, not aggregated, and have homogeneous size and morphology. As can be appreciated in Figure 17, as the F.R. increased, the MS were less defined, more aggregated and heterogeneous. At a F.R. of 8.8 mL/min, the powder was more humid, being affected the powder quality at a F.R. of 10 mL/min. Considering the results, F.R. of 5 mL/min was selected as the optimal for the microencapsulation of NCs. This F.R. was twice as faster (5 mL/min) that the used for the microencapsulation of CS-based NPs (2.5 mL/min) [231,258], resulting in a shorter exposure time to the T_{Inlet}. Surely, it is due to the lipidic nature of the NCs, that requires lower times of exposure to the T_{Outlet} than CS NPs (more thermoresistant).

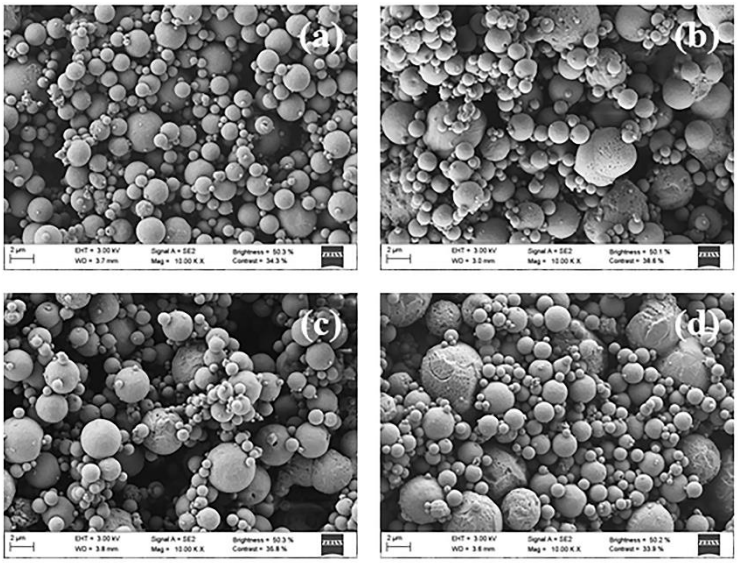

Figure 17. SEM microphotographs of CS NCs-loaded Ma MS spray-dried with a F.R. of: (a) 5 mL/min, (b) 7 mL/min, (c) 8.8 mL/min, and (d) 10 mL/min. (Figure from the work of Fernández-Paz et al. [255], article accepted for publication in Powder Technology)

4.5.2. Preparation and characterization of the dry powder formulations

All dry powder formulations were prepared using the best conditions obtained after adjusting the NCs spray-drying process. The prepared formulations are: Ma MS, CS NCs-loaded Ma MS, HA/CS NCs-loaded Ma MS, pCMV-βGal-Ma MS, pCMV-βGal-CS NCs-loaded Ma MS and pCMV-βGal-HA/CS NCs-loaded Ma MS.

The $T_{Outlets}$ (°C) and P.Y. (*w/w*, %) of the spry-drying processes are collected in the Table 9. As expected, the $T_{Outlets}$ were low (between 55 and 60 °C), suitable for the NCs microencapsulation. In addition, the obtained yields oscillated between 64% and 71%, approximately. These values were high and similar to those reported for the spray-drying of CS-based NPs (CS/TPP NPs, CS/HA/TPP NPs, CS/carboxymethyl-β-cyclodextrin/TPP NPs) (65–70%)

[231,235,248,260], of more compact structure (without liquid oily core) and whose spray-drying temperatures were as high as 160 and 170 °C. Furthermore, the obtained P.Y. were higher than those resulting from the microencapsulation of nanostructures containing lipids, e.g., lipid/CS NPs complexes (approx. 50%) [261] and SLN made of glyceryl tristearate or glyceryl dibehenate (47% to 60%) [238], which were also prepared using a low spray-drying temperature (103 °C) [238].

Table 9. Outlet temperatures ($T_{Outlets}$) and process yields (P.Y.) of the powder samples obtained by spray-drying (feed rate: 5 mL/min, aspirator: 100%, nozzle diameter: 0.7 mm, nozzle cleaner: 5, inlet temperature (T_{Inlet}): 105 ± 2 °C and air flow rate: 600 Nl/h) (mean ± S.D.; n = 3).

Dry Powder	T_{Outlet} (˚C)	P.Y. (*w/w*, %)
Mannitol (Ma) microspheres (MS)	56	64 ± 3
CS NCs-loaded Ma MS	60	67 ± 5
HA/CS NCs-loaded Ma MS	58	67 ± 6
pCMV-βGal-Ma MS	57	70 ± 5
pCMV-βGal-CS NCs-loaded Ma MS	55	69 ± 8
pCMV-βGal-HA/CS NCs-loaded Ma MS	58	71 ± 8

SEM microphotographs (Figure 18) show that individual Ma MS were spherical, somewhat heterogeneous in size, with well-defined limits (Figure 18A). When the CS NCs or HA/CS NCs were included in the Ma MS (Figure 18B,C, respectively), it is important to note that the resulting micro-nanostructures, in addition to being spherical and presenting well-defined limits, were comparatively less aggregated and smaller in size than the previous ones. As expected, the inclusion of plasmid in the MS (pCMV-βGal-Ma MS, pCMV-βGal-CS NCs-

loaded Ma MS and pCMV-βGal-HA/CS NCs-loaded Ma MS) (Figure 18D-F, correspondingly) did not affect their characteristics.

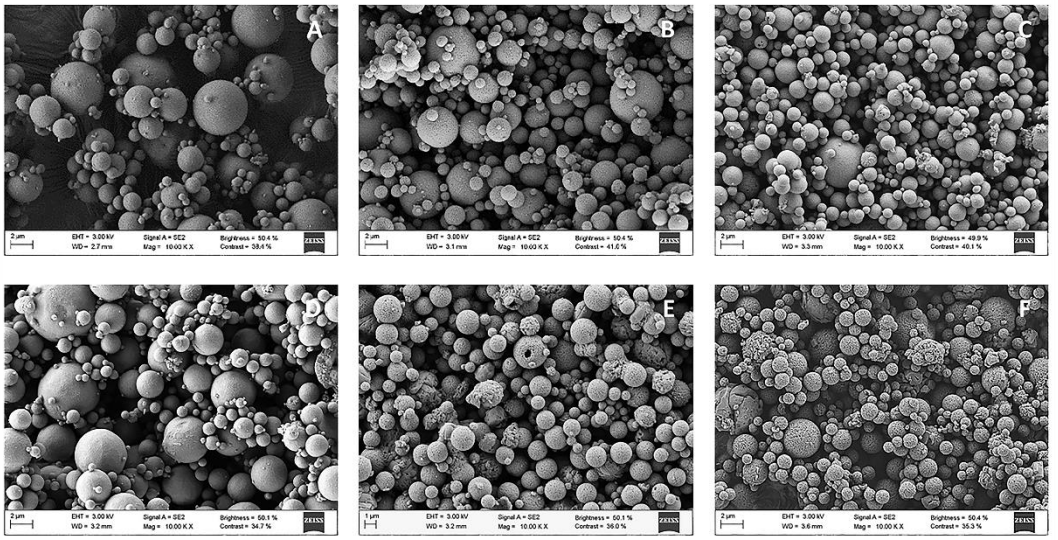

Figure 18. Scanning electron microscopy (SEM) microphotographs of: (A) Ma MS, (B) CS NCs-loaded Ma MS, (C) HA/CS NCs-loaded Ma MS, (D) pCMV-βGal-Ma MS, (E) pCMV-βGal-CS NCs-loaded Ma MS and (F) pCMV-βGal-HA/CS NCs-loaded Ma MS. (Figure from the work of Fernández-Paz et al. [212], Pharm. 13 (2021) 1377. Open access article distributed under the Creative Commons Attribution License)

In addition, all types of MS were generally solid. However, some of the largest obtained were hollow, as the SEM microphotographs showed in the Figure 19. This is consistent with some of the bigger CS NPs-loaded Ma MS, whose hollowness of some broken MS also could be seen [120]. The appearance of some large MS is a random process. Their large holes could be explained by the distribution adopted by the Ma when it is in higher proportion with respect to the nanosystems. At this point, the Ma generates MS of big structure, whose NCs charge is distributed in the Ma shell, but totally lacking of the internal framework of Ma carrying the nanosystems.

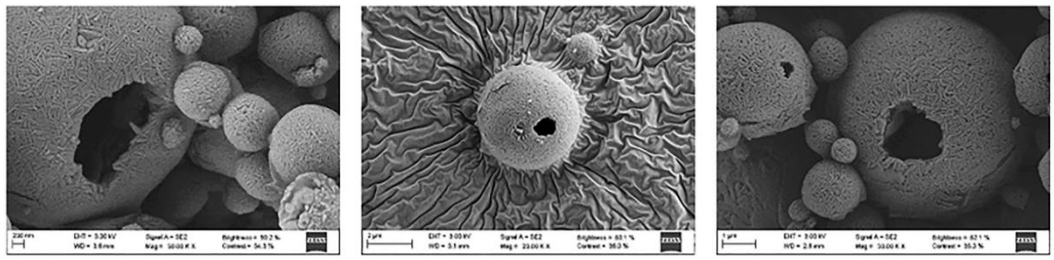

Figure 19. SEM microphotographs of hollow CS NCs-loaded Ma MS. (Figure from the work of Fernández-Paz et al. [255], article accepted for publication in Powder Technology)

Dry powders were characterized in terms of geometric diameter (μm), apparent and real densities (g/cm^3) and theoretical aerodynamic diameter (μm). CS NCs- and HA/CS NCs-loaded Ma MS showed geometric diameters of around 2.10 μm and 2.77 μm, respectively (Table 10), being smaller than that of the control MS (without NCs), whose geometric diameter was of 3.75 μm. The incorporation of pCMV-βGal in the MS (pCMV-βGal-Ma MS, pCMV-βGal-CS NCs-loaded Ma MS and pCMV-βGal-HA/CS NCs-loaded Ma MS) hardly affected their geometric diameters. The apparent density of the Ma MS (approx. 0.50 g/cm^3) was higher than those of the NCs-loaded Ma MS (CS NCs-loaded Ma MS: 0.44 g/cm^3 and HA/CS NCs-loaded Ma MS: 0.42 g/cm^3), but their real density was lower (Ma MS: 1.29 g/cm^3 and NCs-loaded Ma MS: 1.43 g/cm^3). The higher geometric diameter and lower real density of Ma MS compared to the NCs-loaded Ma MS, suggests that the structure of the Ma MS is less compact and more porous than those of the NCs-loaded Ma MS.

Table 10. Physical and aerodynamic properties of the powder samples obtained by spray-drying (feed rate: 5 mL/min, aspirator: 100%, nozzle diameter: 0.7 mm, nozzle cleaner: 5, T_{Inlet}: 105 ± 2 °C and air flow rate: 600 Nl/h) (mean ± S.D.; n = 3).

Dry Powder Samples	Geometric Diameter (μm)	Apparent Density (g/cm^3)	Real Density (g/cm^3)	Theoretical Aerodynamic Diameter (μm)
Ma MS	3.75 ± 1.56	0.50 ± 0.01	1.29 ± 0.01	4.21 ± 0.01
pCMV-βGal-Ma MS	2.85 ± 1.49	-	-	-
CS NCs-loaded Ma MS	2.10 ± 0.86	0.44 ± 0.02	1.43 ± 0.01	2.51 ± 0.02
pCMV-βGal-CS NCs-loaded Ma MS	1.98 ± 0.70	-	-	-
HA/CS NCs-loaded Ma MS	2.77 ± 1.35	0.42 ± 0.02	1.43 ± 0.02	3.35 ± 0.02
pCMV-βGal-HA/CS NCs-loaded Ma MS	2.43 ± 1.32	-	-	-

The Ma MS showed a higher theoretical aerodynamic diameter (4.21 μm) than the NCs-loaded Ma MS (CS NCs-loaded Ma MS: 2.51 μm and HA/CS NCs-loaded Ma MS: 3.35 μm). This was expected taking into account the direct relationship between the D_g and the theoretical D_{aer} (see formula in section 3.11.3.). To achieve an adequate pulmonary delivery, the MS must have approximately an aerodynamic diameter between 1–5 μm [108,262-264]. If they are smaller than 1 μm, the particles will be expelled with the air, but if they are greater than 5 μm, they will remain in the upper respiratory tract [120,263]. In our previous studies, Ma MS containing CS/TPP NPs [231,248,258,260] and SLN [238] showed values of geometric and aerodynamic diameters between 2–5 μm, apparent densities of 0.3–0.6 g/cm^3 and real densities of 1.3–1.5 g/cm^3, suitable to achieve the deep lung. In this work, the theoretical aerodynamic diameters of the dry powders were also within the optimal range (1–5 μm). On other hand, the apparent densities were low, which is generally

associated with good aerodynamic flow behavior [265,266]. Therefore, the micro-nanoplatforms designed and prepared in this work are theoretically suitable for their pulmonary administration and arrival to the deep lung (bronchioles and alveoli) [267].

4.6. Distribution of NCs in Ma MS

To corroborate the presence and investigate the distribution of NCs in Ma MS, RAMAN and CLSM techniques were employed (Section 3.12.).

4.6.1. RAMAN images and spectra

The main objective of this study was to determine the presence of CS NCs both inside and associated on the surface of Ma MS using the RAMAN technique.

Characteristic peaks of lyophilized CS NCs (Figure 20a) and Ma excipient (Figure 20b) were identified in RAMAN spectra: 1657.87 and 1746.52 wavenumber cm^{-1} for CS NCs, and 878.87 wavenumber cm^{-1} for Ma. A surface spectrum of Ma MS containing CS NCs was obtained (Figure 20c), in which the Ma peak was easily identified, and the peaks of CS NCs were also found, but less noticeable. In addition, the peaks of the CS NCs and the Ma corresponding to several planes of the CS NCs-loaded Ma MS were obtained (planes from 21 to 25, from 1.90 to 2.26 µm in depth; MS size: 2.71 µm) in order to find the presence of both components inside of the MS. In fact, in all studied planes, the characteristic peak of Ma was easily detected, demonstrating that MS were not hollow (except for the large MS, Figure 19); while in the case of the CS NCs, their characteristic peaks were more difficult to detect because they were not intense and were masked, as are representatively shown in the plane 21 of the Figure 20. In this case, Ma presence was supposed to frame around the CS NCs and partially cover up the NCs signal. Therefore, the characteristic peaks of the CS NCs and Ma were detected in each spectrum of each plane, remaining practically at the same

wavenumber values, verifying the presence of CS NCs inside and on the surface of the Ma MS.

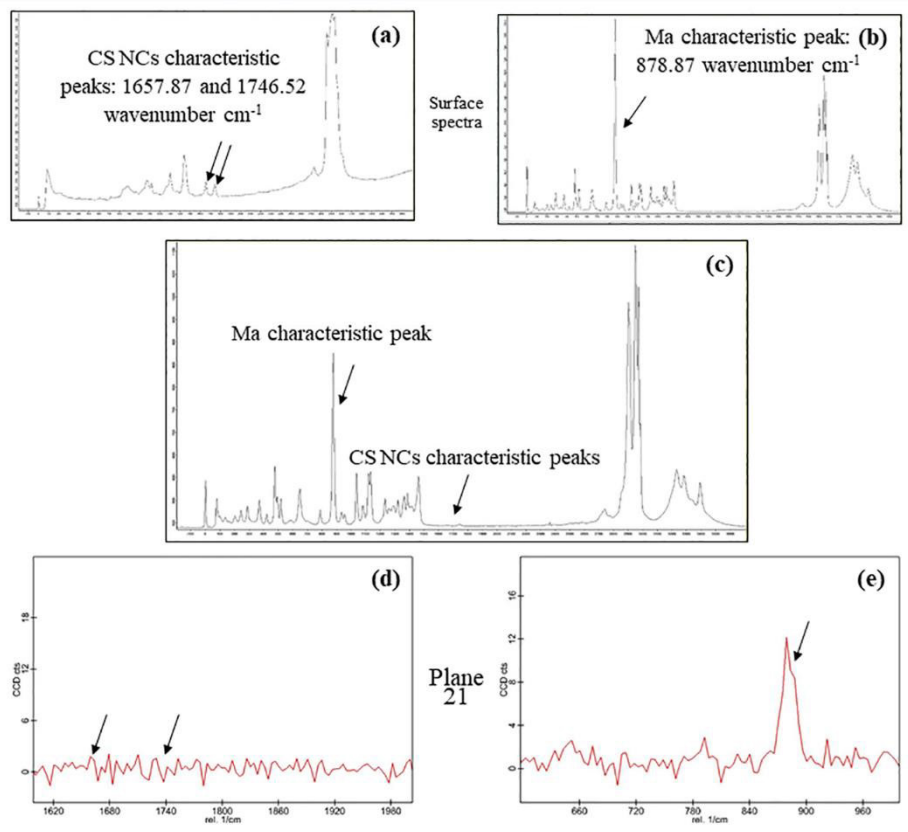

Figure 20. RAMAN spectra of: (a) CS NCs, (b) Ma MS and (c) CS NCs loaded-Ma MS surface; and characteristics peaks of: (d) CS NCs (plane 21: 1.90 nm) and (e) Ma (plane 21: 1.90 nm) of a CS NCs-loaded Ma MS. (New creation figure)

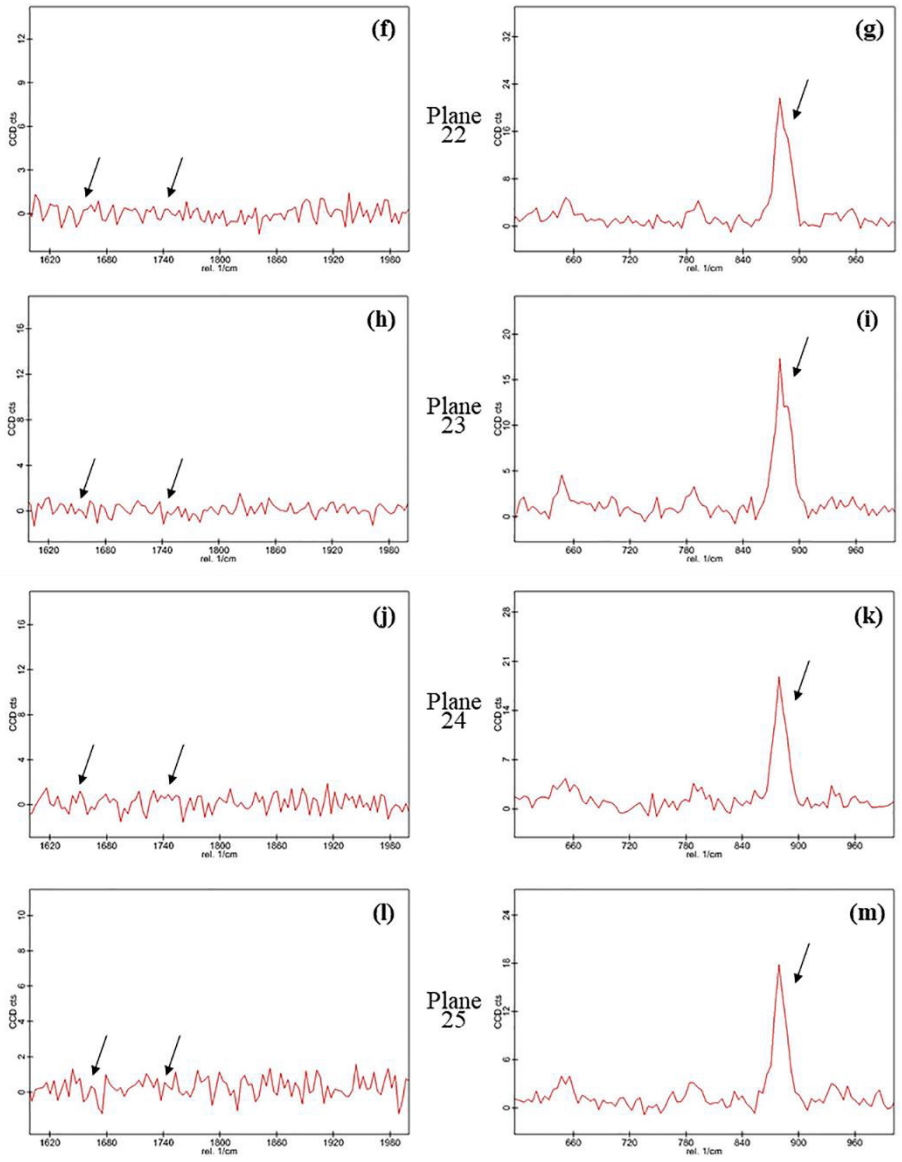

Figure 20 (continuation). Characteristics peaks of: (f) CS NCs (plane 22: 1.99 nm), (g) Ma (plane 22: 1.99 nm), (h) CS NCs (plane 23: 2.08 nm), (i) Ma (plane 23: 2.08 nm), (j) CS NCs (plane 24: 2.17 nm), (k) Ma (plane 24: 2.17 nm), (l) CS NCs (plane 25: 2.26 nm) and (m) Ma (plane 25: 2.26 nm) of a CS NCs-loaded Ma MS. (New creation figure)

The presence of CS NCs (red) in the Ma MS (blue) was further confirmed by RAMAN images obtained at different depths (1.90 nm, 1.99 nm, 2.08 nm, 2.17 nm and 2.26 nm) (Figure 21).These results, led us to conclude that CS NCs were microencapsulated in Ma MS, being widely distributed until reach the edge (Figure 21b). On the other hand, Ma generated an internal lattice (Figure 21a), showing that the MS are generally solid, thus supporting our hypothesis that only the large MS are hollow (see Figure 21).

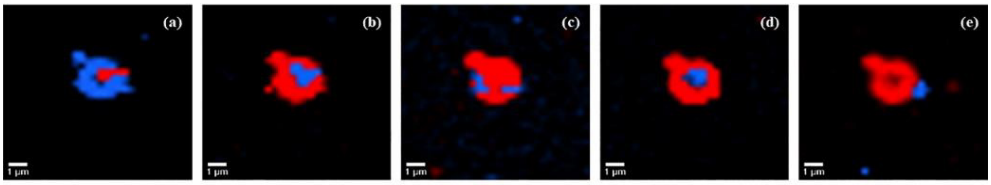

Figure 21. RAMAN images of several planes of a Ma MS (blue) containing CS NCs (red) at different depths: (a) 1.90 nm, (b) 1.99 nm, (c) 2.08 nm, (d) 2.17 nm, and (e) 2.26 nm. (New creation figure)

4.6.2. Confocal Laser Scanning Microscopy (CLSM)

A CLSM study was also carried out to determine the presence and localization of the NCs in the Ma MS. As previously explained (Section 3.12.2.), different fluorescent labels were used in order to visualize clearly each component: CS NCs were labeled with Coumarin 6 (Cu^6) (fluorescent green) and Ma was labeled with Bodipy® (fluorescent red).

To eliminate possible non-encapsulated Cu^6 residues and avoid false signals, the Cu^6-labeled NCs were dialyzed as explained in the Methodology section. In Figure 22, Cu^6-labeled NCs pre- (Figure 22a) and dialyzed (Figure 22b) can be compared. In the first case (Figure 22a), the pre-dialyzed labelled NCs were observed, as well as the fluorescent green signal from the non-encapsulated Cu^6. In the second case (Figure 22b), the dialyzed labeled NCs were observed, but the non-encapsulated Cu^6 signal was non-existent. These microphotographs show that, during the Cu^6-labeled NCs dialysis process, the excess of Cu^6 was successfully eliminated and the

encapsulated Cu^6 was not released from the dialyzed labelled-NCs. This can be explained by the Cu^6 non-polar nature that allows it to stay inside the NC oil core. Furthermore, the pre-dialyzed labelled NCs have a more dispersed distribution (Figure 22a), probably due to the presence of Cu^6 between the nanostructures, whose non-polar character repels them and makes them move away from each other. In contrast, dialyzed labelled NCs showed certain trend to approximate between them in form of groups; however, their physicochemical properties were normal (see Table 6). This tendency of the NCs to approach each other is surely due to the distribution acquired between the slide and the cover during the sample preparation.

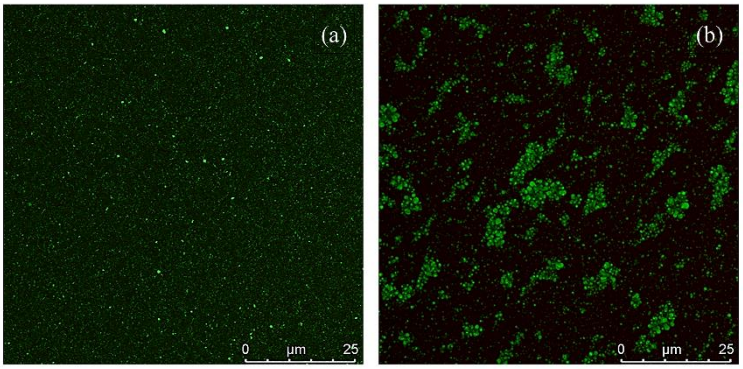

Figure 22. CLSM microphotographs of: (a) pre-dialyzed Cu^6-CS NCs and (b) dialyzed Cu^6-CS NCs. (Figure from the work of Fernández-Paz et al. [255], article accepted for publication in Powder Technology)

According to the CLSM images, Ma was extended throughout the MS forming a matrix (red channel) (Figure 23a), where the Cu^6-NCs were homogeneously distributed in the Ma MS (green channel) (Figure 23b). The confluence of both components can be observed in the overlapping of channels (Figure 23c). This type of micro-nanostructure is different to those seen for microencapsulated CS NPs [248,258], where the CS NPs were distributed inside the MS, but covered by an outer layer of Ma. However, this type of structure agree with that of SLN of glyceryl dibehenate and glyceryl tristearate microencapsulated in Ma MS, in which the outer Ma layer was not present and the nanosystems were distributed up to the edge of the MS

(Figure 23). There are two possible hypotheses that explain the presence of this Ma outer cover in the nanosystems-loaded Ma MS. The first one is based on the T_{Inlet} employed in the spray-drying process. For the CS NPs microencapsulation [248,258,260], the T_{Inlets} were of 160 ºC and 170 ºC, while in the present work was of 105 ºC, similar to that used for the SLN microencapsulation, of 103 °C [238]. At high temperature, there is an increased drying of Ma in the outer layer of the MS compared to the lowest temperatures. The second hypothesis is focused on the concentration of the excipient used during the spray-drying process. A higher Ma concentration, which was used for CS NCs and SLN [238] compared to the CS NPs [248,258,260], is associated to a higher viscosity of the Ma solution. This fact hinders the water and excipient molecules diffusion during the drying process, thus preventing the possible formation of a Ma outer cover.

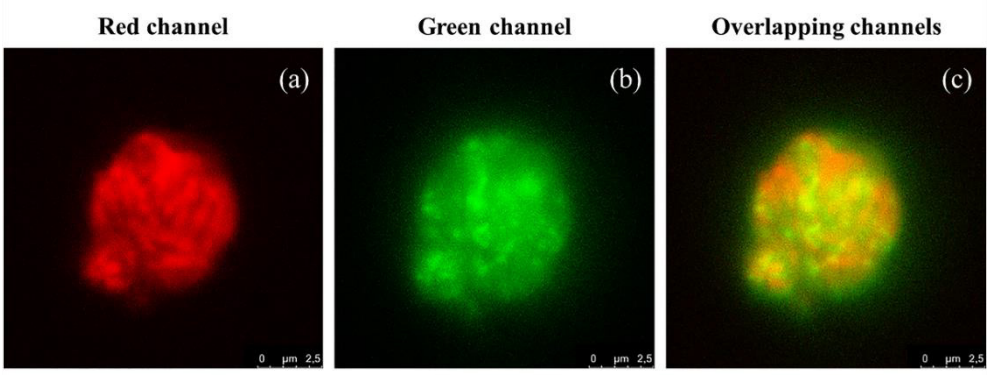

Figure 23. CLSM microphotographs of Cu^{6}-CS NCs-loaded Ma^{B} MS: (a) red channel, (b) green channel and (c) overlapping channels. (Figure from the work of Fernández-Paz et al. [255], article accepted for publication in Powder Technology)

4.7. Release of NCs from the dry powders

To check the *in vitro* capacity of the MS to release NCs, the dry powders were incubated in MilliQ water and in simulated pulmonary medium (Section 3.13.). This is a mixture of the lung surfactant Curosurf® and PBS (0.1% Curosurf® in 10 mM PBS (*v/v*)) with a pH of 7.4, like the pH of the pulmonary fluid, plasma and interstitial fluid [268]. It was observed that in both media, the Ma rapidly dissolved releasing the NCs. As can be seen in the TEM microphotographs (Figure 24), the released NCs were morphologically similar to the freshly prepared NCs (Figure 9), demonstrating that the spray-drying process did not affect to the structure of the NCs, as expected [257]. Therefore, it is expected that NCs will be released also unchanged in the lung fluid.

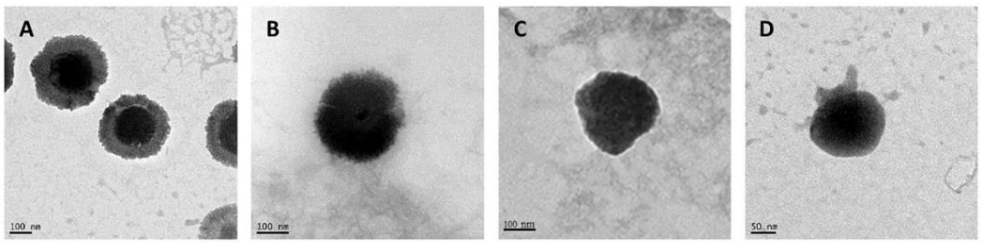

Figure 24. TEM microphotographs of: (A) CS NCs, (B) HA/CS NC, (C) pCMV-βGal-CS NC and (D) pCMV-βGal-HA/CS NC released from Ma MS in MilliQ water. (Figure from the work of Fernández-Paz et al. [212], Pharm. 13 (2021) 1377. Open access article distributed under the Creative Commons Attribution License)

Figure 25 shows the sizes and ζ-potentials of the CS NCs and the HA/CS NCs released from Ma MS in MilliQ water (Figure 25A) and in simulated pulmonary medium (Figure 25B) during 4 h. Following the incubation of the MS in both aqueous media, the NCs showed an increase of size with respect to the fresh NCs, probably due to the presence of Ma remaining of the MS, still in process of release of the NCs and other loose debris of Ma. The increase of size of the NCs released in simulated pulmonary medium was greater than in MilliQ water, surely caused by the electrostatic attraction of negatively charged molecules from the medium to the positive surface of the

NCs, fact that has been reported for other nanosystems microencapsulated in Ma [120]; but it is not relevant. As time progressed, the NCs sizes decreased maintaining themselves above of the fresh NCs sizes, but still within the nanometric range, which is suitable for the purpose of this study. When CS NCs and HA/CS NCs were released in MilliQ water, the ζ-potentials did not vary, but in simulated pulmonary medium the NCs acquired negative ζ-potentials, probably due to the presence of negative molecules of the medium joined by electrostatic attractions to the positive surface of the NCs.

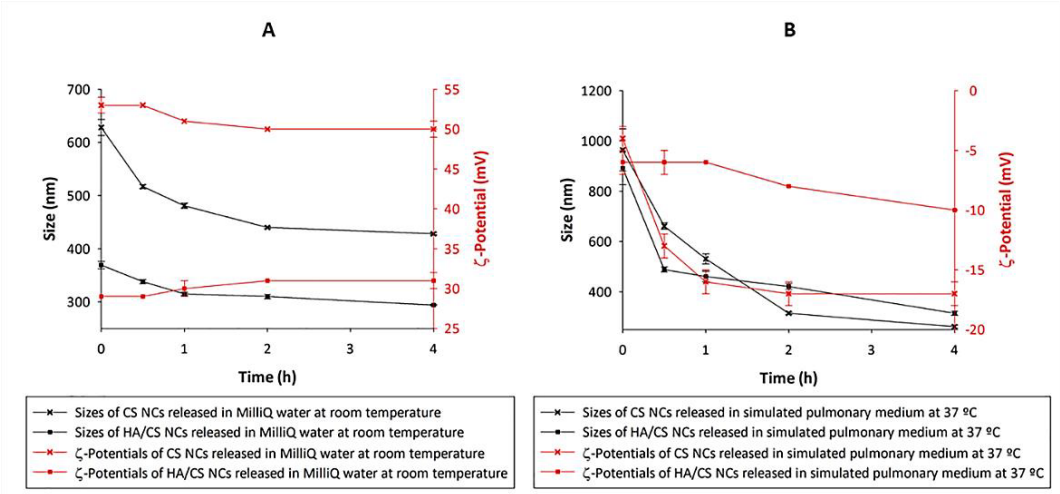

Figure 25. Sizes and ζ-potentials of CS-based NCs released from Ma MS in: (A) MilliQ water at room temperature and (B) simulated pulmonary medium at 37 °C, at different times (0, 0.5, 1, 2 and 4 h) (mean ± S.D.; n = 3). (Figure from the work of Fernández-Paz et al. [212], Pharm. 13 (2021) 1377. Open access article distributed under the Creative Commons Attribution License)

Count rates are shown in Table 11. For fresh CS NCs, the mean was of approx. 273.8 ± 7.3 kcps, being the range from 266 to 281 kcps. The count rate ranges of CS NCs released from 0 to 4 h varied from 262 to 359 kcps and from 280 to 399 kcps when they were released in MilliQ water and in simulated pulmonary medium, respectively. The mean count rate for fresh HA/CS NCs was approx. 198 ± 1.9 kcps, being the range from 196 to 200 kcps. For the released ones (from 0 to 4 h), the ranges varied from 102 to 216 kcps and from

185 to 226 kcps in MilliQ water and in simulated pulmonary medium, correspondingly. This indicates that the CS-based NCs were efficiently released from the Ma MS. Furthermore, at the beginning of the NCs release, a lower count rate was observed compared to that seen at 4 h because the release process was beginning, which is also confirmed by the larger size of the particles at that initial time (Figure 25). This increase in size, as well as a lower number of particles at the beginning of the release process, can be explained by the presence of Ma, which is still releasing NCs. Therefore, as time passed and the Ma dissolved, the mean count rate increased as expected, while a decrease in the particle size occurred.

Table 11. Count rate ranges (kcps) of fresh NCs and NCs released in MilliQ water at room temperature and in simulated pulmonary medium at 37 °C for 4 h (n = 3).

Types of CS-Based NCs	Count Rate (kcps)
CS NCs	266–281
CS NCs released in MilliQ water	262–359
CS NCs released in simulated pulmonary medium	280–399
HA/CS NCs	196–200
HA/CS NCs released in MilliQ water	102–216
HA/CS NCs released in simulated pulmonary medium	185–226

Taking into account the high solubility of Ma in the investigated aqueous media and the results obtained in this study, it is expected that the dry powders administrated *in vivo* release the NCs in the lung fluid.

4.8. Stability of NCs in cell growth medium

The stability of CS NCs and HA/CS NCs in supplemented DMEM and in DMEM without supplementation while mimicking physiological conditions (37 ºC, pH: 7.4), was determined at different times (0, 2 and 4 h), being also checked in MilliQ water as control (Section 3.14.). Specifically, we considered to examine the NCs size and their standard deviations, being desirable that the sizes remain in the nanometric range. Sizes of CS NCs and HA/CS NCs in the different media are shown in Figure 26. Both types of NCs remained practically constant in MilliQ water with time, as expected. However, an increase of size with time was observed when CS-based NCs were incubated in supplemented DMEM, achieving the 500 nm for the CS NCs at 4 h, and being practically constant below the 250 nm for the HA/CS NCs. When NCs were incubated in DMEM without supplementation, the sizes also increased with time, achieving more than 500 nm the CS NCs, and over the 400 nm the HA/CS NCs at 4 h. In addition, the standard deviations were more ample for the CS NCs (around 14-31 nm) than HA/CS NCs (about 3-7 nm), independently of the employed medium. It is remarkable that both sizes and standard deviations were notably higher for the CS NCs than for the HA/CS NCs. The higher stability of the HA/CS NCs can be explained by the presence of HA on their structure, which produces a lower superficial ζ-potential with respect to the CS NCs, so HA/CS NCs interacted less with the media negative components, while the CS NCs were more affected. In this sense, it could have a certain adhesion of the media negative molecules on the NCs positive surface, increasing their sizes. Consequently, HA/CS NCs seem to be more stable than CS NCs in both media. However, both formulations were suitable for the purpose of the *in vitro* cell studies.

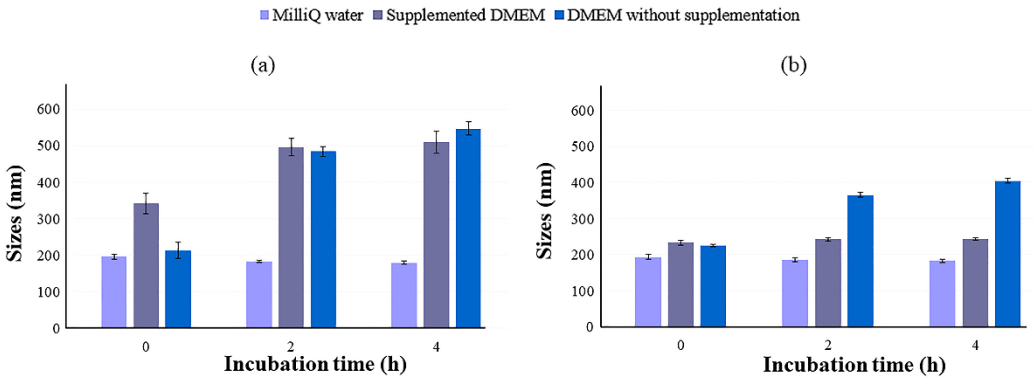

Figure 26. Size (nm) *vs.* incubation time (h) of: (a) CS NCs and (b) HA/CS NCs in MilliQ water, in supplemented DMEM, and in DMEM without supplementation after 0, 2, and 4 h of incubation at 37 ºC (mean ± S.D., n = 3). (Figure from the work of Fernández-Paz et al. [255], article accepted for publication in Powder Technology)

4.9. *In vitro* studies in the A549 cell line

4.9.1. Viability studies

A preliminary cell viability assay was carried out using a Luna II device, under the conditions mentioned in the section 3.15.1. Mean viability values (mean ± SD; n = 3) were calculated and expressed as percentage of live cells (%). Figure 27 shows living cells with a green circle and dead cells with a red circle. Luna II is an automated cell counter, so the obtained images had not scale. The positive control presented a maximum of viability slightly higher than 95% (Figure 27a), whereas the negative control showed a 0% of viability (Figure 27d), as expected. When the cells were incubated with CS NCs and HA/CS NCs presented a viability around 95% in both cases (Figures 27b and 27c). In view of the positive results of this preliminary assay, another viability study was next carried out to assess specifically the metabolic activity of the cells.

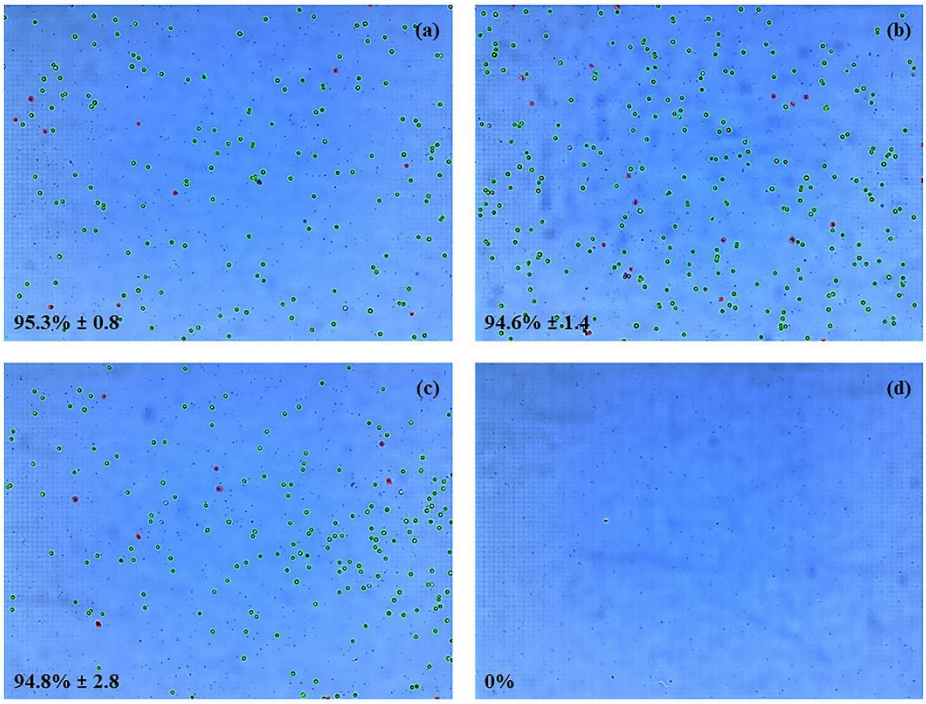

Figure 27. Luna II images of A549 cells incubated in supplemented DMEM with: (a) nothing (positive control), (b) CS NCs, (c) HA/CS NCs, and (d) 1% (*v/v*) Triton (negative control), for 4 h at 37 ºC (% average viability ± S.D.). (Figure from the work of Fernández-Paz et al. [255], article accepted for publication in Powder Technology)

Cell viability of A549 cells was also studied using CellTiter-Blue® (AlamarBlue®, section 3.15.1). The cells were treated with increasing concentrations of CS-based NCs and Ma excipient and incubated for 4 h at 37 ºC. The results are shown in Figure 28, where the viability was expressed as percentage of living cells compared to positive control. After 24 h of the removal of CS NCs the cell viability was comprised between, approximately, 93 and 102% in all the tested concentrations; while in the case of HA/CS NCs, the viability was between 94 and 99%, being similar for both nanosystems. These viability results at 24 h were in agreement with those previously

reported for A549 cells treated with CS/TPP NPs, whose values ranged from approximately 90 to 100% [269,270]. Furthermore, the viabilities were higher than those of SLN (both glyceryl dibehenate and glyceryl tristearate empty or with rifabutin) (80%) [253]. After 48 h of removal CS NCs, the viabilities were between 99 and 119%. In the case of HA/CS NCs the viabilities were of 96 to 118% for all the tested concentrations, being similar for both nanosystems. Taking into account that at 24 h the viabilities were close to 100% for both NCs, it is possible that at 48 h there were so high viabilities due to the recovery of the cells. The opposite occurred with the CS/TPP NPs that, at the lowest concentration, presented a viability of 120% but, as the concentrations increased, the viability decreased to a value of around 90% [269]. This discrepancy could be due to a better recovery of the cell division cycle when the cells were treated with the CS-based NCs compared to the CS/TPP NPs. In addition, constant high viability values around 100% were obtained at 24 and 48 h post-treatment in presence of Ma excipient. These values were higher than those obtained in the work of Grenha et al. [269], showing that Ma, has good *in vitro* biocompatibility. In summary, the results of this study indicated that CS-based NCs and Ma excipient led to high viabilities in the A549 cell line. Therefore, these micro-nanosystems are expected to be suitable for lung delivery.

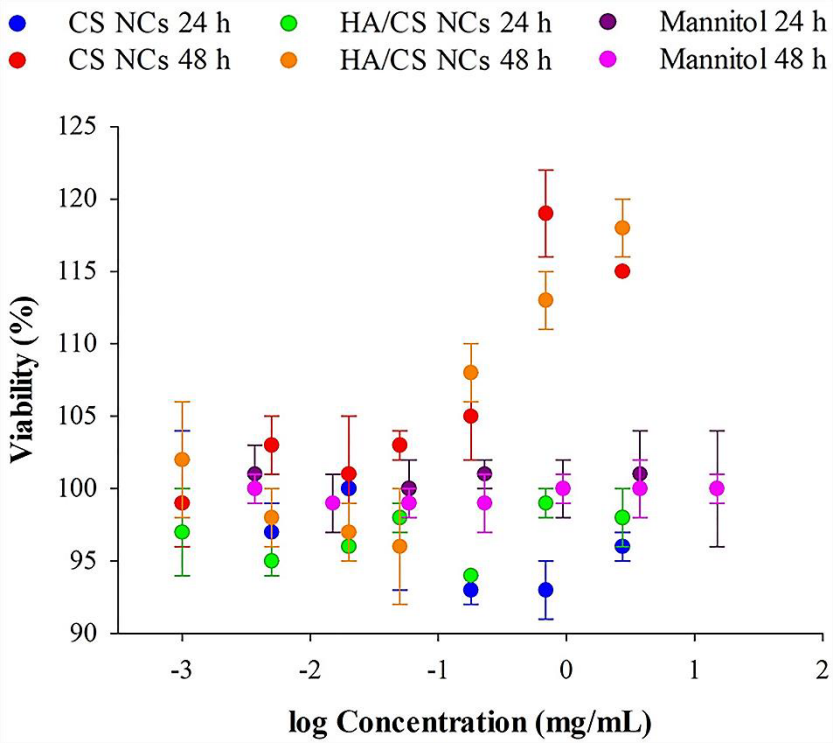

Figure 28. Cell viability after 24 and 48 h of recovery after removal of CS NCs, HA/CS NCs and Ma excipient of the A549 cells, measuring the fluorescence signal of CellTiter-Blue® (mean ± S.D., n = 4). (Figure from the work of Fernández-Paz et al. [255], article accepted for publication in Powder Technology)

4.9.2. Study of intracellular uptake

The study of intracellular uptake was carried out as was explained in the section 3.15.2. The images collected in the Figure 29 verified the internalization of the nanosystems inside cells in comparison with the images of the control cells. The excess of Cu^6-NCs was previously eliminated in the washing processes, so that the Cu^6-NCs observed in the images are within the cells. These results agree with those obtained in previous studies of CS-based nanostructures. Specifically, CS/TPP NPs were also internalized in high quantities in A549 cells [269]. Furthermore, images in Figure 30 (zoom of Figure 29) show

more clearly how the cells maintained their integrity, as well as a more intense fluorescence signal from Cu^6-HA/CS NCs than from Cu^6-CS NCs. This is probably due to the penetration-enhancing effect of the HA [82,271]. In any case, both nanosystems were efficiently uptaked by the A549 cell line.

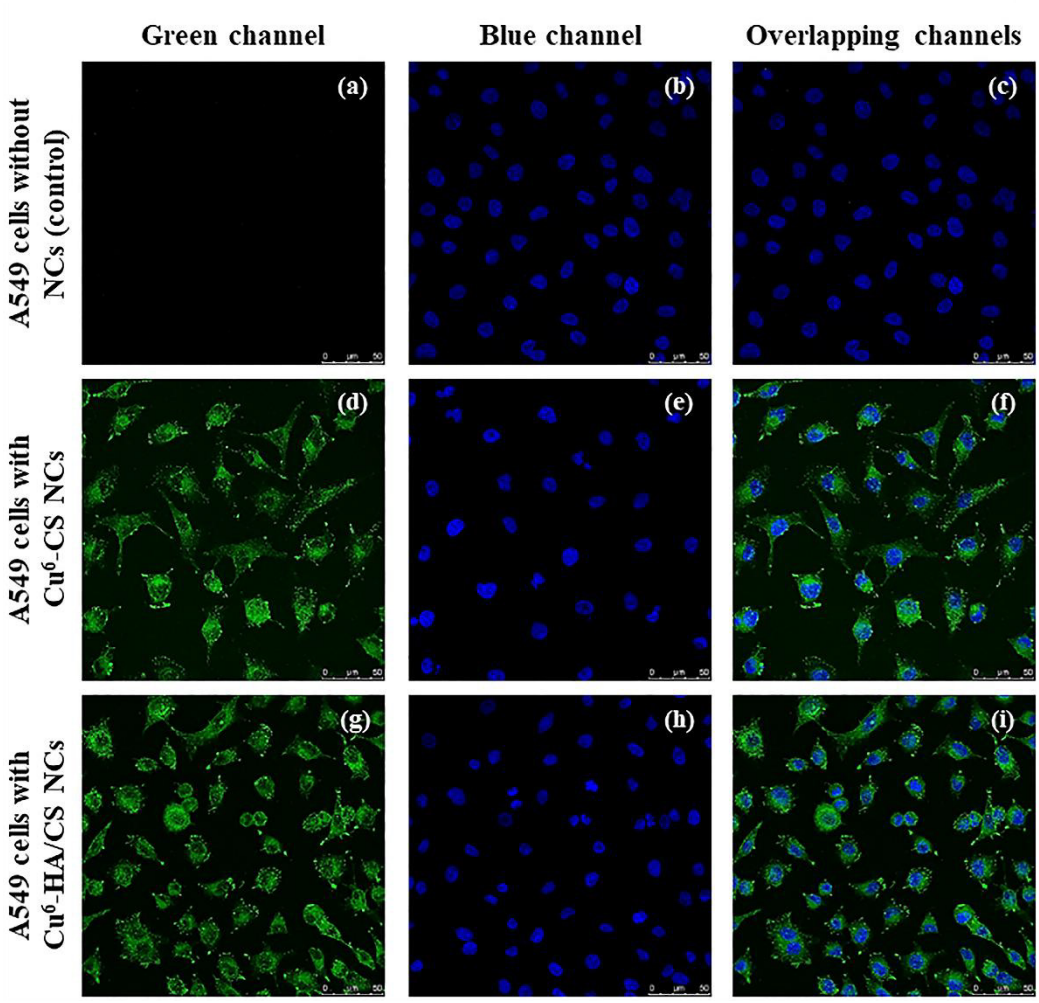

Figure 29. Confocal microscopy images of A549 cells: control (without CS-based NCs) (a-c), treated with 55.2 µg/well of Cu^6-CS NCs (d-f), and treated with 55.2 µg/well of Cu^6-HA/CS NCs (g-i) (green channel). Cell nuclei were stained with

DAPI (blue channel). Scale bar = 50 µm. (Figure from the work of Fernández-Paz et al. [255], article accepted for publication in Powder Technology)

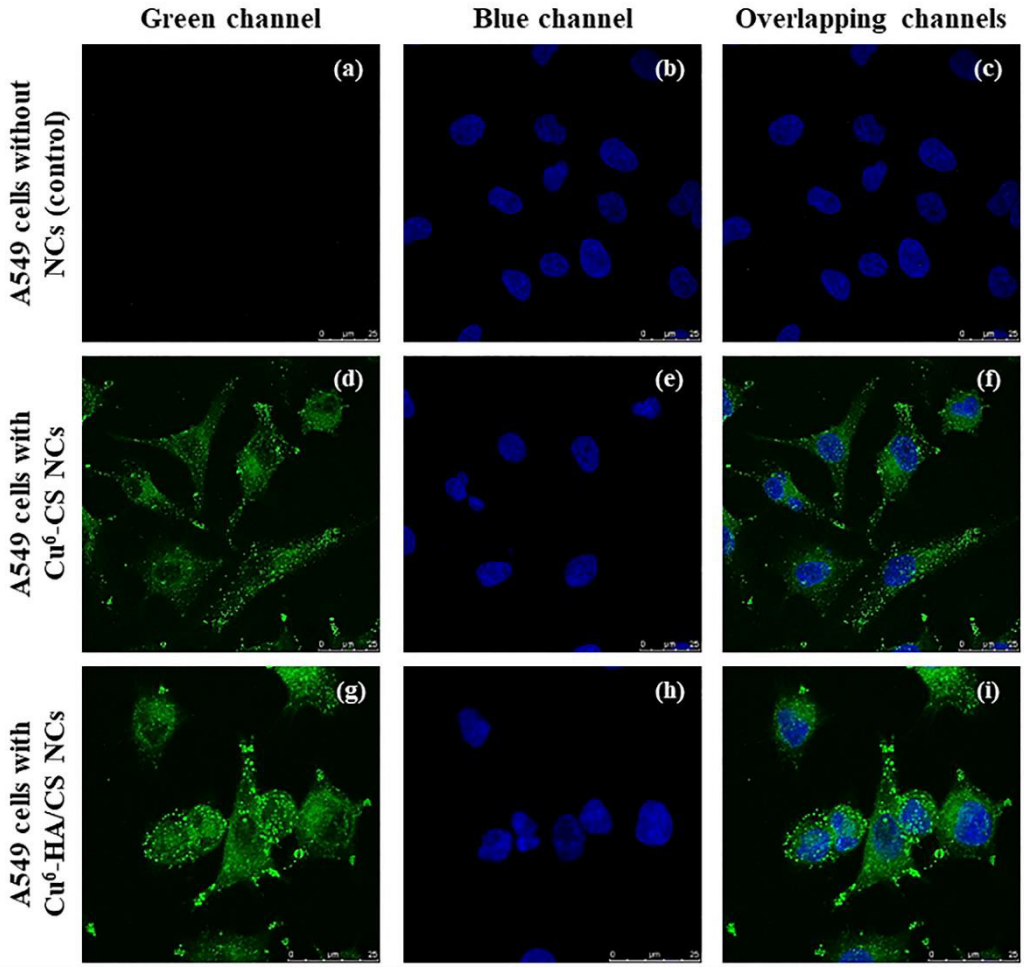

Figure 30. Confocal microscopy images of A549 cells: control (without CS-based NCs) (a-c), treated with 55.2 µg/well of Cu^6-CS NCs (d-f), and treated with 55.2 µg/well of Cu^6-HA/CS NCs (g-i) (green channel). Cell nuclei were stained with DAPI (blue channel). Scale bar = 25 µm. (Figure from the work of Fernández-Paz et al. [255], article accepted for publication in Powder Technology)

4.9.3. Quantification of A549 cells containing NCs

To quantify the A549 cells that have internalized CS NCs and HA/CS NCs, the FACS technique was carried out by the analysis of a minimum of 10000 events per sample (Section 3.15.3.). Table 12 shows the data of number of events (Count) and the percentage of alive cells (%) selected of their corresponding Dot Plot.

Table 12. Number of events (*Count*) and percentage of alive cells (%) of control cells (first column), cells incubated with Cu^6-CS NCs (second column), and cells treated with Cu^6-HA/CS NCs (third column) (mean ± S.D.; n = 3).

Control cells		**Cells with Cu^6-CS NCs**		**Cells with Cu^6-HA/CS NCs**	
Count	Alive cells (%)	Count	Alive cells (%)	Count	Alive cells (%)
10919.0 ± 153.7	80.6 ± 0.5	10646.0 ± 41.2	85.7 ± 0.8	10711.0 ± 299.5	83.3 ± 6.3

The histograms of the control cells were considered the basal signal to correct the signal obtained from the cells treated with Cu^6-NCs. As shows the Figure 31 the histogram of the control cells confirmed a positive viability of 100%, as expected. When the cells were treated with Cu^6-CS NCs and Cu^6-HA/CS NCs, their respective histograms (previously corrected by "color compensation") showed that the cells were negative to Aqua, indicating also a high viability (99.83% and 99.93% on average for Cu^6-CS NCs and Cu^6-HA/CS NCs, respectively).

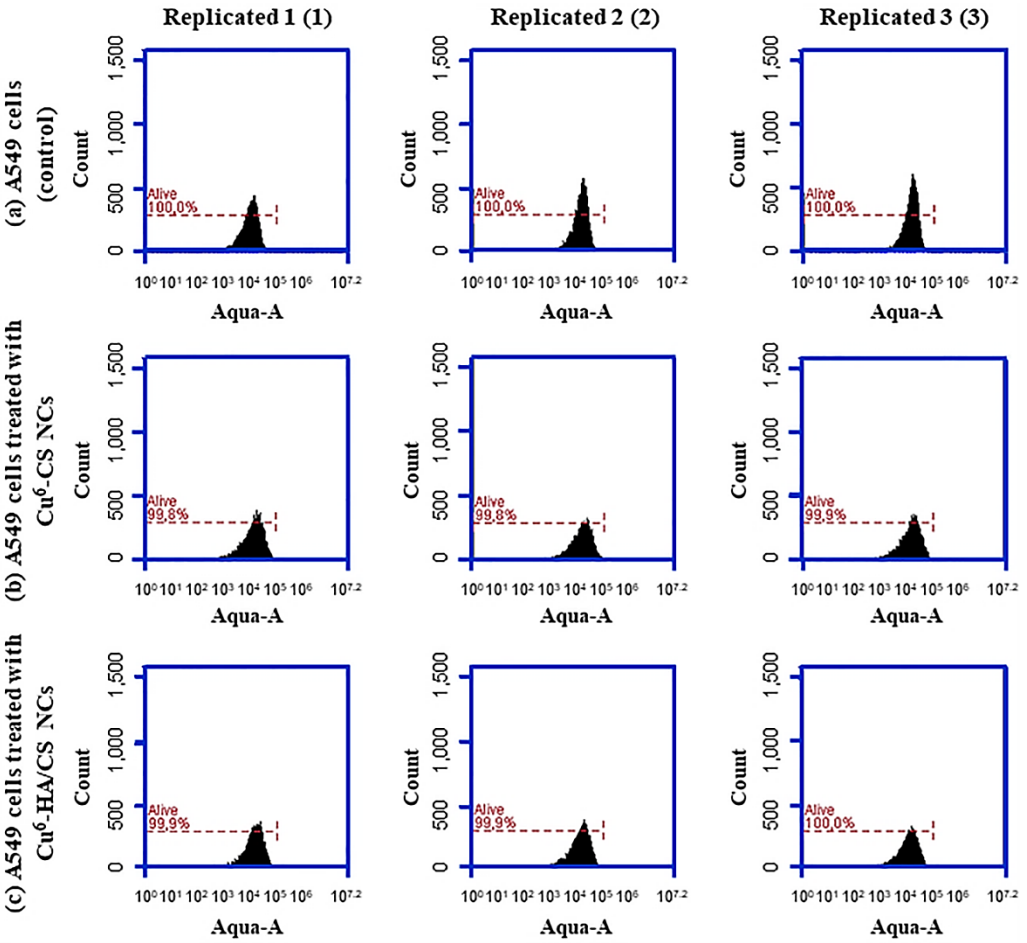

Figure 31. FACS histograms of A549 cells: (a) control (without treatment), (b) treated with 55.2 µg/well of Cu^6-CS NCs, and (c) treated with 55.2 µg/well of Cu^6-HA/CS NCs to evaluate the cell viability. (Figure from the work of Fernández-Paz et al. [255], article accepted for publication in Powder Technology)

To determine the percentage of cells that have internalized NCs, the histogram of control cells was compared with those obtained for the cells treated with Cu^6-CS NCs and Cu^6-HA/CS NCs (Figure 32). As expected, control cells were negative to the signal of Cu^6. When cells were treated with Cu^6-CS NCs and Cu^6-HA/CS NCs, they were

positive to the signal of Coumarin, showing that the nanosystems were internalized into the cells (100%) (Figure 32).

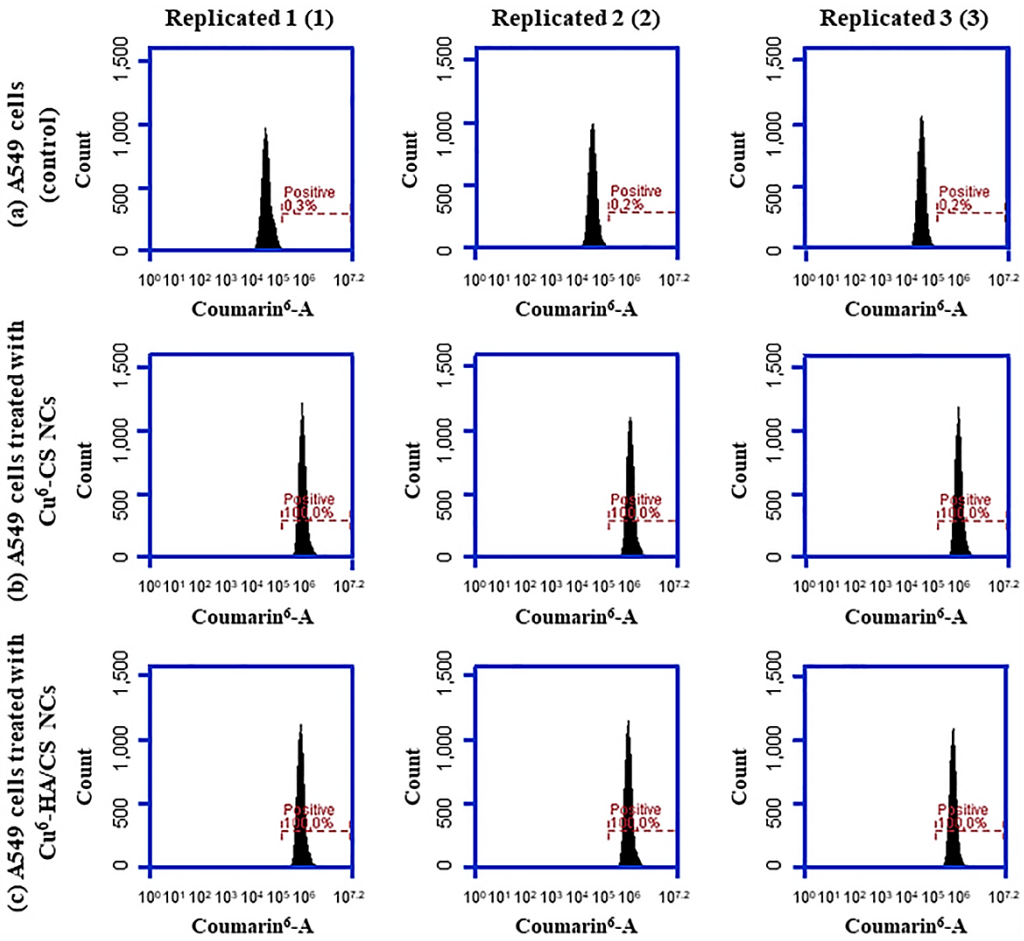

Figure 32. FACS histograms of A549 cells: (a) control (without treatment), (b) treated with 55.2 µg/well of Cu^6-CS NCs, and (c) treated with 55.2 µg/well of Cu^6-HA/CS NCs to evaluate the cell internalization. (Figure from the work of Fernández-Paz et al. [255], article accepted for publication in Powder Technology)

Similar results were obtained in numerous studies of CS-based nanosystems that were loaded with antitumoral drugs [272-274]. On

the contrary, it was found that CS/TPP NPs did not penetrate in A549 and Calu-3 cell lines; but they remained attached to the surface of the cells [269]. Unlike that study, in which the NPs were incubated only for 2 h, in our study the NCs were incubated for 4 h. Therefore, and taking into account the good results of this study and of previous ones based on CS nanosystems, it is very probable that CS/TPP NPs would also internalize in the cells with a longer incubation time. In addition, the results of this study were congruent with those obtained by CLSM (Section 4.9.2.) because we could verify the cellular internalization of the nanosystems, but also quantifying the % of A549 cells internalized with the NCs. It can be concluded that both confocal images and flow cytometry studies showed an efficient internalization of CS-based NCs in the A549 cell line. Furthermore, it was revealed that the internalization of the nanosystems did not affect the cell viability (see Figure 31), which was consistent with the results of previous studies (Section 4.9.1.). Therefore, the microencapsulated CS-based NCs seem to be safe and suitable for their administration by the pulmonary route.

4.10. *In vivo* studies

4.10.1. Lung distribution of microencapsulated NCs

The *in vivo* pulmonary distribution of microencapsulated NCs was investigated using Cu^6-labelled NCs and the CLSM technique, as described in the section 3.16.1. The Cu^6-NCs were dialyzed prior to their microencapsulation to remove the excess of free Cu^6, as it was indicated in the Section 4.6.2.

Representative CLSM images of lung sections obtained following the administration of the Cu^6-labelled micro-nanostructured formulations to rats, are shown in Figure 33, in which the fluorescent green signal associated to the NCs is visible. The images in Figure 33A–C correspond to the control lung tissue (without powder), while those in Figure 33D–F and Figure 33G–I represent lung tissues of rats that were treated with Cu^6-CS NCs-loaded Ma MS and Cu^6-HA/CS NCs-loaded Ma MS, respectively. At 1h post- administration of both

formulations, micro-nanostructures were detected in the lung epithelium (indicated by arrows in Figure 33), being some of them captured by macrophages (Figure 33F,I). Macrophage phagocytosis depend on several factors, including the nature and charge of the particles, size and shape, concentration and contact time, between others [231]. In this sense, macrophages have preference for hydrophobic particles, or with a high surface charge (either positive or negative), with a size between 1–6 μm, spherical and non-porous [119]. For that, we cannot exclude that some NCs still included in the MS were phagocytosed. It must be taking into account that, although it was demonstrated *in vitro* that NCs were rapidly released from MS due to the fast dissolution of the Ma in the aqueous media (Figure 25A,B), it is reasonable to think that the *in vivo* release of the NCs is slower due to the small volume of alveolar fluid [231]. The fact that the micro-nanostructures were distributed in the deep lung, as well as that some MS were phagocytosed, was also observed with the CS/TPP-insulin NPs-loaded Ma MS aimed at protein lung absorption [231]. These results confirm that the new micro-nanostructured platform has a great potential for the pulmonary administration of nanostructures, more specifically of NCs, leading to their release in the deep lung. Next study was aimed to demonstrate the ability of the plasmid-loaded micro-nanostructured dry powders to produce lung transfection after their *in vivo* administration.

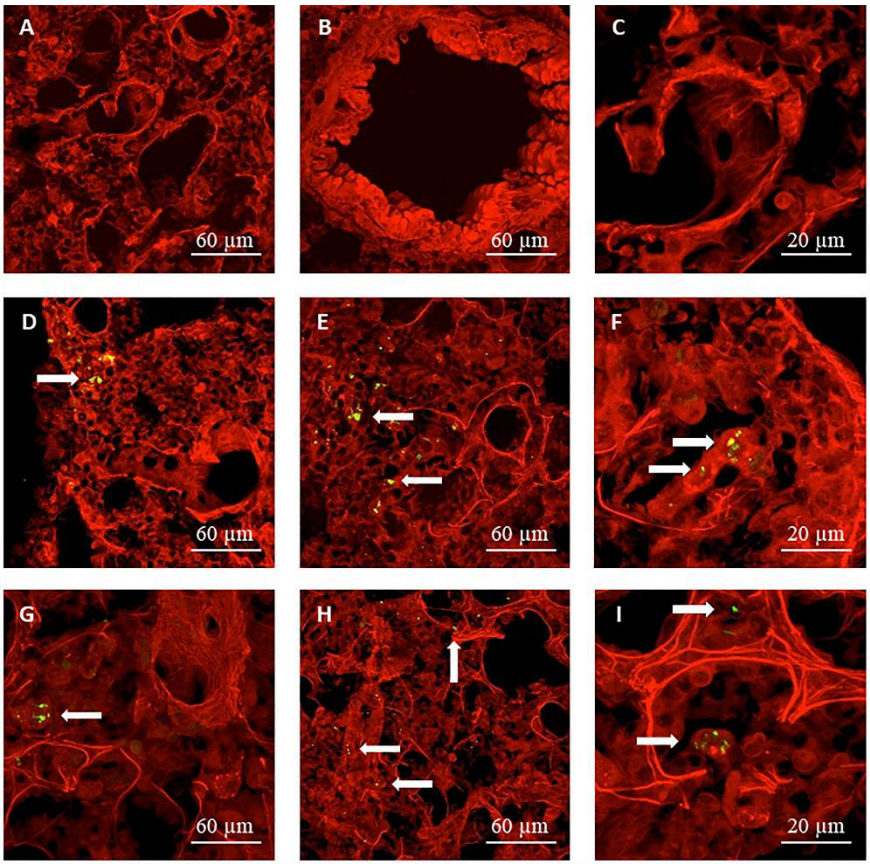

Figure 33. CLSM microphotographs of alveoli: (A–C) control (without powder), (D–F) at 1 h post-administration of Cu^6-CS NCs-loaded Ma MS and (G–I) at 1 h post-administration of Cu^6-HA/CS NCs-loaded Ma MS. (Figure from the work of Fernández-Paz et al. [212], Pharm. 13 (2021) 1377. Open access article distributed under the Creative Commons Attribution License)

4.10.2. *In vivo* gene expression study

The plasmid pCMV-βGal (or LacZ gene) used in this study is one of the most used reporter genes for the evaluation of gene transfection efficiency. It codes the enzyme β-Gal. The substrate used to test the functionality of β-Gal is 5-Bromo-4-chloro-3-indolyl-beta-D-galactopyranoside (X-Gal). When lung tissues of rats treated with

plasmid-loaded formulations were incubated within X-Gal solution, the β-Gal present in the tissues transforms the X-Gal molecules in blue precipitates. It is important to point out that the tissues of mammals also possess endogenous enzymes with the same β-galactosidase activity. Therefore, it was crucial to inhibit the endogenous β-galactosidase activity to avoid false positives. To do that, the tissues were previously processed properly to inhibit these enzymes (by incubation in solutions of pH around 7.4, as previously explained in the section 3.16.2.) [247,275]. In order to inhibit the endogenous β-galactosidase activity [247,275], it was also taken into account that the pH at which the exogenous β-galactosidase activity is highest is above than the pH at which the mammalian β-galactosidase activity is greatest. Therefore, this study was made at a pH of 7.4 to ensure the inhibition of the mammalian β-galactosidase activity and to maintain optimal the exogenous β-galactosidase activity. In addition, it was necessary to find a balance in the incubation time of the lung tissues in the X-Gal solution. This inhibition could be maintained until the 2 h, once the reaction with X-Gal began. Therefore, the lung tissues were incubated for exactly 2 h in the X-Gal solution. Furthermore, it was better to process the lung in sections than in block because it allows a more effective inhibition of the endogenous β-galactosidase activity, as well as a better detection of the exogenous β-galactosidase activity [247]. Therefore, following the pulmonary administration to rats of pCMV-βGal-CS NCs-loaded Ma MS and pCMV-βGal-HA/CS NCs-loaded Ma MS, as well as their controls (CS NCs-loaded Ma MS, HA/CS NCs-loaded Ma MS and pCMV-βGal-Ma MS), the β-Gal expression was studied in sections of the lungs extracted three days after the administration of the powders [75]. As can be seen in the light field optical microscopy images of the Figure 34, the sections of rat lungs that were not treated with powders (Figure 34A–D) show no blue deposits, indicating that the endogenous β-galactosidase activity was correctly inhibited to avoid false positives. Neither appeared blue deposits when the rats were administered with the control powders without plasmid: CS NCs-loaded Ma MS (Figure 34E–H) and HA/CS NCs-loaded Ma MS (Figure 34M–P). On the contrary, blue deposits (indicated with

arrows) clearly and reproducibly appeared in the lungs of rats treated with the plasmid-loaded formulations: pCMV-βGal-CS NCs-loaded Ma MS (Figure 34I–L); pCMV-βGal-HA/CS NCs-loaded Ma MS (Figure 34Q–T); and pCMV-βGal-Ma MS (Figure 34U–X), indicating efficient *in vivo* gene expression.

Blue deposits were evidenced as result of the enzymatic reaction of β-Gal, which was formed thanks to the expression of the intact structure of pCMV-βGal in the lung tissue. Specifically, important differences were observed between the transfection patterns of the plasmid-loaded formulations, depending on whether or not the genetic material was associated to NCs and whether or not the NCs contained HA. Indeed, in the lungs of rats treated with dry powders of Ma MS containing naked plasmid (pCMV-βGal-Ma MS), the blue deposits formed clusters. This might be explained because the MS, in contact with the lung fluid, released the plasmid very rapidly in the lung epithelium (Figure 34U–X). In contrast, when pCMV-βGal was previously incorporated to CS NCs and HA/CS NCs (pCMV-βGal-CS NCs-loaded Ma MS: Figure 34I–L; pCMV-βGal-HA/CS NCs-loaded Ma MS: Figure 34Q–T), the resulting blue deposits were more scattered throughout the lung epithelium. Furthermore, as expected [82,83,276-278], the addition of HA to the coat of the CS NCs improved their transfection properties. As can be seen in Figure 34S,T, for pCMV-βGal-HA/CS NCs-loaded Ma MS, there were blue deposits extended beyond the edge of the pulmonary alveoli and the transfection occurred homogeneously over a wider area. This difference on the transfection patterns demonstrates that HA was attached to the NCs surface, which corroborates the results of the Table 6 and Figure 9B. HA promotes the internalization of nanostructures by increasing both specific and non-specific interactions with cells [83]. During internalization, HA/CS NCs are also expected to enter into non-lysosomal vesicular compartments, accumulating in the perinuclear area and in the cell nucleus [279]. Furthermore, HA promotes the gene expression by acting as a transcriptional activator, probably by loosening the tight bond between the nanosystem and the gene [278]. This improvement in the transfection efficiency was also observed for CS/HA/TPP NPs

prepared using pEGFP, pβ-gal or siRNA [82,83]. In those studies, it was demonstrated that the transfection capacity was strongly related to the composition, increasing the level of gene expression as the amount of HA in the NPs was higher.

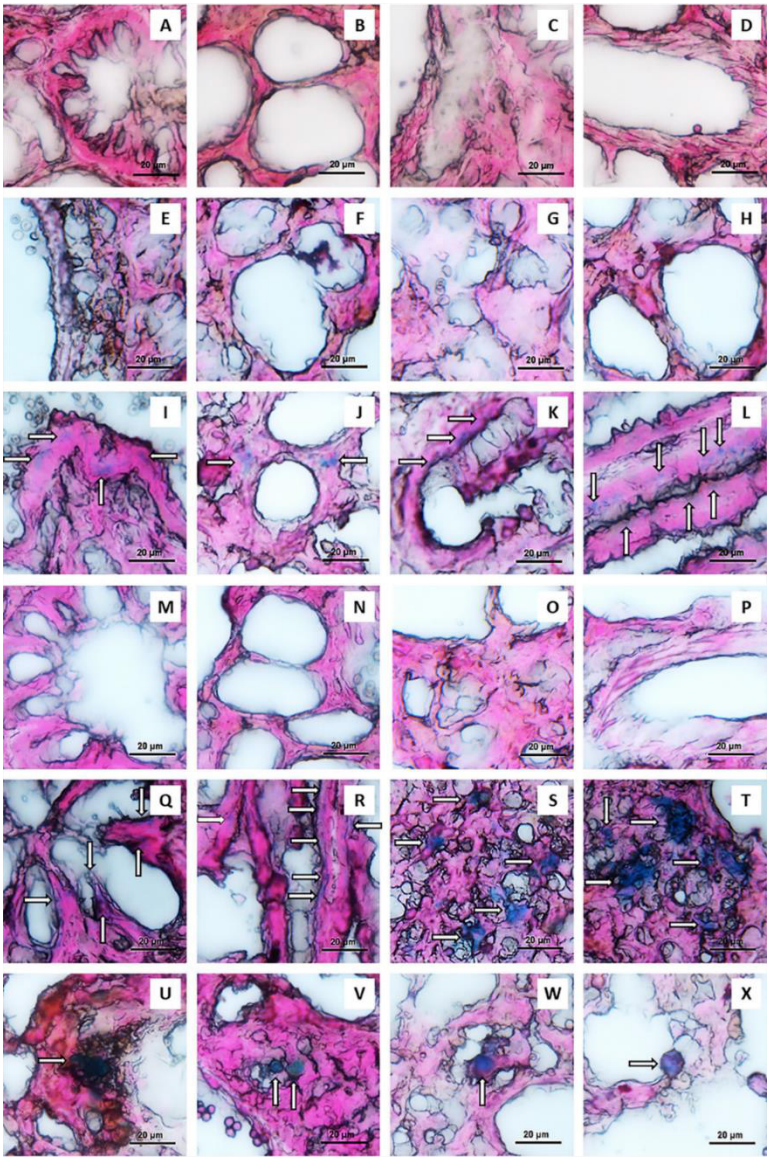

Figure 34. Light field optical microscopy images of rat lung: (A–D) without powder administration, and post-administration of: (E–H) CS NCs-loaded Ma MS, (I–L) pCMV-βGal-CS NCs-loaded Ma MS, (M–P) HA/CS NCs-loaded Ma MS, (Q–T) pCMV-βGal-HA/CS NCs-loaded Ma MS and (U–X) pCMV-βGal-Ma MS. (Figure from the work of Fernández-Paz et al. [212], Pharm. 13 (2021) 1377. Open access article distributed under the Creative Commons Attribution License)

Dry powders are usually preferable for inhalation than their equivalents in liquid formulations due to their better stability [231]. It has been reported the administration of naked pDNA inhaled in form of dry powders prepared with different excipients, resulting in a better transfection than their counterparts in suspension. In that study, the level of transfection was highly dependent on the excipient used for the preparation of the powders, being the MS prepared with HA the ones that gave the best results [280], which could be expected taking into account the HA transfection enhancer effect. CS NCs have already been proposed for lung delivery of genes [140], but they had not been microencapsulated or assessed *in vivo*. The main novelty of our work is the microencapsulation of the genetic material-loaded CS-based NCs in Ma MS to facilitate their pulmonary administration in dry powders form, leading to revealing results. Furthermore, it is very important to highlight that the systems presented in this work are not toxic for the A549 cell line (adenocarcinoma human alveolar basal epithelial cells). Correspondingly, the results of the histopathological examination of the lung sections (Figure 34) are remarkable, taking into account that the lungs were removed 3 days after the administration of the dry powder formulations, sufficient time to evaluate the possible toxicity of the micro-nanosystems. As can be seen in the Figure 34, it was observed the absence of both pulmonary embolism and inflammation, as well as the presence of normal parenchyma, with alveoli of thin wall. These results are comparable to those observed in lung tissue sections not treated with formulations (Figure 34A–D), which visibly confirm the non-toxicity and, hence, the security of the formulations for pulmonary administration. In addition, an interesting advantage of the CS-based NCs is that they can be used for a combined gene therapy, loading the genetic material on the coat and an adjuvant lipophilic molecule, in the core. This can be a molecule that enhances the transfection, like capsaicin [140], which decreases the thickness of the mucus layer [215] and opens the intercellular tight junctions in a reversible way [213,214]. The versatility of the simultaneous transport of HA and different active molecules in the same simple structure allows to carry out a

synergistic transfection effect, being of enormous value for a more effective treatment of genetic lung diseases.

5. CONCLUSIONS

Specific conclusions

From the results of this Doctoral Thesis work, the following conclusions were drawn:

1. CS-based NCs, containing or not HA, capable of carrying a high load of the model plasmid pCMV-βGal were prepared, being the association efficiency of around 90%.

2. pCMV-βGal-loaded CS-based NCs were microencapsulated in Ma MS using a spray-drying technique, giving as result high process yields (> 60%) and microspheres with suitable morphological and aerodynamic characteristics for their pulmonary administration.

3. CS-based NCs released from Ma MS in aqueous media maintained their size in the nanometric range, being hardly affected by the spray-drying process. Consequently, it is expected that after administration *in vivo*, the recovered nanostructures retain their original characteristics in the lung fluid.

4. CS-based NCs and Ma excipient are biocompatible with the A549 cells, leading to viabilities higher than 90%. Furthermore, the cellular uptake was produced by the 100% of the cells.

5. The *in vivo* administration of the developed micro-nanosystems confirmed the arrival of the microencapsulated NCs in the deep lung. In addition, the X-Gal reaction revealed high levels of transfection. The best results were obtained by the pCMV-βGal-HA/CS NCs-loaded Ma MS, producing blue deposits extended homogeneously beyond the edge of the pulmonary alveoli. The light field optical microscopy images visibly confirmed the absence of toxicity and, hence, the safety of the dry powder formulations for pulmonary administration.

General conclusion

In this work we have designed and developed a micro-nanoplatform based on CS NCs and HA/CS NCs microencapsulated in Ma MS in dry powder form for the efficient and safe "in situ" administration of genetic material in the lung. This platform can find an application in gene therapy for the treatment of genetic lung diseases, opening a window of hope for the treatment for those that currently are not well resolved.

6. FUTURE PERSPECTIVES

Microencapsulated CS-based NCs have shown enormous potential for their application in gene therapy by the pulmonary route. Therefore, it arouses the interest of future studies that complement and reinforce the usefulness of this micro-nanoplatform. The possible studies that we contemplate to delve with this line of research are the following:

1. To evaluate the stability of the dry powder formulations (microencapsulated NCs) over time, considering the effect of certain factors such as the temperature and humidity.

2. To improve the characterization of the aerodynamic properties of the selected dry powders with respect to their aerodynamic diameter and *in vitro* distribution, using an Andersen Cascade Impactor.

3. To investigate the association to the HA/CS NCs shell of a therapeutic genetic material for a specific genetic lung disease, together with a lipophilic adjuvant molecule in their oily core, such as capsaicin (proposed as an adjuvant molecule to promote the cell transfection). In addition, we are thinking in the treatment of infectious produced by *A. baumannii* and *M. tuberculosis*, with specific genetic material and antibiotic in their shell and core, respectively. Another idea is to investigate the micro-nanoplatform for the pulmonary delivery of genetic vaccines, like in the case of, for example, COVID-19.

4. To test the *in vitro* viability, transfection and ability to modify the gene expression in altered cells, using the dry powder formulations containing the active ingredients proposed in the point 3.

5. To evaluate the *in vivo* therapeutic efficacy in a suitable animal model (for example, mouse) with a genetic defect that reveals a lung disease, to which could be administered the formulation in dry powder form containing the active molecules proposed in the point 3.

6. To delve into the safety profiles of the proposed micro-nanoplatform.

7. REFERENCES

[1] R. Tang, Z. Xu, Gene therapy: a double-edged sword with great powers, Mol. Cell. Biochem. 474 (2020) 73–81. doi:10.1007/s11010-020-03834-3.

[2] N. Nagoba Shivappa, S. Khurde Sonali, L. Shaikh Atiya, R. Shimge Krishna, Review on gene therapy for the genetic revolution, Indo. Am. J. P. Sci. 05 (2018) 7111–7122.

[3] M. Jafarlou, B. Baradaran, T.A. Saedi, V. Jafarlou, D. Shanehbandi, M. Maralani, F. Othman, An overview of the history, applications, advantages, disadvantages and prospects of gene therapy, J. Biol. Regul. Homeost. Agents. 30 (2016) 315–321.

[4] S. Droz-Georget Lathion, A. Rochat, G. Knott, A. Recchia, D. Martinet, S. Benmohammed, N. Grasset, A. Zaffalon, N.B. Schmutz, E. Savioz-Dayer, J.S. Beckmann, J. Rougemont, F. Mavilio, Y. Barrandon, A single epidermal stem cell strategy for safe ex vivo gene therapy, EMBO Mol. Med. 7 (2015) 380–393. doi:10.15252/emmm.201404353.

[5] J. Serra, C.P.A. Alves, L. Brito, G.A. Monteiro, J.M.S. Cabral, D.M.F. Prazeres, C.L. da Silva, Engineering of human mesenchymal stem/stromal cells with vascular endothelial growth factor-encoding minicircles for angiogenic ex vivo gene therapy, Hum. Gene Ther. 30 (2019) 316–329. doi:10.1089/hum.2018.154.

[6] Z.-Y. He, Y.-G. Zhang, Y.-H. Yang, C.-C. Ma, P. Wang, W. Du, L. Li, R. Xiang, X.-R. Song, X. Zhao, S.-H. Yao, Y.-Q. Wei, In vivo ovarian cancer gene therapy using CRISPR-Cas9, Hum. Gene Ther. 29 (2018) 223–233. doi:10.1089/hum.2017.209.

[7] J.H. Han, S. Han, I.S. Jeong, S.H. Cheon, S.-W. Kim, Minicircle-based GCP-2 ex vivo gene therapy enhanced the reepithelialization and angiogenic capacity, J. Tissue Eng. Regen. Med. 14 (2020) 829–839. doi:10.1002/term.3049.

[8] M. Ramamoorth, A. Narvekar, Non viral vectors in gene therapy - an overview, J. Clin. Diagn. Res. 9 (2015) 1–6. doi:10.7860/jcdr/2015/10443.5394.

[9] D. Wang, G. Gao, State of the art human gene therapy: part II. Gene therapy strategies and clinical applications, Discov. Med. 18 (2014) 151–161.

[10] K.A. Hoadley, C. Yau, T. Hinoue, D.M. Wolf, A.J. Lazar, E. Drill, R. Shen, A.M. Taylor, A.D. Cherniack, V. Thorsson, R. Akbani, R. Bowlby, C.K. Wong, M. Wiznerowicz, F. Sanchez-Vega, A.G. Robertson, B.G. Schneider, M.S. Lawrence, H. Noushmehr, T.M. Malta, J.M. Stuart, C.C. Benz, P.W. Laird, Cell of origin patterns dominate the molecular classification of 10,000 tumors from 33 types of cancer, Cell. 173 (2018) 291–304. doi:10.1016/j.cell.2018.03.022.

[11] E.P. Szymanski, J.M. Leung, C.J. Fowler, C. Haney, A.P. Hsu, F. Chen, P. Duggal, A.J. Oler, R. McCormack, E. Podack, R.A. Drummond, M.S. Lionakis, S.K. Browne, D.R. Prevots, M. Knowles, G. Cutting, X. Liu, S.E. Devine, C.M. Fraser, H. Tettelin, K.N. Olivier, S.M. Holland, Pulmonary nontuberculous mycobacterial infection- a multisystem, multigenic disease, Am. J. Respir. Crit. Care Med. 192 (2015) 618–628. doi:10.1164/rccm.201502-0387OC.

[12] R. Thwaite, G. Pagès, M. Chillón, A. Bosch, AAVrh.10 immunogenicity in mice and humans. Relevance of antibody cross-reactivity in human gene therapy, Gene Ther. 22 (2015) 196–201. doi:10.1038/gt.2014.103.

[13] Y. Deng, C.C. Wang, K.W. Choy, Q. Du, J. Chen, Q. Wang, L. Li, T.K.H. Chung, T. Tang, Therapeutic potentials of gene silencing by RNA interference: Principles, challenges, and new strategies, Gene. 538 (2014) 217–227. doi:10.1016/j.gene.2013.12.019.

[14] G. Cuccato, A. Polynikis, V. Siciliano, M. Graziano, M. di Bernardo, D. di Bernardo, Modeling RNA interference in mammalian cells, BMC Syst. Biol. 5 (2011) 19. doi:10.1186/1752-0509-5-19.

[15] H. Borna, S. Imani, M. Iman, S. Azimzadeh Jamalkandi, Therapeutic face of RNAi: In vivo challenges, Expert Opin. Biol. Ther. 15 (2015) 269–285. doi:10.1517/14712598.2015.983070.

[16] F. Gövert, S.A. Schneider, Huntington´s disease and Huntington´s disease-like syndromes: an overview, Curr. Opin. Neurol. 26 (2013) 420–427. doi:10.1097/WCO.0b013e3283632d90.

[17] M. Kesimer, C. Ehre, K.A. Burns, C.W. Davis, J.K. Sheehan, R.J. Pickles, Molecular organization of the mucins and glycocalyx underlying mucus transport over mucosal surfaces of the airways, Mucosal Immunol. 6 (2013) 379–392. doi:10.1038/mi.2012.81.

[18] MJ. Gutbrod, R.A. Martienssen, Conserved chromosomal functions of RNA interference, Nat. Rev. Genet. 21 (2020) 311–331. doi:10.1038/s41576-019-0203-6.

[19] C. D'Ydewalle, C.J. Sumner, Spinal muscular atrophy therapeutics: Where do we stand? Neurother. 12 (2015) 303–316. doi:10.1007/s13311-015-0337-y.

[20] D. Duan, Duchenne muscular dystrophy gene therapy in the canine model, Hum. Gene Ther. Clin. Dev. 26 (2015) 57–69. doi:10.1089/humc.2015.006.

[21] S.-T. Chou, Q. Leng, A.J. Mixson, Zinc finger nucleases: Tailor-made for gene therapy, Drugs Future. 37 (2012) 183–196. doi:10.1358/dof.2012.037.03.1779022.

[22] H.L. Li, N. Fujimoto, N. Sasakawa, S. Shirai, T. Ohkame, T. Sakuma, M. Tanaka, N. Amano, A. Watanabe, H. Sakurai, T. Yamamoto, S. Yamanaka, A. Hotta, Precise correction of the

dystrophin gene in duchenne muscular dystrophy patient induced pluripotent stem cells by TALEN and CRISPR-Cas9, Stem Cell Rep. 4 (2015) 143–154. doi:10.1016/j.stemcr.2014.10.013.

[23] J. Niu, B. Zhang, H. Chen, Applications of TALENs and CRISPR/Cas9 in human cells and their potentials for gene therapy, Mol. Biotechnol. 56 (2014) 681–688. doi:10.1007/s12033-014-9771-z.

[24] M. Alsaggar, D. Liu, Physical methods for gene transfer, Adv. Genet. 89 (2015) 1–24. doi:10.1016/bs.adgen.2014.10.001.

[25] J. Pahle, W. Walther, Vectors and strategies for nonviral cancer gene therapy, Expert Opin. Biol. Ther. 16 (2016) 443–461. doi:10.1517/14712598.2016.1134480.

[26] L. Sendra, A. Miguel, D. Pérez-Enguix, M.J. Herrero, E. Montalvá, M.A. García-Gimeno, I. Noguera, A. Díaz, J. Pérez, P. Sanz, R. López-Andújar, L. Martí-Bonmatí, S.F. Aliño, Studying closed hydrodynamic models of "in vivo" DNA perfusion in pig liver for gene therapy translation to humans, PLoS One. 11 (2016) e0163898. doi:10.1371/journal.pone.0163898.

[27] T. Suda, D. Liu, Hydrodynamic delivery, Adv. Genet. 89 (2015) 89–111. doi:10.1016/bs.adgen.2014.10.002.

[28] G. Ahlén, L. Frelin, F. Höolmstrm, G. Smetham, S. Augustyn, M. Sällberg, A targeted controlled force injection of genetic material in vivo, Mol. Ther. Methods Clinic. Dev. 3 (2016) 16016. doi:10.1038/mtm.2016.16.

[29] E. Sokol, M. Nijenhuis, K.A. Sjollema, M.F. Jonkman, H.H. Pas, B.N.G. Giepmans, Particle bombardment of ex vivo skin to deliver DNA and express proteins, Methods Mol. Biol. 1559 (2017) 107–118. doi:10.1007/978-1-4939-6786-5_9.

[30] L. Lambricht, A. Lopes, S. Kos, G. Sersa, V. Preat, G. Vandermeulen, Clinical potential of electroporation for gene therapy and DNA vaccine delivery, Expert Opin. Drug Deliv. 13 (2016) 295–310. doi:10.1517/17425247.2016.1121990.

[31] Q. Bi, X. Song, A. Hu, T. Luo, R. Jin, H. Ai, Y. Nie, Magnetofection: Magic magnetic nanoparticles for efficient gene delivery, Chin. Chem. Lett. 31 (2020) 3041–3046. doi:10.1016/j.cclet.2020.07.030.

[32] C.L. Hardee, L.M. Arévalo-Soliz, B.D. Hornstein, L. Zechiedrich, Advances in non-viral DNA vectors for gene therapy, Genes. 8 (2017) 65. doi:10.3390/genes8020065.

[33] C.-K. Chen, P.-K. Huang, W.-C. Law, C.-H. Chu, N.-T. Chen, L.-W. Lo, Biodegradable polymers for gene-delivery applications, Int. J. Nanomed. 15 (2020) 2131–2150. doi:10.2147/IJN.S222419.

[34] K. Ma, C.-L. Mi, X.-X. Cao, T.-Y. Wang, Progress of cationic gene delivery reagents for non-viral vector, Applied Microbiol. Biotechnol. 105 (2021) 525–538. doi:10.1007/s00253-020-11028-6.

[35] S.M. Alnasser, Review on mechanistic strategy of gene therapy in the treatment of disease, Gene. 769 (2020) 1–30. doi:10.1016/j.gene.2020.145246.

[36]https://www.mscbs.gob.es/profesionales/saludPublica/prevPromocion/vacunaciones/covid19/docs/Guia_Tecnica_AstraZeneca.pdf (accessed on 18 January 2022)

[37]https://www.sanidad.gob.es/profesionales/saludPublica/prevPromocion/vacunaciones/covid19/docs/Guia_Tecnica_Janssen.pdf (accessed on 18 January 2022)

[38] X.J. Loh, T.-C. Lee, Gene delivery by functional inorganic nanocarriers, Recent Pat. DNA Gene Seq. 6 (2012) 108–114. doi:10.2174/187221512801327361.

[39] D. Li, K.T. Al-Jamal, siRNA design and delivery based on carbon nanotubes, Methods Mol. Biol. 2282 (2021) 181–193. doi:10.1007/978-1-0716-1298-9_12.

[40] M.J. Molaei, Carbon quantum dots and their biomedical and therapeutic applications: A review, RSC Adv. 9 (2019) 6460–6481. doi:10.1039/c8ra08088g.

[41] V.G. Reshma, P.V. Mohanan, Quantum dots: Applications and safety consequences, J. Lumin. 205 (2019) 287–298. doi:10.1016/j.jlumin.2018.09.015.

[42] T.J. Levingstone, S. Herbaj, J. Redmond, H.O. McCarthy, N.J. Dunne, Calcium phosphate nanoparticles-based systems for RNAi delivery: Applications in bone tissue regeneration, Nanomater. 10 (2020) 146. doi:10.3390/nano10010146.

[43] N.-F. Sun, Z.-A. Liu, W.-B. Huang, A.-L. Tian, S.-Y. Hu, The research of nanoparticles as gene vector for tumor gene therapy, Crit. Rev. Oncol. Hematol. 89 (2014) 352–357. doi:10.1016/j.critrevonc.2013.10.006.

[44] T.V. Mashel, Y.V. Tarakanchikova, A.R. Muslimov, M.V. Zyuzin, A.S. Timin, K.V. Lepik, B. Fehse, Overcoming the delivery problem for therapeutic genome editing: Current status and perspective of non-viral methods, Biomater. 258 (2020) 120282. doi:10.1016/j.biomaterials.2020.120282.

[45] N. Amreddy, A. Babu, R. Muralidharan, A. Munshi, R. Ramesh, Polymeric nanoparticle- mediated gene delivery for lung cancer treatment, Top. Curr. Chem. 375 (2017) 35. doi:10.1007/s41061-017-0128-5.

[46] S.G. Stolberg, The biotech death of Jesse Gelsinger, N. Y. Times Mag [0362-4331]. (1999) 136–140.

[47] D. Wang, G. Gao, State of the art human gene therapy: Part I. Gene delivery technologies, Discov. Med. 18 (2014) 67–77.

[48] M.S. Huh, E.J. Lee, H. Koo, J.Y. Yhee, K.S. Oh, S. Son, S. Lee, S.H. Kim, I.C. Kwon, K. Kim, Polysaccharide-based nanoparticles for gene delivery, Top. Curr. Chem. 375 (2017) 31–50. doi:10.1007/s41061-017-0114-y.

[49] S.J. Hong, M.H. Ahn, J. Sangshetti, P.H. Choung, R.B. Arote, Sugar-based gene delivery systems: Current knowledge and new perspectives, Carbohydr. Polym. 181 (2018) 1180–1193. doi:10.1016/j.carbpol.2017.11.105.

[50] W. Khan, H. Hosseinkhani, D. Ickowicz, P.-D. Hong, D.-S. Yu, A.J. Domb, Polysaccharide gene transfection agents, Acta Biomater. 8 (2012) 4224–4232. doi:10.1016/j.actbio.2012.09.022.

[51] M. Lara-Velázquez, R. Alkharboosh, E.S. Norton, C. Ramirez-Loera, W.D. Freeman, H. Guerrero-Cazares, A.J. Forte, A. Quiñones-Hinojosa, R. Sarabia-Estrada, Chitosan-based non-viral gene and drug delivery systems for brain cancer, Front. Neurol. 11 (2020) 1–10. doi:10.3389/fneur.2020.00740.

[52] R.C. Cheung, T.B. Ng, J.H. Wong, W.Y. Chan, Chitosan: An update on potential biomedical and pharmaceutical applications, Mar. Drugs. 13 (2015) 5156–5186. doi:10.3390/md13085156.

[53] A. Bernkop-Schnurch, S. Dunnhaupt, Chitosan-based drug delivery systems, Eur. J. Pharm. Biopharm. 81 (2012) 463–469. doi:10.1016/j.ejpb.2012.04.007.

[54] J. Zhao, J. Li, Z. Jiang, R. Tong, X. Duan, L. Bai, J. Shi, Chitosan, N,N,N-trimethyl chitosan (TMC) and 2-hydroxypropyltrimethyl ammonium chloride chitosan (HTCC): The

potential immune adjuvants and nano carriers, Int. J. Biol. Macromol. 154 (2020) 339–348. doi:10.1016/j.ijbiomac.2020.03.065.

[55] A.S. Erenler, Capsular polysaccharide biosynthesis from recombinant E. coli and chondroitin sülfate production, Cell. Mol. Biol. 65 (2019) 17–21. doi:10.14715/cmb/2019.65.6.4.

[56] S. Rodrigues, M. Dionísio, C. Remuñán-López, A. Grenha, Biocompatibility of chitosan carriers with application in drug delivery, J. Funct. Biomater. 3 (2012) 615–641. doi:10.3390/jfb3030615.

[57] A. Muxika, A. Etxabide, J. Uranga, P. Guerrero, K. de la Caba, Chitosan as a bioactive polymer: Processing, properties and applications, Int. J. Biol. Macromol. 105 (2017) 1358–1368. doi:10.1016/j.ijbiomac.2017.07.087.

[58] P. Paul, B. Kolesinska, W. Sujka, Chitosan and its derivatives - Biomaterials with diverse biological activity for manifold applications, Mini Rev. Med. Chem. 19 (2019) 737–750. doi:10.2174/1389557519666190112142735.

[59] W. Yu, T. Hu, Conjugation with an inulin-chitosan adjuvant markedly improves the immunogenicity of Mycobacterium tuberculosis CFP10-TB10.4 fusion protein, Mol. Pharm. 13 (2016) 3626–3635. doi:10.1021/acs.molpharmaceut.6b00138.

[60] Z. Hu, S. Lu, Y. Cheng, S. Kong, S. Li, C. Li, L. Yang, Investigation of the effects of molecular parameters on the hemostatic properties of chitosan, Molecules. 23 (2018) 3147. doi:10.3390/molecules23123147.

[61] D. Chuan, T. Jin, R. Fan, L. Zhou, G. Guo, Chitosan for gene delivery: Methods for improvement and applications, Adv. Coll. Interface Sci. 268 (2019) 25–38. doi:10.1016/j.cis.2019.03.007.

[62] B. Santos-Carballal, E. Fernández Fernández, F.M. Goycoolea, Chitosan in non-viral gene delivery: Role of structure, characterization methods, and insights in cancer and rare diseases therapies, Polym. 10 (2018) 444. doi:10.3390/polym10040444.

[63] I.K.D. Dimzon, T.P. Knepper, Degree of deacetylation of chitosan by infrared spectroscopy and partial least squares, Int. J. Biol. Macromol. 72 (2015) 939–945. doi:10.1016/j.ijbiomac.2014.09.050.

[64] Y. Cao, Y.F. Tan, Y.S. Wong, M.W.J. Liew, S. Venkatraman, Recent advances in chitosan-based carriers for gene delivery, Mar. Drugs. 17 (2019) 381. doi:10.3390/md17060381.

[65] M. Alameh, M. Lavertu, N. Tran-Khanh, C.-Y. Chang, F. Lesage, M. Bail, V. Darras, A. Chevrier, M.D. Buschmann, siRNA delivery with chitosan: Influence of chitosan molecular weight, degree of deacetylation, and amine to phosphate ratio on in vitro silencing efficiency, hemocompatibility, biodistribution, and in vivo efficacy, Biomacromol. 19 (2018) 112–131. doi:10.1021/acs.biomac.7b01297.

[66] L.M. Bravo-Anaya, K.G. Fernández-Solís, J. Rosselgong, J.L.E. Nano-Rodríguez, F. Carvajal, M. Rinaudo, Chitosan-DNA polyelectrolyte complex: Influence of chitosan characteristics and mechanism of complex formation, Int. J. Biol. Macromol. 126 (2019) 1037–1049. doi:10.1016/j.ijbiomac.2019.01.008.

[67] J. Yan, Z.-Y. Guan, W.-F. Zhu, L.-Y. Zhong, Z.-Q. Qiu, P.-F. Yue, W.-T. Wu, J. Liu, X. Huang, Preparation of puerarin chitosan oral nanoparticles by ionic gelation method and its related kinetics, Pharm. 12 (2020) 216. doi:10.3390/pharmaceutics12030216.

[68] Y.K. Kim, H.L. Jiang, Y.J. Choi, I.K. Park, M.H. Cho, C.S. Cho, Polymeric nanoparticles of chitosan derivatives as DNA and siRNA carriers, Chitosan Biomater. I. 243 (2011) 1–21. doi:10.1007/12_2011_110.

[69] P.N. Sudha, M.H. Rose, Beneficial effects of hyaluronic acid, Adv. Food Nutr. Res. 72 (2014) 137–176. doi:10.1016/B978-0-12-800269-8.00009-9.

[70] G. Huang, H. Huang, Application of hyaluronic acid as carriers in drug delivery, Drug Deliv. 25 (2018), 766–772. doi:10.1080/10717544.2018.1450910.

[71] G. Tripodo, A. Trapani, M.L. Torre, G. Giammona, G. Trapani, D. Mandracchia, Hyaluronic acid and its derivatives in drug delivery and imaging: Recent advances and challenges, Eur. J. Pharm. Biopharm. 97 (2015) 400–416. doi:10.1016/j.ejpb.2015.03.032.

[72] J.M. Wickens, H.O. Alsaab, P. Kesharwani, K. Bhise, M.C.I.M. Amin, R.K. Tekade, U. Gupta, A.K. Iyer, Recent advances in hyaluronic acid-decorated nanocarriers for targeted cancer therapy, Drug Discov. Today. 22 (2017) 665–680. doi:10.1016/j.drudis.2016.12.009.

[73] E. Karousou, S. Misra, S. Ghatak, K. Dobra, M. Götte, D. Vigetti, A. Passi, N.K. Karamanos, S.S. Skandalis, Roles and targeting of the HAS/hyaluronan/CD_{44} molecular system in cancer, Matrix. Biol. 59 (2017) 3–22. doi:10.1016/j.matbio.2016.10.001.

[74] G. Mattheolabakis, L. Milane, A. Singh, M.M. Amiji, Hyaluronic acid targeting of CD44 for cancer therapy: From receptor biology to nanomedicine, J. Drug Target. 23 (2015) 605–618. doi:10.3109/1061186X.2015.1052072.

[75] N. Csaba, M. Köping-Höggård, M.J. Alonso, Ionically crosslinked chitosan/tripolyphosphate nanoparticles for oligonucleotide and plasmid DNA delivery, Int. J. Pharm. 382 (2009) 205–214. doi:10.1016/j.ijpharm.2009.07.028.

[76] E.P. Rondon, H.A. Benabdoun, F. Vallières, M. Segalla Petrônio, M.J. Tiera, M. Benderdour, J.C. Fernandes, Evidence supporting the

safety of pegylated diethylaminoethyl-chitosan polymer as a nanovector for gene therapy applications, Int. J. Nanomed. 15 (2020) 6183–6200. doi:10.2147/ijn.s252397.

[77] M. Baghaei, F.S.M. Tekie, M.R. Khoshayand, R. Varshochian, M. Hajiramezanali, M.J. Kachousangi, R. Dinarvand, F. Atyabi, Optimization of chitosan-based polyelectrolyte nanoparticles for gene delivery, using design of experiment: In vitro and in vivo study, Mater. Sci. Eng. C. Mater. Biol. Appl. 118 (2021) 111036. doi:10.1016/j.msec.2020.111036.

[78] E. Baghdan, S.R. Pinnapireddy, B. Strehlow, K.H. Engelhardt, J. Schäfer, U. Bakowsky, Lipid coated chitosan-DNA nanoparticles for enhanced gene delivery, Int. J. Pharm. 535 (2018) 473–479. doi:10.1016/j.ijpharm.2017.11.045.

[79] H.M. Aldawsari, H.K. Dhaliwal, B.M. Aljaeid, N.A. Alhakamy, Z.M. Banjar, M.M. Amiji, Optimization of the conditions for plasmid DNA delivery and transfection with self-assembled hyaluronic acid-based nanoparticles, Mol. Pharm. 16 (2019) 128–140. doi:10.1021/acs.molpharmaceut.8b00904.

[80] P.S. Apaolaza, D. Delgado, A. del Pozo-Rodríguez, A. Rodríguez Gascón, M.Á. Solinís, A novel gene therapy vector based on hyaluronic acid and solid lipid nanoparticles for ocular diseases, Int. J. Pharm. 465 (2014) 413–426. doi:10.1016/j.ijpharm.2014.02.038.

[81] L.-J. Yan, X.-H. Guo, W.-P. Wang, Y.-R. Hu, S.-F. Duan, Y. Liu, Z. Sun, S.-N. Huang, H.-L. Li, Gene therapy and photothermal therapy of layer-by-layer assembled AuNCs /PEI/miRNA/ HA nanocomplexes, Curr. Cancer Drug Targets. 19 (2019) 330–337. doi:10.2174/1568009618666181016144855.

[82] S. Al-Qadi, M. Alatorre-Meda, E.M. Zaghloul, P. Taboada, C. Remunán-López, Chitosan– hyaluronic acid nanoparticles for gene silencing: The role of hyaluronic acid on the nanoparticles' formation

and activity, Colloids Surf. B: Biointerfaces. 103 (2013) 615–623. doi:10.1016/j.colsurfb.2012.11.009.

[83] M. de la Fuente, B. Seijo, M.J. Alonso, Novel hyaluronic acid-chitosan nanoparticles for ocular gene therapy, Invest. Ophthalmol. Vis. Sci. 49 (2008b) 2016–2024. doi:10.1167/iovs.07-1077.

[84] A. Masjedi, A. Ahmadi, F. Atyabi, S. Farhadi, M. Irandoust, Y. Khazaei-Poul, M.G. Chaleshtari, M.E. Fathabad, M. Baghaei, N. Haghnavaz, B. Baradaran, M. Hojjat-Farsangi, G. Ghalamfarsa, G. Sabz, S. Hasanzadeh, F. Jadidi-Niaraghg, Silencing of IL-6 and STAT3 by siRNA loaded hyaluronate-N,N,N-trimethyl chitosan nanoparticles potently reduces cancer cell progression, Int. J. Biol. Macromol. 149 (2020) 487–500. doi:10.1016/j.ijbiomac.2020.01.273.

[85] L. Zhao, M. Liu, J. Wang, G. Zhai, Chondroitin sulfate-based nanocarriers for drug/gene delivery, Carbohydr. Polym. 133 (2015) 391–399. doi:10.1016/j.carbpol.2015.07.063.

[86] A. Pathak, P. Kumar, K. Chuttani, Gene expression, biodistribution, and pharmacoscintigraphic evaluation of chondroitin sulfate–PEI nanoconstructs mediated tumor gene therapy, ACS Nano. 3 (2009) 1493-1505. doi: 10.1021/nn900044f.

[87] H. Hosseinkhani, T. Kushibiki, K. Matsumoto, T. Nakamura, Y. Tabata, Enhanced suppression of tumor growth using a combination of NK4 plasmid DNA-PEG engrafted cationized dextran complex and ultrasound irradiation, Cancer Gene Ther. 13 (2006) 479-489. doi:10.1038/sj.cgt.7700918.

[88] Q. Liu, B. Duan, X. Xu, L. Zhang, Progress in rigid polysaccharide-based nanocomposites with therapeutic functions, J. Mater. Chem. B. 5 (2017) 5690–5713. doi:10.1039/c7tb01065f.

[89] L. Knudsen, M. Ochs, The micromechanics of lung alveoli: Structure and function of surfactant and tissue components,

Histochem. Cell Biol. 150 (2018) 661–676. doi:10.1007/s00418-018-1747-9.

[90] P.W. Davenport, A. Von Leupoldt, K. Wheeler-Hegland, I.M. Colrain, Frontiers in respiratory physiology - grand challenge, Front. Physiol. 1 (2010) 139–146. doi:10.3389/fphys.2010.00139.

[91] L. Feng, J. Delacoste, D. Smith, J. Weissbrot, E. Flagg, W.H. Moore, F. Girvin, R. Raad, P. Bhattacharji, D. Stoffel, D. Piccini, M. Stuber, D.K. Sodickson, R. Otazo, H. Chandarana, Simultaneous evaluation of lung anatomy and ventilation using 4D respiratory-motion-resolved ultrashort echo time sparse MRI, J. Magn. Reson. Imaging. 49 (2019) 411–422. doi:10.1002/jmri.26245.

[92] S.M. More, S.S. Kale, A review on pulmonary drug delivery system, World J. Pharm. Pharm. Sci. 10 (2021) 625–641. doi:10.17605/OSF.IO/29J6A.

[93] M. Ochs, J. Hegermann, E. Lopez-Rodriguez, S. Timm, G. Nouailles, J. Matuszak, S. Simmons, M. Witzenrath, W.M. Kuebler, On top of the alveolar epithelium: Surfactant and the glycocalyx, Int. J. Mol. Sci. 21 (2020) 3075. doi:10.3390/ijms21093075.

[94] B. Forbes, C. Ehrhardt, Human respiratory epithelial cell culture for drug delivery applications. Eur. J. Pharm. Biopharm. 60 (2005) 193–205. doi:10.1016/j.ejpb.2005.02.010.

[95] A. Ciechanowicz, Stem cells in lungs, Adv. Exp. Med. Biol. 2101 (2019) 261–274. doi:10.1007/978-3-030-31206-0_13.

[96] Q. Zhong, O.M. Merkel, J.J. Reineke, S.R.P. da Rocha, Effect of the route of administration and PEGylation of Poly(amidoamine) dendrimers on their systemic and lung cellular biodistribution, Mol. Pharm. 13 (2016) 1866–1878. doi:10.1021/acs.molpharmaceut.6b00036.

[97] M. Kolinski, A. Plazinska, K. Jozwiak, Recent progress in understanding of structure, ligand interactions and the mechanism of activation of the β 2-adrenergic receptor, Curr. Med. Chem. 19 (2012) 1155–1163. doi:10.2174/092986712799320547.

[98] A.D. Alves, J.S. Cavaco, F. Guerreiro, J.P. Lourenço, A.M.R. da Costa, A. Grenha, Inhalable antitubercular therapy mediated by locust bean gum microparticles, Mol. 21 (2016) 702. doi:10.3390/molecules21060702.

[99] A. Gupta, G. Pant, K. Mitra, J. Madan, M.K. Chourasia, A. Misra, Inhalable particles containing rapamycin for induction of autophagy in macrophages infected with Mycobacterium Tuberculosis. Mol. Pharm. 11 (2014) 1201–1207. doi:10.1021/mp4006563.

[100] T. Sou, C.A.S. Bergströem, Contemporary formulation development for inhaled pharmaceuticals, J. Pharm. Sci. 110 (2021) 66–86. doi:10.1016/j.xphs.2020.09.006.

[101] Y.-W. Lin, J. Wong, L. Qu, H.-K. Chan, Q.T. Zhou, Powder production and particle engineering for dry powder inhaler formulations, Curr. Pharm. Des. 21 (2015) 3902–3916. doi:10.2174/1381612821666150820111134.

[102] J. Heyder, Deposition of inhaled particles in the human respiratory tract and consequences for regional targeting in respiratory drug delivery, Proc. Am. Thorac. Soc. 1 (2004) 315–320. doi:10.1513/pats.200409-046TA.

[103] J. Brady Scott, R. Kaur, Monitoring breathing frequency, pattern, and effort, Respir. Care. 65 (2020) 793–806. doi:10.4187/respcare.07439.

[104] J. Weers, A. Clark, The impact of inspiratory flow rate on drug delivery to the lungs with dry powder inhalers, Pharm. Res. 34 (2017) 507–528. doi:10.1007/s11095-016-2050-x.

[105] S. Ren, M. Cai, Y. Shi, W. Xu, X. Douglas Zhang, Influence of bronchial diameter change on the airflow dynamics based on a pressure-controlled ventilation system, I. J. Numer. Methods Biomed. Eng. 34 (2017) 2929. doi:10.1002/cnm.2929.

[106] M. Ghadiri, P.M. Young, D. Traini, Strategies to enhance drug absorption via nasal and pulmonary routes, Pharm. 11 (2019) 113. doi:10.3390/pharmaceutics11030113.

[107] S. Bhattacharyya, B.S. Sogali, Inhalation therapy–approaches and challenges, Asian J. Pharm. Clin. Res. 11 (2018) 9–16. doi:10.22159/ajpcr.2018.v11i4.24117.

[108] A. Grenha, D. Carrión-Recio, D. Teijeiro-Osorio, B. Seijo, C. Remuñán-López, Nano-and microparticulate carriers for pulmonary drug delivery. In Handbook of Particulate Drug Delivery; Kumar, M.N.V., Ed.; Ranch, Stevenson; American Scientific Publishers: Valencia, CA, USA, 2008; Volume 2, pp. 165–192.

[109] S.P. Newman, Delivering drugs to the lungs: The history of repurposing in the treatment of respiratory diseases. Adv. Drug Deliv. Rev. 133 (2018) 5–18. doi:10.1016/j.addr.2018.04.010.

[110] S.P. Newman, Drug delivery to the lungs: Challenges and opportunities. Ther. Deliv. 8 (2017) 647–661. doi:10.4155/tde-2017-0037.

[111] T.S. Wilkinson, J.-M. Sallenave, J. Simpson, Pulmonary defense mechanisms, Curr. Respir. Med. Rev. 8 (2012) 149–162. doi:10.2174/157339812800493322.

[112] X.M. Bustamante-Marin, L.E. Ostrowski, Cilia and mucociliary clearance, Cold. Spring Harb. Perspect. Biol. 9 (2017) 028241. doi:10.1101/cshperspect.a028241.

[113] N. Kim, G.A. Duncan, J. Hanes, J.S. Suk, Barriers to inhaled gene therapy of obstructive lung diseases: A review, J. Control Release. 240 (2016) 465–488. doi:10.1016/j.jconrel.2016.05.031.

[114] I.J. Haq, M.A. Gray, J.P. Garnett, C. Ward, M. Brodlie, Airway surface liquid homeostasis in cystic fibrosis: Pathophysiology and therapeutic targets, Thorax. 71 (2016) 284–287. doi:10.1136/thoraxjnl-2015-207588.

[115] M.M. Leiva-Juárez, J.K. Kolls, S.E. Evans, Lung epithelial cells: Therapeutically inducible effectors of antimicrobial defense, Mucosal Immunol. 11 (2018) 21–34. doi:10.1038/mi.2017.71.

[116] S. Chen, S.W.T. Lai, C.E. Brown, M. Feng, Harnessing and enhancing macrophage phagocytosis for cancer therapy, Front. Immunol. 12 (2021) 635173. doi:10.3389/fimmu.2021.635173.

[117] J.M. Rubio, A.M. Astudillo, J. Casas, M.A. Balboa, J. Balsinde, Regulation of phagocytosis in macrophages by membrane ethanolamine plasmalogens, Front. Immunol. 9 (2018) 1723. doi:10.3389/fimmu.2018.01723.

[118] M. Geiser, Update on macrophage clearance of inhaled micro- and nanoparticles, J. Aerosol Med. Pulm. Drug Deliv. 23 (2010) 207–217. doi:10.1089/jamp.2009.0797.

[119] B. Patel, N. Gupta, F. Ahsan, Particle engineering to enhance or lessen uptake by alveolar macrophages and to influence therapeutic outcomes, Eur. J. Pharm. Biopharm. 89 (2015) 163–174. doi:10.1016/j.ejpb.2014.12.001.

[120] A. Grenha, B. Seijo, C. Remuñán-López, Microencapsulated chitosan nanoparticles for lung protein delivery, Eur. J. Pharm. Sci. 25 (2005) 427–437. doi:10.1016/j.ejps.2005.04.009.

[121] A. Hidalgo, A. Cruz, J. Pérez-Gil, Barrier or carrier? Pulmonary surfactant and drug delivery, Eur. J. Pharm. Biopharm. 95 (2015) 117–127. doi:10.1016/j.ejpb.2015.02.014.

[122] S.H. Han, R.K. Mallampalli, The role of surfactant in lung disease and host defense against pulmonary infections, Ann. Am. Thorac. Soc. 12 (2015) 765–774. doi:10.1513/AnnalsATS.201411-507FR.

[123] J.J. Schüer, A. Arndt, C. Wölk, S.R. Pinnapireddy, U. Bakowsky, Establishment of a synthetic in vitro lung surfactant model for particle interaction studies on a Langmuir film balance, Langmuir. 36 (2020) 4808–4819. doi:10.1021/acs.langmuir.9b03712.

[124] S. Grijalvo, A. Alagia, G. Puras, J. Zárate, J.L. Pedraz, R. Eritja, Cationic vesicles based on non-ionic surfactant and synthetic aminolipids mediate delivery of antisense oligonucleotides into mammalian cells, Colloids Surf. B: Biointerfaces. 119 (2014) 30–37. doi:10.1016/j.colsurfb.2014.04.016.

[125] C.-Y. Hsu, C.T. Sung, I.A. Aljuffali, C.-H. Chen, K.-Y. Hu, J.-Y. Fang, Intravenous anti-MRSA phosphatiosomes mediate enhanced affinity to pulmonary surfactants for effective treatment of infectious pneumonia, Nanomed. 14 (2018) 215–225. doi:10.1016/j.nano.2017.10.006.

[126] L. Guillot, N. Nathan, O. Tabary, G. Thouvenin, P. Le Rouzic, H. Corvol, S. Amselem, A. Clement, Alveolar epithelial cells: Master regulators of lung homeostasis, Int. J. Biochem. Cell Biol. 45 (2013) 2568–2573. doi:10.1016/j.biocel.2013.08.009.

[127] A. Costa, C. de Souza Carvalho-Wodarz, V. Seabra, B. Sarmento, C.-M. Lehr, Triple co-culture of human alveolar epithelium, endothelium and macrophages for studying the interaction of nanocarriers with the air-blood barrier, Acta Biomater. 91 (2019) 235–247. doi:10.1016/j.actbio.2019.04.037.

[128] S. Santiwarangkool, H. Akita, I.A. Khalil, M.M.A. Elwakil, Y. Sato, K. Kusumoto, H. Harashima, A study of the endocytosis mechanism and transendothelial activity of lung-targeted GALA-modified liposomes, J. Control. Release. 307 (2019) 55–63. doi:10.1016/j.jconrel.2019.06.009.

[129] N. Rout-Pitt, N. Farrow, D. Parsons, M. Donnelley, Epithelial mesenchymal transition (EMT): A universal process in lung diseases with implications for cystic fibrosis pathophysiology, Respir. Res. 19 (2018) 136. doi:10.1186/s12931-018-0834-8.

[130] C.E. Green, A.M. Turner, The role of the endothelium in asthma and chronic obstructive pulmonary disease (COPD), Respir. Res. 18 (2017) 20. doi:10.1186/s12931-017-0505-1.

[131] A.C. Schamberger, N. Mise, J. Jia, E. Genoyer, AÖ Yildirim, S. Meiners, O. Eickelberg, Cigarette smoke-induced disruption of bronchial epithelial tight junctions is prevented by transforming growth factor-β, Am. J. Respir. Cell Mol. Biol. 50 (2014) 1040–1052. doi:10.1165/rcmb.2013-0090OC.

[132] Adivitiya, M.S. Kaushik, S. Chakraborty, S. Veleri, S. Kateriya, Mucociliary respiratory epithelium integrity in molecular defense and susceptibility to pulmonary viral infections, Biol. 10 (2021) 95. doi:10.3390/biology10020095.

[133] F.A. da Silva da Costa, M.R. Soares, M.J. Malagutti-Ferreira, G.R. da Silva, F.A. Dos Reis Lívero, J.T. Ribeiro-Paes, Three-dimensional cell cultures as a research platform in lung diseases and

COVID-19, Tissue Eng. Regen. Med. 18 (2021) 735–745. doi:10.1007/s13770-021-00348-x.

[134] R. Jain, P. Dandekar, B. Loretz, M. Koch, C.-M. Lehr, Dimethylaminoethyl methacrylate copolymer-siRNA nanoparticles for silencing a therapeutically relevant gene in macrophages, Med. Chem. Commun. 6 (2015) 691–701. doi:10.1039/c4md00490f.

[135] J. Ho, M. Ip, Antibiotic-resistant community-acquired bacterial pneumonia, Infect. Dis. Clin. N. Am. 33 (2019) 1087–1103. doi:10.1016/j.idc.2019.07.002.

[136] W. Zhong, X. Zhang, Y. Zeng, D. Lin, J. Wu, Recent applications and strategies in nanotechnology for lung diseases, Nano Res. (2021) 1–23. doi:10.1007/s12274-020-3180-3.

[137] B. Shin, W. Park, Antibiotic resistance of pathogenic Acinetobacter species and emerging combination therapy, J. Microbiol. 55 (2017) 837–849. doi:10.1007/s12275-017-7288-4.

[138] P.J. Stogios, M.L. Kuhn, E. Evdokimova, M. Law, P. Courvalin, A. Savchenko, Structural and biochemical characterization of Acinetobacter spp. aminoglycoside acetyltransferases highlights functional and evolutionary variation among antibiotic resistance enzymes, ACS Infect. Dis. 3 (2017) 132–143. doi:10.1021/acsinfecdis.6b00058.

[139] C. Lopez, B.A. Arivett, L.A. Actis, M.E Tolmasky, Inhibition of AAC(6')-Ib-mediated resistance to amikacin in Acinetobacter baumannii by an antisense peptide-conjugated 2',4'-bridged nucleic acid-NC-DNA hybrid oligomer, Antimicrob. Agents Chemother. 59 (2015) 5798–5803. doi:10.1128/AAC.01304-15.

[140] A.K. Kolonko, J. Efing, Y. González-Espinosa, N. Bangel-Ruland, W. van Driessche, F.M. Goycoolea, W.-M. Weber, Capsaicin-loaded chitosan nanocapsules for wtCFTR-mRNA delivery

to a cystic fibrosis cell line, Biomed. 8 (2020) 364. doi:10.3390/biomedicines8090364.

[141] Z. Li, G. Lu, G. Meng, Pathogenic fungal infection in the lung, Front. Immunol. 10 (2019) 1524. doi:10.3389/fimmu.2019.01524.

[142] C. Schwarz, C. Brandt, P. Whitaker, S. Sutharsan, H. Skopnik, S. Gartner, C. Smazny, J.F. Röhmel, Invasive pulmonary fungal infections in cystic fibrosis, Mycopathol. 183 (2018) 33–43. doi:10.1007/s11046-017-0199-4.

[143] H. Salvator, N. Mahlaoui, E. Catherinot, E. Rivaud, B. Pilmis, R. Borie, B. Crestani, C. Tcherakian, F. Suarez, B. Dunogue, M.-A. Gougerot-Pocidalo, M. Hurtado-Nedelec, J.-F. Dreyfus, I. Durieu, F. Fouyssac, O. Hermine, O. Lortholary, A. Fischer, L.-J. Couderc, Pulmonary manifestations in adult patients with chronic granulomatous disease, Eur. Respir. J. 45 (2015) 1613–1623. doi:10.1183/09031936.00118414.

[144] M.N. Gamaletsou, T.J. Walsh, N.V. Sipsas, Invasive fungal infections in patients with hematological malignancies: Emergence of resistant pathogens and new antifungal therapies, Turk. J. Haematol. 35 (2018) 1–11. doi:10.4274/tjh.2018.0007.

[145] K.R. Healey, Y. Zhao, W.B. Perez, S.R. Lockhart, J.D. Sobel, D. Farmakiotis, D.P. Kontoyiannis, D. Sanglard, S.J. Taj-Aldeen, B.D. Alexander, C. Jimenez-Ortigosa, E. Shor, D.S. Perlin, Prevalent mutator genotype identified in fungal pathogen Candida glabrata promotes multi-drug resistance, Nat. Commun. 7 (2016) 11128. doi:10.1038/ncomms11128.

[146] R.K. Shields, M.H. Nguyen, E.G. Press, A.L. Kwa, S. Cheng, C. Du, C.J. Clancy, The presence of an FKS mutation rather than MIC is an independent risk factor for failure of echinocandin therapy among patients with invasive candidiasis due to Candida glabrata,

Antimicrob. Agents Chemother. 56 (2012) 4862–4869. doi:10.1128/AAC.00027-12.

[147] P.E. Verweij, A. Chowdhary, W.J.G. Melchers, J.F. Meis, Azole resistance in Aspergillus fumigatus: Can we retain the clinical use of mold-active antifungal azoles? Clin. Infect. Dis. 62 (2016) 362–368. doi:10.1093/cid/civ885.

[148] A. Chowdhary, C. Sharma, J.F. Meis, Azole-resistant aspergillosis: Epidemiology, molecular mechanisms, and treatment, J. Infect. Dis. 216 (2017) 436–444. doi:10.1093/infdis/jix210.

[149] M.W. McCarthy, D.P. Kontoyiannis, O.A. Cornely, J.R. Perfect, T.J. Walsh, Novel agents and drug targets to meet the challenges of resistant fungi, J. Infect. Dis. 216 (2017) 474–483. doi:10.1093/infdis/jix130.

[150] D. Sanchez-Guzman, P. Le Guen, B. Villeret, N. Sola, R. Le Borgne, A. Guyard, A. Kemmel, B. Crestani, J.-M. Sallenave, I. Garcia-Verdugo, Silver nanoparticle-adjuvanted vaccine protects against lethal influenza infection through inducing BALT and IgA-mediated mucosal immunity, Biomater. 217 (2019) 119308. doi:10.1016/j.biomaterials.2019.119308.

[151] P. Sadhukhan, M.T. Ugurlu, M.O. Hoque, Effect of COVID-19 on lungs: Focusing on prospective malignant phenotypes, Cancers. 12 (2020) 3822. doi:10.3390/cancers12123822.

[152] K.S. Park, X. Sun, M.E. Aikins, J.J. Moon, Non-viral COVID-19 vaccine delivery systems, Adv. Drug Deliv. Rev. 169 (2021) 137–151. doi:10.1016/j.addr.2020.12.008.

[153] E.E. Walsh, R.W. Frenck, A.R. Falsey, N. Kitchin, J. Absalon, A. Gurtman, et al., Safety and immunogenicity of two RNA-based Covid-19 vaccine candidates, New Engl. J. Med. 383 (2020) 2439-2450. doi:10.1056/NEJMoa2027906.

[154] L.R. Baden, H.M. El Sahly, B. Essink, K. Kotloff, S. Frey, R. Novak, et al., Efficacy and safety of the mRNA-1273 SARS-CoV-2 vaccine. New Engl. J. Med. 384 (2021) 403–416. doi:10.1056/NEJMoa2035389.

[155] European Medicines Agency: Science Medicines Health. COVID-19 vaccines: Authorised for use in the European Union. https://www.ema.europa.eu/en/human-regulatory/overview/public-health-threats/coronavirus-disease-covid-19/treatments-vaccines/covid-19-vaccines. (Accessed 1 September 2021).

[156] https://www.aemps.gob.es/la-aemps/ultima-informacion-de-la-aemps-acerca-del-covid%e2%80%9119/vacunas-contra-la-covid%e2%80%9119/comirnaty/ (accessed on 18 January 2022)

[157] https://www.aemps.gob.es/la-aemps/ultima-informacion-de-la-aemps-acerca-del-covid%e2%80%9119/vacunas-contra-la-covid%e2%80%9119/covid-19-vaccine-moderna/ (accessed on 18 January 2022)

[158] T. Tagami, S.G. Sakka, X. Monnet, Diagnosis and treatment of acute respiratory distress syndrome, JAMA. 320 (2018) 305. doi:10.1001/jama.2018.5924.

[159] B.E. Levine, Fifty years of research in ARDS. ARDS: How it all began, Am. J. Respir. Crit. Care Med. 196 (2017) 1247–1248. doi:10.1164/rccm.201706-1281ED.

[160] E. Fan, D. Brodie, A.S. Slutsky, Acute respiratory distress syndrome: Advances in diagnosis and treatment, JAMA. 319 (2018) 698–710. doi:10.1001/jama.2017.21907.

[161] H. Dupont, P. Depuydt, F. Abroug, Prone position acute respiratory distress syndrome patients: Less prone to ventilator

associated pneumonia? Intensive Care Med. 42 (2016) 937–939. doi:10.1007/s00134-015-4190-6.

[162] D. Abrams, D. Brodie, Extracorporeal membrane oxygenation for adult respiratory failure: 2017 update, Chest. J. 152 (2017) 639–649. doi:10.1016/j.chest.2017.06.016.

[163] B. Baer, L.M.P. Souza, A.S. Pimentel, R.A.W. Veldhuizen, New insights into exogenous surfactant as a carrier of pulmonary therapeutics, Biochem. Pharmacol. 164 (2019) 64–73. doi:10.1016/j.bcp.2019.03.036.

[164] A. Amigoni, A. Pettenazzo, V. Stritoni, M. Circelli, Surfactants in acute respiratory distress syndrome in infants and children: Past, present and future, Clin. Drug Investig. 37 (2017) 729–736. doi:10.1007/s40261-017-0532-1.

[165] F. Alessandri, F. Pugliese, V.M. Ranieri, The role of rescue therapies in the treatment of severe ARDS, Respir. Care. 63 (2018) 92–101. doi:10.4187/respcare.05752.

[166] X.-P. Zhang, W.-T. Zhang, Y. Qiu, M.-J. Ju, G.-W. Tu, Z. Luo, Understanding gene therapy in acute respiratory distress syndrome, Curr. Gene Ther. 19 (2019) 93–99. doi:10.2174/1566523219666190702154817.

[167] S.T. Holgate, S. Wenzel, D.S. Postma, S.T. Weiss, H. Renz, P.D. Sly, Asthma, Nat. Rev. Dis. Primers. 1 (2015) 15025. doi:10.1038/nrdp.2015.25.

[168] W.T. Gerthoffer, J. Solway, B. Camoretti-Mercado, Emerging targets for novel therapy of asthma, Curr. Opin. Pharmacol. 13 (2013) 324–330. doi:10.1016/j.coph.2013.04.002.

[169] I.P. Shilovskii, M.S. Prozorova, A.R. Gaisina, A.A. Laskin, V.V. Smirnov, A.A. Babakhin, M.R. Khaitov, RNA interference: New

approach to the treatment of allergic asthma (a review), Eksp. Klin. Farmakol. 79 (2016) 35–44.

[170] S.C. Ramelli, W.T. Gerthoffer, MicroRNA targets for asthma therapy, Adv. exp. med. biol. 1303 (2021) 89–105. doi:10.1007/978-3-030-63046-1_6.

[171] P.-J. Chang, C. Michaeloudes, J. Zhu, N. Shaikh, J. Baker, K.F. Chung, P.K. Bhavsar, Impaired nuclear translocation of the glucocorticoid receptor in corticosteroid-insensitive airway smooth muscle in severe asthma, Am. J. Respir. Crit. Care Med. 191 (2015) 54–62. doi:10.1164/rccm.201402-0314OC.

[172] R.A. El-Zein, R.P. Young, R.J. Hopkins, C.J. Etzel, Genetic predisposition to chronic obstructive pulmonary disease and/or lung cancer: Important considerations when evaluating risk, Cancer Prev. Res. 5 (2012) 522–527. doi:10.1158/1940-6207.CAPR-12-0042.

[173] M.J. Abramson, J.L. Perret, S.C. Dharmage, V.M. McDonald, C.F. McDonald, Distinguishing adult-onset asthma from COPD: A review and a new approach, Int. J. Chron. Obstruct. Pulmon. Dis. 9 (2014) 945–962. doi:10.2147/COPD.S46761.

[174] K.F. Rabe, H. Watz, Chronic obstructive pulmonary disease, Lancet. 389 (2017) 1931–1940. doi:10.1016/S0140-6736(17)31222-9.

[175] K. Aoshiba, F. Zhou, T. Tsuji, A. Nagai, DNA damage as a molecular link in the pathogenesis of COPD in smokers, Eur. Respir. J. 39 (2012) 1368–1376. doi:10.1183/09031936.00050211.

[176] L.M. Paardekooper, I. Dingjan, P.T.A. Linders, A.H.J. Staal, S.M. Cristescu, W.C.E.P. Verberk, G. van den Bogaart, Human monocyte-derived dendritic cells produce millimolar concentrations of ROS in phagosomes per second, Front. Immunol. 10 (2019) 1216. doi:10.3389/fimmu.2019.01216.

[177] B.M. Fischer, J.A. Voynow, A.J. Ghio, COPD: Balancing oxidants and antioxidants, Int. J. Chron. Obstruct. Pulmon. Dis. 10 (2015) 261–276. doi:10.2147/COPD.S42414.

[178] E. Mendoza-Coronel, E. Ortega, Macrophage polarization modulates FcγR- and CD13-mediated phagocytosis and reactive oxygen species production, independently of receptor membrane expression, Front. Immunol. 8 (2017) 303. doi:10.3389/fimmu.2017.00303.

[179] D.-D. Wu, J. Song, S. Bartel, S. Krauss-Etschmann, M.G. Rots, M.N. Hylkema, The potential for targeted rewriting of epigenetic marks in COPD as a new therapeutic approach, Pharmacol. Ther. 182 (2018) 1–14. doi:10.1016/j.pharmthera.2017.08.007.

[180] B.S. Comer, M. Ba, C.A. Singer, W.T. Gerthoffer, Epigenetic targets for novel therapies of lung diseases, Pharmacol. Ther. 147 (2015) 91–110. doi:10.1016/j.pharmthera.2014.11.006.

[181] Q. Lin, J. Chen, Z. Zhang, G. Zheng, Lipid-based nanoparticles in the systemic delivery of siRNA, Nanomed. 9 (2014) 105–120. https://doi.org/10.2217/nnm.13.192.

[182] D. Koppers-Lalic, M.M. Hogenboom, J.M. Middeldorp, D.M. Pegtel, Virus-modified exosomes for targeted RNA delivery; a new approach in nanomedicine, Adv. Drug Deliv. Rev. 65 (2013) 348–356. doi:10.1016/j.addr.2012.07.006.

[183] T. Ong, B.W. Ramsey, Update in cystic fibrosis 2014, Am. J. Respir. Crit. Care Med. 192 (2015) 669–675. doi:10.1164/rccm.201504-0656UP.

[184] D.A. Stoltz, D.K. Meyerholz, M.J. Welsh, Origins of cystic fibrosis lung disease, N. Engl. J. Med. 372 (2015) 351–362. doi:10.1056/NEJMra1300109.

[185] S. Kumar, A. Tana, A. Shankar, Cystic fibrosis - what are the prospects for a cure? Eur. J. Intern. Med. 25 (2014) 803–807. doi:10.1016/j.ejim.2014.09.018.

[186] F. Qaisar, A. Habib, M. Riaz, Z.U. Rehman, Barriers and recent advances in non-viral vectors targeting the lungs for cystic fibrosis gene therapy, Nanomed. J. 6 (2019) 75–84. doi:10.22038/NMJ.2019.06.0001.

[187] E. Fernández Fernández, B. Santos-Carballal, W.-M. Weber, F.M. Goycoolea, Chitosan as a non-viral co-transfection system in a cystic fibrosis cell line, Int. J. Pharm. 502 (2016) 1–9. doi:10.1016/j.ijpharm.2016.01.083.

[188] L. Pandolfi, V. Frangipane, C. Bocca, A. Marengo, E. Tarro Genta, S. Bozzini, M. Morosini, M. D'Amato, S. Vitulo, M. Monti, G. Comolli, M.T. Scupoli, E. Fattal, S. Arpicco, F. Meloni, Hyaluronic acid–decorated liposomes as innovative targeted delivery system for lung fibrotic cells, Mol. 24 (2019) 3291. doi:10.3390/molecules24183291.

[189] P. Salahuddin, Gene therapy for alpha-1-antitrypsin deficiency diseases, Gene Ther. Applications. (2011) 375–400. doi:10.5772/17415.

[190] J. Wozniak, T. Wandtke, P. Kopinski, J. Chorostowska-Wynimko, Challenges and prospects for alpha-1 antitrypsin deficiency gene therapy, Hum. Gene Ther. 26 (2015) 709–718. doi:10.1089/hum.2015.044.

[191] C. McCarthy, E.P. Reeves, N.G. McElvaney, The role of neutrophils in alpha-1 antitrypsin deficiency, Ann. Am. Thorac. Soc. 13 (2016) 297–304. doi:10.1513/AnnalsATS.201509-634KV.

[192] M. Mohanka, D. Khemasuwan, J.K. Stoller, A review of augmentation therapy for alpha-1 antitrypsin deficiency, Expert Opin. Biol. Ther. 12 (2012) 685–700. doi:10.1517/14712598.2012.676638.

[193] M.J. Chiuchiolo, R.G. Crystal, Gene therapy for alpha-1 antitrypsin deficiency lung disease, Ann. Am. Thorac. Soc. 13 (2016) 352–369. doi:10.1513/AnnalsATS.201506-344KV.

[194] F. Bray, J. Ferlay, I. Soerjomataram, R.L. Siegel, L.A. Torre, A. Jemal, Global cancer statistics 2018: GLOBOCAN estimates of incidence and mortality worldwide for 36 cancers in 185 countries, CA Cancer J. Clin. 68 (2018) 394–424. doi:10.3322/caac.21492.

[195] W. Zhang, W. Xu, Y. Lan, X. He, K. Liu, Y. Liang, Antitumor effect of hyaluronic-acid-modified chitosan nanoparticles loaded with siRNA for targeted therapy for non-small cell lung cancer, Int. J. Nanomed. 14 (2019) 5287–5301. doi:10.2147/IJN.S203113.

[196] NIH, U.S. National Library of Medicine, ClinicalTrials.gov.: database of clinical trials from around the world. https://www.clinicaltrials.gov. (Accessed 1 September 2021).

[197] S. Deng, M.R. Gigliobianco, R. Censi, P. Di Martino, Polymeric nanocapsules as nanotechnological alternative for drug delivery system: Current status, challenges and opportunities, Nanomater. 10 (2020) 847. doi:10.3390/nano10050847.

[198] C.-S. Chiang, S.-H. Hu, B.-J. Liao, Y.-C. Chang, S.-Y. Chen, Enhancement of cancer therapy efficacy by trastuzumab-conjugated and pH-sensitive nanocapsules with the simultaneous encapsulation of hydrophilic and hydrophobic compounds, Nanomed: Nanotechnol. Biol. Med. 10 (2014) 99–107. doi:10.1016/j.nano.2013.07.009.

[199] A.M. Ledo, M.S. Sasso, V. Bronte, I. Marigo, B.J. Boyd, M. Garcia-Fuentes, M.J. Alonso, Co-delivery of RNAi and chemokine by polyarginine nanocapsules enables the modulation of myeloid-derived

suppressor cells, J. Control. Release. 295 (2019) 60–73. doi:10.1016/j.jconrel.2018.12.041.

[200] C.S. Kim, R. Mout, Y. Zhao, Y.-C. Yeh, R. Tang, Y. Jeong, B. Duncan, J.A. Hardy, V.M. Rotello, Co-delivery of protein and small molecule therapeutics using nanoparticle-stabilized nanocapsules, Bioconjug. Chem. 26 (2015) 950–954. doi:10.1021/acs.bioconjchem.5b00146.

[201] P. Rosa, M.L. Friedrich, J. dos Santos, D.R. Nogueira Librelotto, L.H. Maurer, T. Emanuelli, C.B. da Silva, A.I.H. Adams, Desonide nanoencapsulation with açai oil as oil core: Physicochemical characterization, photostability study and in vitro phototoxicity evaluation, J. Photochem. Photobiol. B: Biol. 199 (2019) 111606. doi:10.1016/j.jphotobiol.2019.111606.

[202] L.A. Frank, R.P. Gazzi, P. de Andrade Mello, A. Buffon, A.R. Pohlmann, S.S. Guterres, Imiquimod-loaded nanocapsules improve cytotoxicity in cervical cancer cell line, Eur. J. Pharm. Biopharm. 136 (2019) 9–17. doi:10.1016/j.ejpb.2019.01.001.

[203] F.A. Dimer, C. de Souza Carvalho-Wodarz, A. Goes, K. Cirnski, J. Herrmann, V. Schmitt, L. Pätzold, N. Abed, C. De Rossi, M. Bischoff, P. Couvreur, R. Müller, C.-M. Lehr, PLGA nanocapsules improve the delivery of clarithromycin to kill intracellular Staphylococcus aureus and Mycobacterium abscessus, Nanomed. 24 (2020) 102125. doi:10.1016/j.nano.2019.102125.

[204] D.M. Rata, A.N. Cadinoiu, L.I. Atanase, S.E. Bacaita, C. Mihalache, O.-M. Daraba, D. Gherghel, M. Popa, “In vitro” behaviour of aptamer-functionalized polymeric nanocapsules loaded with 5-fluorouracil for targeted therapy, Mater. Sci. Eng. C. Mater. Biol. Appl. 103 (2019) 109828. doi:10.1016/j.msec.2019.109828.

[205] A. Castro, N. Berois, A. Malanga, C. Ortega, P. Oppezzo, O. Pristch, A.W. Mombru, E. Osinaga, H. Pardo, Docetaxel in chitosan-

based nanocapsules conjugated with an anti-Tn antigen mouse/human chimeric antibody as a promising targeting strategy of lung tumors, Int. J. Biol. Macromol. 182 (2021) 806–814. doi:10.1016/j.ijbiomac.2021.04.054.

[206] J. Kim, T. Ramasamy, J.Y. Choi, S.T. Kim, Y.S. Youn, H.-G. Choi, C.S. Yong, J.O. Kim, PEGylated polypeptide lipid nanocapsules to enhance the anticancer efficacy of erlotinib in non-small cell lung cancer, Colloids and Surf. B: Biointerfaces. 150 (2017) 393–401. doi:10.1016/j.colsurfb.2016.11.002.

[207] C. Shi, S. Zhong, Y. Sun, L. Xu, S. He, Y. Dou, S. Zhao, Y. Gao, X. Cui, Sonochemical preparation of folic acid-decorated reductive-responsive ε-poly-L-lysine-based microcapsules for targeted drug delivery and reductive-triggered release, Mater. Sci. Eng. C. 106 (2020) 110251. doi:10.1016/j.msec.2019.110251.

[208] M.L. Simionato Gomes, N. Da Silva Nascimento, D.M. Borsato, A.P. Pretes, J. Mendes Nadal, A. Novatski, R. Zanetti Gomes, D. Fernandes, P.V. Farago, S.M. Warumby Zanin, Long-lasting anti-platelet activity of cilostazol from poly(ε-caprolactone)-poly(ethylene glycol) blend nanocapsules, Mater. Sci. Eng. C. 94 (2019) 694–702. doi:10.1016/j.msec.2018.10.029.

[209] V. Dubey, P. Mohan, J.S. Dangi, K. Kesavan, Brinzolamide loaded chitosan-pectin mucoadhesive nanocapsules for management of glaucoma: Formulation, characterization and pharmacodynamic study, Int. J. Biol. Macromol. 152 (2020) 1224–1232. doi:10.1016/j.ijbiomac.2019.10.219.

[210] M.R. Mohd, T.M. Ariff, N. Mohamad, A.Z.A. Latif, W.M.N.W. Nik, A. Mohamed, I.F.M. Suffian, Development of biodegradable sustained-release damnacanthal nanocapsules for potential application in in-vitro breast cancer studies, Pak. J. Pharm. Sci. 32 (2019) 2155–2162.

[211] S. Safwat, R.M. Hathout, R.A. Ishak, N.D. Mortada, Augmented simvastatin cytotoxicity using optimized lipid nanocapsules: A potential for breast cancer treatment, J. Liposome Res. 27 (2017) 1–10. doi:10.3109/08982104.2015.1137313.

[212] E. Fernández-Paz, L. Feijoo-Siota, M.M. Gaspar, N. Csaba, C. Remuñán-López, Microencapsulated chitosan-based nanocapsules: A new platform for pulmonary gene delivery, Pharm. 13 (2021) 1377. doi:10.3390/pharmaceutics13091377.

[213] T. Shiobara, T. Usui, J. Han, H. Isoda, Y. Nagumo, The reversible increase in tight junction permeability induced by capsaicin is mediated via cofilin-actin cytoskeletal dynamics and decreased level of occluding, PLoS One. 8 (2013) e79954. doi:10.1371/journal.pone.0079954.

[214] M. Kaiser, S. Pereira, L. Pohl, S. Ketelhut, B. Kemper, C. Gorzelanny, H.-J. Galla, B.M. Moerschbacher, F.M. Goycoolea, Chitosan encapsulation modulates the effect of capsaicin on the tight junctions of MDCK cells, Sci. Rep. 5 (2015) 10048. doi:10.1038/srep10048.

[215] S. Frydas, G. Varvara, G. Murmura, A. Saggini, A. Caraffa, P. Antinolfi, S. Tetè, D. Tripodi, F. Conti, E. Cianchetti, E. Toniato, M. Rosati, L. Speranza, A. Pantalone, R. Saggini, L.M. Di Tommaso, T.C. Theoharides, P. Conti, F. Pandolfi, Impact of capsaicin on mast cell inflammation, Int. J. Immunopathol. Pharmacol. 26 (2013) 597–600. doi:10.1177/039463201302600303.

[216] J. Li, C. Cai, J. Li, J. Li, J. Li, T. Sun, L. Wang, H. Wu, G. Yu, Chitosan-based nanomaterials for drug delivery, Mol. 23 (2018) 2661. doi:10.3390/molecules23102661.

[217] I.C. Trindade, G. Pound-Lana, D.G.S. Pereira, L.A.M. de Oliveira, M.S. Andrade, J.M. Carneiro Vilela, B. Bueno Postacchini, V.C. Furtado Mosqueira, Mechanisms of interaction of biodegradable

polyester nanocapsules with non-phagocytic cells, Eur. J. Pharm. Sci. 124 (2018) 89–104. doi:10.1016/j.ejps.2018.08.024.

[218] S.U. Frick, M.P. Domogalla, G. Baier, F.R. Wurm, V. Mailänder, K. Landfester, K. Steinbrink, Interleukin-2 functionalized nanocapsules for T cell-based immunotherapy, ACS Nano. 10 (2016) 9216–9226. doi:10.1021/acsnano.5b07973.

[219] C. Ingallina, P.M. Costa, F. Ghirga, R. Klippstein, J.T. Wang, S. Berardozzi, N. Hodgins, P. Infante, S.M. Pollard, B. Botta, K.T. Al-Jamal, Polymeric glabrescione B nanocapsules for passive targeting of Hedgehog-dependent tumor therapy in vitro, Nanomed. 12 (2017) 711–728. doi:10.2217/nnm-2016-0388.

[220] J.-H. Lee, J.-T. Jang, J.-S. Choi, S.H. Moon, S.-H. Noh, J.-W. Kim, J.-G. Kim, I.-S. Kim, K.I. Park, J. Cheon, Exchange-coupled magnetic nanoparticles for efficient heat induction, Nat. Nanotechnol. 6 (2011) 418–422. doi:10.1038/nnano.2011.95.

[221] H.S. Birk, S.J. Han, N.A. Butowski, Treatment options for recurrent high-grade gliomas, CNS Oncol. 6 (2017) 61–70. doi:10.2217/cns-2016-0013.

[222] G. Bottai, M. Truffi, F. Corsi, L. Santarpia, Progress in nonviral gene therapy for breast cancer and what comes next? Expert Opin. Biol. Ther. 17 (2017) 595–611. doi:10.1080/14712598.2017.1305351.

[223] J.P. Kirkpatrick, J.H. Sampson, Recurrent malignant gliomas, Semin. Radiat. Oncol. 24 (2014) 289–298. doi:10.1016/j.semradonc.2014.06.006.

[224] M. Lara-Velazquez, R. Al-Kharboosh, S. Jeanneret, C. Vazquez-Ramos, D. Mahato, D. Tavanaiepour, G. Rahmathulla, A. Quinones-Hinojosa, Advances in brain tumor surgery for glioblastoma in adults, Brain Sci. 7 (2017) 166. doi:10.3390/brainsci7120166.

[225] I.T. Papademetriou, T. Porter, Promising approaches to circumvent the blood-brain barrier: Progress, pitfalls and clinical prospects in brain cancer, Ther. Deliv. 6 (2015) 989–1016. doi:10.4155/tde.15.48.

[226] S. Zhong, H. Zhang, Y. Liu, G. Wang, C. Shi, Z. Li, Y. Feng, X. Cui, Folic acid functionalized reduction-responsive magnetic chitosan nanocapsules for targeted delivery and triggered release of drugs, Carbohydr. Polym. 168 (2017) 282–289. doi:10.1016/j.carbpol.2017.03.083.

[227] F. Danhier, K. Messaoudi, L. Lemaire, J.-P. Benoit, F. Lagarce, Combined anti-Galectin-1 and anti-EGFR siRNA-loaded chitosan-lipid nanocapsules decrease temozolomide resistance in glioblastoma: In vivo evaluation, Int. J. Pharm. 481 (2015) 154–161. doi:10.1016/j.ijpharm.2015.01.051.

[228] M. Van Woensel, T. Mathivet, N. Wauthoz, R. Rosiere, A.D. Garg, P. Agostinis, V. Mathieu, R. Kiss, F. Lefranc, L. Boon, J. Belmans, S.W. Van Gool, H. Gerhardt, K. Amighi, S. De Vleeschouwer, Sensitization of glioblastoma tumor micro-environment to chemo- and immunotherapy by Galectin-1 intranasal knock-down strategy, Sci. Rep. 7 (2017) 1217. doi:10.1038/s41598-017-01279-1.

[229] S.U.I. Islam, A. Shehzad, M.B. Ahmed, Y.S. Lee, Intranasal delivery of nanoformulations: A potential way of treatment for neurological disorders, Mol. 25 (2020) 1929. doi:10.3390/molecules25081929.

[230] I. Posadas, S. Monteagudo, V. Ceña, Nanoparticles for brain-specific drug and genetic material delivery, imaging and diagnosis, Nanomed. 11 (2016) 833–849. doi:10.2217/nnm.16.15.

[231] S. Al-Qadi, A. Grenha, D. Carrión-Recio, B. Seijo, C. Remuñán-López, Microencapsulated chitosan nanoparticles for

pulmonary protein delivery: In vivo evaluation of insulin-loaded formulations, J. Control. Rel. 157 (2012) 383–390. doi:10.1016/j.jconrel.2011.08.008.

[232] C. Fernández-Paz, S. Rojas, P. Salcedo-Abraira, T. Simón-Yarza, C. Remuñán-López, P. Horcajada, Metal-organic frame-work microsphere formulation for pulmonary administration, ACS Appl. Mater. Interfaces. 12 (2020) 25676–25682. doi:10.1021/acsami.0c07356.

[233] H.L. Ohrem, E. Schornick, A. Kalivoda, R. Ognibene, Why is mannitol becoming more and more popular as a pharmaceutical excipient in solid dosage forms? Pharm. Dev. Technol. 19 (2014) 257–262. doi:10.3109/10837450.2013.775154.

[234] U.S. Food and Drug Administration, Inactive Ingredient Search for Approved Drug Products. https://www.accessdata.fda.gov/scripts/cder/iig/index.cfm. (Accessed 1 September 2021).

[235] S. Al-Qadi, P. Taboada, C. Remuñán-López, Micro/nanostructured inhalable formulation based on polysaccharides: Effect of a thermoprotectant on powder properties and protein integrity, Int. J. Pharm. 551 (2018) 23–33. doi:10.1016/j.ijpharm.2018.08.049.

[236] S.G. Maas, G. Schaldach, E.M. Littringer, A. Mescher, U.J. Griesser, D.E. Braun, P.E. Walzel, N.A. Urbanetz, The impact of spray drying outlet temperature on the particle morphology of mannitol, Powder Technol. 213 (2011) 27–35. doi:10.1016/j.powtec.2011.06.024.

[237] A. Teper, A. Jaques, B. Charlton, Inhaled mannitol in patients with cystic fibrosis: A randomised open-label dose response trial, J. Cyst. Fibros. 10 (2011) 1–8. doi:10.1016/j.jcf.2010.08.020.

[238] D.P. Gaspar, M.M. Gaspar, C.V. Eleutério, A. Grenha, M. Blanco, L.M.D. Gonçalves, P. Taboada, A.J. Almeida, C. Remuñán-López, Microencapsulated solid lipid nanoparticles as a hybrid platform for pulmonary antibiotic delivery, Mol. Pharm. 14 (2017) 2977–2990. doi:10.1021/acs.molpharmaceut.7b00169.

[239] D.A. Scheinberg, J. Grimm, D.A. Heller, E.P. Stater, M. Bradbury, M.R. McDevitt, Advances in the clinical translation of nanotechnology, Curr. Opin. Biotechnol. 46 (2017) 66–73. doi:10.1016/j.copbio.2017.01.002.

[240] A. Cadete, A. Olivera, M. Besev, P.K. Dhal, L. Gonçalves, A.J. Almeida, G. Bastiat, J.-P. Benoit, M. de la Fuente, M. García-Fuentes, M.J. Alonso, D. Torres, Self-assembled hyaluronan nanocapsules for the intracelular delivery of anticancer drugs, Sci. Rep. 9 (2019) 11565. doi:10.1038/s41598-019-47995-8.

[241] G. Lollo, P. Hervella, P. Calvo, P. Avilés, M.J. Guillén, M. García-Fuentes, M.J. Alonso, D. Torres, Enhanced in vivo therapeutic efficacy of plitidepsin-loaded nanocapsules decorated with a new poly-aminoacid-PEG derivative, Int. J. Pharm. 483 (2015) 212–219. doi:10.1016/j.ijpharm.2015.02.028.

[242] M. Peleteiro, E. Presas, J.V. González-Aramundiz, B. Sánchez-Correa, R. Simón-Vázquez, N. Csaba, M.J. Alonso, A. González-Fernández, Polymeric nanocapsules for vaccine delivery: Influence of the polymeric shell on the interaction with the immune system, Front. Immunol. 9 (2018) 791. doi:10.3389/fimmu.2018.00791.

[243] P. Calvo, C. Remuñán-López, J.L. Vila-Jato, M.J. Alonso, Development of positively charged colloidal drug carriers: Chitosan-coated polyester nanocapsules and submicron-emulsions, Colloid Polym. Sci. 275 (1997) 46–53. doi:10.1007/s003960050050.

[244] A. Ziaee, A.B. Albadarin, L. Padrela, T. Femmer, E. O'Reilly, G. Walker, Spray drying of pharmaceuticals and biopharmaceuticals:

Critical parameters and experimental process optimization approaches, Eur. J. Pharm. Sci. 127 (2019) 300–318. doi:10.1016/j.ejps.2018.10.026.

[245] A. Ousset, J. Meeus, F. Robin, M.A. Schubert, P. Somville, K. Dodou, Comparison of a novel miniaturized screening device with Büchi B290 Mini Spray-Dryer for the development of spray-dried solid dispersions (SDSDs), Process. 6 (2018) 129. doi:10.3390/pr6080129.

[246] I. El-Gibaly, Development and in vitro evaluation of novel floating chitosan microcapsules for oral use: Comparison with non-floating chitosan microspheres, Int. J. Pharm. 294 (2002) 7–21. doi:10.1016/S0378-5173(02)00396-4.

[247] P. Bell, M. Limberis, G. Gao, D. Wu, M.S. Bove, J.C. Sanmiguel, J.M. Wilson, An optimized protocol for detection of E. Coli β-Galactosidase in lung tissue following gene transfer, Histochem. Cell Biol. 124 (2005) 77–85. doi:10.1007/s00418-005-0793-2.

[248] S. Al-Qadi, A. Grenha, C. Remuñán-López, Microspheres loaded with polysaccharide nanoparticles for pulmonary delivery: Preparation, structure and surface analysis, Carbohydr. Polym. 86 (2011) 25–34. doi:10.1016/j.carbpol.2011.03.022.

[249] M. De la Fuente, B. Seijo, M.J. Alonso, Design of novel polysaccharidic nanostructures for gene delivery, Nanotechnol. 19 (2008a) 075105. doi:10.1088/0957-4484/19/7/075105.

[250] C. Prego, D. Torres, M.J. Alonso, Chitosan nanocapsules: A new carrier for nasal peptide delivery, J. Drug Del. Sci. Tech. 16 (2006) 331–337. doi:10.1016/s1773-2247(06)50061-9.

[251] C. Prego, D. Torres, E. Fernandez-Megia, R. Novoa-Carballal, E. Quiñoá, M.J. Alonso, Chitosan–PEG nanocapsules as new carriers

for oral peptide delivery effect of chitosan pegylation degree. J. Control. Release 111 (2006) 299–308. doi:10.1016/j.jconrel.2005.12.015.

[252] C. Prego, M. Fabre, D. Torres, M.J. Alonso, Efficacy and mechanism of action of chitosan nanocapsules for oral peptide delivery, Pharm. Res. 23 (2006) 549–556. doi:10.1007/s11095-006-9570-8.

[253] D.P. Gaspar, V. Faria, L.M.D. Gonçalves, P. Taboada, C. Remuñán-López, A.J. Almeida, Rifabutin-loaded solid lipid nanoparticles for inhaled antitubercular therapy: Physicochemical and in vitro studies, Int. J. Pharm. 497 (2016) 199–209. doi:10.1016/j.ijpharm.2015.11.050.

[254] H. Rouco, P. Diaz-Rodriguez, D.P. Gaspar, L.M.D. Gonçalves, M. Cuerva, C. Remuñán-López, A.J. Almeida, M. Landin, Rifabutin-loaded nanostructured lipid carriers as a tool in oral anti-mycobacterial treatment of Crohn's disease, Nanomater. 10 (2020) 2138. doi:10.3390/nano10112138.

[255] E. Fernández-Paz, C. Fernández-Paz, S. Barrios-Esteban, I. Santalices, N. Csaba, C. Remuñán-López, Dry powders containing chitosan-based nanocapsules for pulmonary administration: Adjustment of spray-drying process and in vitro evaluation in A549 cells, Powder Technol. Accepted article (pending publication).

[256] G. Pilcer, K. Amighi, Formulation strategy and use of excipients in pulmonary drug delivery, Int. J. Pharm. 392 (2010) 1–19. doi:10.1016/j.ijpharm.2010.03.017.

[257] J. Broadhead, S.K. Edmond-Rouan, C.T. Rhodes, The spray drying of pharmaceuticals, Drug Dev. Ind. Pharm. 18 (1992) 1169–1206. doi:10.3109/03639049209046327.

[258] A. Grenha, B. Seijo, C. Serra, C. Remuñán-López, Chitosan nanoparticle-loaded mannitol microspheres: Structure and surface characterization, Biomacromol. 8 (2007) 2072–2079. doi:10.1021/bm061131g.

[259] A. Bhardwaj, S. Mehta, S. Yadav, S.K. Singh, A. Grobler, A.K. Goyal, A. Mehta, Pulmonary delivery of antitubercular drugs using spray-dried lipid – polymer hybrid nanoparticles, Artif. Cell. Nanomed. Biotechnol. 44 (2015) 1544–1555. doi:10.3109/21691401.2015.1062389.

[260] S. Al-Qadi, C. Remuñán-López, A micro-and nano-structured drug carrier based on biocompatible, hybrid polymeric nanoparticles for potential application in dry powder inhalation therapy, Polymer. 55 (2014) 4012–4021. doi:10.1016/j.polymer.2014.06.046.

[261] A. Grenha, C. Remuñán-López, E.L.S. Carvalho, B. Seijo, Microspheres containing lipid/chitosan nanoparticles complexes for pulmonary delivery of therapeutic proteins, Eur. J. Pharm. Biopharm. 69 (2008) 83–93. doi:10.1016/j.ejpb.2007.10.017.

[262] I. Khan, M. Apostolou, R. Bnyan, C. Houacine, A. Elhissi, S.S. Yousaf, Paclitaxel-loaded micro or nano transfersome formulation into novel tablets for pulmonary drug delivery via nebulization, Int. J. Pharm. 575 (2020) 118919. doi:10.1016/j.ijpharm.2019.118919.

[263] C. Bosquillon, C. Lombry, V. Préat, R. Vanbever, Influence of formulation excipients and physical characteristics of inhalation dry powders on their aerosolization performance, J. Control. Release. 70 (2001) 329–339. doi:10.1016/s0168-3659(00)00362-x.

[264] J.C. Mejias, K. Roy, In-vitro and in-vivo characterization of a multi-stage enzyme-responsive nanoparticle-in-microgel pulmonary drug delivery system. J. Control. Release. 316 (2019) 393–403. doi:10.1016/j.jconrel.2019.09.012.

[265] C. Sinsuebpol, J. Chatchawalsaisin, P. Kulvanich, Preparation and in vivo absorption evaluation of spray dried powders containing salmon calcitonin loaded chitosan nanoparticles for pulmonary delivery, Drug Des. Dev. Ther. 7 (2013) 861–873. doi:10.2147/DDDT.S47681.

[266] M.M. Bailey, E.M. Gorman, E.J. Munson, C. Berkland, Pure insulin nanoparticle agglomerates for pulmonary delivery, Langmuir. 24 (2008) 13614–13620. doi:10.1021/la802405p.

[267] M. Paranjpe, C.C. Müller-Goymann, Nanoparticle-mediated pulmonary drug delivery: A review. Int. J. Mol. Sci. 15 (2014) 5852–5873. doi:10.3390/ijms15045852.

[268] A.R. Berkebile, P.B. McCray, Effects of airway surface liquid pH on host defense in cystic fibrosis, Int. J. Biochem. Cell Biol. 52 (2014) 124–129. doi:10.1016/j.biocel.2014.02.009.

[269] A. Grenha, C.I. Grainger, L.A. Dailey, B. Seijo, G.P. Martin, C. Remuñán-López, B. Forbes, Chitosan nanoparticles are compatible with respiratory epithelial cells in vitro, Eur. J. Pharm. Sci. 31 (2007) 73–84. doi:10.1016/j.ejps.2007.02.008.

[270] N. Changsan, C. Sinsuebpol, Dry powder inhalation formulation of chitosan nanoparticles for co-administration of isoniazid and pyrazinamide, Pharm. Dev. Technol. 26 (2020) 181–192. doi:10.1080/10837450.2020.1852570.

[271] H. Mok, J.W. Park, T.G. Park, Antisense oligodeoxynucleotide-conjugated hyaluronic acid/protamine nanocomplexes for intracellular gene inhibition, Bioconjugate Chem. 18 (2007) 1483–1489. doi:10.1021/bc070111o.

[272] Y. Tao, J. Han, H. Dou, Paclitaxel-loaded tocopheryl succinate-conjugated chitosan oligosaccharide nanoparticles for synergistic

chemotherapy, J. Mater. Chem. 22 (2012) 8930–8937. doi:10.1039/c2jm30290j.

[273] E. Yan, Y. Fu, X. Wang, Y. Ding, H. Qian, C.-H. Wang, Y. Hu, X. Jiang, Hollow chitosan-silica nanospheres for doxorubicin delivery to cancer cells with enhanced antitumor effect in vivo, J. Mater. Chem. 21 (2011) 3147–3155. doi:10.1039/c0jm03234d.

[274] A. Portero, C. Remuñán-López, H.M. Nielsen, The potential of chitosan in enhancing peptide and protein absortion across the TR146 cell culture model-an in vitro model of the buccal epithelium, Pharm. Res. 19 (2002) 169–174. doi:10.1023/a:1014220832384.

[275] D.J. Weiss, D. Liggitt, J.G. Clark, Histochemical discrimination of endogenous mammalian β-Galactosidase activity from that resulting from Lac-Z gene expression, Histochem. J. 31 (1999) 231–236. doi:10.1023/a:1003642025421.

[276] I. Serrano-Sevilla, A. Artiga, S.G. Mitchell, L. de Matteis, J.M. de la Fuente, Natural polysaccharides for siRNA delivery: Nanocarriers based on chitosan, hyaluronic acid, and their derivatives, Mol. 24 (2019) 2570. doi:10.3390/molecules24142570.

[277] K. Shah, S. Chawla, A. Gadeval, G. Reddy, R. Maheshwari, K. Kalia, R.K. Tekade, Nanostructured hyaluronic acid-based materials for the delivery of siRNA, Curr. Pharm. Des. 24 (2018) 2678–2691. doi:10.2174/1381612824666180807123705.

[278] T. Ito, N. Iida-Tanaka, T. Niidome, T. Kawano, K. Kubo, K. Yoshikawa, T. Sato, Z. Yang, Y. Koyama, Hyaluronic acid and its derivative as a multi-functional gene expression enhancer: Protection from non-specific interactions, adhesion to targeted cells, and transcriptional activation, J. Control. Release. 112 (2006) 382–388. doi:10.1016/j.jconrel.2006.03.013.

[279] S.P. Evanko, T.N. Wight, Intracellular localization of hyaluronan in proliferating cells, J. Histochem. Cytochem. 47 (1999) 1331–1341. doi:10.1177/002215549904701013.

[280] T. Ito, T. Okuda, Y. Takashima, H. Okamoto, Naked pDNA inhalation powder composed of hyaluronic acid exhibits high gene expression in the lungs, Mol. Pharm. 16 (2019) 489–497. doi:10.1021/acs.molpharmaceut.8b005

8. STATEMENTS: CONFLICT OF INTEREST, IMAGES USE AND PUBLISHED CONTENT

DECLARATION OF ABSENCE OF CONFLICT OF INTEREST OF THE PhD STUDENT

In accordance with the guidelines of the International Doctoral School (EDI) in Health Sciences of the University of Santiago de Compostela (USC) (agreement of May 3, 2018), the PhD student Estefanía Fernández Paz declares that she has no possible conflict of interest in relation to the present doctoral thesis.

Narón, …… 2022

Fdo. Estefanía Fernández Paz

DECLARATION OF USE OF IMAGES OF THE PhD STUDENT

The images presented in this Thesis Book, entitled: New pulmonary delivery platform based on chitosan nanocapsules with potential application in gene therapy, were prepared by the doctoral student: Estefanía Fernández Paz by,

a) new creation. Figures: 2, 4, 20, 20 (continuation) and 21.

b) adaptation/modification of original figures from an article published by the PhD student. Figures: 8, 9, 10, 18, 24, 25, 33 and 34.

c) adaptation/modification of original figures from an article accepted for publication of the PhD student. Figures: 11, 12, 13, 14, 15, 16, 17, 19, 22, 23, 26, 27, 28, 29, 30, 31 and 32.

d) adaptation/modification of non-original figures (that is, of figures from articles not published by the PhD student). Figures: 3, 5, 6 and 7.

e) copyright free. Figure: 1.

All the figures are adequately cited at the bottom of the same, with reference to their original source and copyright in the corresponding cases.

Narón, …… 2022

Fdo. Estefanía Fernández Paz

DECLARATION OF THE CONTENT PUBLISHED/ACCEPTED FOR PUBLICATION OF THE PhD STUDENT

The present Book of Thesis: "New pulmonary delivery platform based on chitosan nanocapsules with potential application in gene therapy" is structured in a monographic mode and in English, with partial reproduction of published and accepted articles derived from the research work of the PhD student: Estefanía Fernández Paz.

The sections published and accepted for publication, as well as the quality indexes of the journals, are described below:

PUBLISHED/ACCEPTED FOR PUBLICATION SECTIONS:

1. Studies related to CS-based NCs-loaded Ma MS: preparation, characterization, microencapsulation and *in vitro* studies are accepted in a research article, in a peer-reviewed journal.

2. Studies related to plasmid-loaded CS-based NCs-loaded Ma MS: preparation, characterization, microencapsulation and *in vivo* studies are published in a research article, in a peer-reviewed journal.

TITLES OF THE ARTICLES:

1. Dry powders containing chitosan-based nanocapsules for pulmonary administration: Adjustment of spray-drying process and *in vitro* evaluation in A549 cells.

2. Microencapsulated Chitosan-Based Nanocapsules: A New Platform for Pulmonary Gene Delivery.

AUTHORS AND AFFILIATIONS:

1. Estefanía Fernández-Paz[1], Cristina Fernández-Paz[1], Sheila Barrios-Esteban[2], Irene Santalices[1,2], Noemi Csaba[2], Carmen Remuñán-López[1]

   [1]Nanobiofar Group, Department of Pharmacology, Pharmacy & Pharmaceutical Technology, Faculty of Pharmacy, University of Santiago de Compostela, 15782 Santiago de Compostela, Spain.
   [2]Nanobiofar Group, Center of Research in Molecular Medicine and Chronic Diseases (CiMUS), University of Santiago de Compostela, Campus Vida, 15706 Santiago de Compostela, Spain

2. Estefanía Fernández-Paz[1], Lucía Feijoo-Siota[2], Maria Manuela Gaspar[3], Noemi Csaba[4] and Carmen Remuñán-López[1]

   [1]Nanobiofar Group, Department of Pharmacology, Pharmacy & Pharmaceutical Technology, Faculty of Pharmacy, University of Santiago de Compostela, 15782 Santiago de Compostela, Spain.
   [2]Department of Microbiology & Parasitology, Faculty of Pharmacy, University of Santiago de Compostela, 15782 Santiago de Compostela, Spain

[3]Research Institute for Medicines (iMed.ULisboa), Faculty of Pharmacy, University of Lisboa, Av. Professor GamaPinto, 1649-003 Lisbon, Portugal
[4]Nanobiofar Group, Center of Research in Molecular Medicine and Chronic Diseases (CiMUS), University of Santiago de Compostela, Campus Vida, 15706 Santiago de Compostela, Spain

DATE OF PUBLISHING/ACCEPTANCE:

1. 18/01/2022 (date of acceptance)
2. 31/08/2021 (date of publishing)

JOURNAL:

1. Powder Technology
2. Pharmaceutics

DOI, VOLUME, PAGES/ARTICLE NUMBER:

1. Article accepted for publication in Powder Technology.
2. doi:10.3390/pharmaceutics13091377, volumen:13, número de artículo: 1377.

CONTRIBUTION OF THE PhD STUDENT TO THE ARTICLES:

In both articles, the PhD student contributed in:

1. Conceptualization: formulation of ideas and statement of general objectives of the research.
2. Methodology: design and development of methodology.

3. Research: conducting experiments and collecting results.
4. Validation: verification of the replication and general reproducibility of the experiments and results.
5. Software: handling of different softwares.
6. Data processing: collection, purification and interpretation of research results.
7. Formal analysis: application of statistical, mathematical and computational techniques to analyze the results of the studies.
8. Resources: management of obtaining laboratory material, reagents and instrumentation.
9. Visualization: visualization and presentation of data.
10. Writing: preparing of the original draft.

The PhD student carried out all the studies presented in the articles and in the Thesis, with the exception of certain studies:

1. Help received for the plasmid preparation: Lucía Feijoo Siota (Department of Microbiology, Faculty of Pharmacy) and Noemi Csaba (CiMUS).
2. Help received for taking SEM, TEM, CLSM and RAMAN images: personnel specialized in the handling of the CACTUS and CiMUS microscopes.
3. Help received to carry out the *in vitro* cell studies. Specifically, the PhD student was allowed the use of facilities and protocols, thanks to the generosity of Noemi Csaba, but the PhD student performed the experiments.
4. *In vivo* studies carried out by Manuela Gaspar, who was in charge of the processes associated with the handling of rats. The PhD student prepared the dry powder samples and she was in charge of the interpretation, writing and discussion of the results.

QUALITY CRITERIA:

The journals where the articles were publicated/accepted present:

1. Impact factor: 5.134 (2020); CiteScore Index: 7.7 (calculated by Scopus in 2020); Quartile 1 (Q1) in "Chemical Engineering (miscellaneous, including *Applications of particle technology in production of pharmaceuticals*)" (SJR 2020 1.079) calculated by Scimago: https://www.scimagojr.com/journalsearch.php?q=13717&tip=sid&clean=0
2. Impact factor: 6.321 (2020); CiteScore Index: 4.7 (calculated by Scopus in 2020); Quartile 1 (Q1) in "Pharmaceutical Science" (SJR 2020 1.054) calculated by Scimago: https://www.scimagojr.com/journalsearch.php?q=19700188360&tip=sid&clean=0

ETHICAL CONSIDERATIONS:

In this Thesis Book, they have been included certain data and figures that were adapted/modified from:

a) Original data and figures, published/accepted in:

1. **Powder Technology.** The original article was accepted for publication in this journal (see page 326). Figures: 11, 12, 13, 14, 15, 16, 17, 19, 22, 23, 26, 27, 28, 29, 30, 31 and 32.
2. **Pharmaceutics.** It has not required permission for partial reproduction of content and figures (Figures 8, 9, 10, 18, 24, 25, 33 and 34) from the journal because the published article is an open access article distributed under the terms and conditions of the Creative Commons Attribution (CC BY) License.

b) Non-original figures, previously published in**:**

1. **Journal of Functional Biomaterials.** It has not required permission for the employment and modification of a figure (Figure 3) from the journal because the published article is an open access article distributed under the terms of the Creative Commons Attribution License.
2. **Drug Delivery.** It has not required permission for the employment and modification of a figure (Figure 5) from the journal because the published article is an open access article distributed under the terms of the Creative Commons CC BY License.
3. **Journal of Pharmaceutical Sciences.** It has not required permission for the employment and modification of two figures (Figures 6 and 7) from the journal because the published article is an open access article.

9. PERMISSIONS

This article of "Pharmaceutics" is an open access article distributed under the terms and conditions of the Creative Commons Attribution (CC BY) License. It was used to employ original figures (Figures 8-10, 18, 24, 25, 33 and 34) and modified text.

Open Access Article

Microencapsulated Chitosan-Based Nanocapsules: A New Platform for Pulmonary Gene Delivery

by Estefanía Fernández-Paz [1], Lucía Feijoo-Siota [2], María Manuela Gaspar [3], Noemi Csaba [4] and Carmen Remuñán-López [1,*]

[1] Nanobiofar Group, Department of Pharmacology, Pharmacy & Pharmaceutical Technology, Faculty of Pharmacy, University of Santiago de Compostela, 15782 Santiago de Compostela, Spain
[2] Department of Microbiology & Parasitology, Faculty of Pharmacy, University of Santiago de Compostela, 15782 Santiago de Compostela, Spain
[3] Research Institute for Medicines (iMed.ULisboa), Faculty of Pharmacy, University of Lisboa, Av. Professor GamaPinto, 1649-003 Lisbon, Portugal
[4] Nanobiofar Group, Center of Research in Molecular Medicine and Chronic Diseases (CiMUS), University of Santiago de Compostela, Campus Vida, 15706 Santiago de Compostela, Spain
* Author to whom correspondence should be addressed.

Academic Editors: Vanessa Carla Furtado Mosqueira and Raquel Silva Araújo

Pharmaceutics 2021, *13*(9), 1377; https://doi.org/10.3390/pharmaceutics13091377

(Top on the page)

(Bottom on the page)

Abstract

In this work, we propose chitosan (CS)-based nanocapsules (NCs) for pulmonary gene delivery. Hyaluronic acid (HA) was incorporated in the NCs composition (HA/CS NCs) aiming to promote gene transfection in the lung epithelium. NCs were loaded with a model plasmid (pCMV-βGal) to easily evaluate their transfection capacity. The plasmid encapsulation efficiencies were of approx. 90%. To facilitate their administration to the lungs, the plasmid-loaded NCs were microencapsulated in mannitol (Ma) microspheres (MS) using a simple spray-drying technique, obtaining dry powders of adequate properties. In vivo, the MS reached the deep lung, where the plasmid-loaded CS-based NCs were released and transfected the alveolar cells more homogeneously than the control formulation of plasmid directly microencapsulated in Ma MS. The HA-containing formulation achieved the highest transfection efficiency, in a more extended area and more homogeneously distributed than the rest of tested formulations. The new micro-nanostructured platform proposed in this work represents an efficient strategy for the delivery of genetic material to the lung, with great potential for the treatment of genetic lung diseases. View Full-Text

Keywords: chitosan nanocapsules; in vivo study; microspheres; pCMV-βGal; pulmonary gene delivery; spray-drying

► Show Figures

Acceptance of the article "Dry powders containing chitosan-based nanocapsules for pulmonary administration: Adjustment of spray-drying process and *in vitro* evaluation in A549 cells" by the Powder Technology journal.

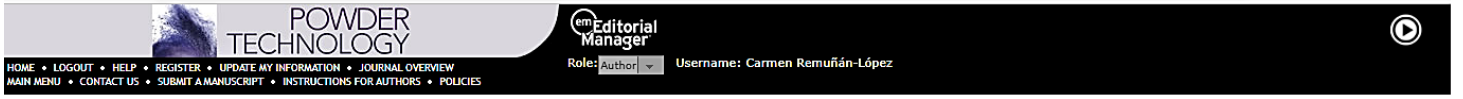

Submissions with an Editorial Office Decision for Author Carmen Remuñán-López, PhD

Page: 1 of 1 (1 total completed submissions) Results per page 10

Action	Manuscript Number	Title	Initial Date Submitted	Status Date	Current Status	Date Final Disposition Set	Final Disposition
Action Links	POWTEC-D-21-03042	Dry powders containing chitosan-based nanocapsules for pulmonary administration: Adjustment of spray-drying process and in vitro evaluation in A549 cells	Nov 06, 2021	Jan 18, 2022	Completed - Accept	Jan 18, 2022	Accept

Page: 1 of 1 (1 total completed submissions) Results per page 10

<< Author Main Menu

You should use the free Adobe Reader 10 or later for best PDF Viewing results.

Get ADOBE READER

This article of "Journal of Functional Biomaterials" is an open access article distributed under the terms of the Creative Commons Attribution License. It was used for the modification of a non-original figure (Figure 3 of the Thesis Book).

GOVERNO DE PORTUGAL | MINISTÉRIO DA AGRICULTURA E MAR

dgav

Exma Senhora
Doutora Maria Manuela Gaspar
Faculdade de Farmácia da Universidade de Lisboa
Departamento de Farmácia Galénica e Tecnologia Farmacêutica
Campus do Lumiar
Estrada do Paço do Lumiar, 22, Edifício F, R/C
1649 – 038 LISBOA

2013-09-02 023517

Nossa referência	Vossa referência	Vossa data
0421/000/000 /2013		

Assunto: **PROTEÇÃO DOS ANIMAIS UTILIZADOS PARA FINS EXPERIMENTAIS E/OU OUTROS FINS CIENTÍFICOS – PEDIDO DE AUTORIZAÇÃO PARA REALIZAÇÃO DE PROJECTO DE EXPERIMENTAÇÃO ANIMAL**

Na sequência do pedido efetuado por V. Exª no sentido de poder ser autorizada a realização do projeto experimental designado **"Development of microparticulate systems to target alveolar macrophages in tuberculosis therapy"**, tendo como investigadora responsável a **Doutora Ana Grenha**, cabe-me informar que o mesmo foi levado à consideração dos membros da Comissão Consultiva prevista na alínea b) do nº 49, da Portaria nº 1005/92, de 23 de Outubro, sendo que os mesmos não levantaram qualquer objeção à solicitação supra referida.

Mais se informa V. Exª que esta Direção Geral, depois de esclarecidas as dúvidas que a sua análise nos levantou, nada teve a opôr ao projeto apresentado, pelo que o mesmo foi autorizado, ao abrigo do nº 8º do mesmo diploma legislativo.

Com os melhores cumprimentos,

A Diretora Geral

As) Maria Teresa Villa de Brito

DBEA/APM

SEDE : LARGO DA ACADEMIA NACIONAL DE BELAS ARTES, 2 – 1249-105 LISBOA TELEF. 21 323 95 00 FAX. 21 346 35 18

DGV
Direcção Geral
de Veterinária
Ministério da Agricultura,
do Desenvolvimento Rural e das Pescas

CERTIFICADO DE ATRIBUIÇÃO DE CREDITAÇÃO

Ao abrigo do ponto iii), da alínea e), do nº 3 da Portaria nº 1005/92, de 23 de Outubro, é atribuída a MARIA MANUELA GASPAR, creditação como pessoa competente para a prática de experimentação animal.

Lisboa, 19 de Setembro de 2005

O Director Geral

As) Carlos Agrela Pinheiro

FERNANDO BERNARDO
Subdiretor-Geral

LARGO DA ACADEMIA NACIONAL DE BELAS ARTES, 2 – 1249-105 LISBOA TLF. 21 323 95 00 FAX 21 323 95 65

10. CHECKLISTS

Checklist for Thesis that include experimental animals. **EXPERIMENTAL ANIMALS ARRIVE**

Yes/No/NA		Page
	Title	
Yes	Provide as accurate and concise a description of the content of the article as possible.	191-193
	Abstract	
Yes	Provide an accurate summary of the background, research objectives, including details of the species or strain of animal used, key methods, principal findings and conclusions of the study.	191-193, 237-245, 249
	Background	
Yes	Provide an accurate summary of the background, research objectives, including details of the species or strain of animal used, key methods, principal findings and conclusions of the study.	191-193, 237-245, 249
Yes	Explain how and why the animal species and model being used can address the scientific objectives and, where appropriate, the study's relevance to human biology.	191
	Objectives	
Yes	Clearly describe the primary and any secondary objectives of the study, or specific hypotheses being tested.	170-172, 191-193
	Ethical statement	
Yes	Indicate the nature of the ethical review permissions, relevant licenses, and national or institutional guidelines for the care and use of animals, that cover the research.	191, 316, 317
	Study design	
Yes	Number of experimental and control groups	191
Yes	Steps taken to minimize the effects of subjective bias when allocating animals to treatment (e.g. randomization procedure) and when assessing results (e.g. if done, describe who was blinded and when).	191

Yes	The experimental unit (e.g. a single animal, group or cage of animals). A time-line diagram or flow chart can be useful to illustrate how complex study designs were carried out.	191
	Experimental procedures	
Yes	How (e.g. drug formulation and dose, site and route of administration, anesthesia and analgesia used [including monitoring], surgical procedure, method of euthanasia). Provide details of any specialist equipment used, including supplier(s).	191-193
NA	When (e.g. time of day).	
Yes	Where (e.g. home cage, laboratory, water maze).	191
Yes	Why (e.g. rationale for choice of specific anesthetic, route of administration, drug dose used).	191-193
	Experimental animals	
Yes	Provide details of the animals used, including species, strain, sex, developmental stage (e.g. mean or median age plus age range) and weight (e.g. mean or median weight plus weight range).	191
Yes	Provide further relevant information such as the source of animals, international strain nomenclature, genetic modification status (e.g. knock-out or transgenic), genotype, health/immune status, drug or test naïve, previous procedures, etc.	191
	Housing and husbandry	
Yes	Housing (type of facility e.g. specific pathogen free [SPF]; type of cage or housing; bedding material; number of cage companions; tank shape and material etc. for fish).	191
Yes	Husbandry conditions (e.g. breeding program, light/dark cycle, temperature, quality of water etc for fish, type of food, access to food and water, environmental enrichment).	191
Yes	Welfare-related assessments and interventions that were carried out prior to, during, or after the experiment.	191, 193
	Sample size	
Yes	Specify the total number of animals used in each experiment, and the number of animals in each experimental group.	191
NA	Explain how the number of animals was arrived at.	

	Provide details of any sample size calculation used.	
NA	Indicate the number of independent replications of each experiment, if relevant.	
	Allocating animals to experimental groups	
Yes	Indicate the number of independent replications of each experiment, if relevant.	191
NA	Describe the order in which the animals in the different experimental groups were treated and assessed.	
	Experimental outcomes	
Yes	Clearly define the primary and secondary experimental outcomes assessed (e.g. cell death, molecular markers, behavioral changes).	237-245
	Statistical methods	
NA	Provide details of the statistical methods used for each analysis.	
Yes	Specify the unit of analysis for each dataset (e.g. single animal, group of animals, single neuron).	191
NA	Describe any methods used to assess whether the data met the assumptions of the statistical approach.	
	Results and discussion	
	Basal data	
Yes	For each experimental group, report relevant characteristics and health status of animals (e.g. weight, microbiological status, and drug or test naïve) prior to treatment or testing (this information can often be tabulated).	191
	Numbers analyzed	
Yes	Report the number of animals in each group included in each analysis. Report absolute numbers (e.g. 10/20, not 50%).	191
NA	If any animals or data were not included in the analysis, explain why.	
	Outcomes and estimation	
Yes	Report the results for each analysis carried out, with a measure of precision (e.g. standard error or confidence interval).	237-245
	Adverse events	
NA	Give details of all important adverse events in each	

	experimental group.	
NA	Describe any modifications to the experimental protocols made to reduce adverse events.	
	Interpretation/scientific implications	
Yes	Interpret the results, taking into account the study objectives and hypotheses, current theory and other relevant studies in the literature.	237-245
NA	Comment on the study limitations including any potential sources of bias, any limitations of the animal model, and the imprecision associated with the results.	
NA	Describe any implications of your experimental methods or findings for the replacement, refinement or reduction (the 3Rs) of the use of animals in research.	
	Generalizability/translation	
Yes	Comment on whether, and how, the findings of this study are likely to translate to other species or systems, including any relevance to human biology.	244-245
	Funding	
Yes	List all funding sources (including grant number) and the role of the funder(s) in the study.	329

Based on The ARRIVE guidelines: Animal Research: Reporting of In Vivo Experiments.

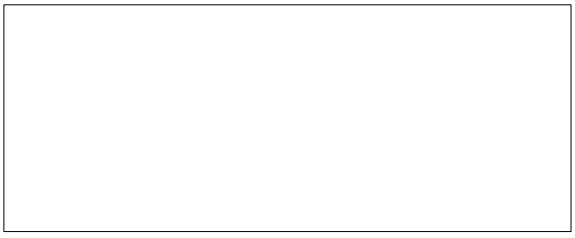

Checklist for recommendations of **Thesis EDI saúde. GENERAL**

Yes-No-N/A		Page
For all Thesis		
Yes	Declaration of potential conflicts of interests	299
Yes	Declaration on the origin and copyright status of non-original figures, with permission if necessary. Include them in the text of each figure	43, 112, 121, 135, 142, 301, 309, 313-315
N/A	Checklist of statistics adequacy if no other checklists apply.	
For Thesis involving human experimentation, human samples, or personal data.		
N/A	Declaration on approval by the research ethics committee.	
N/A	Code number of the study.	
N/A	Copy of ethics report.	
N/A	Declaration that data are based on anonymous information, and no approval of the ethics committee is needed.	
N/A	If it is an observational study, STROBE checklist.	
For Thesis that include a clinical assay		
N/A	Declaration of its authorization by the Agencia Española de Medicamentos y productos sanitarios.	
N/A	Copy of the authorization	
N/A	CONSORT Checklist	
For Thesis that use embryonic or induced human stem cells		
N/A	Declaration on its authorization	
N/A	Reference of the authorization	
N/A	Copy of the authorization	
For Thesis that include animal experimentation		

Yes	Declaration of its authorization	316
Yes	Code number of the authorization of the animal experimentation Project.	191, 316
No	Register number of the authorized user center if experiments were made in Spain	
No	Copy of the capacitation certificate if the experiments were made by the Thesis author.	
Yes	Person, company or service that performed the experiments if applicable.	306, 317
Yes	ARRIVE Checklist	321-324

PhD Student signature

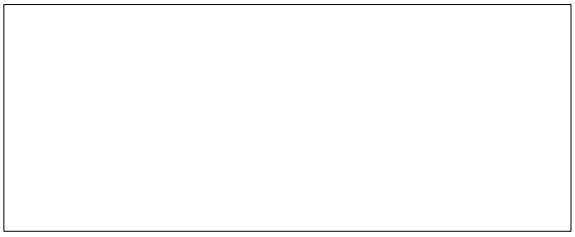

11. FUNDING

FUNDING

The PhD student Estefanía Fernández Paz thanks to the entities that have supported her research studies:

- I+D+I Grant PID2019-107500RB-I00, funded by MCIN/AEI/10.13039/501100011033
- Instituto de Salud Carlos III of Spain (Strategic Health Action, Grants FIS PS09/00816 and FIS PSI14/00059)
- Xunta de Galicia (Consellería de Cultura, Educación e Ordenación Universitaria, Project PGIDIT, 09CSA022203PR; Projects Competitive Reference Groups ED431C 2017/09-FEDER and ED431C 2021/17-FEDER)
- FCT, Portugal PTDC/DTP- FTO/0094/2012, UIDB/04138/2020 and UIDP/04138/2020

Gene therapy offers hope of cure for rare and other serious diseases that currently have no established effective treatments. It has become a valuable therapeutic strategy for congenital or acquired genetic lung diseases, such as α1-antitrypsin deficiency, infections and some types of lung cancer, among others. In this Thesis work, a new pulmonary delivery platform consisting of mannitol microspheres (Ma MS) containing chitosan-based nanocapsules (CS-based NCs) loaded with the model plasmid pCMV-βGal is proposed for its direct delivery to the lung. The designed micro-nanostructures have suitable aerodynamic properties, are biocompatible with the A549 lung cell line and are distributed in
the deep lung, producing transfection.